

# **Somatosensory Cortical Input to the Basal Ganglia.**

Elizabeth Anne May Hutton

Thesis submitted for the degree of PhD.

University of Edinburgh

August 1998



## **Declaration.**

I hereby declare that the work contained within this thesis was all my own work except for the following:

The tissue for figure 1 was kindly produced by Ann Wright.

Figure 2 was reprinted by Colin Warwick from an original drawing by Ann Wright.

Figures 44, 46, 78 and 79 were drawn by Ann Wright.

None of the work presented here has been published previously, nor has it been presented for consideration for any other award either in this establishment or any other

Elizabeth Anne May Hutton

August 1998

## Acknowledgements

I would like to thank the following people for all their help and support during both the experimental and writing phases of this work.

Prof. Gordon Arbuthnott for all his help, encouragement and support throughout and for the faith he had in my abilities (even when I didn't). I would also like to thank him for sharing some of his knowledge in neuronal recording, tracing and his knowledge of the cortex and basal ganglia. I never thought I would be able to fill single neurons and now, thanks to you Gordon I can! I would also like to thank Ann Wright who has helped and encouraged me in the anatomical tracing, histology, neuronal reconstruction and photography, she too had faith in my abilities long before I did. I never thought I was good at art, maybe thanks to you Ann I might be average! Thanks also to Linda Norrie for her help in teaching me histological processing and photography. All three have given me great support and friendship throughout, in a way it's a shame to finish this work . I'll never be able to thank them enough.

I would like to thank the electrical and mechanical workshops within the Dick Vet for building the hydraulic and piezoelectric whisker stimulators (and Andy MacRae for his super glue and accelerator for fixing the piezoelectric stimulators!). I would also like to thank Colin Warwick for his photographic help throughout.

I would also like to thank my friends both within the Dick Vet and outside for their support and understanding especially throughout the writing phase of this thesis. Thank you, it meant a lot to me.

Last but not least I would like to thank Donald for 'putting up with me' through some of my tantrums and fits whilst I was writing this. All I can say is, thanks to you, I did it, one bite at a time!

## Abstract

The mystacial vibrissae in rodents provide the major peripheral input to primary somatosensory cortex via a topographically arranged ascending system to cortex. The cortex in turn integrates this information and provides the major input to the basal ganglia and thalamus. Whilst the ascending system and the cortical integration have been studied extensively the efferent projections from cortex have not. The aim of this study was to investigate the corticostriatal pathways in a highly organised and topographically arranged cortical area using an intracellular *in vivo* method for the recording, filling and tracing of single corticostriatal neurons.

In order to do so a successful intracellular recording protocol had to be developed (from an existing extracellular method) to ensure maximum neuronal filling. This process was an ongoing and the various stages of development are highlighted. Alongside this a suitable biocytin method had to be developed for the visualisation of terminal fields arising from single neuronal fills. The various stages in the development of this method are also described.

This study has resulted in recordings from all four types of layer V pyramidal projection neurons described *in vitro*. Whilst the morphology was identical to that observed *in vitro* for the IB and RS neurons the physiological responses to whisker deflection were more complex, especially in IB neuronal firing patterns. In general there was a lot more background synaptic activity observed in all the cellular records. The IB neurons tended to show more complex firing patterns, firing either as mainly single action potentials with occasional burst or predominantly bursts with occasional action potentials. Only rarely did they fire the typical burst firing observed *in vitro*.. It was apparent from this study that the RS2 and IB1 neurons

were very similar in both their physiology and morphology and were more difficult to classify.

The study revealed two different classes of ipsilateral corticostriatal neurons. One class is similar to the innervation pattern seen in motor cortex. This innervation arose from a lateral branch of the axons of pyramidal tract neurons as they run through the fibre bundles within the striatum. In this case the neuron has the physiology and the morphology of an RS2 neuron. The second class of corticostriatal innervation arose from a typical IB1 neuron that innervated the striatum in a topographic manner similar to that described in anatomical studies of rat primary somatosensory cortex. The topography appears to be arranged within rows. In the ascending vibrissal system, and within cortex, there appears to be an in-row preference generated in cortex by intracortical connections. The IB input may also be arranged in rows as it may obey the general rules observed in monkey corticostriatal connections where more heavily interconnected cortical regions are more likely to overlap and innervate the same regions of the striatum whilst still retaining a topographically arranged innervation pattern. The conclusions drawn are that the RS2 innervation may result in the initial short latency activation of the striatum whereas the topographic IB innervation may provide a longer latency and more detailed input to the striatum

# CONTENTS

INTRODUCTION		Page
<b>1.0</b>	<b>General Introduction</b>	<b>1</b>
	1.1 Vibrissal arrangement	1
	1.2 Whisker use	1
	1.3 Somatosensory cortex	2
	1.4 Septae	3
	1.5 Sensory relay	3
<b>2.0</b>	<b>Whisker Follicles</b>	<b>6</b>
	2.1 Musculature of the whisker pad	6
	2.2 Vibrissal nerves	7
	2.3 Whisker follicles	8
	2.4 Inner conical body	10
	2.5 Outer conical body	10
	2.6 Slowly adapting receptors	10
	2.7 Rapidly adapting receptors	11
	2.8 Common fur innervation	11
	2.9 Directional sensitivities	12
<b>3.0</b>	<b>Trigeminal Patterns</b>	<b>13</b>
	3.1 General introduction	13
	3.2 Subnucleus Principalis (PrV)	14
	3.3 Subnucleus Interpolaris (SpVi)	14
	3.4 Subnucleus Caudalis (SpVc)	15
	3.5 Subnucleus Oralis (SpVo)	15

<b>4.0</b>	<b>Thalamic Introduction</b>	<b>18</b>
4.1	VentroPosteromedial thalamic nucleus (VPm)	18
4.2	VentroPosteromedial thalamic neurons	18
4.3	Thalamocortical and corticothalamic connections	21
4.4	Posteromedial thalamic nucleus (POm)	22
4.5	Trigeminal inputs to POm	22
4.6	Thalamocortical and corticothalamic connections	22
<b>5.0</b>	<b>Primary Somatosensory Cortex</b>	<b>26</b>
5.1	Thalamic inputs	26
5.2	General cortical introduction	26
5.3	Centre receptive fields (CRF)	28
5.4	Surround receptive fields (SRF)	30
5.5	Connection with other cortical areas	35
5.6	Subcortical projection targets	37
<b>6.0</b>	<b>Physiology and Morphology of Cortical Neurons</b>	<b>39</b>
6.1	General physiology and morphology	39
6.2	Spiny stellate cells	40
6.3	Spiny stellate morphology	40
6.4	Fast spiking (FS) neurons	41
6.5	Regular spiking (RS) neuronal physiology	43
6.6	RS neuronal morphology	44
6.7	Intrinsic bursting (IB) neuronal physiology	45
6.8	IB neuronal morphology	47
<b>7.0</b>	<b>Anaesthesia and Cortical Physiology</b>	<b>52</b>

<b>8.0 Conclusions</b>	<b>53</b>
<b>MATERIALS AND METHODS</b>	
<b>9.0 Methods Introduction</b>	<b>56</b>
9.1 Anaesthesia	56
9.2 Basic surgery	56
9.3 Contralateral stimulating electrode	57
9.4 Whisker stimulation	58
9.5 Hydraulic whisker stimulator	58
9.6 Electrical stimulation of the whisker pad	60
9.7 Piezoelectric whisker stimulation	62
9.8 Perfusion	63
9.9 Biocytin Histology	64
<b>10.0 Extracellular Recordings</b>	<b>65</b>
10.1 Surgery	65
10.2 Recording of surface evoked potentials	65
10.3 Extracellular recording	66
10.4 Extracellular marking and perfusion	66
<b>11.0 Initial Intracellular Recording Protocol</b>	<b>70</b>
11.1 Anaesthesia and surgery	70
11.2 Whisker stimulus	70
11.3 Maclab data acquisition packages	70
11.4 Recording set up	72
11.5 Intracellular recording	72
11.6 Physiological classification of neurons	73

11.7 Intracellular filling	74
11.8 Further recordings	74
<b>12.0 Final Intracellular Recording Protocol</b>	<b>76</b>
12.1 Anaesthesia and surgery	76
12.2 Surgical adaptations	76
12.3 Advantages and disadvantages of the surgical adaptations	77
<b>13.0 Anaesthetic Considerations</b>	<b>82</b>
<b>14.0 Electrodes</b>	<b>84</b>
<b>15.0 Biocytin Methods Introduction</b>	<b>86</b>
15.1 Perfusion	86
15.2 Cutting	86
15.3 Washes	86
15.4 Mounting	87
15.5 Coverslipping	87
<b>16.0 Extracellular Biocytin Visualisation Protocol</b>	<b>88</b>
16.1 Fixation and cutting	88
16.2 Reaction and visualisation	88
<b>17.0 Cytochrome Oxidase Histochemistry</b>	<b>91</b>
17.1 Tissue considerations	91
17.2 Visualisation	91
17.3 Considerations	91

<b>18.0</b>	<b>Freeze Thaw Ethanol Technique</b>	<b>93</b>
	18.1 Membrane disruption	93
	18.2 Considerations	94
<b>19.0</b>	<b>Osmium Tetroxide</b>	<b>95</b>
	19.1 Osmication	95
	19.2 Dehydration and mounting	95
	19.3 Technical considerations	96
	19.4 Lead citrate	128
<b>20.0</b>	<b>Triton and Elite Histology Methods</b>	<b>99</b>
	20.1 Quenching of endogenous peroxidase activity	99
	20.2 Biocytin visualisation	99
	20.3 Adaptations	100
	20.4 Morphological recordings	129
<b>21.0</b>	<b>Final Intracellular Biocytin Protocol</b>	<b>101</b>
	21.1 Biocytin visualisation	101
	21.2 Morphological recordings	132
<b>22.0</b>	<b>Biocytin Histology Methods</b>	<b>102</b>
	22.1 Methanol quenching	102
	22.2 Triton-X100	102
	22.3 Elite versus standard ABC	103
	22.4 Cell classification	146
<b>23.0</b>	<b>Erroneous Fills</b>	<b>106</b>
	23.1 Subcortical Projections	148
<b>24.0</b>	<b>Investigation at the Light Microscope Level</b>	<b>110</b>
	24.1 Morphological classification of neuron	110
	24.2 Subcortical projections	112
<b>25.0</b>	<b><u>In Vivo</u> Versus <u>In Vitro</u></b>	<b>114</b>

<b>26.0</b>	<b>Intracellular Recordings in vivo</b>	<b>116</b>
	26.1 Small animals	120
<b>27.0</b>	<b>Electrophysiology Results</b>	<b>118</b>
	27.1.1 Electrophysiology in vivo	127
<b>28.0</b>	<b>Scope/VCR Analysis</b>	<b>125</b>
	28.1 Introduction	125
	28.2 Scope records	125
	28.3 Latency values	126
	28.4 Single whisker recordings	126
	28.5 Multi-whisker recordings	126
	28.6 Inhibitory period	129
	28.7 Single whisker recordings	129
	28.8 Multi-whisker recordings	129
	28.9 Classification criteria	130
<b>29.0</b>	<b>Firing Patterns/Cell Class Across Whiskers</b>	<b>132</b>
	29.1 Scope records versus VCR/chart	132
	29.2 VCR/chart recordings of multiple whiskers	133
	29.3 Firing patterns and cell class across whiskers	138
<b>30.0</b>	<b>Morphology Results</b>	<b>145</b>
	30.1 Morphology of single whisker recordings	145
	30.2 Morphology of multiple whisker recordings	146
<b>31.0</b>	<b>Cell Classification</b>	<b>146</b>
	31.1 Cell classification criteria	146
	31.2 Cell classification results	147
<b>32.0</b>	<b>Subcortical Projections</b>	<b>148</b>
	32.1 Intracortical recording locations and spatial distribution	148
<b>33.0</b>	<b>Terminal Fields</b>	<b>149</b>
	33.1 Terminal field locations and spatial distribution	149
	33.2 Terminal field morphology	150
	33.3 Terminal field classification	151
	33.4 Terminal field morphology and classification	152
	33.5 Terminal field morphology and classification	153
	33.6 Terminal field morphology and classification	154
	33.7 Terminal field morphology and classification	155
	33.8 Terminal field morphology and classification	156
	33.9 Terminal field morphology and classification	157
	33.10 Terminal field morphology and classification	158
	33.11 Terminal field morphology and classification	159
	33.12 Terminal field morphology and classification	160
	33.13 Terminal field morphology and classification	161
	33.14 Terminal field morphology and classification	162
	33.15 Terminal field morphology and classification	163
	33.16 Terminal field morphology and classification	164
	33.17 Terminal field morphology and classification	165
	33.18 Terminal field morphology and classification	166
	33.19 Terminal field morphology and classification	167
	33.20 Terminal field morphology and classification	168
	33.21 Terminal field morphology and classification	169
	33.22 Terminal field morphology and classification	170
	33.23 Terminal field morphology and classification	171
	33.24 Terminal field morphology and classification	172
	33.25 Terminal field morphology and classification	173
	33.26 Terminal field morphology and classification	174
	33.27 Terminal field morphology and classification	175
	33.28 Terminal field morphology and classification	176
	33.29 Terminal field morphology and classification	177
	33.30 Terminal field morphology and classification	178
	33.31 Terminal field morphology and classification	179
	33.32 Terminal field morphology and classification	180
	33.33 Terminal field morphology and classification	181
	33.34 Terminal field morphology and classification	182
	33.35 Terminal field morphology and classification	183
	33.36 Terminal field morphology and classification	184
	33.37 Terminal field morphology and classification	185
	33.38 Terminal field morphology and classification	186
	33.39 Terminal field morphology and classification	187
	33.40 Terminal field morphology and classification	188
	33.41 Terminal field morphology and classification	189
	33.42 Terminal field morphology and classification	190
	33.43 Terminal field morphology and classification	191
	33.44 Terminal field morphology and classification	192
	33.45 Terminal field morphology and classification	193
	33.46 Terminal field morphology and classification	194
	33.47 Terminal field morphology and classification	195
	33.48 Terminal field morphology and classification	196
	33.49 Terminal field morphology and classification	197
	33.50 Terminal field morphology and classification	198
	33.51 Terminal field morphology and classification	199
	33.52 Terminal field morphology and classification	200
	33.53 Terminal field morphology and classification	201
	33.54 Terminal field morphology and classification	202
	33.55 Terminal field morphology and classification	203
	33.56 Terminal field morphology and classification	204
	33.57 Terminal field morphology and classification	205
	33.58 Terminal field morphology and classification	206
	33.59 Terminal field morphology and classification	207
	33.60 Terminal field morphology and classification	208
	33.61 Terminal field morphology and classification	209
	33.62 Terminal field morphology and classification	210
	33.63 Terminal field morphology and classification	211
	33.64 Terminal field morphology and classification	212
	33.65 Terminal field morphology and classification	213
	33.66 Terminal field morphology and classification	214
	33.67 Terminal field morphology and classification	215
	33.68 Terminal field morphology and classification	216
	33.69 Terminal field morphology and classification	217
	33.70 Terminal field morphology and classification	218
	33.71 Terminal field morphology and classification	219
	33.72 Terminal field morphology and classification	220
	33.73 Terminal field morphology and classification	221
	33.74 Terminal field morphology and classification	222
	33.75 Terminal field morphology and classification	223
	33.76 Terminal field morphology and classification	224
	33.77 Terminal field morphology and classification	225
	33.78 Terminal field morphology and classification	226
	33.79 Terminal field morphology and classification	227
	33.80 Terminal field morphology and classification	228
	33.81 Terminal field morphology and classification	229
	33.82 Terminal field morphology and classification	230
	33.83 Terminal field morphology and classification	231
	33.84 Terminal field morphology and classification	232
	33.85 Terminal field morphology and classification	233
	33.86 Terminal field morphology and classification	234
	33.87 Terminal field morphology and classification	235
	33.88 Terminal field morphology and classification	236
	33.89 Terminal field morphology and classification	237
	33.90 Terminal field morphology and classification	238
	33.91 Terminal field morphology and classification	239
	33.92 Terminal field morphology and classification	240
	33.93 Terminal field morphology and classification	241
	33.94 Terminal field morphology and classification	242
	33.95 Terminal field morphology and classification	243
	33.96 Terminal field morphology and classification	244
	33.97 Terminal field morphology and classification	245
	33.98 Terminal field morphology and classification	246
	33.99 Terminal field morphology and classification	247
	33.100 Terminal field morphology and classification	248

<b>34.0</b>	<b>Neurons With Terminal Fields</b>	<b>150</b>
34.1	Striatal terminals	150
34.1.1	Topographic innervation 1	150
34.1.2	Topographic innervation 2	157
34.1.3	Limited lateral branch innervation 1	165
34.1.4	Limited lateral branch innervation 2	174
34.2	Thalamic innervation	181
34.2.1	Layer V innervation	181
34.2.2	Layer VIa innervation	191
34.3	Layer III neurons	197
<b>DISCUSSION</b>		<b>200</b>
35.0	Different classes of layer V pyramidal projection neurons	200
35.1	Classification Criteria	200
35.2	Physiology data	203
35.3	Principal versus adjacent whisker	204
35.4	RS and IB firing patterns with respect to striatal innervation	205
35.5	Pyramidal tract neurons and striatal innervation in rat motor cortex	208
35.6	Vibrissal region of primary somatosensory cortex	210
35.7	Limited lateral branch innervation of the striatum	211
35.8	Topographic innervation of the striatum	212
35.9	Relation to ascending sensory systems	212
35.10	Relation to other cortical regions	213
35.11	Intrinsically bursting neurons and striatal innervation	214
<b>36.0</b>	<b>CONCLUSION</b>	<b>218</b>
<b>37.0</b>	<b>BIBLIOGRAPHY</b>	<b>222</b>
<b>38.0</b>	<b>APPENDIX</b>	<b>A1</b>

## FIGURE LIST

### INTRODUCTION

Page

- 1 Tangential section taken from the vibrissal region of primary somatosensory stained for cytochrome oxidase 4
- 2 Diagram showing the arrangement of the whiskers on a rodent's snout 5
- 3 Drawing of a whisker follicle 9
- 4 Trigemino-trigeminal and trigemiothalamic connections 17
- 5 VentroPosteriomedial thalamic inputs to primary somatosensory cortex 20
- 6 Posteriomedial thalamic inputs to primary somatosensory cortex 24
- 7 Summary diagram of thalamocortical inputs 25
- 8 Activation of cortical columns 34
- 9 Physiological and morphological differences between RS, IB and FS neurons 49
- 10 Examples of typical firing patterns of RS, IB and FS neurons in vitro 50
- 11 Lamina locations of RS, IB and FS neurons 51
- 12 Examples of the morphology of RS and IB neurons seen in vitro 55

## MATERIALS AND METHODS

13	Extracellular record of a neuron responding to hydraulic whisker deflection	59
14	Extracellular record of a neuron responding to electrical stimulation of the whisker pad	61
15	Tangential section stained for cytochrome oxidase and marked with an extracellular injection of the dye pontamine sky blue	68
16	Tangential section stained for cytochrome oxidase and marked with extracellular injection of biocytin	69
17	Photomicrographs of recording area used in the final intracellular recording protocol	78
18	Photomicrographs showing a dental cement well	79
19	Photomicrograph showing the triple piezoelectric whisker stimulator	80
20	Photomicrograph showing the final intracellular recording set up	81
21	Photomicrograph highlighting a cortical column	89
22	Tangential section stained for cytochrome oxidase and biocytin	90
23	Example of a neuron visualised using the osmium tetroxide method	97

24 Photomicrograph showing the intense staining seen with osmium tetroxide 98

25 Example of a ghost like filling of a single neuron 109

## RESULTS

26 A table showing the various recordings made 116

27 A table highlighting the correlation between morphological and physiological classification 116

28 Camera lucida reconstruction of a typical RS1 neuron and its response to whisker deflection 119

29 Camera lucida reconstruction of a typical RS2 neuron and its response to whisker deflection 120

30 Camera lucida reconstruction of a typical IB1 neuron and its response to whisker deflection 121

31 Camera lucida reconstruction of a typical IB2 neuron and its response to whisker deflection 122

32 Variations in latency between the IB and RS neurons recorded in this study 127

33 Histogram highlighting latency variations within IB and RS neurons 128

34 Latency and inhibitory period data for centre barrel recordings in an IB and an RS neuron 130

35	Latency and inhibitory period data for barrel side or septal recordings in an IB neuron	131
36	Typical examples of pattern 1 and pattern 2 firing	134
37	Example of the switch between pattern 2 and pattern 1 firing upon whisker deflection	135
38	'Scope' overlays highlighting RS synchronicity	136
39	'Scope' overlays highlighting IB synchronicity and rhythmicity	137
40	Centre barrel recordings for three whiskers	139
41	Centre barrel recordings for three whiskers and a contralateral stimulating electrode	140
42	Side/septal recordings for three whiskers	142
43	Side/septal recordings for three whiskers and a contralateral stimulating electrode	143
44	Photomicrograph of the topographic innervation neuron 1	152
45	Camera lucida reconstruction of topographic innervation neuron 1	153
46	Camera lucida reconstruction of the topographic innervation 1 terminal field	154
47	Photomicrograph of the topographic innervation 1 terminal field	155

48	Camera lucida reconstruction of the topographic innervation 1 neuron and its striatal terminal field	156
49	Photomicrograph of the topographic innervation 2 neurons	159
50	Camera lucida reconstruction of a topographic innervation 2 neurons	160
51	Photomicrograph of the topographic innervation 2 terminal field within striatum	161
52	Photomicrograph of the SII innervation from topographic innervation 2 neuron	162
53	Camera lucida reconstruction of the topographic innervation 2 neuron and its striatal terminal field	163
54	Examples of neuronal firing to whisker deflection of the two neurons filled in the topographic innervation 2	164
55	Photomicrograph of one of the neurons filled in the lateral branch innervation	166
56	Camera lucida reconstruction of one of the neurons filled in the lateral branch innervation 1	167
57	Photomicrograph of the other neuron filled in the limited lateral branch innervation 1	168
58	Camera lucida reconstruction of the other neuron filled in the limited lateral branch innervation 1	169

59	Photomicrograph of the limited lateral branch innervation 1 terminal field	170
60	Camera lucida reconstruction of the limited lateral branch innervation 1 terminal field	171
61	Camera lucida reconstruction of both the neurons and the striatal terminal field	172
62	Examples of both the neurons response to whisker deflection	173
63	Photomicrograph of the neuron resulting in the limited lateral branch innervation 2	175
64	Camera lucida reconstruction of the neuron resulting in the limited lateral branch innervation 2 of the striatum	176
65	Photomicrograph of the limited lateral branch innervation 2 terminal field in striatum	177
66	Camera lucida reconstruction of the limited lateral branch innervation 2 terminal field within striatum	178
67	Camera lucida reconstruction of the neuron and terminal field described in the limited lateral branch innervation 2	179
68	Example of the limited lateral branch innervation 2 neuronal response to whisker deflection	180
69	Photomicrograph of the layer V corticothalamic neuron	183

70	Camera lucida reconstruction of the layer V cortico-thalamic neuron	184
71	Photomicrograph of the thalamic terminal field of the layer V corticothalamic neuron	185
72	Camera lucida reconstruction of the thalamic terminal field of the layer V corticothalamic neuron	186
73	Photomicrograph of the second thalamic terminal field of the layer V corticothalamic neuron	187
74	Camera lucida reconstruction of the second thalamic terminal field of the layer V corticothalamic neuron	188
75	Camera lucida reconstruction of the layer V cortico-thalamic neuron and its terminal fields	189
76	Example of the layer V corticothalamic neuronal response to whisker deflection	190
77	Photomicrograph of the layer VIa corticothalamic neuron	192
78	Camera lucida reconstruction of the layer VIa cortico-thalamic neuron	193
79	Photomicrograph of the layer VIa corticothalamic neuronal terminal field	194
80	Camera lucida reconstruction of the layer VIa cortico-thalamic neuronal terminal field	195

1.0 GENERAL INTRODUCTION

81	Camera lucida reconstruction of the layer VIa cortico-thalamic neuron in its entirety	196
82	Low power photomicrograph of a typical layer III neuron	198
83	Higher power photomicrograph of a typical layer III neuron	199

DISCUSSION

84	Summary diagram of cortical inputs to the basal ganglia from this study	221
----	---	-----

## 1.0 GENERAL INTRODUCTION.

### 1.1 Vibrissal Arrangement.

The mystacial vibrissae (whiskers) provide rodents with the major source of sensory information from their environment. From this information the rodent is then able to execute an appropriate motor action. This system is especially important in the assessment of (routine) stimuli surrounding the snout of the animal. Rats rely heavily upon their vibrissae as they live in dark environments and compared to cats and primates have a poorly developed visual system.

The large mystacial vibrissae are arranged in five rows either side of the snout running dorsal to ventral (rows A-E). Within rows the more caudal whiskers are relatively coarse and long whereas the more rostral ones are much shorter and finer (whiskers within a row are labelled numerically 1-8 running caudal to rostral). Whiskers that run across rows i.e. B1, C1, D1 are termed arcs (Woolsey and Van der Loos, 1970; Gustafson and Felbain-Keradamis, 1977). It is thought that there is a preferential relay of information within rows rather than between arcs of whiskers (Durham and Woolsey, 1978; 1985; Simons, 1978; Simons and Woolsey, 1979; 1984; Armstrong-James and Fox, 1987; McCasland and Woolsey, 1988; Bernardo et al, 1990b). There are four vibrissae located at the most caudal end of the vibrissae between the arc of A1-E1 termed straddlers and are labelled  $\alpha$ - $\delta$  (Woolsey and Van der Loos, 1970). The remainder of the snout is covered with fine short fur known as common fur.

### 1.2 Whisker Use

Rodents receive their sensory information from their whiskers in two basic ways i.e. an active or passive mode. The whiskers are usually used in the active mode

("whisking") where the whiskers are actively palpated at a regular frequency of approximately 8 Hz (Carvell and Simons, 1990; 1996). The large caudal whiskers move together during whisking whereas the more rostral ones do not (Carvell and Simons, 1990). This whisking behaviour develops around the middle of the second postnatal week (Welker, 1964). In roughness discrimination the more rostral whiskers remain protracted and motionless when approaching the object. Upon contact they remain in constant contact with it whilst the more caudal whiskers whisk across it (Carvell and Simons, 1990). This repeated scanning of an object produces a refined cortical representation (Simons, 1995). The whisking cycles themselves are very complex with each cycle lasting between 100-125 mS.

The whiskers can also be used in the static phase which relays sensory information by detecting rapid and usually larger whisker deflections. Whisker deflection occurs in two preferential ways- in rows or in a rostral to caudal direction (Welker et al., 1993). The groups of vibrissae are thought to be used for different purposes. The larger more caudal ones are thought to be important for roughness discrimination whereas the finer more rostral whisker are thought to be important in object location (Simons, 1995).

### **1.3 Somatosensory Cortex**

The vibrissal information is processed within the vibrissal region of primary and secondary somatosensory cortex (SI and SII). The vibrissal region of SI occupies approx. 20% of SI (Welker and Woolsey, 1974) and mirrors the facial topography in sections of SI cut tangentially to the pial surface and stained for the enzyme cytochrome oxidase (Wong-Riley, 1979). A whisker pattern can be clearly seen in posterior SI as blobs of cytochrome oxidase rich areas termed barrels (Woolsey and Van der Loos, 1970). These areas correspond in a 1:1 manner with the facial vibrissae. The whisker representation seen in the posterior of the field is termed the

PosteriorMedial Barrel Subfield (PMBSF) (Woolsey and Van der Loos, 1970). The more anterior barrels in the vibrissal region appear to have no clear arrangement or topography and are termed the AnterioMedial Barrel SubField representing the common fur on the snout. The barrelfield in rats contains 165-220 barrels per hemisphere (Woolsey and Van der Loos, 1970; Welker and Woolsey, 1974) with the PMBSF occupying approximately 40-50% of the barrelfield (Woolsey and Van der Loos, 1970). The larger barrels in rats are 400  $\mu\text{m}$  in the long axis (Welker and Woolsey, 1974). The arrangement of blood vessels within SI also appears to be linked with the barrels themselves as the highest density of blood vessels are associated with layer IV and the pattern is consistent between animals (Patel, 1983).

#### **1.4 Septae**

Barrels within SI are characterised by an unusually cell dense layer IV and are separated by areas of less cell dense cytochrome oxidase poor areas termed septa (Woolsey and Van der Loos, 1970). The septae in rats are known to be wider between rows than they are between arcs (Woolsey et al., 1975). It is thought that the distance between two barrel centres is approximately 500  $\mu\text{m}$  (Welker and Woolsey, 1974).

#### **1.5 Sensory Relay**

The relay of sensory information from the whisker pad to the cortex and the subsequent execution of the appropriate motor action is a complex system. This process involves the whole of the ascending sensory system (vibrissal follicles, the trigeminal nuclei, thalamus, cortex) as well as inputs from the descending system (thalamus and striatum) and other cortical areas. Each of the systems will be dealt with separately in a bid to understand the vibrissal input to the cortex and how it may be possible for the cortex to modulate the input it receives from the snout.

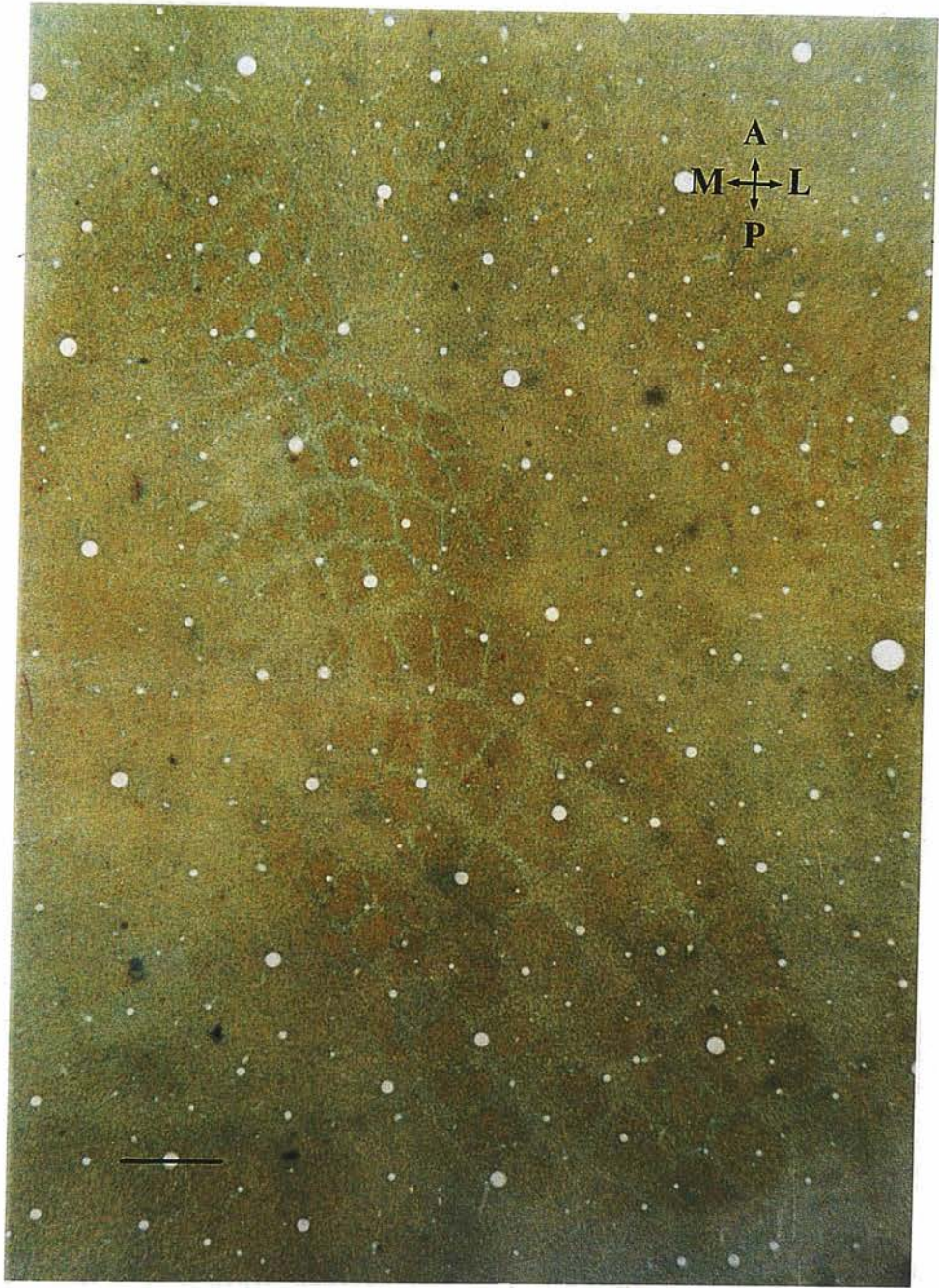


Figure 1. A tangential section taken from the vibrissal region of primary somatosensory cortex and stained for the enzyme cytochrome oxidase (and counterstained with methyl green). Note the positioning of the posterior (P) and anterior (A) barrels as well as the septa (S). Scale bar 500  $\mu$ m.

## 2.2 WHISKER FOLLILES

Whisker follicles are arranged in a regular pattern on the snout of rodents. The arrangement of whisker follicles is such that they are arranged in a regular pattern on the snout of rodents. The arrangement of whisker follicles is such that they are arranged in a regular pattern on the snout of rodents.

## 2.3 MAINTENANCE OF THE WHISKER PAD

Whisker follicles are arranged in a regular pattern on the snout of rodents. The arrangement of whisker follicles is such that they are arranged in a regular pattern on the snout of rodents. The arrangement of whisker follicles is such that they are arranged in a regular pattern on the snout of rodents.

The arrangement of whisker follicles is such that they are arranged in a regular pattern on the snout of rodents. The arrangement of whisker follicles is such that they are arranged in a regular pattern on the snout of rodents.

The arrangement of whisker follicles is such that they are arranged in a regular pattern on the snout of rodents. The arrangement of whisker follicles is such that they are arranged in a regular pattern on the snout of rodents.

The arrangement of whisker follicles is such that they are arranged in a regular pattern on the snout of rodents. The arrangement of whisker follicles is such that they are arranged in a regular pattern on the snout of rodents.

Figure 2. A drawing showing the arrangement of the whiskers on a rodents snout. Note the arrangement of arcs and rows. The lower figure shows a cartoon of the barrel arrangement within the vibrissal region of somatosensory cortex.

## 2.0 WHISKER FOLLICLES

Whiskers must operate in such a way as to provide relevant sensory information for relay throughout the system. The whisker system must be capable of encoding the variety of responses seen in the whisker follicles i.e. direction, amplitude, onset, duration and velocity of deflection (Zucker and Welker, 1969)

### 2.1 Musculature of the Mystacial Pad

Whisking animals are able to palpate their whiskers as desired through a complex intrinsic and extrinsic muscle arrangement within the mystacial pad and innervated by branches of the facial nerves (Dorfl, 1982; 1985). The extrinsic muscles move the upper lip and nose and innervate the mystacial pad by running between the vibrissae. The intrinsic (follicular muscles) are associated exclusively with the mystacial follicles (Dorfl, 1985). The follicular muscles form a sling around the vibrissae connecting two adjacent whiskers within the same row and are responsible for whisking behaviour (Dorfl, 1985) with the largest being associated with the straddlers at the back of the field. In rats follicular muscles are associated with all the vibrissae in rows A and B and only the first 6 or possibly 7 of the remaining rows.

In whisking behaviour a smooth movement is achieved through the control of four muscles. The m. levator labii superioris, m. transversus nasi, m. maxillolabialis and m. nasalis (Dorfl, 1985). Whilst this appears to be the case in a behaving animal anaesthesia results in the whisker follicles being directed forward as there is no active muscle tone to retract the vibrissae (Dorfl, 1985). This is an important consideration for *in vivo* recordings as the whiskers appear to be in a position that is the reverse of normal behavioural conditions. Muscular activity within the mystacial pad allows a

variation in the set point around which activity is detected (Carvell et al., 1991). The musculature is also responsible for the retraction and protraction patterns of the vibrissae.

## 2.2 Vibrissal Nerves

The whiskers are innervated by two distinct nerves: the deep and superficial vibrissal nerves (DVN and SVN respectively). The superficial vibrissal nerves innervate the rete ridge collar of the follicle and the inner conical body (ICB). The deep vibrissal nerves innervate the ring sinus. The deep vibrissal nerves derive from a row fascicle of the infraorbital nerve (Dorfl, 1985) and innervate a single vibrissal hair follicle (Dorfl, 1985; Rice et al., 1986). The superficial nerves innervate more than 1 whisker follicle as well as sinus and vellus hairs of the vibrissal pad (Waite and Jacquin, 1992). The superficial nerves exclusively innervate the inner conical body (ICB) (Rice et al., 1986). Within the whisker follicle the SVN innervate the neck and the DVN innervate the base of the follicle at the cavernous sinus forming a network of fine innervations (Rice et al., 1993). The DVN project to lamina III, IV and V of the trigeminal nucleus caudalis in a topographical columnar arrangement. The superficial nerves project to lamina I-III (and occasionally lamina V) although not in this tight topographical arrangement (Arvidsson and Rice, 1991).

The deep vibrissal nerves are directionally sensitive. Over half of the cells respond to sustained displacements of the whiskers and to a push-pull pattern of whisker activation and almost half of the cells will respond to injury. The SVN generally are more responsive to sustained whisker stimuli than the DVN and are also non-responsive to whisker pulling although almost half the cells will respond to whisker pushing.

### 2.3 Whisker Follicles

The whisker follicle itself can be subdivided (see Rice et al, 1986). The whole structure is termed the follicle sinus complex (F-SC) (Rice et al., 1986) and can be subdivided into the conical body. The conical body can be subdivided into the inner (ICB) and outer conical (OCB) bodies and the ringwulst at the top of the hair follicle. The receptors associated with the follicle are a mixture of rapidly and slowly adapting receptors.



Figure 3. A drawing of the whisker follicle showing the position and types of mechanoreceptors it contains (from Rice et al., 1986).

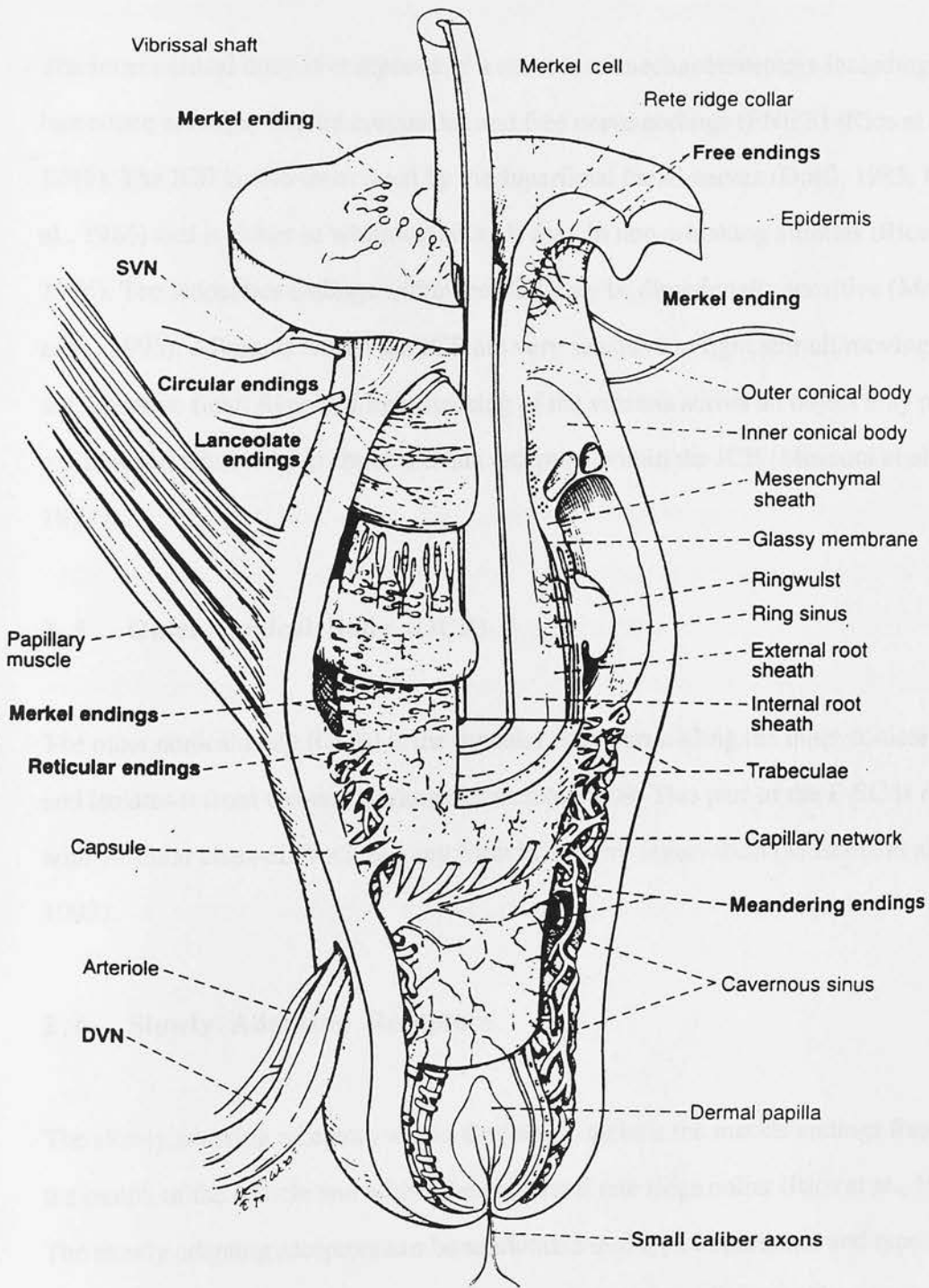


Figure 3. A drawing of the whisker follicle showing the position and type of mechanoreceptors it contains (from Rice et al., 1993)

## **2.4 Inner Conical Body (ICB)**

The inner conical body is composed of a number of mechanoreceptors including lanceolate endings, Ruffini corpuscles and free nerve endings (FNE'S) (Rice et al., 1986). The ICB is also innervated by the superficial facial nerves (Dorfl, 1985; Rice et al., 1986) and is richer in whisking animals than in non-whisking animals (Rice et al., 1986). The lanceolate endings within the ICB may be directionally sensitive (Mosconi et al., 1993). Afferents within the ICB are very sensitive to light stimuli moving across the receptive field. Repeated light stroking of the vibrissa across an object may provide a prolonged stimulus that could activate receptors within the ICB (Mosconi et al., 1993).

## **2.5 Outer Conical Body (OCB)**

The outer conical body (OCB) is the capsular coat surrounding the inner conical body and isolates it from the surrounding connective tissue. This part of the F-SC is rich with vascular channels but lacks any form of sensory innervation (Mosconi et al., 1993).

## **2.6 Slowly Adapting Receptors**

The slowly adapting receptors within the follicle include the merkle endings found in the mouth of the follicle and within the epidermal rete ridge collar (Rice et al., 1986). The slowly adapting receptors can be subdivided into type I epidermal and type II dermal mechanoreceptors with merkel endings being classed as type II receptors. Slowly adapting fibres may also respond to compression (Johansson and Vallbo, 1979; Johansson and Arvidsson, 1994). Slowly adapting receptors are ideally suited to the detection and relay of directionally specific information and may also encode

precisely the intensity of a steady stimulus (Gotteschaldt et al., 1973; Dykes, 1975; Halata and Munger, 1980). The ringwulst provides the dampening mechanism for the deflections (Yohoro, 1977). The vibrissal nerves are also subdivided according to their response properties with the superficial nerves being more responsive to slowly adapting receptors.

## **2.7 Rapidly Adapting Receptors**

Rapidly adapting fibres are predominantly the lanceolate endings found within the ring or cavernous sinuses of the mesenchymal sheath (Rice et al., 1986). The receptors can be subdivided into either high or low velocity threshold receptors. The rapidly adapting receptors are ideally suited to the detection of vibration in the mystacial pad and for the detection of stimulus frequency and velocity (Dykes, 1975, 1983). The lanceolate endings within the ICB are known to be directionally insensitive (Halata and Munger, 1980; Lichtenstein et al., 1990; Mosconi et al., 1993). The rapidly adapting mechanoreceptor information does not appear to be the most dominant input to the somatosensory system with only approximately 25% of the trigeminal ganglion cells responding to rapidly adapting inputs (Lichtenstein et al., 1990).

## **2.8 Common Fur Innervation**

The common fur is composed of two elements, large guard hairs within the fur, surrounded by small vellus hairs. The vellus hairs are innervated by free nerve endings whereas the guard hairs possess similar mechanoreceptors to the vibrissae but the main difference is that the guard hairs do not possess the blood sinuses of the vibrissae. The receptors from the common fur of the snout are most likely to be rapidly adapting and not directionally sensitive (Zucker and Welker, 1969).

## 2.9 Directional Sensitivities

Within the trigeminal nerve there is a strong relay of slowly adapting directionally sensitive information with over 75% of the cell responding to slowly adapting inputs (Zucker and Welker, 1969). The remainder respond to rapidly adapting inputs (Lichtenstein et al., 1990). Within the thalamus there is also a preference for directionally selective information (Simons and Carvell, 1989). In cortex of anaesthetised animals however only approximately 15% of neurons are directionally sensitive (Simons and Carvell, 1989).

### 3.0 TRIGEMINAL PATTERNS

#### 3.1 General Introduction

The trigeminal brainstem nucleus (V) can be subdivided into two major nuclei: the principal sensory nucleus (PrV) and the spinal trigeminal nucleus (SpV). The SpV can be divided into the subnuclei caudalis (SpVc), interpolaris (SpVi) and oralis (SpVo). All these nuclei except the SpVo contain discrete and topographically arranged areas of CO rich staining corresponding to the vibrissal representation on the snout. These areas are termed barrelettes (although they occupy less neural tissue than the corresponding barrel) and are separated by low density CO stained septae (Ma and Woolsey, 1984; Ma, 1991). The trigeminal nuclei are innervated by the infraorbital branch of the trigeminal nerve (ION) (Dorfl, 1982; 1985). The primary afferents of the trigeminal nerve innervate the barrelette hollows (Ma and Woolsey, 1984; Ma, 1991) relaying information from the vibrissae, common fur and the skin via the infraorbital nerve (Jacquin and Rhoades, 1983) with up to 75% of the axons being slowly adapting (Zucker and Welker, 1969; Lichtenstein et al., 1990). Barrelettes may integrate and relay sensory information whilst still maintaining the topographic map (Ma, 1991).

As a general rule, within the brainstem trigeminal nuclei smaller cell bodies tend to have more confined dendritic trees and are in turn associated with smaller vibrissal receptive fields e.g. a single whisker (Renehan et al., 1986; Jacquin et al., 1988a; 1988b; Bennett-Clarke et al., 1992).

### **3.2 Subnucleus Principalis (PrV)**

The PrV is innervated by the maxillary branch of the ION (Bates et al., 1982) and provides the main topographically arranged vibrissal somatosensory input to the ventrobasal thalamus (Shipley, 1974; Jacquin et al., 1988b).

Parvalbumin staining, often generally associated with an increased cellular activity (including increased cytochrome oxidase activity and increased 14C-2-deoxyglucose uptake) (Braun et al., 1985; Karmy et al., 1991). Within PrV parvalbumin immunoreactivity is associated with single whisker receptive fields (RF) trigeminothalamic neurons (Renehan et al., 1986; Jacquin et al., 1988a; 1989b; Bennett-Clarke et al., 1992). Inputs from higher brain centres (via reciprocal connections) affect the character of the receptive field in PrV rather than its size. Inputs from SpVi and SpVc also serve to modulate responses within PrV (Doherty et al., 1992).

### **3.3 Subnucleus Interpolaris (SpVi)**

The SpVi neurons can be divided into two groups: the (majority) local circuit (LC) neurons and the projection neurons (Jacquin et al., 1989b). The local circuit arrangement corresponds with primary afferent inputs (Jacquin et al., 1989b) and parvalbumin staining (Bennett-Clarke et al., 1992) and are likely to be GABAergic (Celio, 1990).

There are two classes of projection neurons present: the calbindin positive trigeminothalamic (Bennett-Clarke et al., 1992) and the trigeminocerebellar neurons (Jacquin et al., 1989a). The majority of the vibrissal projection neurons have multi-vibrissal receptive fields (Jacquin et al., 1986; Gibson, 1987; Bennett-Clarke et al.,

1992) which may arise from the extensive dendritic trees crossing the CO boundaries (Ma, 1991). The projection neurons are also topographically arranged with respect to the primary afferent inputs (Jacquin and Rhoades, 1983; Jacquin et al., 1986; Bennett-Clarke et al., 1992).

### **3.4 Subnucleus Caudalis (SpVc)**

Caudalis is also referred to as the Medullary Dorsal Horn (MDH) and projects somatotopically to the ventrobasal thalamus (Belford and Killackey, 1979a). The deep vibrissal nerves innervate calbindin positive layers II, IV and VI whereas the superficial nerves innervate parvalbumin positive layers I-III (Renehan et al., 1986; Jacquin et al., 1986; Arvidsson and Rice, 1991; Bennett-Clarke et al., 1992).

This lighter parvalbumin staining in layers III/IV is associated with the vibrissal sensitive trigeminothalamic projection neurons (Bennett-Clarke et al., 1992; Renehan et al., 1986; Jacquin et al., 1989b). Intratrigeminal neurons of caudalis innervate interpolaris and oralis (Jacquin et al., 1990). Both the vibrissal and guard hair primary afferents terminate in layers III and V (Renehan et al., 1986) with the non-vibrissal afferents being more widespread than the vibrissal ones (Jacquin et al., 1986). The excitatory connections between the vibrissal axon collaterals in caudalis may produce the multi-vibrissal receptive fields (Renehan et al., 1986).

### **3.5 Subnucleus Oralis (SpVo)**

The majority of neurons are single whisker receptive field local circuit neurons (Jacquin and Rhoades, 1987). Parvalbumin positive neurons are the smallest neurons and the calbindin positive neurons represent the multi-vibrissal receptive field trigeminothalamic neurons (Jacquin and Rhoades, 1987; Bennett-Clarke et al., 1992).

Thus oralis, with its predominant collection of single whisker receptive field local circuit neurons, may be concerned with the detection and response to weaker vibrissal stimuli (Gibson, 1987).

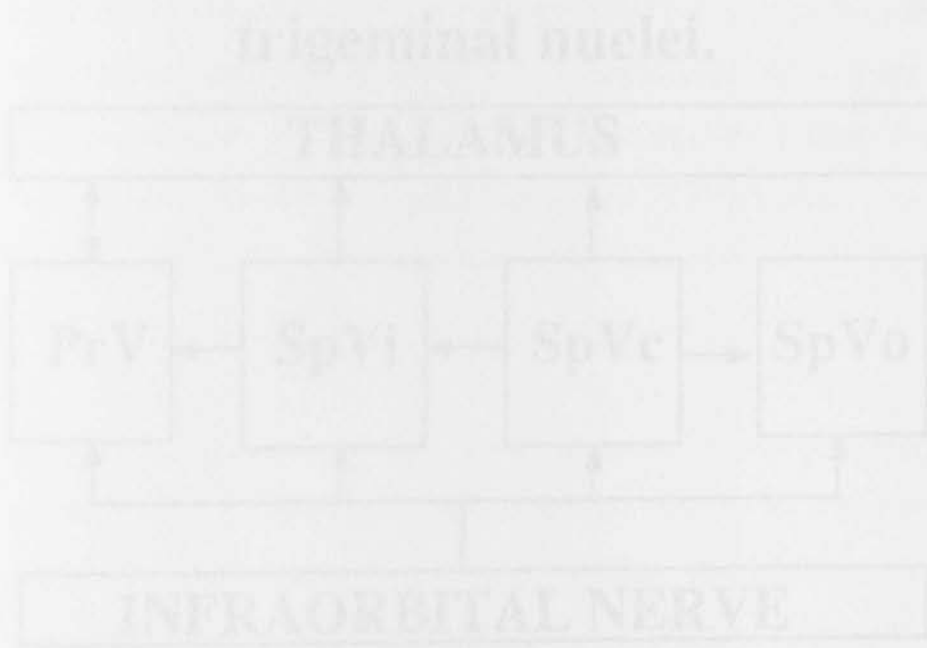


Figure 4. A simple schematic diagram illustrating the trigeminothalamic and trigeminothalamic connections.

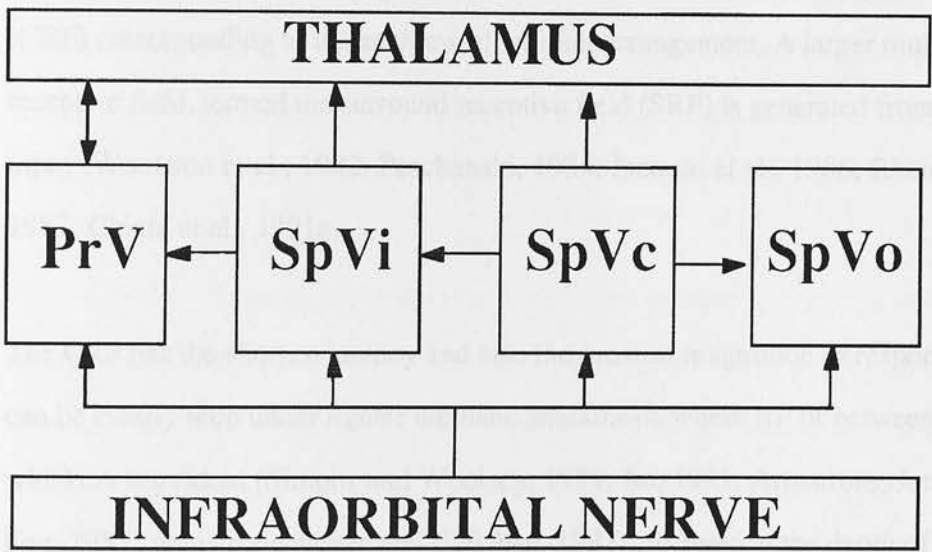
## 4.0 THALAMIC INTRODUCTION

### 4.1 VentrOPosteriorMedial Thalamic nucleus (VPM)

Thalamically arranged clusters of CO rich sensory neural lamellae (VPM) (Vielicki

and Lee, 1975; Land and Kornhuber, 1975) are innervated by the trigeminal ganglion. This ganglion is the peripheral receptive field

## trigeminal nuclei.



innervation, especially nuclei in single whisker receptive fields (Amaral, Jones and Culbert, 1991). The sensory receptive fields in VPM with their longer lamellae are most likely to arise from multi-whisker receptive fields within the trigeminothalamic nucleus (Chagan et al., 1986) and provide direct cortical inputs (Chodzko et al., 1989). The subthalamic connections between VPM and VPM (Wain, 1970)

### 4.2 VentrOPosteriorMedial Thalamic Nucleus

Within VPM all vibrissa receptive areas are confined to the (CO rich) lamellae (Wain, 1970). There are no inhibitory interneurons within VPM (Sjostrom and

Figure 4. A simple schematic diagram illustrating the trigeminothalamic and trigeminothalamic connections.

## **4.0 THALAMIC INTRODUCTION**

### **4.1 VentroPosteriomedial thalamic nucleus (VPm)**

Topographically arranged clusters of CO rich staining termed barreloids (Van der Loos, 1976; Land and Simons, 1985) are innervated in a 1:1 manner by the trigeminal barrelettes (Ma and Woolsey, 1984; Ma, 1991) producing a centre receptive field (CRF) corresponding to the anatomical whisker arrangement. A larger multi whisker receptive field, termed the surround receptive field (SRF) is generated from the SpVi input (Woolston et al., 1982; Peschanski, 1984; Jacquin et al., 1986; Rhoades et al., 1987; Chiaia et al., 1991a).

The CRF has the shortest latency and also the greatest magnitude of response. SRF can be clearly seen under lighter urethane anaesthesia where RF of between 3-5 whiskers is evident (Simons and Woolsey, 1979; Ito, 1981; Armstrong-James and Fox, 1987; Armstrong-James and Callahan, 1991). Increasing the depth of anaesthesia, eventually results in single whisker receptive fields (Armstrong-James and Callahan, 1991). The surround receptive fields in VPm with their longer latencies are most likely to arise from multi-vibrissal receptive fields within the trigeminothalamic neurons (Jacquin et al., 1986) and possibly from cortical inputs (Chmielowska et al., 1989). The whisker representation occupies between 1/3 and 1/2 of total VPm (Waite, 1973).

### **4.2 VentroPosteriomedial Thalamic Neurons**

Within VPm all vibrissae sensitive neurons are confined to the (CO rich) barreloids with the areas in between barreloids occupied by fibres of passage (Land and Simons, 1985; Harris, 1986). There are no inhibitory interneurons within VPm (Saporta and

Kruger, 1977; McAllister and Wells, 1981; Barbaresi et al., 1986; Harris, 1986; Williams and Faull, 1987). Inhibitory mechanisms are thought to be generated through an input from the reciprocal connections with the reticular nucleus via thalamocortical axons en route to cortex (Peschanski, 1984; Barbaresi et al., 1986; Harris, 1987; De Biasi et al., 1988). Within VPM there is no distinction between the rapidly or slowly adapting relay cells (Peschanski, 1984; Harris, 1987). Vibrissal neurons within VPM respond best to light mechanical whisker stimulations (Waite, 1973; Gonzalez and Sharp, 1985; Harris, 1986; Rhoades et al., 1987; Simons and Carvell, 1989; Armstrong-James and Callahan, 1991; Chiaia et al., 1991b; Diamond et al., 1992a; 1992b).

Neurons within VPM do not respond to maintained whisker displacements and large static displacements reduce or abolish the response (small static displacements fail to produce a response). The most common response to stimulation is a rapidly adapting short latency response with as many as two thirds of VPM neurons showing some directional sensitivity (Waite, 1973). There are two response groups to be found within VPM (Ito, 1988). Sustained neurons have short latencies, small RF's, depend upon stimulus amplitude rather than velocity and represent the small rostral whiskers. They also possess lower threshold velocities and higher directional sensitivity (i.e. they are slowly adapting) unlike the rapidly adapting transient cells. The excitatory responses within VPM are generated through NMDA and non-NMDA receptors. The early component of the response in VPM neurons is mediated via non-NMDA receptors whereas the later phase is mediated via NMDA receptors (Salt, 1987). The later NMDA phase is dependent upon the presence of the non-NMDA response (Salt and Eaton, 1989).

### 4.3 Thalamocortical and Corticothalamic Connections

The cytoarchitectural layers comprising the layers IV and lower layers V and VI terminate in the vibrissal region of primary somatosensory cortex. The corresponding VPm thalamic afferents, with secondary and tertiary afferents, terminate in layers II, III, IV, Va, Vb, and VI (Diamond et al., 1975; Killackey et al., 1976; Diamond and Mountcastle, 1980; Hock and White, 1981; White et al., 1982; Mountcastle and Washburn, 1987; Mountcastle and Killackey, 1987; Sanjak et al., 1989; Constantinidis et al., 1990; Mountcastle et al., 1990; Mountcastle and Washburn, 1990; Mountcastle et al., 1991; Mountcastle et al., 1992; Mountcastle et al., 1993; Mountcastle et al., 1994; Mountcastle et al., 1995; Mountcastle et al., 1996; Mountcastle et al., 1997; Mountcastle et al., 1998; Mountcastle et al., 1999; Mountcastle et al., 2000; Mountcastle et al., 2001; Mountcastle et al., 2002; Mountcastle et al., 2003; Mountcastle et al., 2004; Mountcastle et al., 2005; Mountcastle et al., 2006; Mountcastle et al., 2007; Mountcastle et al., 2008; Mountcastle et al., 2009; Mountcastle et al., 2010; Mountcastle et al., 2011; Mountcastle et al., 2012; Mountcastle et al., 2013; Mountcastle et al., 2014; Mountcastle et al., 2015; Mountcastle et al., 2016; Mountcastle et al., 2017; Mountcastle et al., 2018; Mountcastle et al., 2019; Mountcastle et al., 2020; Mountcastle et al., 2021; Mountcastle et al., 2022; Mountcastle et al., 2023; Mountcastle et al., 2024; Mountcastle et al., 2025).

## VPm INPUT TO CORTEX.

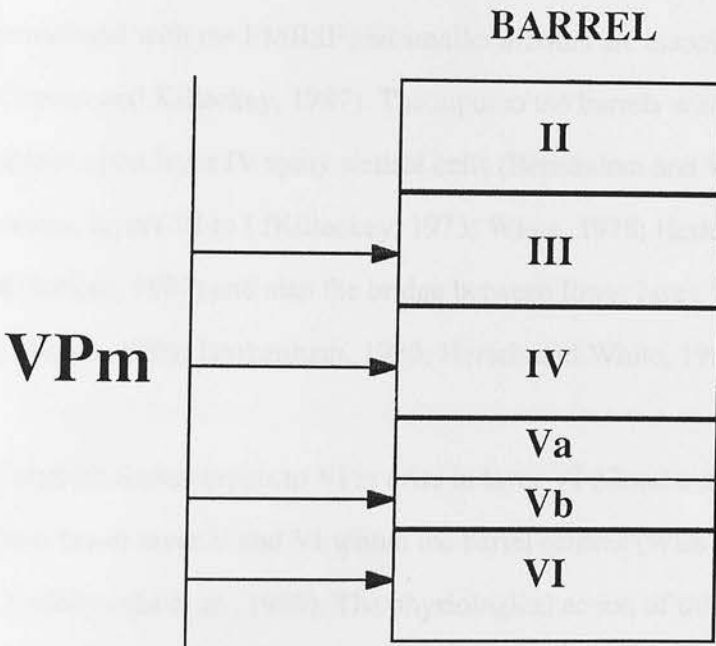


Figure 5. A cartoon highlighting the VentroPosteriomedial thalamic nucleus input to the vibrissal region of primary somatosensory cortex.

### 4.3 Thalamocortical and Corticothalamic Connections

Thalamocortical axons innervating the layer IV and lower layer III of the barrels of SI arise from the corresponding VPM barreloids (Killackey, 1973; Killackey and Leshin, 1975; Donaldson et al., 1975; Killackey et al., 1976; White and Rock, 1979; Herkenham, 1980; Hersch and White, 1981b; White et al., 1984; Bernardo and Woolsey, 1987; Jenson and Killackey, 1987; Koralek et al., 1988; Chmielowska et al., 1989; Armstrong-James and Callahan, 1991; Fabri and Burton, 1991; Agmon and Connors, 1991; 1992; Lu and Lin, 1993; Staiger et al., 1996). Larger arbours are associated with the PMBSF and smaller arbours are associated with the anterior field (Jensen and Killackey, 1987). The input to the barrels within cortex is mainly to the spines upon layer IV spiny stellate cells (Benshalom and White, 1986) and, to a lesser extent, layers III to I (Killackey, 1973; White, 1978; Herkenham, 1980; Jensen and Killackey, 1987) and also the bridge between lower layer V and VI (Agmon and Connors, 1991; Herkenham, 1980; Hersch and White, 1981a; 1981b; White, 1978).

Corticothalamic inputs to VPM arise in layer VI (Good and Killackey, 1992) and also from lower layer V and VI within the barrel centres (Wise and Jones, 1978; Chmielowska et al., 1989). The physiological action of this input is minimal and abolition merely results in more vigorous VPM responses to whisker deflection perhaps with slightly increased latencies (Diamond et al., 1992b). The cortical innervation to the VPM is not a strict 1:1 barrel to barreloid. The barrels innervate an arc of barreliods rather than individual barreliods (Hoogland et al., 1987; Chmielowska et al., 1989). The role of VPM neurons with their restricted RF's may be to encode stimulus locality and magnitude (Chiaia et al., 1991b).

#### **4.4 Posteromedial Thalamic Nucleus (POm)**

#### **4.5 Trigeminal Inputs to POm**

The POm receives a topographic input from the brainstem trigeminal nuclei (Chiaia et al., 1991a; Williams et al., 1993). The receptive field sizes within POm are larger than those seen within VPm (approximately 5 whiskers) but do not contain a CRF (Diamond et al., 1992a). The neuronal population is more heterogeneous than that seen in VPm. The multivibrissal inputs are generated from the single whisker inputs from the PrV (Lu and Lin, 1993).

#### **4.6 Thalamocortical and Corticothalamic Connections**

The POm appears to innervate the septa in SI (White and DeAmicis, 1977; Lin et al., 1987; Koralek et al., 1988; Nothias et al., 1988; Chmielowska et al., 1989; Fabri and Burton, 1991; Lu and Lin, 1993). The innervation also includes input to upper layer V and layer I of the barrel area (Lu and Lin, 1993). The septa area itself is relatively cell sparse compared to the barrels (Woolsey and Van der Loos, 1970; Welker and Woolsey, 1974) and also receives callosal inputs (Olavarria et al., 1984).

The corticothalamic input to POm is much larger than either the POm input to cortex or the trigeminothalamic input to POm (Hoogland et al., 1987; Welker et al., 1988; Fabri and Burton, 1991; Chiaia et al., 1991a; Diamond et al., 1992b) and may be entirely dependant upon an intact cortex (Armstrong-James, 1995). The POm innervates SII and motor cortex (Carvell and Simons, 1987). POm neurons themselves are more responsive to brush stroking of the whisker field rather than individual whisker displacement and are associated with active vibrissal movements after electrical stimulation of the ipsilateral motor cortex (Sharp and Evans, 1982). Thus it appears

that with their different cortical innervation patterns and physiological characteristics POm and VPm neurons have different roles in the processing, interpretation, and relay of vibrissal information to SI.

### POm input to barrel cortex.



Figure 6. A cartoon showing the POm inputs to the vibrissal region of primary somatosensory cortex. Note how these inputs mirror those of the VPm (see Figure 3).

## POm input to barrel cortex.

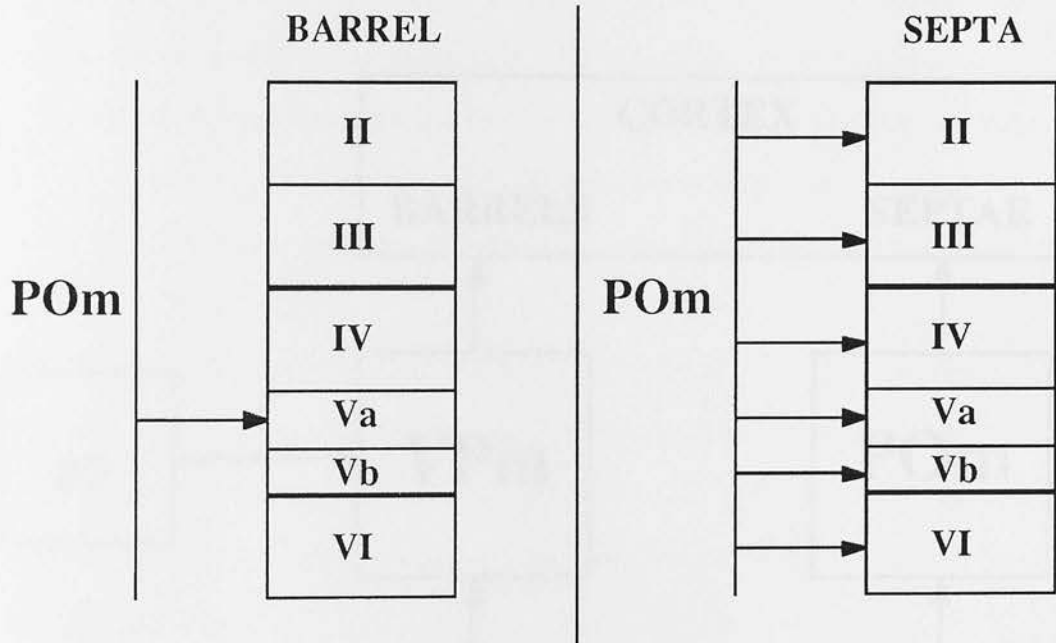


Figure 6. A cartoon showing the POm inputs to the vibrissal region of primary somatosensory cortex. Note how these inputs mirror those of the VPm (seen in Figure 5)

## 5.0 PRIMARY SOMATOSENSORY CORTEX

### 5.1 Thalamic Inputs

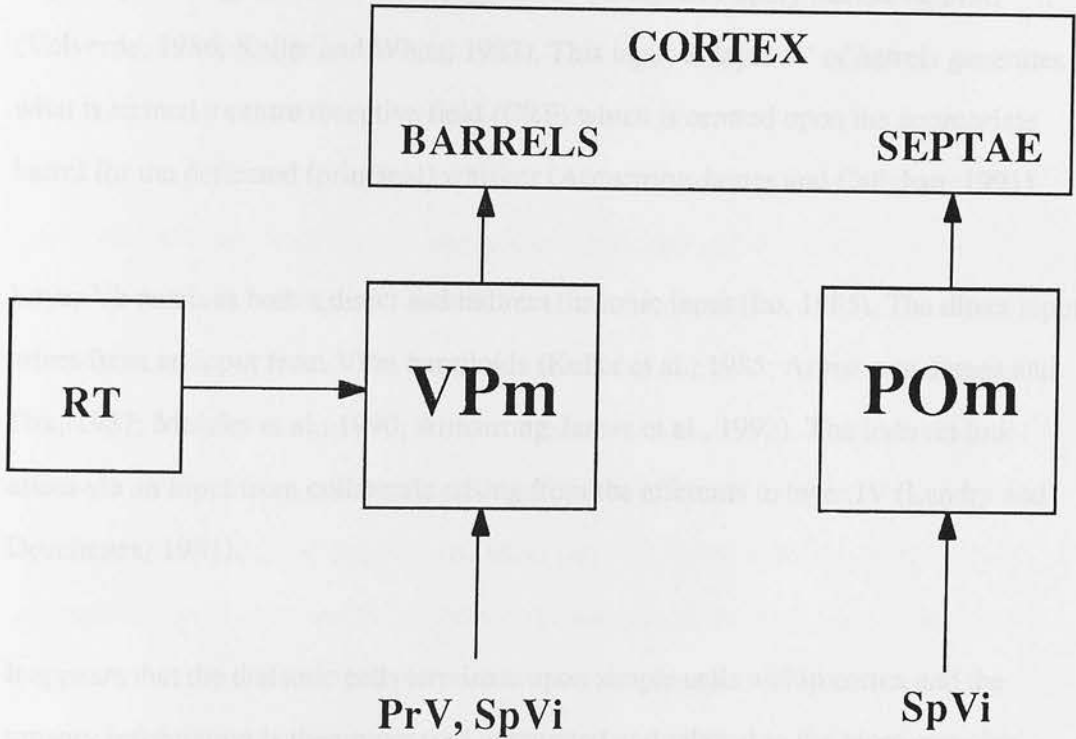


Figure 7. A schematic diagram summarising the inputs of the ascending somatosensory system.

## **5.0 PRIMARY SOMATOSENSORY CORTEX**

### **5.1 Thalamic Inputs**

The thalamic input to the vibrissal region of SI terminates within all cortical layers (except layer Va which receives an input from POm (Koralek et al., 1988) with the major input being onto the dendritic spines of the layer IV spiny stellate neurons (Valverde, 1986; Keller and White, 1987). This input to layer IV of barrels generates what is termed a centre receptive field (CRF) which is centred upon the appropriate barrel for the deflected (principal) whisker (Armstrong-James and Callahan, 1991).

Layer Vb receives both a direct and indirect thalamic input (Ito, 1985). The direct input arises from an input from VPM barreloids (Keller et al., 1985; Armstrong-James and Fox, 1987; Mercier et al., 1990; Armstrong-James et al., 1992). The indirect link arises via an input from collaterals arising from the afferents to layer IV (Landry and Deschenes, 1981).

It appears that the thalamic cells terminate upon simple cells within cortex and the sensory information is then processed, integrated and relayed to the more complex neurons of cortex (White et al., 1984). The VPM input to cortex is always excitatory and any inhibitory responses are generated within cortex (Carvell and Simons, 1988).

### **5.2 General Cortical Introduction**

The lamination pattern within the vibrissal region (and in SI in general) is distinct from other cortical regions. The barrels appear, in coronal sections, as a cell dense cytochrome oxidase rich cell layer. This staining is concentrated within the barrels. The septal regions (dysgranular regions) between the barrels are less cell dense and are

not as rich with the enzyme cytochrome oxidase. The barrels are the most cell dense and cytochrome oxidase rich areas within cortex. The richness of layer IV clearly contrasts with the relatively cell sparse and cytochrome oxidase poor layer Va beneath. The cytochrome oxidase staining and cell density increase again within layers Vb and VI. Lower layer III possesses the same characteristics as layer IV with layer II being slightly less cell dense and less cytochrome oxidase rich.

The cortical areas lying directly above and below a cortical barrel make up an anatomical cortical column. A functional column however is slightly larger than an anatomical one (Chmielowska et al., 1986a). Descriptions of activation patterns are made with reference to principal and adjacent whiskers and centre and surround receptive fields. A principal whisker (PW) is the facial whisker that corresponds anatomically and physiologically with a cortical barrel. Upon deflection this produces the strongest inhibitory and excitatory responses seen within the corresponding barrel (Simons, 1985). The centre receptive field (CRF) is generated from the direct thalamic input from the equivalent thalamic barreliod and roughly coincides with the corresponding cortical barrel. The surround receptive field (SRF) is generated via intracortical relay of PW sensory information across neighbouring barrels (Armstrong-James and Fox, 1987; Welker et al., 1988; Simons and Carvell, 1989; Agmon and Connors, 1992; Armstrong-James et al., 1992). Receptive fields within cortex vary although generally those corresponding to whiskers within the centre of the whisker set appear to be more symmetrical than those on the edges (Diamond et al., 1993; Armstrong-James, 1995). Full descriptions of CRF and SRF properties will be dealt with in separate sections.

The deflection of a PW will produce a stronger excitatory and inhibitory response within a barrel than the deflection of adjacent whiskers (Simons, 1985).

Cortical activity within the rat barrelfield is not uniform. The activity declines from the anteriomedial to posteriolateral in the barrel field (Simons and Carvell, 1989; McCasland et al., 1991). There is a relay of information from the less active to the more active barrels (those in the anterior of the field are more active than those in the more posterior aspect of the field (Durham and Woolsey, 1985; McCasland and Woolsey, 1988; Simons and Carvell, 1989; Bernardo et al., 1990a; McCasland et al., 1991; Weiss and Keller, 1994).

The role of the barrel cortex in sensory processing appears to be, by active whisking, to produce a refined map within cortex of the object being actively palpated. This is aided by the whisking frequency and the set length and curvature of the whiskers themselves (Simons, 1995). A barrel also contains more neurons than the corresponding barreloid and provides a very important initial stage of cortical processing. This information is then passed through the functional hierarchy of the cortex (Simons, 1978; Hutson and Masterton, 1986) for refinement, integration and co-ordination. This is achieved through receptive field properties, influences from other whisker deflections and the preferential relay pathways. All these stages occur prior to the activation of other cortical and subcortical targets.

### **5.3 Centre Receptive Fields (CRF)**

Central receptive fields are generated through a direct input from the corresponding barreliod onto the cortical barrel (Killackey and Leshin, 1975; Caviness, 1976; Durham and Woolsey, 1978; Kossut and Hand, 1984; Armstrong-James and Fox, 1987; McCasland and Woolsey, 1988; Armstrong-James and Callahan, 1991).

The CRF is initially confined to the corresponding vibrissal barrel by the morphology of the layer IV neurons which appear to have very poor horizontal connections

(Bernardo et al., 1990a; 1990b). The neurons within layer IV and lower III (where the RFs are smaller than in layer IVb (Welker and Woolsey, 1974; Simons and Woolsey, 1984; Chapin, 1986) are the spiny stellates (type I) and the GABAergic inhibitory interneurons (type II) (Simons and Woolsey, 1984; Benshalom and White, 1986). The majority of the stellate neurons (85%) have dendritic processes that are confined to their parent barrel and thus tend to respond to the deflection of a single whisker. Type II neurons are the non-spiny multiform and bipolar cells (Simons and Woolsey, 1984) and are possibly GABAergic interneurons (White, 1978; White and Rock, 1981; White et al., 1984; Lin et al., 1985; Chmielowska et al., 1986b; 1988; Keller and White, 1986; 1987). The smooth cells are more concentrated within layers III and deep layer IV (Simons and Woolsey, 1984). Thus the input into lower layer III and IV is initially onto the least complex cortical cells before being relayed to more complex ones.

Upon principal whisker deflection layers IV and Vb are activated first (Ito, 1985; Armstrong-James et al., 1992) and there is an initial excitation followed by a period of inhibition (Simons, 1995). The information is then relayed from layer IV to layers II and III and towards the pia within the same column (Burkhalter, 1989; Armstrong-James et al., 1992). The layer IV neurons appear to be more dependent upon stimulus amplitudes and sometimes show a sustained response to whisker deflection. The relay from layer IV to layer Vb appears to convey directionally sensitive information (Ito, 1985).

Layer Va is generally activated after the radial relay to the pia via a reciprocal connection with layers II and III (Ryugo et al., 1975; Ackers and Killackey, 1978; Valverde, 1986; Chapin et al., 1987; Fonesca et al., 1988; Bernardo et al., 1990a; 1990b; Armstrong-James et al., 1992). It appears that within a barrel there is a flow of sensory information from the supra to infragranular layers (Di et al., 1990). Layer Va

does not appear to obey the columnar arrangement observed to varying degrees in the other cortical layers (McCasland and Woolsey, 1988; Armstrong-James et al., 1992). This is reflected in the fact that there is no difference in the response latencies between principal and adjacent whiskers in layer Va. In other cortical layers the PW elicits a shorter latency response to the deflection of the principal whisker compared to adjacent whiskers (Armstrong-James et al., 1992). Unlike other cortical layers layer Va neurons do not vary in their magnitude of response seen between principal and adjacent whiskers (Armstrong-James et al., 1992).

Responses to PW deflection can be altered by deflection of adjacent whiskers prior to the deflection of PW. Even where the response to adjacent whisker stimulation is weak there is a suppression of the response to principal whisker deflection (Simons, 1985; 1995; Simons and Carvell, 1989; Armstrong-James et al., 1992) with the greatest effects seen in layer IV and the smallest in the infragranular layers (McCasland et al., 1991). Thus barrels may influence responses within other barrels and cortical layers (Simons, 1995).

Centre receptive fields are smallest within lower layer III and layer IV. The CRFs in these layers are characterised by sharp drop-off in response at the edges of the RF and are typically more circular (especially within the centre of the barrel field. The RFs within the infragranular layers (e.g. layer V) can be 2-3 times those observed within layer IV (Chapin, 1986).

#### **5.4 Surround Receptive Fields (SRF)**

The surround receptive fields are generated through intracortical relay mechanisms incorporating both near and far adjacent whisker barrel territory (Armstrong-James and Fox, 1987; Bernardo et al., 1990a; 1990b; Armstrong-James et al., 1991; Armstrong-

James and Callahan, 1991) and are generally weaker than CRFs (Armstrong-James et al., 1992). They do not appear to arise from multi vibrissal inputs from their afferent input (from VPM) as they do in the thalamus (Armstrong-James et al., 1991). As a result they have longer latencies and lower response magnitudes than the CRFs (Armstrong-James et al., 1991, Armstrong-James and Callahan, 1991). The horizontal relay occurs primarily in the adjacent septae before relay to the immediately adjacent barrel centres (Armstrong-James et al., 1992).

Within the SRF there is almost a reversal of the activation pattern observed within the CRF i.e. layer Va is activated initially although there is no significant difference in the latencies between principal and adjacent barrels. This horizontal spread of activity only occurs after the relay though the principal barrel is complete. The relay to adjacent barrels occurs approximately 13 mS post-stimulus and the spread to approximately 6-8 barrels occurs more than 20 mS post-stimulus (Armstrong-James et al., 1992).

After the activation of layer IV there is an activation of layers II/III through the reciprocal connections (Burkhalter, 1989; Bernardo et al., 1990a; 1990b; Armstrong-James et al., 1992) and subsequently layer IV (Armstrong-James et al., 1992). Far neighbour barrel activation occurs 12-14 mS after CRF generation (Armstrong-James et al., 1992). The layer VI activation within barrel cortex generally falls outside the columnar organisation and is activated at a time when SRFs are generated (Armstrong-James et al., 1992).

The spread of activation within the SRF is not generally symmetrical and is most likely to expand across barrels in the same row rather than across an arc (Simons, 1978; Simons and Woolsey, 1979; 1984; Chapin, 1986; Chmielowska et al., 1986a; Armstrong-James and Fox, 1987; Bernardo et al., 1990a; 1990b; Fabri and Burton, 1991; Armstrong-James et al., 1992; McCasland et al., 1992; Simons et al., 1992;

Diamond et al., 1993; Welker et al., 1993). These asymmetric RFs are more commonly found in deeper cortical layers (between 1000-1200  $\mu\text{m}$ ) and are most likely to mirror the movement path of an object across the vibrissal field (Simons, 1985). Overlapping SRFs seen in SI may also play a role in processing inputs from adjacent arcs in the field, may be important in modifications in light of sensory experiences and may show preferential relay patterns for the processing of sensory information (McCasland et al., 1991). Thus a preferential relay mechanism is present to ensure rapid activation of the relevant neuronal populations. The asymmetric RFs are also associated with neuronal groups displaying angular preferences to whisker displacement (Simons, 1985). The spread of activity within rows ensures that there is a weak activation of a barrel by an adjacent whisker prior to PW deflection and ensures that the response to PW deflection is elicited (Armstrong-James, 1995). The shape and size of RFs within cortex are influenced by early sensory experiences (McCasland et al., 1992; Diamond et al., 1993). Sensory experience also dictates the strength of the cortical connections (McCasland and Woolsey, 1988) through establishing preferential relay routes through cortex. Intracortical connections do not develop fully until after the barrel pattern is evident and is strictly dependent upon the presence of an intact periphery (McCasland et al., 1992). SRF sizes within the cortex vary from the small SRFs seen within supragranular layers (1.5 whiskers) and the moderately large one in the granular layers (2.6 whiskers) to the large weak SRFs seen in the infragranular layers (3.5 whiskers) (Armstrong-James and Fox, 1987). The multi whisker RFs are largest within the infragranular cell layers (Simons, 1985; Armstrong-James et al., 1992) and tend to be associated with the more complex stages of cortical processing and integration (White, 1978).

Increasing the depth of anaesthesia tends to decrease SRF size until they are eliminated altogether and in deep anaesthesia CRFs may also be affected (Armstrong-James and George, 1988; Armstrong-James and Callahan, 1991).

Anaesthesia, through its NMDA effects, alters the bursting behaviour of cortical neurons (Armstrong-James and Fox, 1984; Simons et al., 1992). Increasing the depth of anaesthetic results in a decrease in bursting and an increase in the inter burst period (i.e. there is a decrease in neuronal firing). With light urethane anaesthesia (resembling slow wave sleep) there is a synchronisation of activity throughout the cortex (Armstrong-James and Fox, 1984). Whilst urethane affects RF size it has little effect upon the other properties of the RF e.g. angular preferences (Simons et al., 1992). Urethane may also be responsible for uncovering horizontal connections within cortex (Simons et al., 1992; Simons, 1995) and receptive fields under chloralose are larger than those seen in either urethane or barbiturate anaesthesia (Harding et al., 1979).



Figure 4. A schematic diagram outlining the activation of a PW neuron (generating a CCF) and the activation of adjacent columns (classified as ACF).

## 5.3 Connection With Other Cortical Areas

The cytoarchitectural regions projecting both ipsilaterally and contralaterally appear to be primarily pyramidal cortex (White and Purcell, 1981; Carroll and Slomovitz, 1987; Elman and White, 1990). The distal end of primary somatosensory cortex projects both ipsilaterally and contralaterally to the cerebral neocortex. SI is ipsilaterally connected with ipsilateral SI (Winer and DeArchi, 1977; Carroll and Slomovitz, 1987), but also with contralateral SI (Winer and DeArchi, 1977; Carroll and Slomovitz, 1987; Elman and White, 1990). SI also projects to contralateral SI (Winer and DeArchi, 1977; Carroll and Slomovitz, 1987; Elman and White, 1990). SI also projects to contralateral SI (Winer and DeArchi, 1977; Carroll and Slomovitz, 1987; Elman and White, 1990).

# ACTIVATION OF CORTICAL COLUMNS.

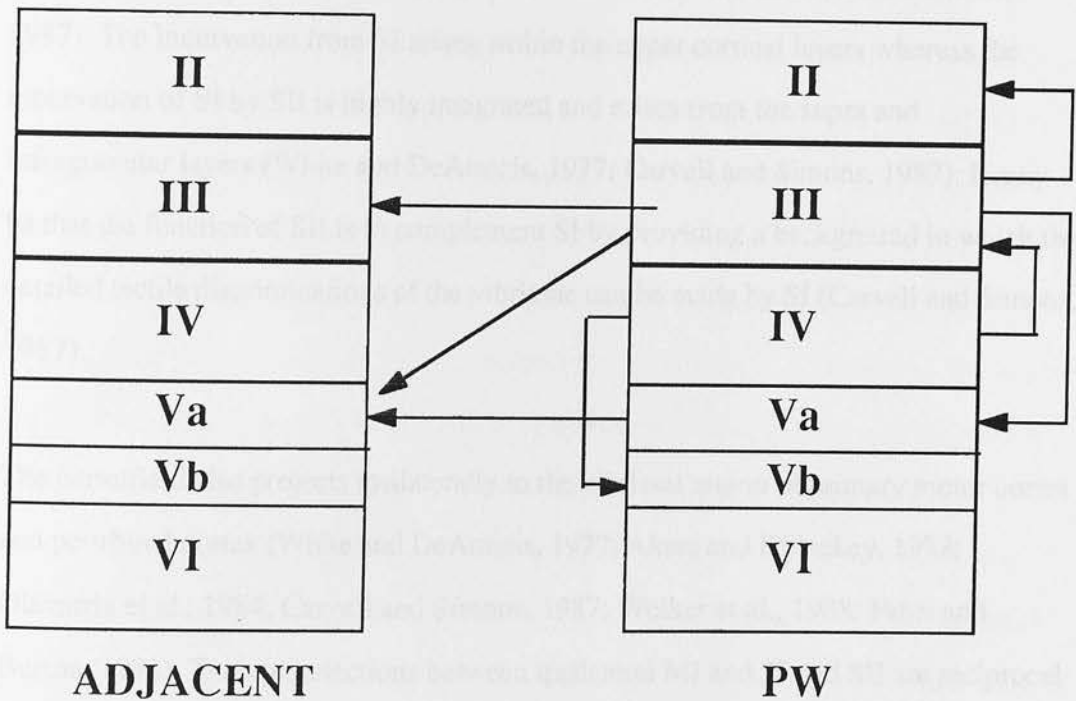


Figure 8. A schematic diagram outlining the activation of a PW barrel (generating a CRF) and the activation of adjacent columns (generating an SRF)

## 5.5 Connection With Other Cortical Areas

The corticocortical neurons projecting both ipsilaterally and contralaterally appear to be primarily pyramidal in shape (White and Hersch, 1981; Carvell and Simons, 1987; Elhanany and White, 1990). The vibrissal region of primary somatosensory cortex projects both ipsilaterally and contralaterally to other cortical regions. SI is reciprocally connected with ipsilateral SII (White and DeAmicis, 1977; Carvell and Simons, 1987). Intralaminar connections with SII are different from those seen in SI barrels (Bernardo et al., 1990a; 1990b). SII receives a greater input from the POm than VPM and has larger RFs than SI and a greater proportion of bilateral RFs (Carvell and Simons, 1987). The innervation from SI arises within the upper cortical layers whereas the innervation of SI by SII is highly integrated and arises from the supra and infragranular layers (White and DeAmicis, 1977; Carvell and Simons, 1987). It may be that the function of SII is to complement SI by providing a background in which the detailed tactile discriminations of the vibrissae can be made by SI (Carvell and Simons, 1987).

The barrelfield also projects ipsilaterally to the vibrissal region of primary motor cortex and perirhinal cortex (White and DeAmicis, 1977; Akers and Killackey, 1978; Olavarria et al., 1984; Carvell and Simons, 1987; Welker et al., 1988; Fabri and Burton, 1991). These connections between ipsilateral MI and SI and SII are reciprocal (White and DeAmicis, 1977; Porter and White, 1983; Carvell and Simons, 1987; Fabri and Burton, 1991; Porter and Izraeli, 1992; Miyashita et al., 1994). The ipsilateral connections arise from layers III and V in barrel SI (White and DeAmicis, 1977; Carvell and Simons, 1987; Elhanany and White, 1990; Miyashita et al., 1994) i.e. there is a projection from the supra and infragranular layers. The neurons projecting to motor cortex also appear to have extensive axon collaterals within layers III and V in barrel cortex (Elhanany and White, 1990) and many of the superficial projection

neurons have dendrites within layer IV (White and Hersch, 1981). The motor cortex barrel SI inputs to layers II/III and V of barrel cortex (White and Hersch, 1981; Porter and White, 1983). The motor cortex is also reciprocally connected with SII (Miyashita et al., 1994).

The vibrissal region of SI also projects to contralateral cortical areas (SI, SII and MI) (Wise and Jones, 1976; Ackers and Killackey, 1978; White and Hersch, 1981; Porter and White, 1983; Olavarria et al., 1984; Carvell and Simons, 1987; Chapin et al., 1987; Elhanany and White, 1990; Miyashita et al., 1994). The contralateral connections within SI are very rare and the connection is not extensive. The contralaterally projecting neurons arise in all cortical layers (but especially within layers III and V) (Wise and Jones, 1976; White and Hersch, 1981; Porter and White, 1983; Carvell and Simons, 1987; Chapin et al., 1987; Miyashita et al., 1994). The contralateral connection is a reciprocal one with the contralateral fibres terminating within deep layer III, superficial layer V and layer VI (Wise and Jones, 1976). The contralateral connection with SII is reciprocal and topographic (Carvell and Simons, 1987). The connection with contralateral SI terminate within vertical columns and is reciprocal (Wise and Jones, 1976) with the connections found within deep layer IV and V. Commisurally projecting neurones are more commonly located within layers III and V (Jacobson and Trojanowski, 1974) terminating within layers IV-VI (Cipolloni and Peters, 1979). The callosal fibres terminate within the dysgranular (septal) areas in a more widespread and less topographic arrangement than the ipsilateral connections (Ackers and Killackey, 1978; Olavarria et al., 1984; Welker et al., 1988). The efferent connections within barrel cortex arise from layer V neurons within barrel columns (Olavarria et al., 1984).

## 5.6 Subcortical Projection Targets

The vibrissal region of SI projects to various subcortical sites both ipsilaterally and contralaterally. Ipsilateral SI projects to the striatum (McGeorge and Faull, 1987; 1989; Mercier et al., 1990; Levesque et al., 1996), thalamus (Royce, 1983; Levesque et al., 1996; Pare and Smith, 1996) and brainstem (Mercier et al., 1990). Contralateral projections include thalamus (Caretta et al., 1996) and striatum (McGeorge and Faull, 1987; 1989; Berendse et al., 1992).

The corticothalamic input arises in lower layer V and upper layer VI (Jacobson and Trojanowski, 1975; Crandall et al., 1986; Chmielowska et al., 1989) and terminates across an arc of barreliods (Hoogland et al 1987; Welker et al., 1989). This is in contrast with the afferent thalamocortical input which is arranged in a 1 barreliod : 1 barrel arrangement (Van der Loos, 1976). Corticothalamic cells are mainly within the infragranular layers and have axon collaterals that project to and terminate within barrel centres (Hersch and White, 1981b; Hersch and White, 1982; White and Keller, 1987; Chmielowska et al., 1988). The apical dendrites of these neurons ascend through layer V with little or no branching and terminate within layer IV (Hersch and White, 1982; White and Keller, 1987; Chmielowska et al., 1989).

The corticostriatal pathway in general can be divided into two separate pathways (Cowan and Wilson, 1994). There is a corticostriatal pathway arising in the superficial layer V (Va) neurons (Mercier et al., 1990). There is also a pathway arising from fine axon collaterals from deeper layer V corticopontine neurons (Mercier et al., 1990; Cowan and Wilson, 1994).

The corticostriatal projection neurons are described as having thinner apical dendrites than the corticospinal or the corticopontine neurons and have apical dendrites that have

side branches within layer V and have terminal tufts through layers III-I (Hersch and White, 1982). The striatal input from the corticofugal neurons arises from a lateral axon collateral branch of the axon innervating the striatum as it passes through the striatal fibre bundles (Donoghue and Kitai, 1981).

The layer Va input to the striatum arises from the non-columnar layer Va pyramids to form a more slowly conducting input to the striatum than the corticofugal input. The layer Va input is also independent of the brainstem and spinal pathways and is less directly influenced by the specific sensory thalamus (due to the lack of thalamic input (Agmon and Connors, 1992) and is more likely to be influenced by cortical interactions and processing. The layer Vb input as well as being rapid is more likely to be under thalamic influences (due to its monosynaptic input from VPM) and also provides a parallel input to the brainstem and the spinal systems (Donoghue and Kitai, 1981).

As a general rule layer V pyramids provide the subcortical projecting neurons within cortex. The most superficial neurons project to the striatum, spinal cord neurons are the deepest in layer V and the cells projecting to the pons and medulla are situated throughout layer V. Corticotectal neurons are situated within superficial layer Vb in SI and SII and possess overlapping RFs. It appears that overlapping RFs are important in orientation of the animal with respect to its environment (Robinson, 1972; Schiller and Stryker, 1972; Stryker and Schiller, 1975).

## 6.0 PHYSIOLOGY AND MORPHOLOGY OF CORTICAL NEURONS

### 6.1 General Physiology and Morphology

The physiology and morphology in SI is similar to that described in motor and visual cortices (Gilbert and Wiesel, 1979; Wilson, 1987; Larkman and Mason, 1990; Larkman, 1991). Neurons are classed as either spiny pyramidal neurons and non-spiny or sparsely spiny non-pyramidal neurons. Spiny non-pyramidal neurons tend to be the spiny stellate cells of layer IV and the aspiny non-pyramidal neurons are the GABAergic interneurons. In general terms neuronal firing patterns of neocortical neurons can be divided into three main classes: Fast spiking (FS), Regular spiking (RS) and Intrinsically bursting (IB). RS and IB neurons are the spiny pyramidal cells (McCormick et al., 1985) and the FS neurons are the aspiny GABAergic interneurons (for a review see Connors and Gutnick, 1990).

The spiny neurons within SI comprise about 70-85% of the total cell population (DeFelipe and Farinas, 1992) and it is the spiny layer V pyramids that form the output neurons (Connors and Gutnick, 1990). It is the combination of the morphology and physiology of a neuron that will indicate the inputs it receives, how it processes the information and the output signal it generates. For example the in row preferences seen within the cortex are generated as a result of dendritic (and axon collateral) orientation (Bernardo et al., 1990b; Fabri and Burton, 1991; McCasland et al., 1992). The physiology of SI neurons and their interactions produce cycles of excitation and inhibition upon whisker deflection (Simons, 1995). The apical dendrites of the pyramidal neurons allow the cell to combine inputs from the more superficial cortical layers (Kim and Connors, 1993). The ion channels and receptors present within a cell membrane affect the firing pattern and to a certain extent the response properties of the

neuronal population. The apical dendrites of the layer V neurons are arranged in clusters as they ascend towards the pia (Peters and Walsh, 1972; Feldman and Peters, 1974; Patel-Viadya, 1985). The dendrite clusters as they ascend vertically are joined by the dendrites from the more superficial layers (White and Peters, 1993). Other morphological variations (seen within the RS and IB neurons) are assumed to provide at least subtle changes in the information received from the different cortical layers. Comparisons between the *in vivo* and *in vitro* recording systems are very rare (see Bindman et al., 1988). Other studies have stated that when aiming to study layer IV neurons the electrodes invariably impale the apical dendrites of layer V neurons (Kim and Connors, 1993). Although intracellular apical dendrite and basilar dendrite recordings can be identified (Pockberger, 1991) it is more reliable to reconstruct and identify the exact cell.

## 6.2 Spiny Stellate Cells

The neurons in layer IV relay information within the same parent barrel before the information is processed intracortically in other barrels (Bernardo et al., 1990a; 1990b; Armstrong-James et al., 1992). The neuronal response seen upon the deflection of principal and adjacent whiskers is quite distinctive in this cell class. PW deflection results in a short latency response in PW layer IV neurons as a result of the monosynaptic thalamocortical input (Armstrong-James et al., 1992).

## 6.3 Spiny Stellate Cell Morphology

Within SI the clusters of spiny stellate cells are co-localised with the cytochrome oxidase rich barrels (Woolsey and Van der Loos, 1970). This neuronal group can be divided further into the star pyramidal neurons and the spiny stellate cells (Simons and Woolsey, 1984). The spiny stellates are more commonly found in upper layer IV than

in lower layer IV (Welker and Woolsey, 1974; Simons and Woolsey, 1984). The neuronal morphology of the class I neurons reflects the small almost single barrel receptive fields seen in layer IV neurons. The dendrites of these neurons are most likely to be confined to its parent barrel (Harris and Woolsey, 1983; Simons and Woolsey, 1984). These dendrites are more likely to be orientated towards the centre of a barrel within layer IV (Woolsey et al., 1975; Harris and Woolsey, 1983; Greenhough and Chang, 1988). These neurons also have poorer horizontal connections than those of other cortical layers which may account for the small (almost single barrel) RFs (Bernardo et al., 1990a; 1990b). An equivalent columnar arrangement can be seen within visual cortex although the neuronal response is not as clearly correlated to a specific individual peripheral stimulus.

#### **6.4 Fast Spiking (FS) Neurons**

Fast spiking neurons are located within layers II-IV and VI especially layer IV i.e. layers receiving a monosynaptic input from VPM (Keller and White, 1986; 1987; Simons, 1978; Hersch and White, 1982; McCormick et al., 1985; Chmielowska et al., 1988b; Simons and Carvell, 1989; Agmon and Connors, 1992). The neurons themselves are GABAergic interneurons (Huettner and Baughman, 1988; Kawaguchi and Kubota, 1993). The direct thalamic input coupled with the repetitive high frequency non-adaptive firing patterns (McCormick et al., 1985; Chagnac-Amitai and Connors, 1989b; Simons and Carvell, 1989; Kawaguchi, 1993; Kawaguchi and Kubota, 1993) means that the FS neurons are able to provide a reliable relay of sensory information from their thalamic input to their targets within cortex (Connors and Gutnick, 1990). In spite of the various morphologies the physiology of these neurons is unique in cortex and neurons can easily be distinguished from those of IB or RS neurons (Simons, 1978; McCormick et al., 1985; Connors and Gutnick, 1990). They tend to have brief characteristic action potentials and deep but brief single

component after hyperpolarisations (McCormick et al., 1985) unlike IB neurons (Kawaguchi, 1993). They have more negative resting membrane potentials than either IB or RS neurons (Kawaguchi, 1993). These parvalbumin positive GABA neurons are also co-localised with the cytochrome oxidase rich barrel centres, sides and rarely in the septa (Chmielowska et al., 1986b; Celio, 1990; van Bredreode et al., 1990; McCasland and Hibbard, 1991). This may explain the restriction of the RFs in layer IV to the parent barrel if the excitatory neurons are intermingled with and restricted by GABAergic interneurons and may also function to suppress responses in neurons to subsequent whisker deflections (Simons, 1978; McCormick et al., 1985, Simons and Carvell, 1989). The distribution of calbindin complements that of parvalbumin in that it is co-localised in the pyramidal neurons of layers II-III and V-VI (van Brederode et al., 1991).

The FS neurons within layer IV are equivalent to the class II neurons described in the literature (Simons, 1978; White, 1978; White et al., 1984; White and Rock, 1981; Simons and Woolsey, 1984; Lin et al., 1985; Chmielowska et al., 1986b; 1989b; Keller and White, 1986; Simons and Carvell, 1989). They have thin axons that are directed towards the white matter and recurrent axon collaterals that are largely confined within the parent barrel (Harris and Woolsey, 1983). Dendritic field extension is more likely to occur in rows (Simons and Woolsey, 1984) and neurons are driven by ventral rather than dorsal rows (McCasland et al., 1991). As a rule the morphology is more varied than that seen in either RS or IB neurons but the one common feature is that they all have aspiny or sparsely spiny dendrites (McCormick et al., 1985; Naegele and Katz, 1990; Foehring et al., 1991).

Generally GABA decreases RF size and increases the angular tuning of excitatory neurons within cortex. The inhibition also functions to increase the signal to noise ratio

in the cortex and has a close link with RS neurons that appear to receive the bulk of GABAergic inputs in cortex.

## 6.5 Regular Spiking (RS) Neuronal Physiology

Regular spiking neurons are the most commonly recorded neuronal cell group within cortex (Mountcastle et al., 1969; Simons, 1978; Agmon and Connors, 1989) extending from layers II to VI (Oshima, 1969; Simons, 1978; Connors et al., 1982; Stafstrom et al., 1984; McCormick et al., 1985; Montoro et al., 1988; Agmon and Connors, 1989; Chagnac-Amitai and Connors, 1989a; Tseng and Prince, 1993; White et al., 1994; Franceschetti et al., 1995). The more superficial RS neurons receive a disynaptic thalamic input whereas the deeper ones receive a monosynaptic input from VPM (Agmon and Connors, 1992). Their most common response to a stimulus is to fire a single action potential (Amitai and Connors, 1995). They have relatively slow action potentials and do not show a tendency to burst (even with current injection) (McCormick et al., 1985; Connors and Gutnick, 1990; Franceschetti et al., 1995). The action potentials generated in RS neurons show a variety of afterpotentials (Calvin and Sypert, 1976; Connors et al., 1982; Lorenzon and Foehring, 1992). The firing rate of RS neurons is linked to the stimulus intensity. RS neurons also show adaptation of their spike frequency (Connors and Gutnick, 1990) and are sensitive to changes in the stimulus current and amplitude (Stafstrom et al., 1984). Responses in RS neurons are affected by adjacent whisker stimulation (Simons and Carvell, 1989). Caudally adjacent whiskers produce greater inhibition than rostrally deflected whiskers and likewise ventral whiskers produce greater inhibitory effects than dorsal ones (Brumberg et al., 1996). This may reduce the amount of 'unpreferred' information getting through the system and may increase the effectiveness of the PW information. They differ from their thalamic input neurons as they appear to have more focused excitatory centre receptive fields and stronger inhibitory surrounds but they are less

spontaneously active and show less vigorous PW on responses (Simons, 1995). Their response to strong and temporarily coherent thalamic inputs is more vigorous than their response to weaker and more widespread inputs (Simons, 1995). The group can be further divided into RS1 and RS2 neurons (Chagnac-Amitai and Connors, 1989a; Agmon and Connors, 1992). RS1 neurons appear to be the major class of neurons within cortex and RS2 neurons are preferentially located within the infragranular layer only (Chagnac-Amitai and Connors, 1989b; Agmon and Connors, 1992; van Brederode and Snyder, 1992). RS1 neurons can adapt to a strong stimulus by changing from a high firing rate to a much lower and more regular firing pattern within approximately 200 mS with a firing rate that rarely exceeds 50-100 Hz (Connors and Gutnick, 1990; Stafstrom et al., 1984). RS2 neurons however adapt to high stimulus intensities by stopping firing. Further depolarisation may result in the neurons firing in an irregular manor (Chaganc-Amitai and Connors, 1989a; 1989b; Amitai and Connors, 1995). RS1 neurons tend to be evenly distributed through the cortex whereas RS2 neurons tend to be concentrated within layer IV and V (Chagnac-Amitai and Connors, 1989b; Agmon and Connors, 1992; van Brederode and Snyder, 1992).

Some reports suggest that regular spiking neurons within cortex may be connected with the reticular thalamus and play a role in the control of sensory information through the thalamus (Pollard and Angel, 1990). The role of RS neurons may be important in accurate encoding of incoming thalamic information with a high degree of sensitivity (Franceschetti et al., 1995).

## **6.6 RS Neuronal Morphology**

RS neurons as a group tend to have the smaller soma of the pyramidal output neurons (28.1 +/- 5.3  $\mu\text{m}$ ) and are spherical in shape (Chagnac-Amitai and Connors, 1989b). Their apical dendrites can be clearly seen ascending from the soma towards the pial

surface terminating in a relatively sparse apical tree. The basilar dendrites appear to have a horizontal extension of approximately 400  $\mu\text{m}$  around the cell body. They have 2-8 axon collaterals that ascend vertically through the cortex terminating in either the supragranular layers or extending towards the pial matter (Chagnac-Amitai and Connors, 1989b; Chagnac-Amitai et al., 1990).

### **6.7 Intrinsic Bursting (IB) Neuronal Physiology**

Intrinsically bursting neurons have a distinct, unique firing pattern. In response to a stimulus IB neurons will typically fire a "high frequency cluster of action potentials" termed a burst. Bursts typically comprise 3-5 action potentials with decreasing spike amplitude seen within a burst (Connors et al., 1982; McCormick et al., 1985; Montoro et al., 1988; Agmon and Connors, 1989; Connors and Gutnick, 1990; Mason and Larkman, 1990; Tseng and Prince, 1993; Francshetti et al., 1995; Schwindt et al., 1997) with the response typical being stimulus dependant (Agmon and Connors, 1989). This bursting behaviour is most apparent with the injection of current (neither RS nor FS neurons fire bursts under these conditions) typically firing with a mean burst frequency of 9 Hz (Agmon and Connors, 1989) and generally within the range of 5-15 Hz (Agmon and Connors, 1989; Chagnac-Amitai et al., 1990; Silva et al., 1991a; Wang and McCormick, 1993; Flint and Connors, 1996). This frequency ties in with whisking frequencies of 8-12 Hz (Carvell and Simons, 1996). The action potentials within cortical bursts are essentially the same as those observed within RS neurons although they do appear to have a more prominent depolarising aspect to their afterpotentials (Amitai and Connors, 1995). The IB neurons also have a slightly lower spike amplitude than the RS neurons (Chagnac-Amitai et al., 1990). The IB neurons can either fire a mixture of cortical bursts or they can fire single action potentials similar to those described in RS neurons. They can switch between the two firing patterns as they mainly fire an initial burst followed by a train of single action

potentials (Connors et al., 1982; McCormick et al., 1985; Chagnac-Amitai et al., 1990; Connors and Gutnick, 1990; Mason and Larkman, 1990; Agmon and Connors, 1992; Franceschetti et al., 1995). As with RS neurons, increasing the stimulus intensity decreases in the response latency (Silva, 1991a; Amitai and Connors, 1995). They fire relatively slow action potentials (McCormick et al., 1985) and never receive a direct monosynaptic input from VPM (Agmon and Connors, 1992), typically firing at longer latencies than other cortical neurons (Armstrong-James et al., 1992; Agmon and Connors, 1992). IB neurons can be subdivided like RS neurons into either recurrently bursting or single bursting neurons (Montoro et al., 1988) but they cannot be distinguished morphologically. The only distinction is in the physiology of their bursting behaviour (Franceschetti et al., 1995). These neurons are concentrated within lower layer V (Agmon and Connors, 1989; Chagnac-Amitai and Connors, 1990; Miller et al., 1990; Larkman and Mason, 1990; Silva et al., 1991a; 1991b; Kasper et al., 1991; Wang and McCormick, 1993) or in the case of rat sensorimotor cortex in lower layer IV and Va (Connors et al., 1982; McCormick et al., 1985; Chagnac-Amitai and Connors, 1989a; 1989b; Armstrong-James et al., 1992; Agmon and Connors, 1992). They are however absent from layers II and III (Silva et al., 1991b; Agmon and Connors, 1992; van Brederode and Snyder, 1992). To date there have been no studies describing any preferential location in the rodent barrelfield with respect to the barrels or the septae.

There is evidence to suggest that synchronicity within local populations of neurons is initiated by processes that are intrinsic to the cortex (Connors et al., 1984; Chagnac-Amitai and Connors, 1989a; 1989b) and that IB neurons are capable of co-ordinating this synchronous activity (Agmon and Connors, 1989; Chagnac-Amitai and Connors, 1989a; 1989b; Chagnac-Amitai et al., 1990; Mason and Larkman, 1990; Tseng and Prince, 1993; Guetteo et al., 1994; Flint and Connors, 1996). It appears that IB neurons normally receive little or no inhibition compared to RS neurons (Silva and

Connors, 1986; Chagnac-Amitai and Connors, 1989a; Chagnac-Amitai et al., 1990; Connors and Gutnick, 1990; Nichol et al., 1993).

The development of burst firing in cortex around P15 (Armstrong-James, 1975) coincides with the development of whisking behaviour (Welker, 1964). Thus exploration before this happens when the cortex and GABAergic influences are not fully developed (Luhman and Prince, 1991; DeCharms and Merzenich, 1996; Micheva and Beaulieu, 1996). Thus this time is important for the development of sensory dependant cortical connections and the formation of experience dependent asymmetric SRFs.

## 6.8 IB Neuronal Morphology

It is possible that there are two sets of IB neurons within cortex distinguished by their laminar location (i.e either layer IV or layer Vb with the layer Vb neurons making up as much as 50% of the lower layer V cell population). The basal dendrites of intrinsically bursting neurons have more widespread basal dendrites than the RS neurons (Armstrong-James and Fox, 1987; Chagnac-Amitai et al., 1990), expanding beyond their parent barrel. This may explain the low numbers of single whisker RFs seen within layer V (Ito, 1981). The fact that the axon collaterals of intrinsically bursting neurons appear to be confined to the output layers of SI indicates that they may have a greater influence over the cortical output than the RS neurons (Chagnac-Amitai et al., 1990).

IB neurons tend to have larger soma than the RS neurons within cortex ( $37.6 \pm 3.1 \mu\text{m}$  compared to  $28.1 \pm 5.3 \mu\text{m}$ ) (Chagnac-Amitai and Connors, 1989a). They have extensive apical dendritic arborisations that extend to the pia and arborise extensively at the surface (Chagnac-Amitai et al., 1990). The axon collaterals of IB neurons extend

up to 1.5-2.0 mm horizontally within cortex (Chagnac-Amitai et al., 1990) i.e. far beyond the confines of even the largest caudal barrel (approximately 400 or 500  $\mu\text{m}$  in the long axis in rats) (Armstrong-James et al., 1992).

The apical dendrite gradually emerges from the soma and extends vertically towards the pia and frequently bifurcates in layers II/III. The apical dendrites are more spiny than the RS equivalent and extend over a much larger area. The basilar dendrites arise from 6-8 branches from the soma and they can extend up to 600  $\mu\text{m}$  horizontally from the soma. The axon collaterals extend horizontally throughout layer V and IV rather than extending towards the pia as in RS neurons. It has been estimated that the IB neurons have approximately 50% more basilar dendritic branching, over 100% more apical dendritic branching and over twice the cumulative dendritic length of RS neurons (Chagnac-Amitai et al., 1990).

Characteristics	Physiological class		
	Regular-spiking (RS)	Intrinsically bursting (IB)	Fast-spiking (FS)
Single-spike: rate of rise rate of fall	++ +	++ +	++ ++
Single-spike afterpotential	Complex, AHPs and ADP	Complex, AHPs and ADP	Simple, AHP alone
Frequency adaptation	++	Variable	-
Spike bursts during injected current	-	++	-
Laminar location of soma	II to VI	IV or V	II to VI
Presumed morphology	Pyramidal or spiny stellate	Pyramidal or spiny stellate	Spiny or sparsely spiny non-pyramidal
Presumed synaptic function	Excitatory (glutamate or aspartate)	Excitatory (glutamate or aspartate)	Inhibitory (GABA)

Symbols: +, the presence and relative strength of a characteristic; -, the absence of a characteristic. Abbreviations: AHP, afterhyperpolarization; ADP, afterdepolarization. Table adapted from Ref. 15, and compiled from data in the following Refs: 7-12, 16, 18, Gutnick, M. J. and White, E. L., unpublished observations, and Agmon, A., PhD Thesis, Stanford University, CA, 1988.

Figure 9. A table highlighting the morphological and physiological difference between RS, IB and FS neurons (From Connors and Gutnick, 1990).

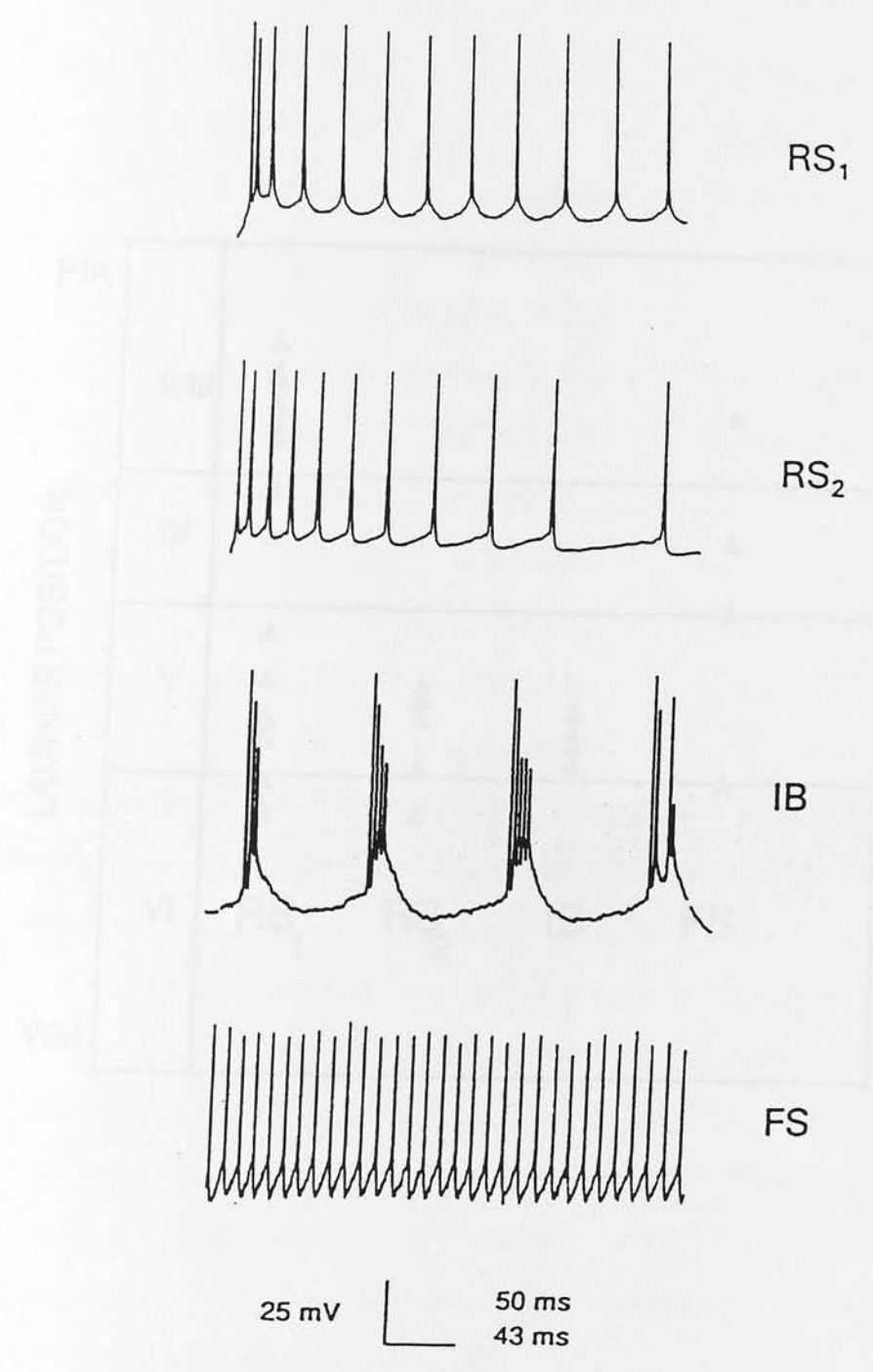


Figure 10. Examples of the physiological firing patterns of RS, IB and FS neurons. Note how FS neurons are quite distinct from the RS and IB neurons with their characteristically high firing frequency and repetitive firing patterns (From Agmon and Connors, 1992)

The present data are consistent with the view that the majority of neurons in the vibrissa region of primary somatosensory cortex are pyramidal cells (Agmon and Connors, 1992). The majority of these neurons are located in layers II/III, IV, and V, with a smaller number located in layer VI. The majority of these neurons are located in layers II/III, IV, and V, with a smaller number located in layer VI.

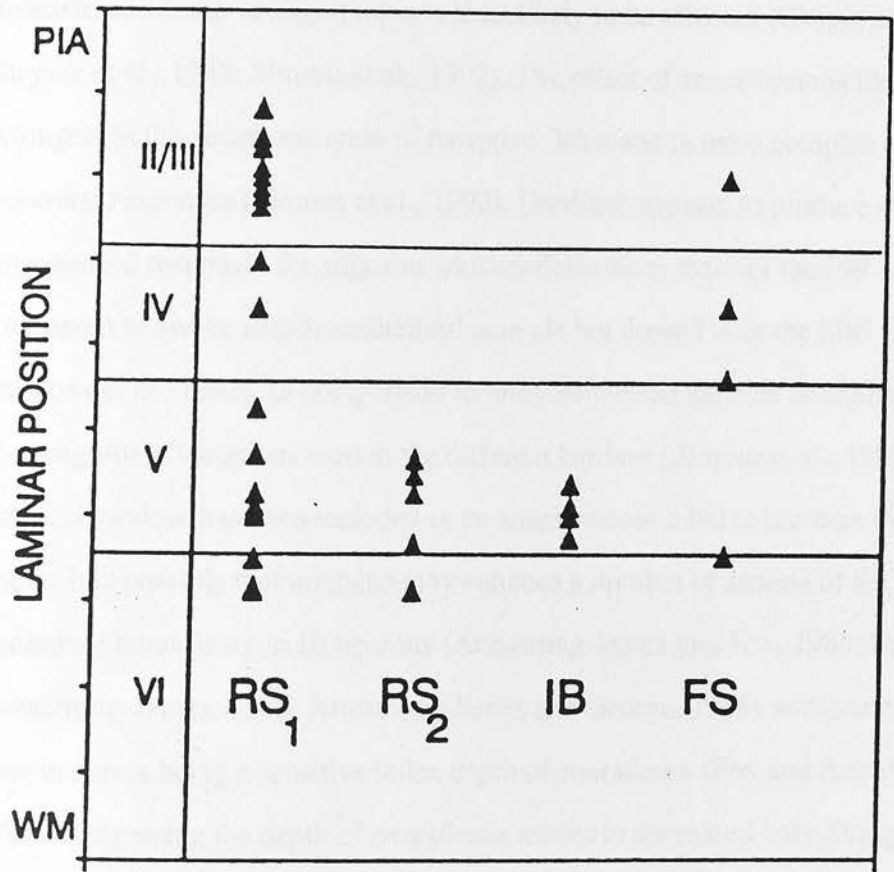


Figure 11. A chart showing the lamina location of the RS, IB and FS neurons within the vibrissa region of primary somatosensory cortex. Notice overlap of FS and RS neurons and the lack of overlap between IB and FS neurons (From Agmon and Connors, 1992)

## 7.0 Anaesthesia and Cortical Physiology

It appears that anaesthetics play an important part in the physiology of recording performed *in vivo* (Simons et al., 1992). The response of a barrel neuron to deflection of the principal whisker (at the preferred deflection angle) is least affected by anaesthesia i.e. the strongest input is least likely to be affected (Chapin and Lin, 1984; Stryker et al., 1988; Simons et al., 1992). The effect of anaesthesia is likely to be strongest in the peripheral areas of receptive fields and in more complex aspects of neuronal responses (Simons et al., 1992). Urethane appears to produce more pronounced responses for adjacent whisker deflections than for the PW when compared to awake non-anaesthetised animals but doesn't alter the SRF shape (Simons et al., 1992). In comparison to unanaesthetised animals urethane abolishes the magnitude variations seen in the different laminae (Simons et al., 1992). In this study chloralose has been included as an anaesthetic in a bid to increase the peripheral input. It is possible that urethane may enhance a number of aspects of the response including burst firing in IB neurons (Armstrong-James and Fox, 1984; Fox and Armstrong-James, 1986; Armstrong-James and George, 1988) with burst repetition rate in cortex being a sensitive index depth of anaesthesia (Fox and Armstrong-James, 1986). Increasing the depth of anaesthesia results in decreased burst firing and an increase in the interburst period (Fox and Armstrong-James, 1986) as well altering the excitability within some intracortical horizontal connections (Simons et al., 1992). Light urethane anaesthesia results in synchronised bursting behaviour (Armstrong-James and Fox, 1984). Burst firing itself is associated with large amplitude focal EEG waves (Armstrong-James and Fox, 1984).

## 8.0 Conclusions

From the physiological, morphological and lamina location of the corticocortical and subcortically projecting neurons it appears that the IB neurons form subcortically projecting neurons only, FS neurons are inhibitory cortically restricted interneurons and the RS neurons are a heterogeneous group. The majority of the neurons within cortex are however excitatory (Giuffrida and Rustioni, 1989). The RS neurons are in the majority within cortex and function as both subcortically projecting neurons and excitatory cortico-cortical neurons. Intrinsically bursting neurons in layer V and especially lamina Va appear to coincide with the laminar location for the corticostriatal projection (Mercier et al., 1990). Specifically the pathway appears to be under limited thalamic input control and more under the influence of and concerned with, the relay of cortically integrated sensory information. From the literature available for rat vibrissal primary somatosensory cortex it appears that the IB neurons are capable of receiving inputs from a wide area of sensory cortex including several barrels. The RS neurons however, with their location throughout cortex including the more superficial layers project both to other areas of cortex (e.g. the excitatory pyramidal neurons that activate layer Va neurons) and subcortically to the thalamus and brainstem. The subcortical RS projection neurons located predominantly in layer V (especially layer Vb) appear to receive inputs from thalamus (especially VPM) and thus produce an output signal to subcortical structures that is more directly under thalamic influence than those displayed by IB neurons. The RS neurons also appear to provide inputs to a variety of subcortical structures including the thalamic nuclei and brainstem as well as possibly an axon collateral input to the striatum from axons that run through the striatal fibre bundles to other targets (Mercier et al., 1990). Regardless of the target site of the neurons the asymmetric RFs observed within layer V may reflect the angular preferences of the neurons and the ideal deflection angle of the whisker. The aim of this study therefore is to provide an insight into the morphology and physiology of

specifically identified subcortically projecting neurons in the vibrissal region of rat SI. From the literature it appears that the IB neurons within the middle cortical layers can amplify, initiate, co-ordinate and synchronise their activity to act as a network and can generate a cortically based rhythm (Chagnac-Amitai and Connors, 1989a; Connors and Gutnick, 1990; Agmon and Connors, 1992; Francescetti, 1995). These neurons normally fire independently but upon activation with an appropriate stimulus their firing can become co-ordinated even in the face of strong inhibition (Chagnac-Amitai and Connors, 1989a; 1989b).

Thus the barrel system provides an initial stage of cortical processing (layer IV) and there is then a relay through the various cortical laminae that produces increasing levels of contrast between the sensory information generated through individual whiskers. This increasing contrast is generated through the synchrony within cortex and is enhanced through the whisking action. The synchronisation also increases synaptic effectiveness and provides a clear contrast between strong and weak inputs (Simons, 1995).

The literature concerning other cortical areas and other species will be discussed, in relation to this work, in a later section (see discussion).

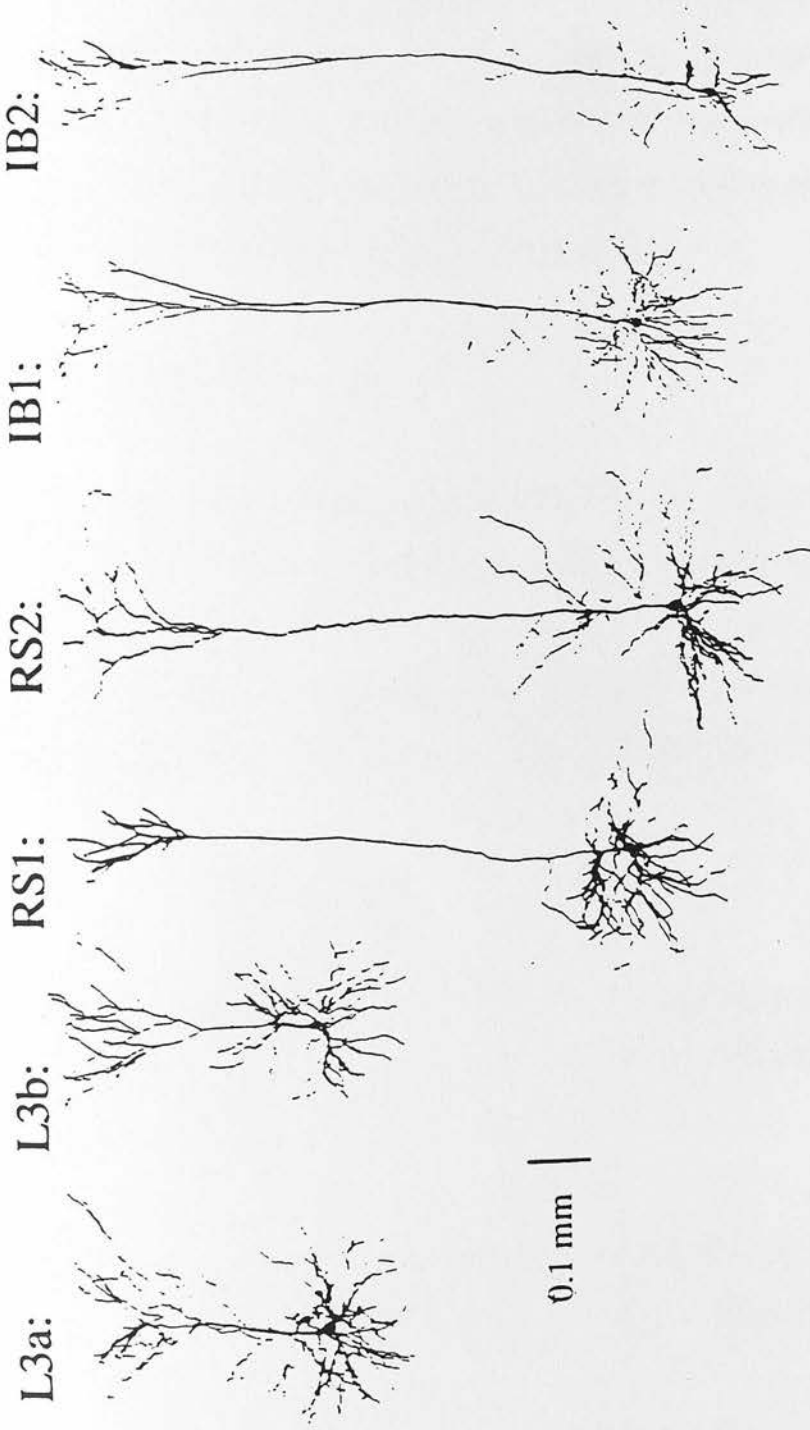


Figure 12. Shows the different classes of pyramidal neurons in the vibrissal region of primary somatosensory cortex. Notice in the case of IB and RS neurons the difference in the depth in the cortex at which the apical dendrite branches. RS neurons characteristically have apical dendrites that branch much closer to the pia than IB neurons (From Cauller and Connors, 1994).

## **9.0 METHODS INTRODUCTION**

As a large part of this work was the development of an intracellular recording protocol from an extracellular one, the progressive development of the method will be described. All of the methods for electrophysiology and biocytin visualisation will be described together with their advantages, disadvantages and the reasons why the method was developed further. In all the methods described the following procedures remained unchanged throughout their development:

### **9.1 Anaesthesia**

A total of 178 male Sprague Dawley rats (300-400 g, Harlan Olac) were used. On each experimental day a single rat was anaesthetised intraperitoneally with 0.8-1.1 ml/100 g of a 10% urethane 1% chloralose mix. Stable levels of anaesthesia were maintained throughout and additional anaesthetic (10% of original dose) was administered when required, to ensure the absence of a foot withdrawal reflex.

### **9.2 Basic Surgery**

A tracheostomy was performed and the head was secured in a stereotaxic frame via ear and tooth bars. Body temperature was maintained at 37°C throughout using a homeothermic blanket and rectal probe.

The skull was exposed by deflecting the scalp from the base of the skull to anterior of bregma and the skull surface cleared to reveal both bregma and the midline.

The levator duris longus muscle at the base of the skull was separated to reveal the atlanto-occipital membrane. A slit was made to reveal the underlying brainstem. A

CSF drain was created by taking a saline soaked cotton wool strip subcutaneously from the base of the skull to a slit created in the skin above the forepaw. The drain was inserted into the slit in the atlanto-occipital membrane.

The anterior superficial masseter and posterior deep masseter muscles were teased away from the skull so as to expose the parietal bone down to the origin of the zygomatic arch. The masseter muscles and the scalp were secured, using silk suture, to a brass ring situated directly above the skull (in order to keep the entire area clear). A unilateral craniotomy was then performed to expose the entire area of the right cerebral cortex from lateral of the midline just past the zygomatic arch and covering the area just posterior of bregma and anterior of lambda. The dura was not deflected until recording was about to take place. Prior to deflection it was covered with a cotton wool ball soaked in physiological saline. Once exposed the dura covering the entire area was deflected by creating a slit in the membrane as far posterior of the recording site as possible and bathed in physiological saline prior to recording. In all cases after dura deflection the preparation was allowed to recover electrical activity for at least 30 min prior to recording either surface evoked potentials or extracellular recordings within cortex.

### **9.3 Contralateral stimulating electrode**

In some experiments (intracellular recording protocol) a stimulating electrode was placed contralateral to the recording electrode (AP -3 mm, L 5.5 mm, DV 2 mm) in a bid to identify bilaterally projecting neurons. An area of similar area of cortex compared to the recording area was exposed and once the stimulating electrode was in place it was secured using agar for the duration of the experiment. Surface evoked potentials from increasing intensity of stimulus (typically 10-20 mV) were recorded to establish stimulus intensity for intracellular recordings. Once whisker responses were

noted for a neuron the response to the stimulating electrode was established. If the neuron responded to the stimulating electrode it was thought that the neuron was bilaterally projecting and located either within the side of a barrel in the septa between two barrels.

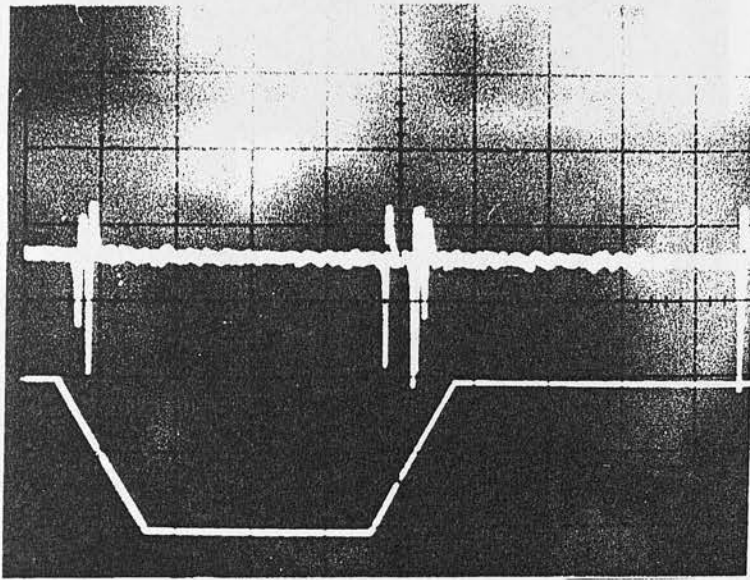
The stimulating electrode was eventually removed from the recording protocols as very few neurons responded to the stimulating electrode and also because the additional surgery increased the possibility of cortical damage causing either uncontrollable bleeding or spreading depression. Either way any damage affected the viability of the preparation for successful intracellular recordings. Examples of neuronal responses to contralateral stimulation can be seen in figures 39 and 41.

#### **9.4 WHISKER STIMULATION**

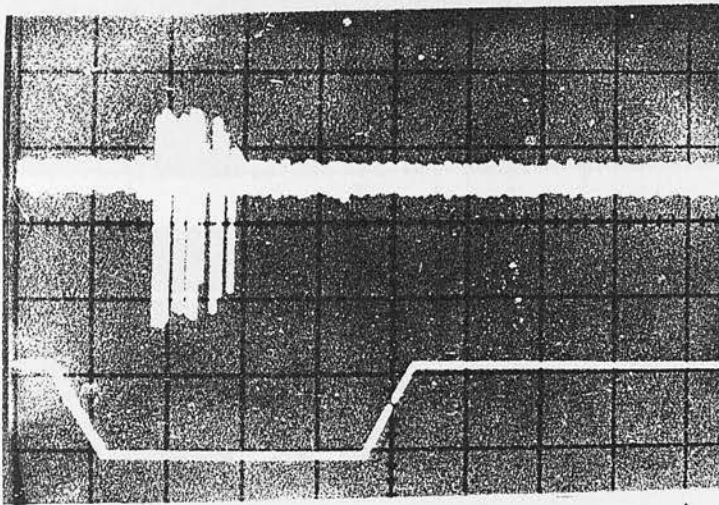
In all whisker stimulation experiments a single whisker is deflected at any one time. Whilst this allows the detection and recording of a cell's response to whisker deflection it must be remembered that in a naturally behaving animal a single whisker is rarely, if ever, deflected in isolation.

#### **9.5 Hydraulic Whisker Stimulator**

The hydraulic whisker stimulator provided a method for the slow deflection (typically 1 cm amplitude, 80-300 mS duration) of a whisker in a forwards-backwards direction via a bent hypodermic needle hooked around the chosen whisker. Due to the design of the stimulator rapid whisker deflection was not possible. Thus this stimulator allowed the recording of a specific group of neurons that responded to slow whisker deflections.

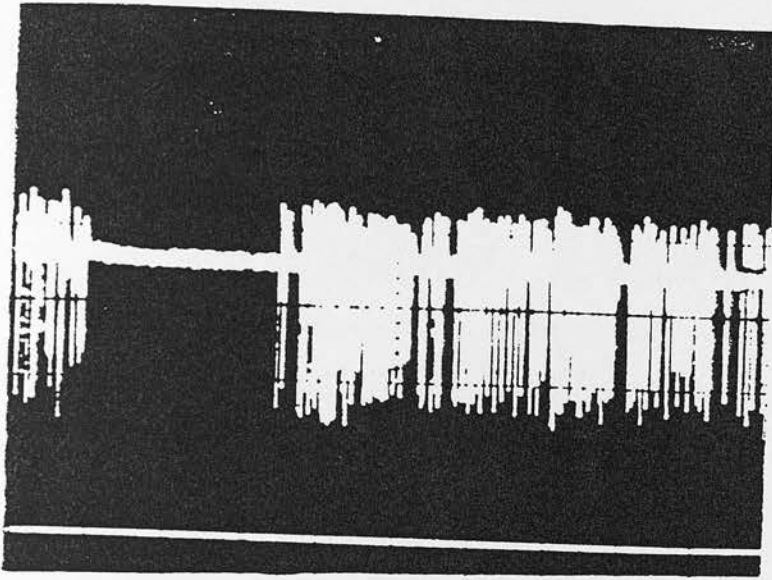


20 mV  
50 mS

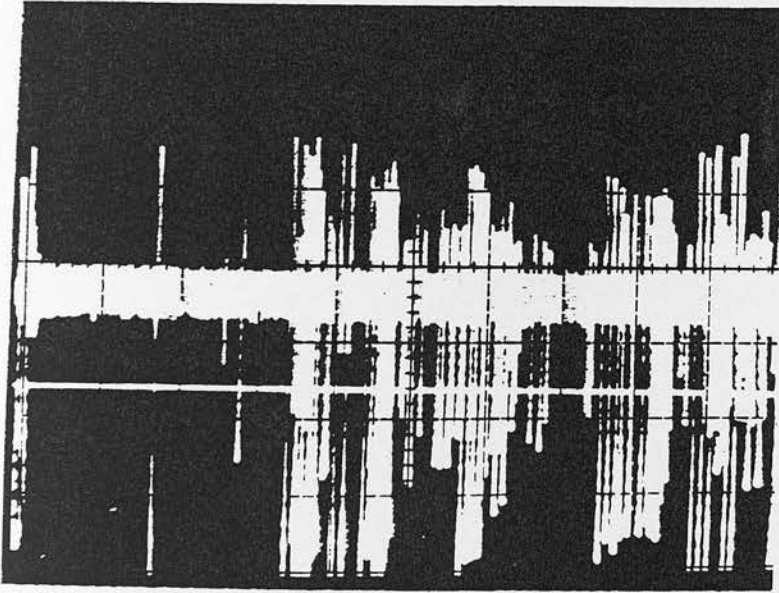


5 mV  
10 mS

Figure 13. An example of extracellularly recorded neurons responding to hydraulic whisker deflection. The stimulus position is displayed as the ramp like trace on the photograph. The plateau represents the full extension of the vibrissae in either the fully forwards or backwards direction. The ramps on either side represent whisker movements.



10 mV  
50 mS



2 mV  
50 mS

Figure 14. An example of extracellular recordings taken during electrical stimulation of the whisker pad.

## 9.6 Electrical Stimulation of the Whisker Pad

The electrical stimulator consisted of a pair of exposed wires 2-4 mm in length, 2 mm apart, inserted into a piece of cork (typically 10 mV amplitude, 1 ms duration). These pins were pushed into the whisker pad around a chosen whisker and electrical current was passed across the pins in order to elicit a muscular twitch in the whisker pad. The stimulus was adjusted so as to produce a detectable twitch in a single whisker and cellular responses in cortex.

The electrical stimulation of the whisker pad provided short latency responses within what were thought to be whisker sensitive neurons. The two disadvantages with this method are that it is impossible to say that the neuronal response is specifically to the deflection of a whisker rather than to the electrical activation of other receptors within the muzzle. In order to counteract this both electrical and hydraulic stimulation were carried out on each neuron. The other problem is that if the neuronal response is taken to be to whisker deflection then there is no way of clearly defining the stimulated whisker. In most cases at any one of at least an arc of whiskers surrounding the area in which the electrodes are implanted could be producing a response. If neurons responded to both stimuli it was assumed that they were vibrissae sensitive. If they responded to the electrical stimulus but not to the hydraulic one then they could either be sensitive to rapid but not slow vibrissal deflection or they could be sensitive to other elements within the whisker pad.

## 9.7 Piezoelectric Whisker Stimulation

The main reason for the use of a rapid short lived stimulus was that in previous studies using hydraulic and electrical stimulation it was found that the majority of cells responded to a rapid electrical stimulus whereas very few responded to a slow whisker stimulation. Because of this it was felt that a rapid whisker deflection was most likely to be the best stimulus to use for the detection and filling of the layer V pyramidal projection neurons (Simons, 1995). The piezoelectric stimulation of single vibrissae provided the ideal whisker stimulation method. Single whiskers could be reliably isolated from each other and stimulated independently (2 mm amplitude, 4 mS duration). In each experiment where recordings to a complement of three whiskers were made the deflection order was noted in case the previous whisker deflection in some way influenced subsequent whisker deflections (Simons, 1995). In each case what was thought to be the principal whisker for the stereotaxic electrode position in cortex according to the stereotaxic map drawn up by Armstrong-James (personal communication) was deflected initially in a bid to achieve the best principal whisker response as possible.

This method was ideal for multiple whisker deflections as the piezoelectric bimorphs were sufficiently small to allow the positioning of three stimulators in close proximity to each other (not possible with either hydraulic or electrical). Arranging any more than three stimulators in an experiment would prove difficult to use. In this study the vibrissae were fed into glass holders attached to the bimorph chips in a stimulator holder that allowed 180° movement of each chip. The glass tubes were adjusted so that the vibrissae lay parallel to each other in as close to a natural resting position as possible with respect to the animal's face. This was in order to eliminate any possibility that the position of the stimulator could elicit cellular responses even when the bimorphs were not activated.

In a bid to remove the possibility of deflecting adjacent non selected whiskers, adjacent whiskers were trimmed before the chosen whiskers were fed into the electrode glass holders. The selected whiskers were trimmed slightly to remove the fine tips of the large caudal whiskers to make them more flexible and easier to handle. The bimorphs were then situated approx. 1 cm from the animal's face.

For the majority of cells the whiskers responses were recorded on VCR tape before the neuron was filled. In order to decide which, if any of the whiskers was the principal whisker CRO paper printouts were taken of the typical response of the cell for the deflection of that whisker. A time base of 10 mS per division was used to determine response latency and another with a timebase of 100 mS per division in order to determine if the neuron was either a RS or IB neuron. This ensured that only electrically stable vibrissae sensitive neurons were filled.

## **9.8 Perfusion**

Animals were given a terminal dose of the chloralose urethane anaesthetic used in the recording phase. The thoracic cavity was then exposed and the animal was perfused transcardially with 25 ml of heparinised (10 U/ml) saline (0.9%) followed by 300 ml of a fixative. In initial (extracellular) experiments the fix contained 4% paraformaldehyde and 0.05% glutaraldehyde in 0.1 M phosphate buffer pH 7.4. In the intracellular experiments the fix was modified to include a greater glutaraldehyde content (to ensure biocytin was fixed in the presynaptic terminals (Smith, 1992)). This fixative contained 2% paraformaldehyde and 1.25% glutaraldehyde in 0.1 M phosphate buffer pH 7.4.

Once perfused the brains were removed and stored in 10% buffered sucrose fixative to ensure that the tissue is cryoprotected before cutting on a freezing microtome. The

buffered fixative was made by diluting the fixative 1:1 with of 20 % sucrose in water. Once placed in the sucrose/fix the brains were stored at least overnight (and longer in less well fixed tissue) to ensure the tissue was both fixed and cryopreserved.

## **9.9 Biocytin Histology**

The biocytin histology protocols will be described in a later section (see biocytin histology protocols, sections 15-22).

## **10.0 EXTRACELLULAR RECORDINGS**

### **10.1 Surgery**

The basic surgical procedures were the same as those described previously. A unilateral craniotomy was performed on the right side to expose an area of cortex from the midline to dorsal of the zygomatic arch and approximately 6 mm posterior of bregma. The whiskers were stimulated using the hydraulic and electrical stimuli described earlier. A total of 26 rats were used in these experiments.

### **10.2 Recording of Surface Evoked Potentials**

To record surface evoked potentials the dura was carefully removed to expose the entire cortical surface and was flooded with warmed physiological saline (37°C) and an amplifier earth secured to the scalp. For recording purposes the entire cortical area was bathed in light liquid paraffin (37°C). The whole preparation was isolated from ground vibration by resting on an inflated bicycle inner tube. In all experiments a single contralateral whisker was stimulated using either the hydraulic or electrical stimulation methods described earlier (section 9.4 and 9.5).

Surface evoked potentials were recorded using either a steel or silver wire electrode. The cortex was mapped for around the co-ordinate AP- 3 mm, L 5.5 (assumed to be the location of the C1 barrel) by dividing it into a grid of points 500  $\mu\text{m}$  apart. The co-ordinate giving the shortest latency and greatest magnitude response was assumed to correspond to the principal whisker barrel. This position was noted with respect to the surface blood vessels and was used for the positioning of glass recording electrodes in subsequent recordings.

### **10.3 Extracellular Recording**

Glass microelectrodes filled with biocytin hydrochloride (5% in either 1 M sodium or potassium acetate) were advanced 100  $\mu\text{m}$  into the cortex and electrode resistance and capacitance compensation balanced before covering the surface with agar (4% in physiological saline). For extracellular recordings the electrodes used had a typical resistance of 6-20  $\text{M}\Omega$ . The electrode was advanced in 5  $\mu\text{m}$  steps manually using a Narishinge micromanipulator. Neuronal activity was searched for using electrical stimulation of the whisker pad. Once a cell was recorded extracellularly the response to whisker deflection was established. The response was recorded as a photographic record of an oscilloscope screen (from 10 sweeps of a CRO triggered in sequence with the stimulus). The electrode was advanced to a maximum depth of 2000  $\mu\text{m}$  for each track (corresponding to the start of the corpus callosum), typically concentrating in the 600- 1200  $\mu\text{m}$  region (corresponding to layers IV and V). Between glass microelectrode recordings the exposed area was cleared of liquid paraffin in order to improve refraction for the exact positioning of electrodes. Once positioned the area was flooded with liquid paraffin again.

### **10.4 Extracellular Marking and Perfusion**

At the end of the recording session the electrode was placed in a physiologically responsive area and biocytin was applied by iontophoretic injection at an appropriate depth (negative current, 10-20  $\mu\text{A}$  min) for extracellular tracing studies. In some cases the electrode was filled with pontamine sky blue (2% in 0.5 M sodium acetate) and current applied for approximately 20  $\mu\text{A}$  min in order to make a small, discrete, stereotaxic mark.

The animal was allowed to survive 3-6 hours post injection after which it was sacrificed by transcardial perfusion with 25 ml of heparinised (10 U/ ml) saline (0.9%) followed by 300 ml of 4% paraformaldehyde, 0.05% glutaraldehyde in 0.1 M phosphate buffer pH 7.4. The brain was removed and stored in 10% sucrose buffered fixative overnight at 4°C. The brain was then cut into serial sections using a freezing microtome either coronally or, in the case of cortical sections for cytochrome oxidase histochemistry, tangential to the pial surface.

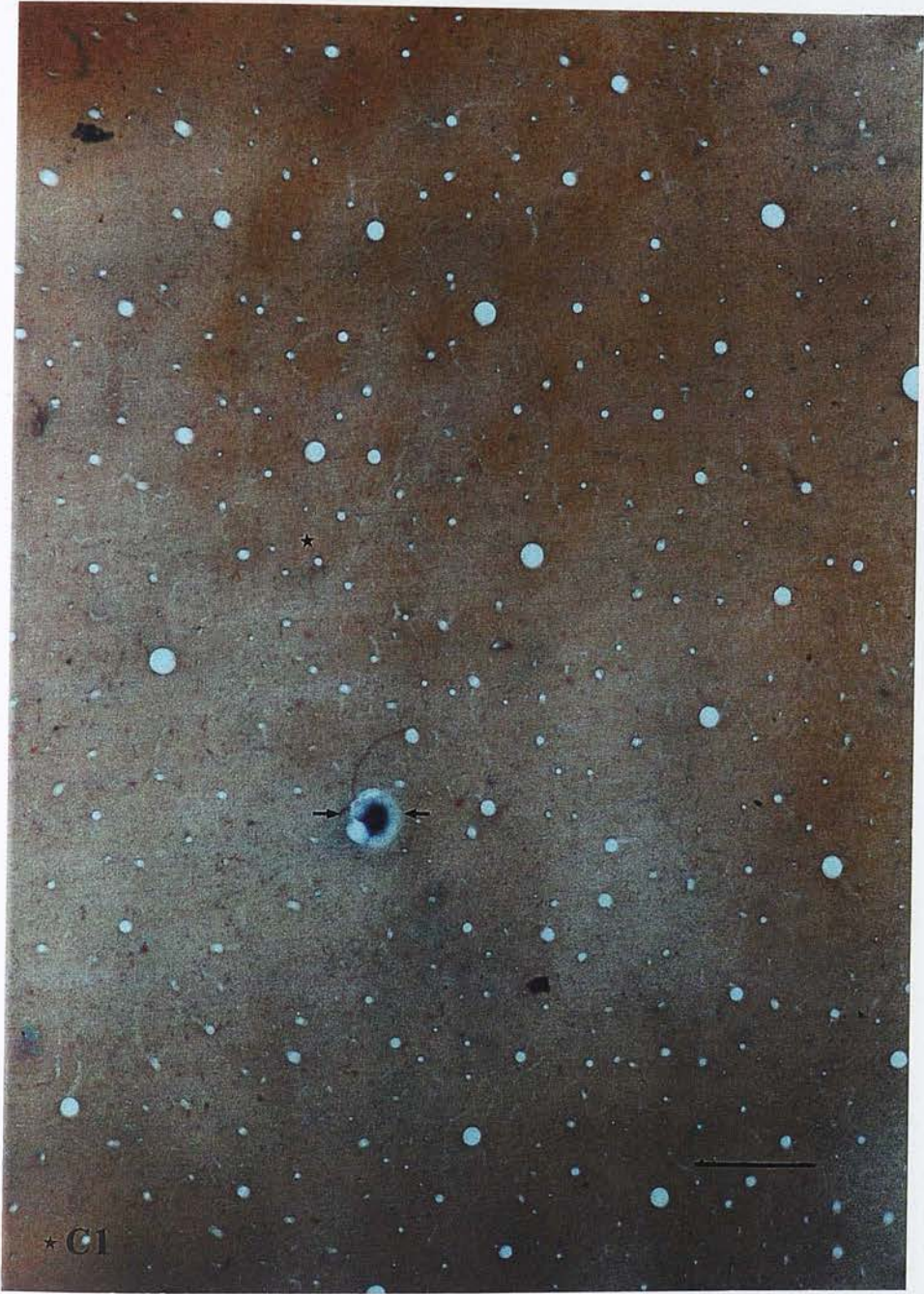


Figure 15. Tangentially cut cortical sections stained for the enzyme cytochrome oxidase marked with pontamine sky blue (see section 17.0 for a description of the staining procedure). The orientation is as follows: Anterior to the top of the photograph, posterior to the bottom and the midline to the left. Scale bar 500  $\mu\text{m}$ .



Figure 16. Tangentially cut cortical sections stained for the enzyme cytochrome oxidase marked with biocytin and revealed using the initial biocytin histology protocol. (See section 17.0 for a description of the staining procedure). The orientation is as follows: Anterior to the top of the photograph, posterior to the bottom and the midline to the left. Scale bar 500  $\mu\text{m}$ .

## **11.0 INITIAL INTRACELLULAR RECORDING PROTOCOL**

### **11.1 Anaesthesia and Surgery**

The surgical procedure was the same as described for extracellular recordings using an anaesthetic dose of 1 ml/100 g. The liquid paraffin used in the extracellular studies was replaced with agar (4% in physiological saline) in order to increase recording stability. The total area of cortex exposed was the same in the two experiments and surface evoked potentials were also recorded. A total of 103 rats were used in these experiments

### **11.2 Whisker Stimulus**

The stimulus used was the piezoelectric bimorph system and the micromanipulator a piezoelectric driven Burleigh microdrive. The electrode was advanced in 3  $\mu\text{m}$  rapid steps through the cortex in order to achieve a quick and clean penetration of a neuron. Upon cell penetration in the later experiments neuronal responses to 3 separately deflected pre-chosen whiskers (B1, C1 and D1) were examined in order to achieve an insight into the positioning of the neuron within the barrel field.

### **11.3 Maclab Data Acquisition Packages**

In order to achieve more detailed information from the electrophysiological data the photographic recording of CRO traces was replaced in the intracellular recording with a Macintosh based 'Scope' and 'Chart' data acquisition package (MacLab).

## **'Scope'**

Using the 'Scope' option it was possible to capture consecutive CRO like traces triggered by the stimulus. Once captured it was possible to accurately measure response amplitudes and latencies as well as inhibitory periods (in this case between the initial response and the resumption of firing). For an example of a 'Scope' record see figures 34-39.

## **'Chart' Records**

The 'Chart' program was used to analyse video based records that contained a minute or more of a cell's responses to prolonged whisker deflection. Analysis of this data allowed the experimenter to analyse a continuous physiological response to whisker deflection rather than an individual episode.

'Chart' analysis provided a clear record of any adaptive behaviour displayed by the neuron to a single whisker or, in the case of later experiments, the variety of responses seen in a single cell when a single whisker within an arc was deflected. 'Chart' analysis also allowed a more accurate method of classification of neurons than either the 'Scope' package or a conventional CRO.

Therefore in these experiments 'Scope' records were used to determine response latencies and length of inhibitory periods to whisker deflection. 'Chart' records were used for cell classification and identification of a PW and for determining the position of a cell across an arc of three barrels (see results chapter).

#### **11.4 Recording Set Up**

Neuronal responses were recorded either on a Macintosh based data acquisition package (MacLab 'Scope' package) or as a VCR record. In both cases they were later analysed using the MacLab 'Chart' program. In the initial intracellular experiments the preparations were isolated from ground vibration using the inflated bicycle inner tube. In later experiments a nitrogen filled isolation table was used.

#### **11.5 Intracellular Recording**

Glass microelectrodes containing biocytin (5% in 1 M potassium acetate) with resistances of between 100-200 M $\Omega$  were advanced through the cortex in 3  $\mu$ m steps to a maximum depth of 1200  $\mu$ m typically concentrating within the 600-1200  $\mu$ m area (corresponding to layers IV and V). Electrodes were advanced until a neuron was impaled by either advancement alone or by a combination of advancement and electrode 'buzzing' where a brief pulse of high current was passed through the electrode. The cell detection stimulus used was an intracellular current pulse (500 mS cycle length) which ensured rapid cell detection. The whisker deflection method used a stimulus with a cycle duration of 2.5 S in order to ensure that there was full electrical recovery of the cortex between stimuli. Once the cell was impaled the response to whisker stimulation was tested and the response pattern of the cell was also noted to verify whether it was an RS, IB or FS neuron.

When intracellular recordings were performed no holding current was used when data was recorded to either 'Scope' or to vcr. Holding current was only ever used to stabilise intracellular fillings. Holding current in these cases was used either to reduce firing rates in high firing neurons or to stabilise resting membrane potentials in neurons with decreasing resting membrane potentials and/or neurons whose firing patterns mimicked those of FS neurons (i.e. high frequency, repetitive firing).

## 11.6 Physiological Classification of Neurons

The physiological classification of RS, IB and FS neurons was determined by comparing their firing patterns to the firing patterns observed within the in vitro literature (for a review see Connors and Gutnick, 1990).

RS neurons were identified by their inability to generate burst firing (a burst being a high frequency cluster of typically 3-5 or more action potentials riding on a depolarising envelope) in response to the deflection of any of the preselected whiskers. In all cases 'Scope' and 'Chart' recordings were examined independantly. Where morphological classification was available from intracellular filling the morphological and physiological classifications were determined independantly.

IB neurons were identified by their ability to fire at least one burst in response to the deflection of at least one of the preselected whiskers. Again, 'Scope', 'Chart' and morphological classifications were performed independantly. Although the neuron was classed as intrinsically bursting if it fired at least one burst the recordings obtained from these neurons contained numerous characteristic bursts (for examples see figures 36-37 and 54).

FS neurons were rarely encountered and were not classified either electrophysiologically or morphologically as these neurons were unstable under these reording conditions. The neurons were identifiable by their high frequency non-adaptive firing patterns which were the similar to those described in vitro (see Connors and Gutnick, 1990).

## 11.7 Intracellular Filling

If the neuron was deemed stable (i.e. low resting membrane potential, spike heights of more than 30 mV and a stable firing pattern) it was filled with biocytin. Filling was achieved using hyperpolarising current (-2 nA, 200 mS on / 200 mS off cycle) continuing until either the membrane became more depolarised, the firing pattern changed, and/or there was a decrease in the amplitude of the EPSP's or the action potentials. Filling was then terminated and the electrode carefully removed from the cortex.

## 11.8 Further Recordings

Any further recordings were performed away from the region of an intracellular fill in order to prevent any damage to a viable transporting cell and also to make histological identification easier. In any one animal a maximum of two neurons were filled for ease of post-histological identification. Where the fill times of the neurons were less than a couple of minutes further neurons would be filled and as poorly filled neurons were either not detectable after histological processing or appeared as 'ghosts' with little basilar dendritic or axonal filling and staining (see figure 25), filling further neurons would be attempted in a bid to achieve two successes.

After recordings ceased animals were maintained at 37°C until sufficient time had elapsed for axonal transport and terminal filling to have taken place. The animals were then perfused as described previously.

In the majority of experiments in this and the following section use the stimulators in an up-down stimulus rather than back-front position for two reasons. Firstly it allows easier positioning of the piezoelectric chips in a stack and ensures that the whiskers are

more likely to be in a natural state. Secondly it is thought that there are very few directionally very specific cells within barrel cortex (Armstrong-James, 1995).

The methods described here provided the most complete longitudinal records of this study and were a result of the existing method development.

### 12.1 Anaesthesia and Surgery

The main surgery and the general anaesthesia of the animals were the same as described previously. The animals within the barrel cortex were anaesthetized with increasing recording stability. A total of 49 recordings were made.

### 12.2 Surgical Adaptations

The goal of cortex exposure for recording was to get to 2 mm depth (midline) i.e. large enough to allow very dense electrode and surgical instruments (generally 2 mm diameter) to reach and be positioned in the area of interest. The skull was held in place during the recording. The procedure was similar to the previous method (see 2.1) but the 1.5 mm depth of the electrode was maintained in the area of the skull was marked with a small amount of cyanoacrylate glue, with particular care. The hole was drilled using a dental drill with speed control. Once the skull was removed the dura was carefully dehydrated and the exposed area was covered by gently filling the area with cotton wool saturated with physiological saline. Once exposed, several layers of skull around the hole were drilled and a small amount of glue was applied. Once the well was formed, the dura was removed and the well was filled with physiological saline.

The recording procedure was similar to the one described for the previous animals. The recording procedure was similar to the one described for the previous animals.

## **12.0 FINAL INTRACELLULAR RECORDING PROTOCOL**

The method described here provided the most stable intracellular records of this study and was a result of the ongoing method development.

### **12.1 Anaesthesia and Surgery**

The basic surgery and the piezoelectric stimulation of the whiskers were the same as described previously. The variations within the method were all concerned with increasing recording stability. A total of 49 rats were used in these experiments.

### **12.2 Surgical Adaptations**

The area of cortex exposed for recording was kept to a workable minimum i.e. large enough to allow easy access for electrodes and surgical instruments (generally 2 mm diameter). The area used corresponded to the area in extracellular and initial intracellular recordings that provided physiologically responsive neurons (AP - 3.0 mm, L 5.5 mm). Once the stereotaxic point was noted the area on the skull was marked with a broken recording electrode filled with pontamine sky blue. The hole was drilled using a dental drill with a trephine burr bit. Once the skull was removed the dura was carefully deflected and the exposed area was covered by gently filling the area with cotton wool soaked in 40°C physiological saline. Once securely covered the area of skull around the hole was dried and a dental cement well approx. 1 cm tall was built. Once the well was constructed the cotton wool was removed and the well was filled with physiological saline.

The recording procedures were essentially the same as described for the previous intracellular recording protocol although the recordings were stabilised with low

setting point paraffin wax rather than agar (paraffin wax proved to be much harder and more stable). The perfusion procedure was also the same.

### **12.3 Advantages and Disadvantages of the Surgical Adaptations**

Whilst this method produced intracellular fills in excess of 20 min the number of successful experiments was reduced for various reasons related to the surgical procedure. Bleeding from and damage to the cortical surface (which may not interfere with recording in subcortical areas) is one of the main reasons for failure in cortical recording studies. Bleeding, even when minimal, causes spreading depression and electrical shutdown. In experiments where there appeared to be no responsive neurons cortical evoked potentials were checked to establish whether the preparation was electrically active. In cases where it was not the experiment was terminated.

When the exposed area was larger (as in the initial protocol) large blood vessels could be avoided much more easily than when the area of exposed cortex was much smaller. In most intracellular recording experiments the aim was to achieve stable recordings as quickly as possible. This ensured that there was minimal damage to the cortex from electrode placements and from the constant removal and application of paraffin wax.

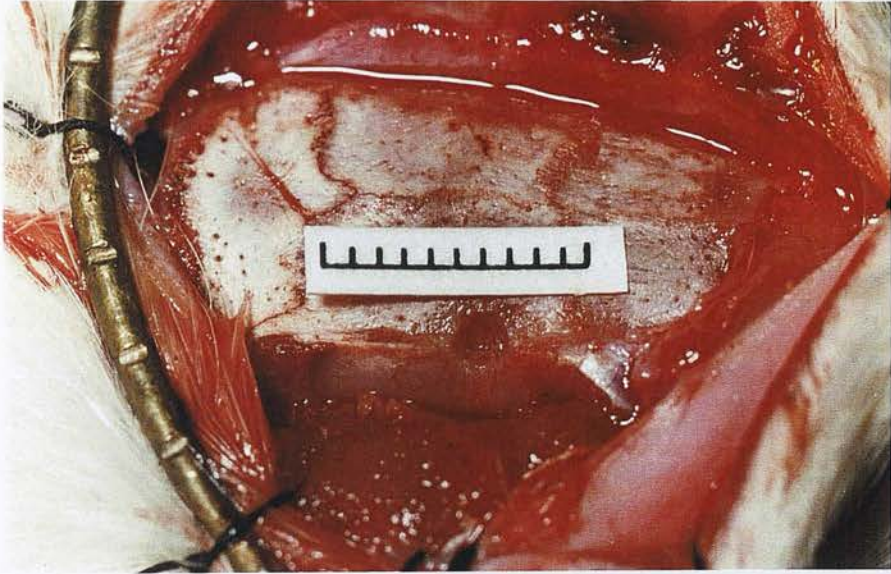


Figure 17. Low and higher power photomicrographs of the typical area exposed for intracellular recording. Note the positioning on the parietal bone which makes the drilling of the hole more technically difficult. In the higher power photomicrograph note the steep sides of the hole (which makes skull and dura removal easy) and the rich innervation of blood vessels. Anterior = right, posterior = left, midline = top and lateral = bottom. Scale bar 1 cm.

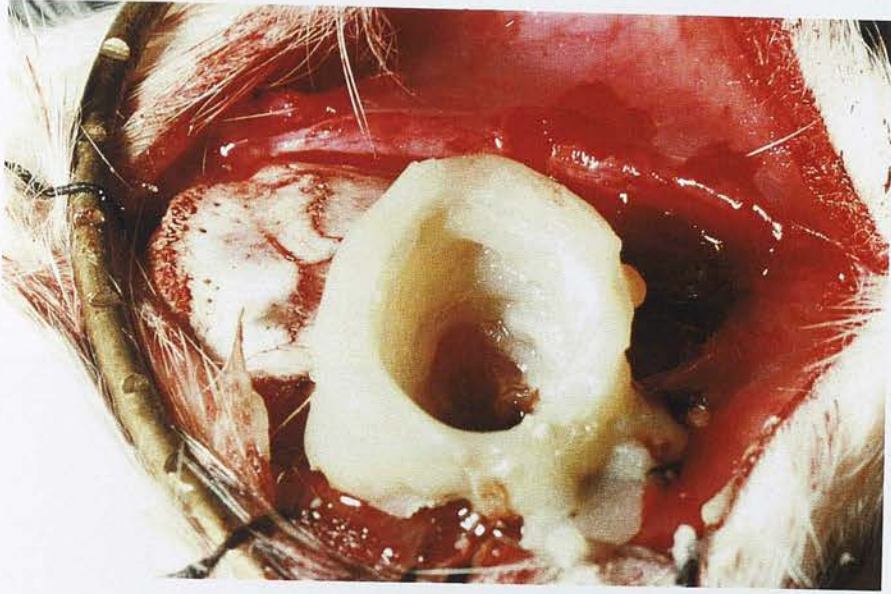


Figure 18. Low and higher power photomicrographs showing the dental cement well built around the exposed cortex. Note the height of the column and the roughness of the sides. Scale bar 1 cm.

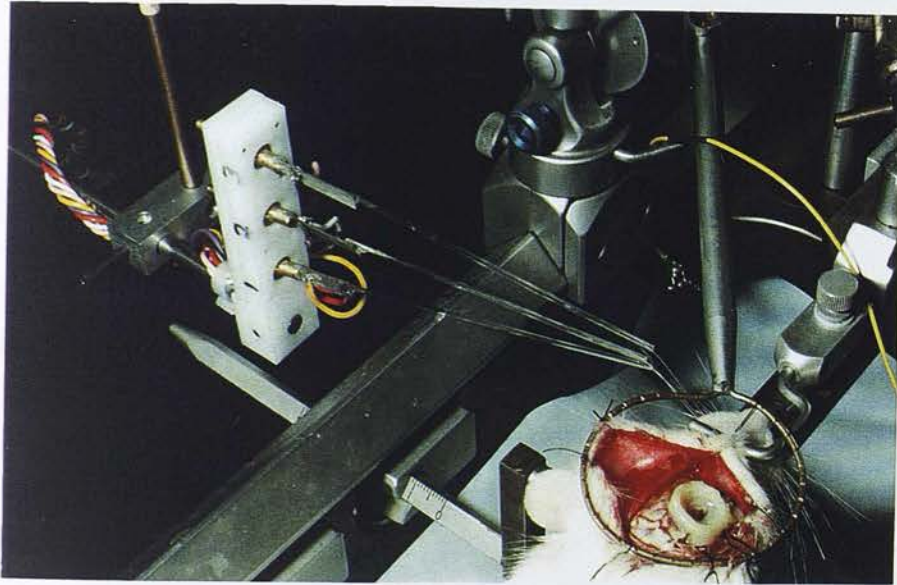


Figure 19. A photomicrograph clearly showing the triple piezoelectric whisker stimulator in an experimental set up (note that in this experiment whiskers are set in a front/back arrangement and that each piezoelectric chip is able to operate independently. Scale bar 1 cm.

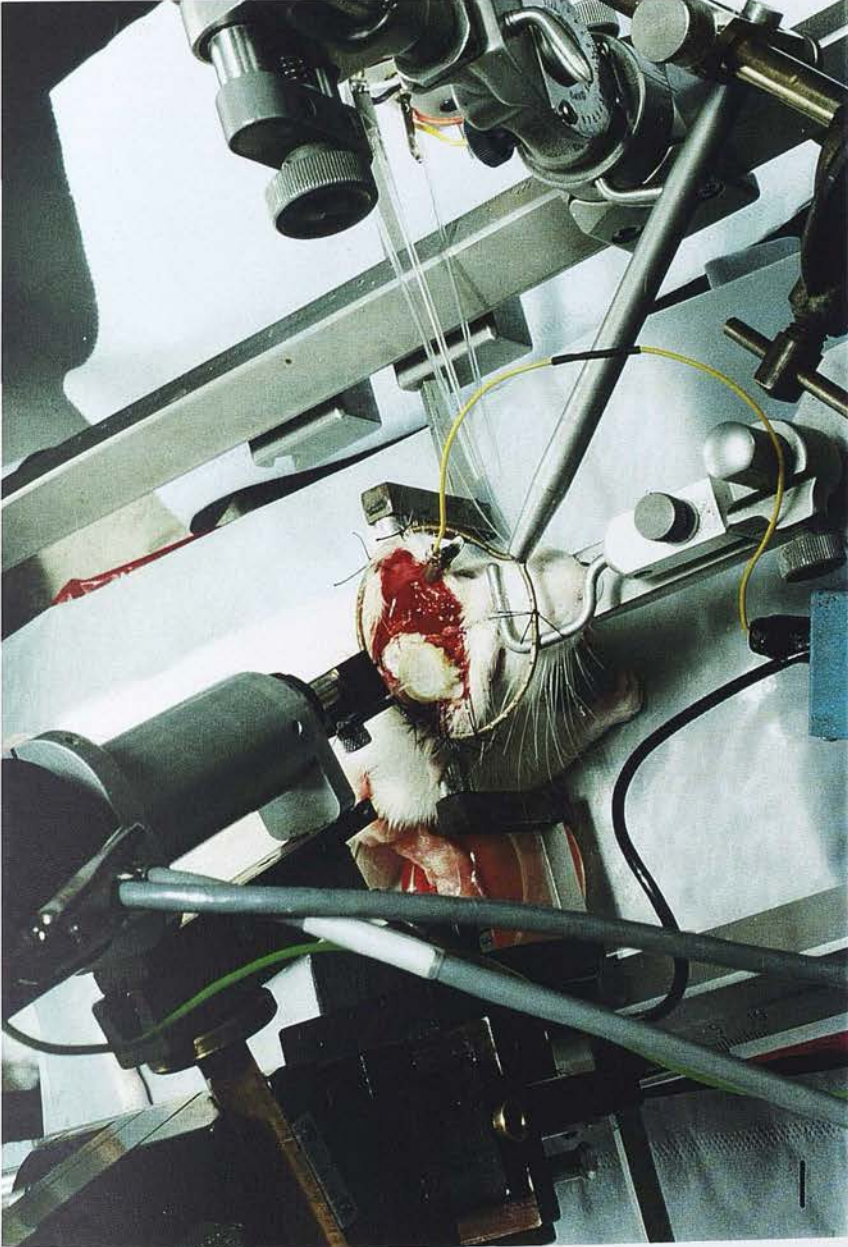


Figure 20. A photomicrograph showing an intracellular recording set up. Note the fixation of the Burleigh microdrive onto a Narishige manual micromanipulator. Scale bar 1 cm.

### 13.0 ANAESTHETIC CONSIDERATIONS

The majority of recordings were performed on Sprague Dawley rats under a chloralose-urethane mix anaesthesia.

In a few cases urethane alone was used in a bid to highlight the burst firing projection neurons of layer V. Such experiments proved difficult to perform as it became clear that in this study at least, Sprague Dawley rats required greater doses of urethane (up to 1 ml/100 g body weight) to ensure that the foot withdrawal reflex had been completely abolished. This anaesthetic dose proved to be very close to the lethal dose. Thus for practical reasons all future experiments were performed under the chloralose urethane mix described.

In the majority of the chloralose urethane experiments the  $\alpha$ -chloralose was replaced on a monthly basis to ensure that as little as possible of the  $\beta$  isomer was present. In some cases where the  $\alpha$ -chloralose was older, it took longer and greater amounts of anaesthetic to ensure that the foot withdrawal reflex had been abolished. The  $\beta$ -chloralose increased the likelihood of respiratory problems including laboured and erratic breathing resulting in unstable recordings and a blocking of the tracheal cannula with mucous which could kill the animal. This resulted in a poor perfusion of the animal and fixation of the brain. Poor tissue preservation resulted in bloody tissue with high levels of endogenous peroxidase activity which it was not always possible to remove completely through methanol quenching. This made histological processing unpredictable, especially with respect to whether or not any filled neuron would be detectable at LM and how high the background staining would be. The background staining was especially important when examining the tissue for the axon and terminal fields.

In all cases fresh anaesthetic was made daily and only reheated to dissolve the anaesthetic when top-ups were required. The anaesthetic was always heated gently and was never allowed to boil.

## 14.0 ELECTRODES

The best results for successfully impaling and filling layer V neurons were achieved using electrodes with a resistance of approximately 100 M $\Omega$  filled with 1M potassium acetate. Electrodes with much higher resistances proved difficult to clear and continually became blocked as they were advanced through cortex. This caused erroneous fills in cortex. Also, in trying to clear these electrodes the tip would frequently break back leaving an electrode with a resistance of less than 20 M $\Omega$  (more suited to extracellular recordings). Removing the broken electrode and replacing it with an electrode with a more suitable resistance caused more cortical damage by a) the advancement of a second electrode through cortex and b) extra surface damage (and an increased risk of causing unstoppable bleeding) caused by the repeated removal and reapplication of the dampening material. The advantage of the higher resistance electrodes was that dendritic recordings were more likely and more successful. Lower resistance electrodes were more likely to be electrically less noisy but were less likely to result in longer more stable intracellular fills.

In order to ensure that the intracellular recordings were as stable as possible, the neurons were carefully analysed to see that the firing pattern was stable, the resting membrane potential was greater than -40 mV and the action potential heights were in excess of 40 mV. In cases where the resting membrane potential was less than -60 mV and the spike heights were nearer 20 mV the recording was deemed too unstable to withstand prolonged intracellular filling without disappearing. In more stable recordings stability was further increased by the injection of sufficient hyperpolarising current to switch the cell from an actively firing mode to a hyperpolarised state where it barely fired. Filling was continually monitored to check that there was little variation in the resting membrane potential and the firing pattern of the cell. In order to check these two important criteria the filling was halted briefly from time to time (depending

upon the condition of the neuron) and checked. Filling was also stopped if the cell appeared to change its firing pattern to a firing pattern resembling that of a typical FS neuron i.e. high frequency and non-adaptive. In these cases, ceasing filling was sometimes sufficient to ensure that a normal firing pattern returned but it was generally a sign that the recording was becoming unstable and the filling was stopped. The action of filling (with hyperpolarising current) was sometimes sufficient to cause an increase in the stability of a cellular recording. In some cases where stability was decreasing, reversing the electrode 3  $\mu\text{m}$  back out of the cell was sufficient to increase the stability.

## **15.0 BIOCYTIN METHODS INTRODUCTION**

All of the biocytin histology protocols described in this section were based on the method described by King et al., 1989. The method was based on an avidin-biotin peroxidase system using 3, 3' diaminobenzidine (DAB) as the chromagen.

Throughout the development of the method, the cutting and perfusions remained constant.

### **15.1 Perfusion**

See section 9.7

### **15.2 Cutting**

In all experiments the brains were sectioned coronally using a freezing microtome taking 50  $\mu$ m serial sections and processing the tissue as free floating sections prior to mounting onto chrome alum subbed microscope slides.

### **15.3 Washes**

All buffer washes took 10 min and the sections were washed and reacted under constant agitation with 0.05 M phosphate buffered saline (0.9%) pH 7.4 (PBS) either with or without the inclusion of the non-ionic detergent Triton-X100 (0.3%; PBS-TX) for membrane disruption.

## 15.4 Mounting

All sections were mounted on chrome alum subbed microscope slides and oven dried (at 40°C) for one week prior to coverslipping.

## 15.5 Coverslipping

Once dried the sections were either rehydrated through a graded series of alcohols, counterstained with methyl green (5%), dehydrated and coverslipped with DPX or dehydrated without counterstaining and coverslipped using DPX. In cases where the background staining was low (all cases except sections stained with cytochrome oxidase and the final intracellular recording protocol) the sections were counterstained. In cases where the background staining was higher the sections were dehydrated and coverslipped.

## 16.0 EXTRACELLULAR BIOCYTIN VISUALISATION PROTOCOL

### 16.1 Fixation and Cutting

The animals used in this procedure were fixed using a low gluteraldehyde fixative (4% paraformaldehyde, 0.05% glutaraldehyde in 0.1 M phosphate buffer pH 7.4).

### 16.2 Reaction and Visualisation

Coronally cut sections were initially washed in 0.05 M phosphate buffer pH 7.4 containing 0.9% sodium chloride (PBS) to remove any residual fixative. The sections were incubated in a standard ABC solution (1:200 in PBS for 1 hour at room temperature, Vector Laboratories, UK) before washing with 3 times with PBS. The sections were then visualised by reacting with a DAB solution (with or without nickel enhancement (Adams, 1981)) for 10 min. The sections were then rinsed 3 times in PBS before mounting, drying, dehydrating, counterstaining and coverslipping with DPX. When counterstaining, the sections were slightly overstained in a bid to differentiate the cell dense layer IV from the underlying cell sparse layer Va (see figure 44). It was hoped that this would give a clearer lamina location for iontophoretic injections and the soma of single cell fills.

Every sixth section from these sections were processed for the enzyme cytochrome oxidase (see cytochrome oxidase histology section) as well as for biocytin.

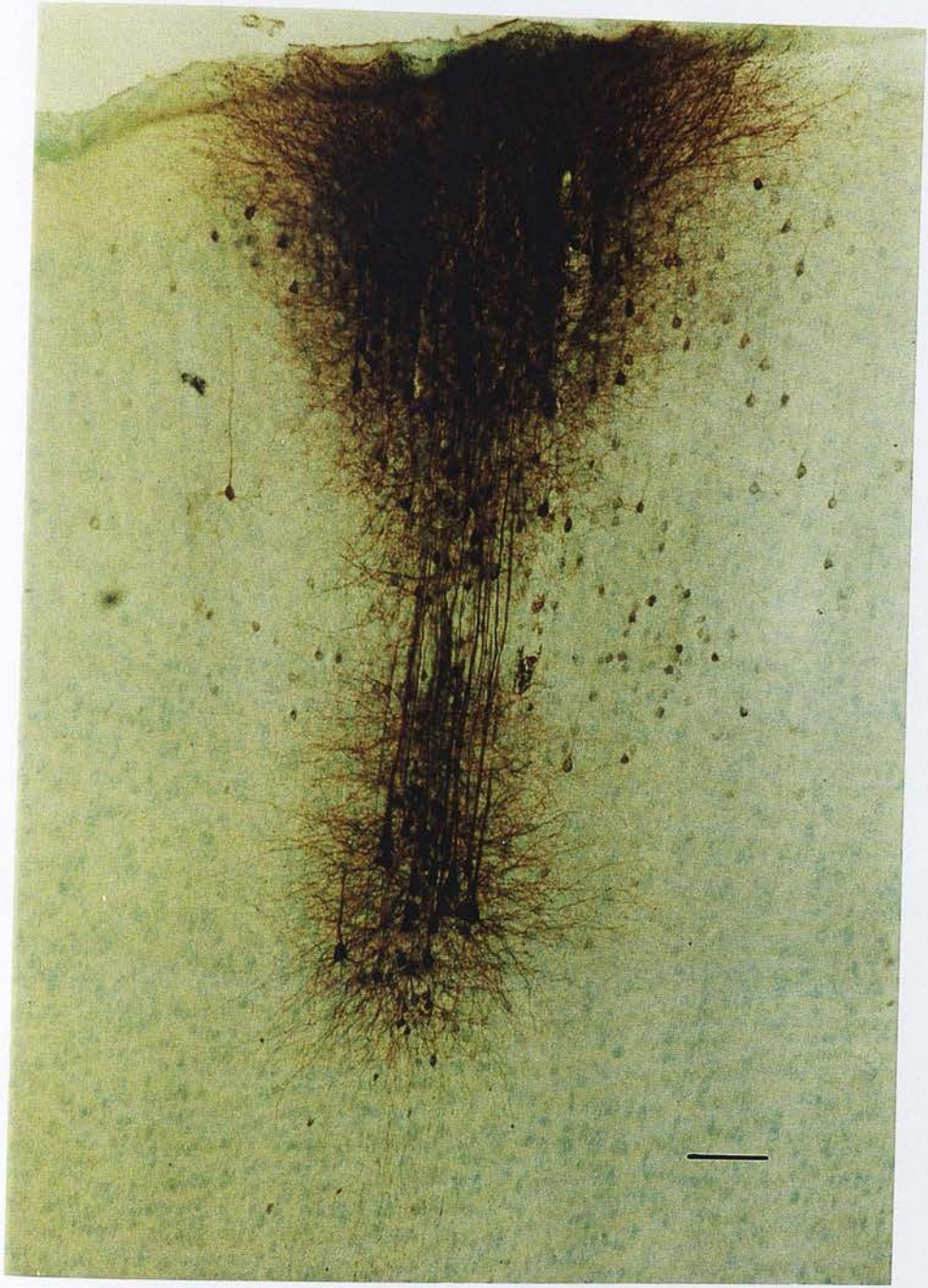


Figure 21. A photomicrograph of an extracellular iontophoretic injection of biocytin made at a depth of 1000  $\mu\text{m}$ . The biocytin was visualised using the above method. Note the columnar arrangement of the axons and dendrites. The orientation is as follows: The pia is at the top of the photograph, the corpus callosum to the bottom and the midline to the left. Scale bar 100  $\mu\text{m}$ .

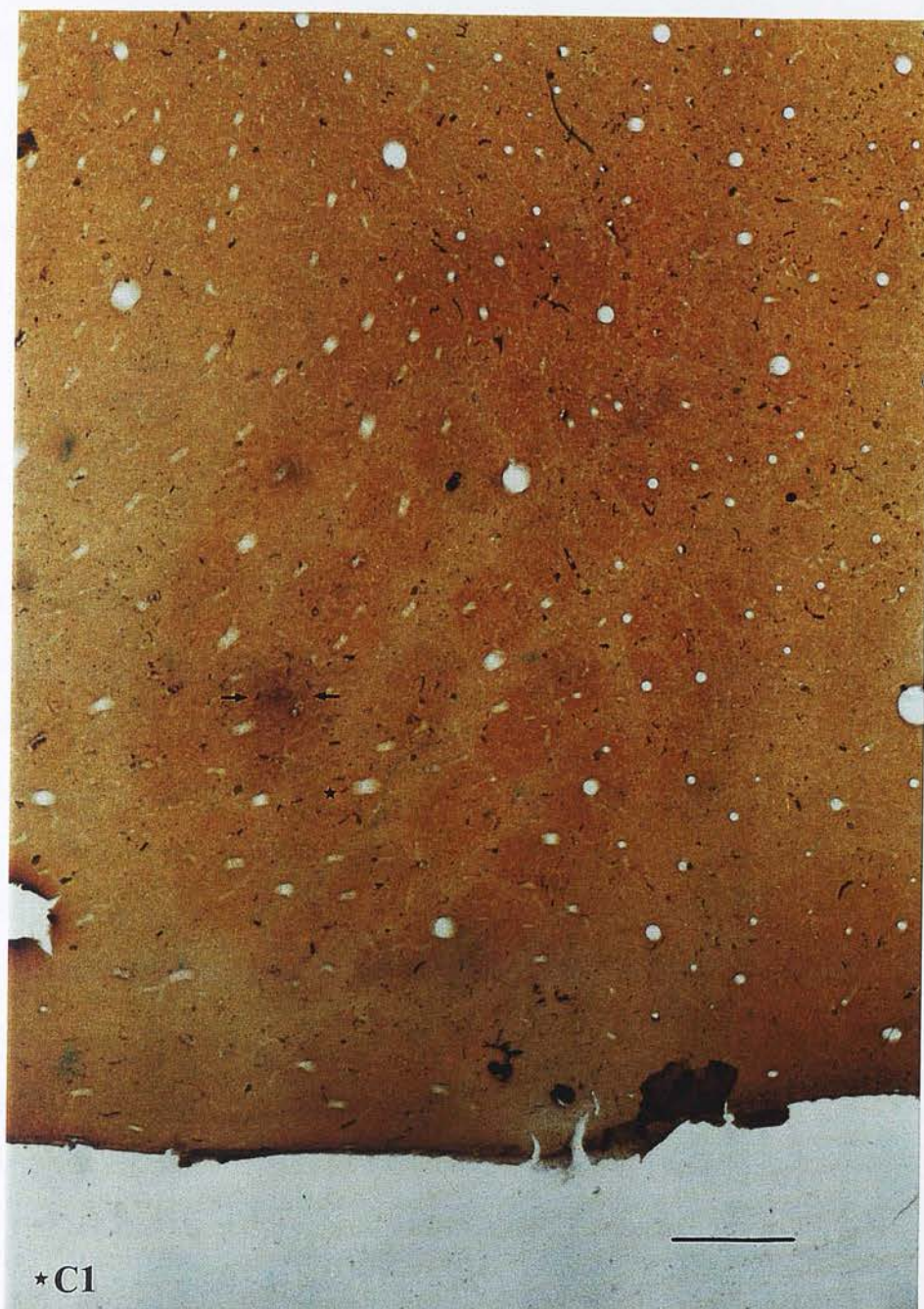


Figure 22. A photomicrograph of a tangentially cut cortical section from a brain containing a small extracellular iontophoretic injection of biocytin. The orientation is as follows: Anterior is to the top of the photograph, posterior to the bottom and the midline to the left. Scale bar 500  $\mu\text{m}$ .

## **17.0 CYTOCHROME OXIDASE HISTOCHEMISTRY**

### **17.1 Tissue Considerations**

This histochemical technique was only performed on tangentially cut cortical sections and coronal sections where the animal was perfused with a low gluteraldehyde fixative (4% paraformaldehyde, 0.05% gluteraldehyde). The method was a modification of the method described by Wong-Riley, 1979.

### **17.2 Visualisation**

Sections were initially washed in 0.1 M phosphate buffer pH 7.4 (PB) in order to remove any fixative from this tissue. The sections were then incubated in a mixture containing 0.03% cytochrome C, 0.025% 3, 3', diaminobenzidine hydrochloride and 4% sucrose in PB for approximately 3 hours at 37°C.

The stain was monitored visually throughout to ensure that the barrel field pattern could be clearly distinguished from the background staining. Once the reaction had developed to the required depth it was stopped by washing in at least 3 changes of PB over 30 min. The sections were then mounted, air dried and coverslipped using DPX. Example of a tangentially cut cortical sections stained for the enzyme cytochrome oxidase can be seen in Figures 1, 15 and 23.

### **17.3 Considerations**

The best results were achieved with the protocol described above. The method was compatible with staining for biocytin as long as the biocytin was visualised with nickel enhanced DAB. There was no preferential order in which to combine the two

techniques. The use of cytochrome oxidase histochemistry was most useful in tangential sections for barrel visualisation. Cytochrome oxidase staining in coronal sections produced the characteristic barrel shape, but did not provide a method for determining which individual barrel had been filled within the barrel field. This produced the problem that the ideal method to determine single cell morphology was using coronal sections but the best way of locating which barrel contained the neuron was using tangential sections.

As cellular morphology was a priority in this study all brains were sectioned coronally rather than tangentially.

## **18.0 FREEZE THAW ETHANOL TECHNIQUE**

In some of the intracellular filling experiments an alternative method to increase ABC binding was used. This method employed an electron microscopic technique rather than the much later light microscope technique of triton membrane disruption.

### **18.1 Membrane Disruption**

The penetration of large molecules (e.g. ABC) into the tissue was improved by a freeze thaw technique. The sections are initially incubated in a solution of 1% sodium borohydride (in 0.1 M phosphate buffer pH 7.4) for 25 min. The sections were then treated with a graded series of solutions containing dimethyl sulphoxide (DMSO) (5%, 10% and 20% for ten min each).

Once the sections had been subjected to the final DMSO solution they underwent a set of 3 cycles of freezing and thawing using dry ice. Excess DMSO solution was removed from the tissue pots and the sections were frozen on dry ice for 30-40 S before being gently thawed at 4°C. Once the cycles were completed the sections were reacted to reveal the biocytin.

The sections were thoroughly washed with PBS before incubation in ABC overnight at 4°C (1:100 in PBS, Vector Laboratories). The sections were then rinsed thoroughly in PBS before being visualised with nickel enhanced DAB for 10 min. The excess DAB solution was washed from the sections before mounting, drying, counterstaining and coverslipped with DPX.

## 18.2 Considerations

This method provided a reliable if more time consuming way of visualising stained neurons. Using this method it was possible to visualise terminal fields from filled cells (see section 34.2.1). The method was simplified for the light microscope by replacing the sodium borohydride and freeze thaw steps with triton X-100 incubations. This method would however provide a reliable method when combined with electron microscope investigation.

For an example of a neuron visualised using this method see figures 69 and 70.

## **19.0 OSMIUM TETROXIDE**

In two cases the sections were treated with osmium tetroxide following a basic em protocol. The protocol was the same as the basic light microscope protocol used at that time except for the DAB development stages.

The sections were quenched for endogenous peroxidase activity using the alcohol method described previously (Metz et al.,1989). The cell membranes were disrupted and the biocytin visualised using the freeze thaw method described previously.

### **19.1 Osmication**

Once the sections had been treated with DAB they were reacted with osmium. The sections were incubated in a 1% osmium tetroxide solution for a total of 30 min at room temperature. Sections were then washed in two changes of phosphate buffer for 5 min each and then in distilled water for two washes of 5 min.

### **19.2 Dehydration and Mounting**

Sections were then dehydrated in a graded series of alcohols starting at 50% for 5 min. The sections were then incubated in 70% ethanol for 20 min and 95% for 15 min and in 100% alcohol for two 15 min washes. Sections were then incubated in propylene oxide for two 10 min washes. To embed the sections they were submerged in durcupan resin (Fluka) for 12 h and then mounted on greased microscope slides and heated to 60°C for 48 h in order to polymerise the resin.

### 19.3 Technical Considerations

Osmication of sections for investigation at the light microscope level was not continued because although the stain produced was intense, there was reduced contrast with the background and the staining of the fibre bundles within the striatum was so dark it made axon visualisation difficult and terminal visualisation impossible. The use of osmium and the durcupan mounting technique provided a method whereby the sections could be placed onto the slides and mounted without air drying them first. However, this method would be required if electron microscopic confirmation of synaptic contacts is attempted.



Figure 23. A photomicrograph of a neuron visualised and mounted using the method described above. Note the similarity of the background contrast with the final intracellular biocytin visualisation protocol. The section is orientated with the pia towards the top of the photograph, the corpus callosum the bottom and the midline to the left. Scale bar 100  $\mu\text{m}$ .

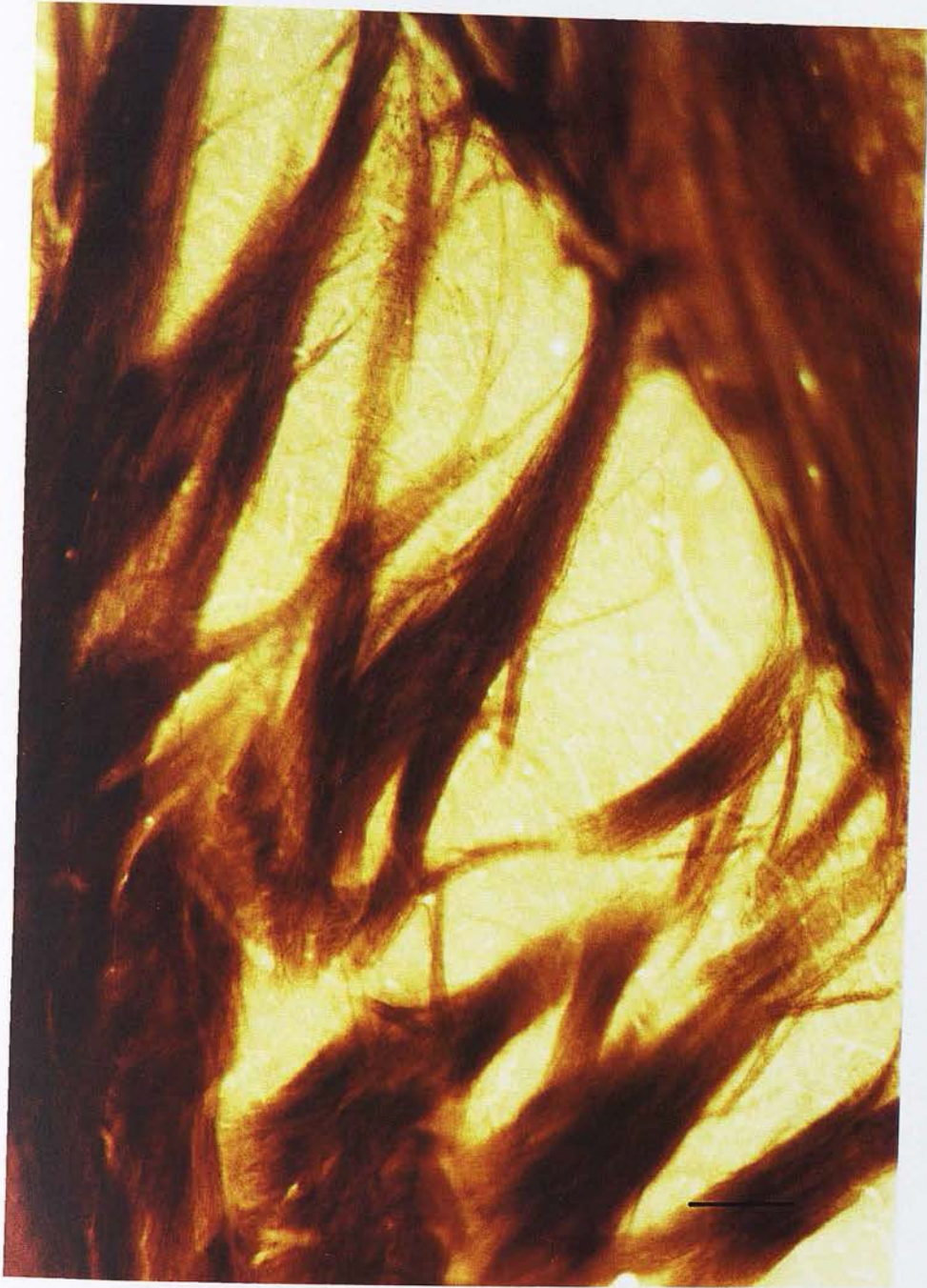


Figure 24. A photomicrograph showing the osmicated striatal fibre bundles. In routine tissue screening it would be almost impossible to distinguish terminals from the intense background stain. The section is orientated with the pia towards the top of the photograph and the midline to the left. Scale bar 100  $\mu$ m.

## **20.0 TRITON AND ELITE HISTOLOGY METHODS**

The previous biocytin protocol was adjusted to include a better peroxidase quenching technique, an easier light microscope tissue disruption technique and a more sensitive and quicker ABC stage. Some experiments used the technique of triton membrane disruption to increase the penetration and binding of ABC molecules to biocytin.

### **20.1 Quenching of Endogenous Peroxidase Activity**

Serial sections were taken and washed to remove residual fixative. Once washed the sections were reacted in a peroxidase quenching solution containing 70% PBS, 30% methanol and 0.03% hydrogen peroxide. The sections were quenched for at least 30 min. The time was, to a certain extent, dictated by the success of the perfusion, the presence of obvious blood throughout the brain when cutting or the presence of blood on the cortical surface.

### **20.2 Visualisation**

After quenching the sections were washed at least seven times in BS in an attempt to remove the peroxide reaction mixture from the sections. Residual quenching solution resulted in the entire section turning a brown colour (or black in the case of nickel enhanced DAB) masking the specific reaction product. This quenching stage was performed prior to the ABC stage. The resulting sections had a low level of background staining and the staining of erythrocytes across the tissue was minimal.

In order to visualise the sections were incubated initially in PBS-TX for one and a half hours prior to incubation with the ABC solution. This was performed in order to increase binding between the and the ABC molecule. The sections were then incubated

in ABC standard kit (1:100 in BS-XT; Vector Laboratories) at 4°C overnight or in ABC elite kit (1:50) for 1 hour at room temperature. The sections were then rinsed in BS and visualised using a vector DAB kit with nickel enhancement for 10 min. The sections were then washed three times in BS and mounted on microscope slides. Once mounted the sections were oven dried and then counter stained with methyl green prior to coverslipping with DPX.

### **20.3 Adaptations**

The triton elite protocol described previously was refined even further to increase ABC penetration and binding (the method still used the methanol quenching technique described previously).

The exposure to triton X100 in a PBS prewash was increased to 3 hours and the exposure to the elite ABC was extended to 18 hours (1:50 in PBS-TX at 4°C). The DAB was visualised, mounted and coverslipped in the same way as described above.

## 21.0 FINAL INTRACELLULAR BIOCYTIN PROTOCOL

### 21.1 Biocytin Visualisation

The final biocytin method used was a result of developing the previous methods. The sections were washed to remove the fixative as usual but were not peroxidase quenched. The sections were incubated for 5 hours in PBS-TX before being incubated in ABC elite (1:50 in PBS-TX) at 4°C for 60 h. The sections were then washed three times in PBS to remove any residual ABC and visualised using DAB and washed three times in PBS prior to mounting. The sections were not treated for a set time in DAB as in previous protocols but were incubated in the DAB solution until the sections developed a dark brown colour (approximately the same colour as successful cytochrome oxidase stained sections). This brown colouration gave the best contrast between background and stain colour for terminal visualisation. The sections were then well rinsed in PBS before being mounted onto chrome alum subbed microscope slides, dried and coverslipped with DPX. The sections were not counterstained with methyl green as the colouration produced with the DAB background provided sufficient contrast and also allowed the clear distinction between layers IV and Va. For examples of neurons visualised using this method see figures 49 and 77.

## **22.0 BIOCYTIN HISTOLOGY METHODS**

All the biocytin histology methods employed throughout this study appeared to be successful for the recovery of filled neurons. They all gave successful terminal visualisation (see results section) in a few cases.

### **22.1 Methanol Quenching**

Methanol quenching of endogenous peroxidase activity (i.e. from erythrocytes) may have been advantageous where the animal was not successfully perfused, where the tissue appeared partially fixed or where the recording procedure or surgery resulted in tissue damage and bleeding. Such damage was almost unavoidable due to the high density of blood vessels in the vibrissal region of somatosensory cortex (Patel, 1983). The quenching method was eventually dropped from the protocol as the presence of endogenously stained peroxidase provided an inbuilt control to prove that the DAB reaction had been successful.

### **22.2 Triton-X100**

The use of triton in the histology protocols helped destroy the membranes surrounding the filled neurons. This aided the binding of the large ABC molecules to the biocytin. Whilst the triton produced an increase in binding it didn't allow complete visualisation of the axon. Elements of the filled cell that were located within the heavily myelinated areas e.g. fibre bundles of the striatum and the internal capsule proved difficult to disrupt with triton for complete visualisation.

### 22.3 Elite Versus Standard ABC

The elite vector kit increased the sensitivity of the reaction to biocytin by anything up to a factor of 5 (manufactures literature). In a bid to visualise the biocytin filled terminals the initial fix of 0.05% glutaraldehyde was replaced by a higher (1.25%) glutaraldehyde fix. From the literature (Smith, 1992) it appears that high gluteraldehyde fixation is necessary for the visualisation of biocytin filled terminals. These two factors ensured that if biocytin filled terminals were present in the tissue it was more than likely that they would be visible.

The use of increased incubations in triton and elite in the last protocol and the development of the reaction product to produce a high background were all aimed at maximum development and visualisation

Using all the biocytin histology methods the majority of cells were recovered in their entirety (i.e. cell body, spiny apical, basilar dendrites and axon collaterals). The few cells that were not recovered from intracellular fills were lost due to biocytin breakdown within the tissue which may occur via two routes. Firstly it is possible that if the time between intracellular fill and sacrifice was too long then the biocytin may have been broken down. Biocytin is a very rapid antrograde tracer (e.g. labelling of the corticostriatal path may take as little as 4 hours (Smith, 1992) compared with HRP or PHaL and too long an incubation may have resulted in biocytin that was injected directly into a cell being broken down. In these experiments an incubation time of around 3 hours was used. This was based on previous extracellular biocytin injections where terminal fields were observed in striatum after survival times of 5 hours. Thus working on the assumption that the 5 hour incubation must also have included a period where the cells were actively taking up sufficient biocytin to be detected at the post-synaptic terminal site, a reduced period seemed valid for direct intracellular fills. This

success can be seen in the case highlighted in figures 45 and 47 where post-synaptic terminal fields are clearly visible in the striatum.

Lack of biocytin filled neurons may also have been due to the presence of tissue damage to the cortex setting off a cascade of reactions which resulted in biocytin being degraded or the fact that the neuron itself died.

The initial methods of reduced incubation in elite, triton and DAB produced tissue with a low background stain. This may provide a quick method for biocytin visualisation at the LM level. In producing a low background stain make this method made axon and terminal field visualisation relatively easy in serial sections. The nickel enhanced DAB was used in a bid to increase the contrast between the stain and the background (black DAB versus a green counterstain) (see figure 44). The nickel enhancement was eventually abandoned because in cases where the background was high the black stain produced by the nickel makes it especially difficult to distinguish the axon and terminal fields in subcortical structures (more so than with the brown DAB colour).

The later method of increased elite and DAB incubations were made in a bid ensure that all aspects of the filled cells were revealed. However, as a by-product it also made the background level much higher, thus reducing contrast. Therefore a careful balance between developing cellular aspects and obscuring them by increasing the background must be maintained.

This method did however provide an interesting point. The increased brown background produced a stain that had similarities with the cytochrome oxidase reaction product i.e. cortical lamination patterns and a distinction, albeit weak, between barrels and septa. Thus in some cases it was possible to determine, to a certain extent, the laminar location and location with respect to barrels. In earlier cases the background

stain was provided by the methyl green (nuclear) counterstain. When this stain was kept deliberately darker than usual it was possible to clearly see the cortical lamination pattern (especially layer IV, Va and Vb divisions) but visualisation of the barrels in layer IV was impossible with any degree of accuracy (see figures 47 and 49). For comparisons of a dark DAB brown background and dark methyl green background for lamination and barrel determination see figures 44 and 77. Essentially the preferred method may be down to personal choice of background to stain contrast.

In all cases the serial sections were air and oven dried onto subbed slides prior to coverslipping. This method of mounting and drying the sections caused the snake like path and corkscrew like appearance of the dendrites within sections. This artefact could be reduced by treating sections with osmium tetroxide (onto slides in resin which was then polymerised under coverslips). By this technique the sections were not allowed to dry in air. For air dried sections correction factors can be applied (but not in these cases) but the true extent of shrinkage cannot be known.

### 23.0 ERRONEOUS FILLS

In some rare cases, examination of the tissue after histological processing revealed the presence of 'extra' neurons that were not filled via intracellular recordings. There are two possible causes for the presence of these extra neurons.

In some cases (where these filled neurons were close to the pia) the presence of ghost like neurons may have been a result of the preparation procedure for intracellular recording. Electrodes were initially advanced 100  $\mu\text{m}$  into cortex and then 'cleared' using a brief hyperpolarising current to correct any blockages before their resistance (and suitability for intracellular recording) were established with a bridge balance amplifier. In the process of clearing the electrode it is possible that sufficient current passed through the electrode to allow biocytin to be ejected from the electrode, taken up by a cell and later revealed histochemically. This method of non-physiological filling might also have happened in deeper cortical layers where in the process of electrode advancement during recording the electrode became blocked.

A second means non-physiological filling is via leakage from a physiologically defined and filled neuron. In these cases the seal around the electrode in an impaled neuron was poor enough to allow the biocytin ejected during the filling procedure to leak from the filled cell and be actively taken up by neighbouring cells. Another possibility is that even in cases where the seal is tight there may have been leakage of the tracer through junctions and channels connecting neighbouring cells e.g. gap junctions. These cases can be determined as they appear as ghost like fills of a cell body, or the cell body and the apical dendrite, close to neurons that have been successfully filled and are more heavily stained (see figure 25). In some cases the link between the two cells can even be seen. Where it is possible to determine that a neuron was filled by one of the methods described above they have not been included in the morphological data.

Neurons that were classed as being filled from direct intracellular current injection were examined initially for the success of filling, success of staining and classification of cortical layer. In cases where the neuron appeared to be poorly filled (from direct current injection) it was only possible to reconstruct the soma and the ascending apical dendrite. Thus the only information available from these neurons was whether or not the apical dendrite could be clearly seen to ascend from the soma, a recorded depth value and in which cortical layer the apical dendrite branched. In cases where the neuron was successfully filled and recovered histologically the neuron was investigated for the presence of an axon that left the cortex.

In general terms, fill times of at least 2 min resulted in cells that could be detected, albeit weakly, in cortex with the soma and apical dendrite present. With these short fill times it was unlikely that the axon left the cortex and resulted in filled terminals. In the last surgical protocol the small hole in the cortex made it difficult to introduce further electrodes into cortex for recording after a successful intracellular fill without causing damage to the cell or even killing the actively transporting cell or filling two cells very close together (see section 34.1.2). It may be possible, especially with the extensive basilar dendrite, to impale the same neuron. Thus generally if a neuron was filled for less than approx. 2 min it was assumed that the cellular staining would prove poor and other electrodes were advanced into cortex in a bid to achieve a single successful intracellular fill. In these cases it was assumed that only the successful fill would be identifiable and any axons or terminals present would have arisen only from it.

In the earlier experiments it was easier to reposition the electrode successfully and make a note of one cell's position with respect to another (see section 34.1.3) but it was almost impossible to say which axon (and axonal path) belonged to which cell in serial sections and in cases where terminals were present it was impossible to assign them to a particular cell. In later experiments where the working area was greatly

reduced two filled neurons made it impossible to dissect even the basilar dendrites of each cell. In cases where layer III and layer V pyramidal neurons were filled together (see figure 44) there are problems assigning axon collaterals as both layer Va and layer III neurons have extensive axon collaterals in layer Va. Axonal and terminal field problems did not arise as the layer III neurons filled in this study did not project subcortically.

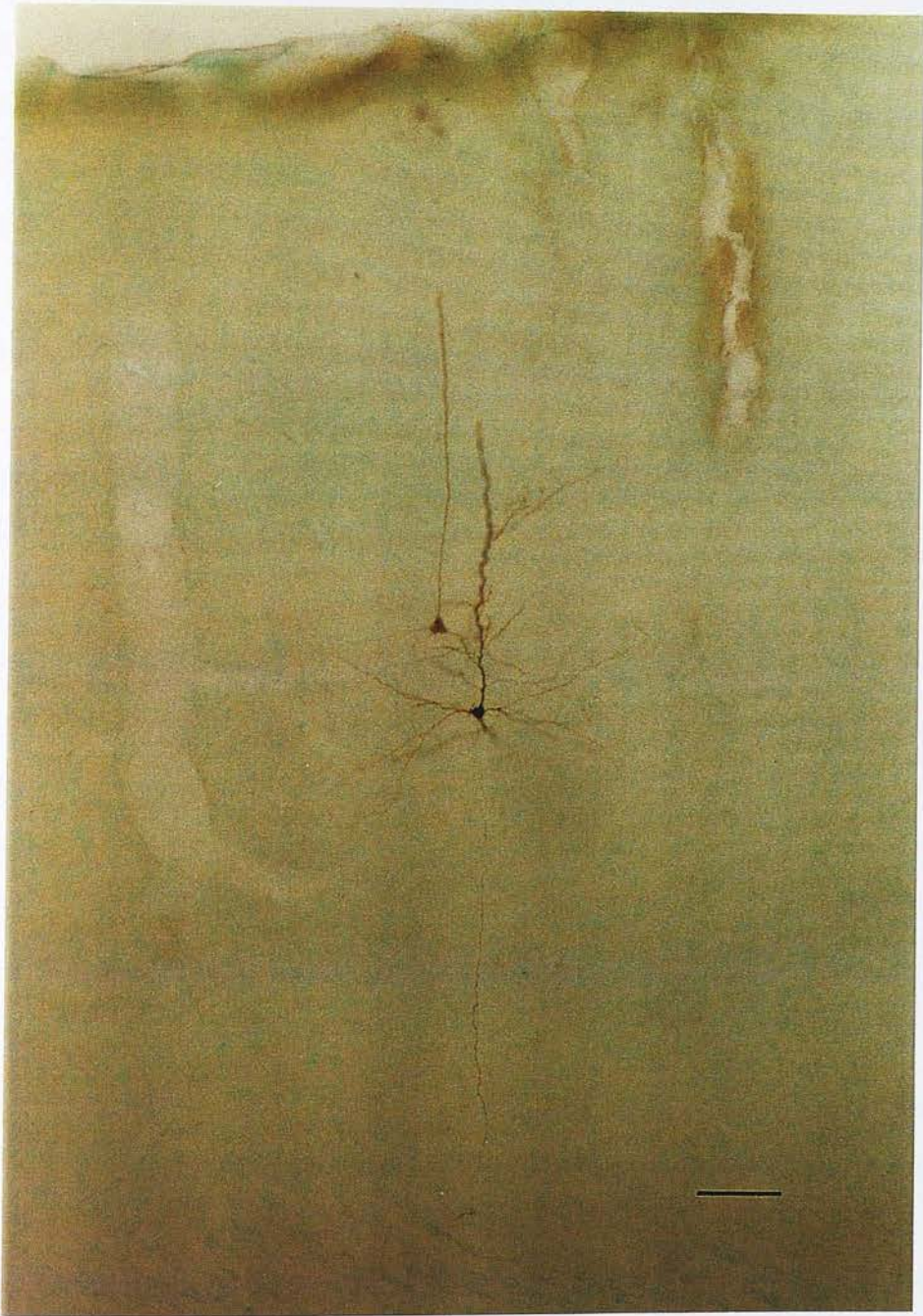


Figure 25. A photomicrograph showing an example of a ghost like cell resulting from poor filling. Note that only the soma and the apical dendrite are clearly visible. The section is orientated with the pia towards the top of the photograph, the corpus callosum the bottom and the midline to the left. Scale bar 100  $\mu\text{m}$ .

## 24.0 INVESTIGATION AT THE LIGHT MICROSCOPE LEVEL

In all cases where cells were filled with biocytin the serial sections were investigated at the light microscope level. The sections were searched for the presence of an intact neuron i.e. the presence of a soma, apical dendrite, basilar dendritic tree and an axon leaving the cortex.

### 24.1 Morphological Classification of Neurons

Once a neuron had been filled and visualised using any one of the biocytin histology protocols described (see sections 18.0 to 21.0) the serial sections were examined to determine the morphology of the neuron. In order to reliably determine the morphology of the neuron the following had to be present:

Soma

Apical Dendrite

Apical and Basilar Dendritic Trees

Axon Collaterals (whilst an aid to classification the presence of these was not essential)

Examination of the serial section could reliably produce a morphological classification prior to camera lucida reconstructions as in many neuron the soma, apical dendrite and the apical and basilar dendritic trees were visible within the one section. The apical and dendritic trees extended over several sections (depending upon the cell and the case but generally the extent of the trees could be established).

The classification used for classification were the same as those described in vitro (for a review see Connors and Gutnick, 1990). The criteria used were as follows:

### **1) The Branch Point of the Apical Dendrite**

In the case of IB neurons the apical dendrite branches within layer IV/III. In RS neurons the apical dendrite branch occurs more dorsal (within layers III/II or in some cases close to the pial surface).

### **2) The Horizontal Extension of the Apical and Basilar Dendritic Trees**

Intrinsically bursting neurons have more extensive apical and basilar dendritic trees than RS neurons. These dendrites also extend further horizontally in cortex (see Introduction and Connors and Gutnick, 1990).

### **3) The Laminar Distribution of the Axon Collaterals**

Examination of the serial sections revealed that the axon collaterals of the IB neurons extend horizontally within layer V whereas the axon collaterals of the RS neurons are localised in the region of the basilar dendrites and extend vertically towards the pia (as in vitro).

The most reliable classification can be determined by examining the branch point of the apical dendrite and the horizontal extension of the apical and basilar dendritic trees. The use of the axon collaterals for classification was used to confirm a classification established through the first two criteria as axon collaterals do not appear clearly in every filled neuron. In neurons where either the neuron is poorly filled, visualised or fixed within the tissue axon collaterals can be absent. In some cases where they are present they may not be present in their entirety (and hence may be little use for classification).

## 24.2 Subcortical Projections

The axonal pathway was followed to confirm if the axon entered the corpus callosum and if it innervated subcortical structures e.g. the ipsilateral thalamus and striatum. The passage of the axon through the striatum was also noted to establish if the axon ran through the fibre bundles within the striatum *en route* to the thalamus and brainstem or if the axon ran into the striatal matrix and also for axonal branching giving several possible terminal fields.

The serial sections were examined to establish the final section on which the final piece of the cell could be detected and whether the cell sent an axon to the internal capsule, thalamus or the substantia nigra. Once the extent of the axon was established the tissue was examined for the presence of terminals i.e. possible pre-synaptic contacts. The presence of terminals was established using a x100 oil immersion objective.

Terminals were established on 4 criteria:

- 1) The suspected terminals appeared to run through the entire depth of the section in question. If they did not they were classed as either surface contamination of the section or background tissue staining.
- 2) They could be clearly traced back to the axon either in the section in which they occur or in an immediately adjacent section.
- 3) In some cases the presence of boutons was noted (although not in all cases). The terminal field was also viewed with the terminal field patterns see in anatomical tracing studies in somatosensory cortex (Wright et al, 1998). The patterns and descriptions from comparable studies from in vivo intracellular studies from rat motor cortex were

also considered (Jinnai and Matsuda, 1979; Donoghue and Kitai, 1981; Wilson et al., 1982; Landry et al., 1984; Wilson, 1986; Cowan and Wilson, 1994).

4) The suspected terminal fields were also examined by two people with experience in the detection and characterisation of terminal fields both generally and specifically in the barrel region of primary somatosensory cortex.

The neurons were then reconstructed using a conventional camera lucida attached to a Nikon microscope. In some cases the cells were photographed in black and white (developed in house) or colour (developed by a commercial company).

## 25.0 IN VIVO VERSUS IN VITRO

In this study an intracellular in vivo technique was used in a bid to study the corticostriatal pathway rather than an in vitro preparation. The reasons for this choice are several:

1) An in vivo preparation is superior to an in vitro preparation in that it is possible to record cortical responses to as near natural peripheral stimuli as possible. In this study the stimulus was a rapid whisker deflection via a piezoelectric bimorph chip attached to an individual whisker. In an in vitro preparation the stimulus would involve direct electrical stimulation of the thalamus or cortex.

2) In an in vivo preparation the somatosensory information from the periphery is directed through an entire intact ascending system including the trigeminal and thalamic stations. Thus in this case the cortical responses are as near natural as possible. With the intact in vivo system the corticothalamic as well as cortico-cortical systems and the interactions between the substantia nigra, the striatum and the cortical inputs are also intact. In the in vitro preparation the facial and trigeminal processing stages have been severed as well as intrathalamic, thalamocortical and intracortical connections.

3) In studying the subcortical projections from somatosensory cortex filling a neuron and its subcortical targets in their entirety may be impossible with a slice preparation (max. thickness 500  $\mu\text{m}$ ). In the case of cell body and dendritic filling, especially the IB neurons that have basilar dendrites that extend upto 600  $\mu\text{m}$  from the soma. In the case of terminal fields visualisation may be impossible since neurons projecting to the brainstem cannot have their terminal targets within the slice. As another example, in this study it was observed that it was possible for neurons that projected to the striatum and brainstem targets to send a branch of the axon running in an anterior direction and

innervate the striatum as well as a branch running in a posterior direction towards the brainstem. The only way to visualise both is in an in vivo preparation.

4) In vitro may also offer advantages over in vivo in that the recording stability is greater in vitro e.g. in the case of cortex the maximum recording time of the layer V pyramids was approx. 30 min (the majority of this time taken up with neuronal filling). Recordings in vitro on the other hand may be stable for at least an hour. Other advantages are that it is possible in vitro to isolate and record solely from layer V much more easily than in vivo. This is highlighted by cases in this study where for example a recording at a depth that would suggest layer III was actually a recording from the apical dendrite of a layer V neuron that innervated the thalamus (see section 34.2.1 and figures 69 and 76).

With in vitro recordings it is also possible to identify the barrels within layer IV (See Agmon and Connors, 1991) and record specifically layer V projection neurons that are associated with the barrels. In this in vivo study some neurons have been assigned to barrel centre or sides or septae according to response latencies and inhibitory periods between the initial phase of firing and resumed firing. As location has not been confirmed histologically the position with respect to barrels is by no means certain.

## 26.0 INTRACELLULAR RECORDINGS IN VIVO

An important consideration when analysing the results of intracellular tracing studies is the rarity of successful recordings with complete filling and tracing of the axon path and terminal fields.

In studies of this kind very few recordings result in successful terminal field fillings. As the methods developed (see methods chapter) a variety of recordings were made. These recordings included:

	Unfilled	Filled Not visible	Filled Visible	Filled V.T.F.*	Total
<b>Recorded</b>	75	30	24	4	133
<b>Unrecorded</b>	0	0	2	2	4
<b>Totals</b>	75	30	26	6	137

\* Visible Terminal Field

Figure 26. A table showing the variety of recordings that were made in this study.

	Morphology IB	Morphology RS
Physiology IB	11	none
Physiology RS	none	12

Figure 27. A table highlighting the correlation between the physiological and morphological classification of neurons in this study. Note that whilst IB neuron can be mistaken for RS neurons based on their physiology alone RS neuron are never mistaken for IB neurons based on their physiology. In no case was any cell for which there was both physiology and morphology misclassified from any of the physiological records.

Only in a very small minority of experiments, was a neuron traced in it's entirety. However, if all of the other classes of neuronal records were disregarded the richness and complexity of neuronal responses to whisker stimulation and the variation in

morphological characteristics within the neuronal subgroups would be lost. Thus, the results section describes neurons that reveal their terminals and their cellular morphology alongside a physiological response to whisker deflection. These cells will be classed according to the system described in the introduction using their morphology and their physiology. Cells possessing only morphology can be classed according to their morphology; neurons possessing only physiology can be classed according to physiology.

Initially in this section, the physiological characterisation of all intracellular recorded neurons will be described. Once these are established, the morphological characteristics of the subset that have been filled will then be discussed. The final cells to be examined will be those with probable pre synaptic contacts visible. Although the physiology and the morphology will be discussed separately the two have been very closely linked in the studies in vitro (for a review see Connors and Gutnick, 1990). We will present evidence that a similar but not identical relationship exists in vivo.

## 27.0 ELECTROPHYSIOLOGY RESULTS

In this study all 4 classes of the layer V pyramidal neurons were studied both morphologically and electrophysiologically.

The stimulation and recordings in this study differ from those recorded in vitro and quoted in the literature. In these studies the stimulus was maintained throughout the recording. In this in vivo study the stimulation was a brief whisker deflection and thus the response recorded was to a short lived stimulus.

In all cases one important difference was consistently observed between the in vitro literature and this in vivo study. The recordings were never as 'clean' as those observed in vitro. In the in vivo study there was always a significant background synaptic activity associated with the resting membrane potential. It is impossible to say what the cause of this activity is although it is possible that it may be a result of synaptic interactions either in cortex itself or activity that is arising from the thalamus. This background activity can be clearly seen in all the physiological traces in this work. Both 'Scope' and 'VCR/Chart' records are shown here. 'Scope' records can be identified as traces with timebases recorded as either a 100 or 10 mS scale bar. In these cases the stimulus occurs 10 mS into the recording. In 'VCR/Chart' records the time base shown is a time frame taken a stated time from the start of recording (onset of stimulation = time 0). The exact location of the stimulus within these records is unknown. In these cases the record highlights the typical firing pattern of the neuron.

As there is a difference in the activity of neurons and their firing patterns between in vivo and in vitro, the neurons recorded here have been classed as being either RS or IB. Only cells that have been recorded and identified morphologically have been classified further (IB and RS 1 or 2) (Cauller and Connors, 1994).

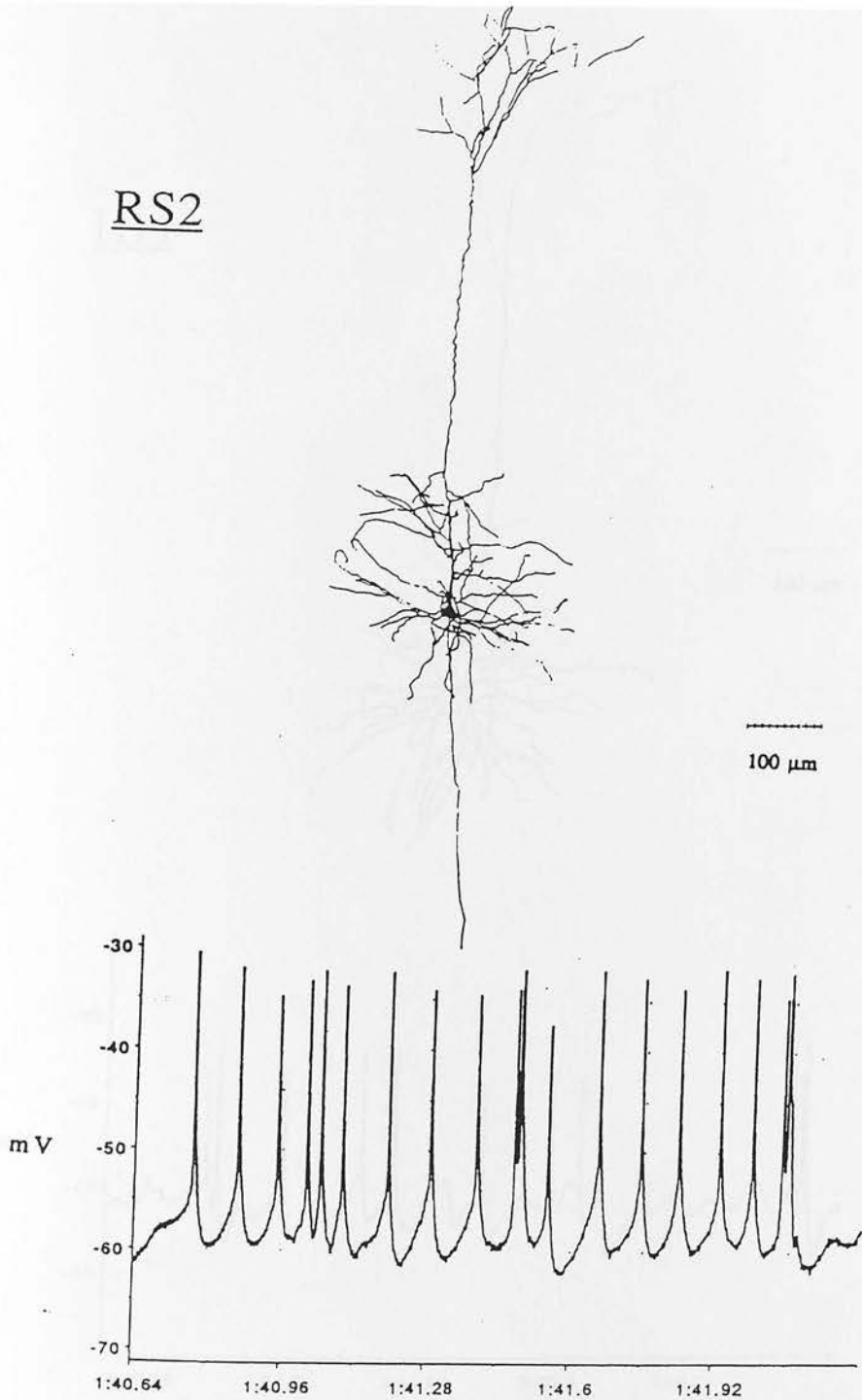
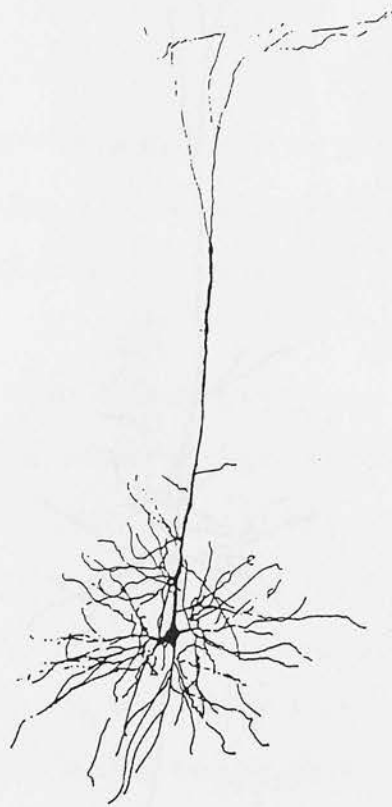


Figure 29. A typical example of a camera lucida reconstructed RS2 neuron (scale bar 100  $\mu\text{m}$ ) and its response to piezoelectric whisker stimulation. The trace shown is a 'Chart' recording and as a result the position of the stimulus is unknown (although the stimulus amplitude and duration remains the same) ( see sections 11.3 and 27.0). The neuron is orientated with the pia towards the top of the page, the callosum to the bottom and the midline to the left.

IB1



100  $\mu\text{m}$

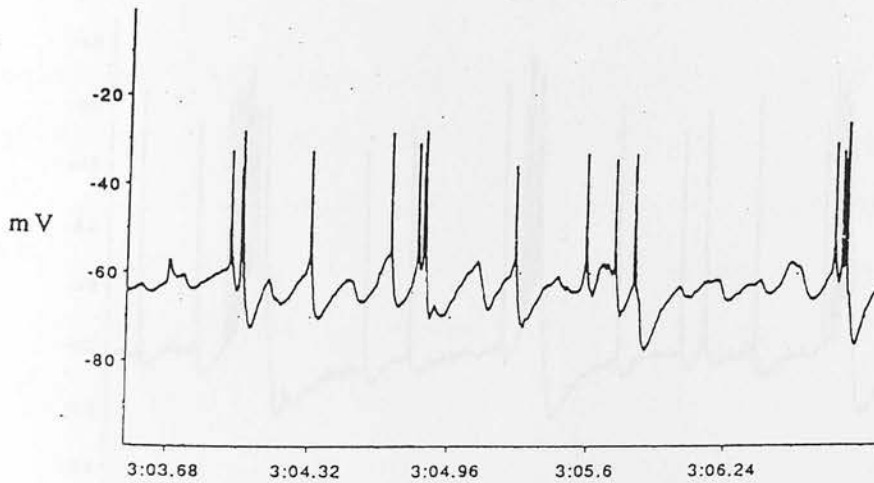
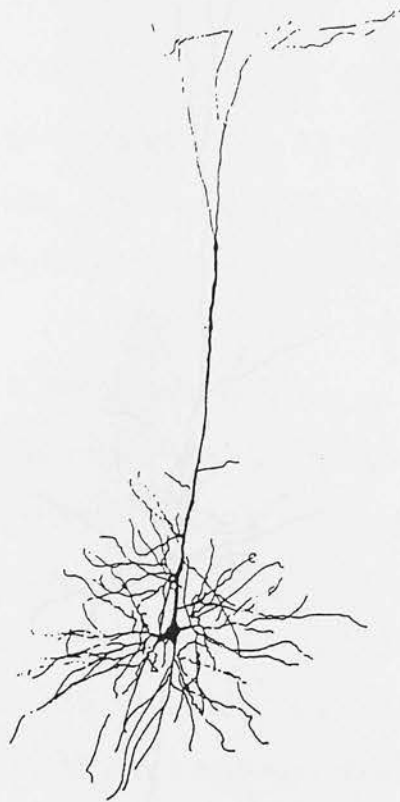


Figure 30. A typical example of a camera lucida reconstructed IB1 neuron (scale bar 100  $\mu\text{m}$ ) and its response to piezoelectric whisker stimulation. The trace shown is a 'Chart' recording and as a result the position of the stimulus is unknown (although the stimulus amplitude and duration remains the same) ( see sections 11.3 and 27.0). The neuron is orientated with the pia towards the top of the page, the callosum to the bottom and the midline of the left.

IB1



100  $\mu\text{m}$

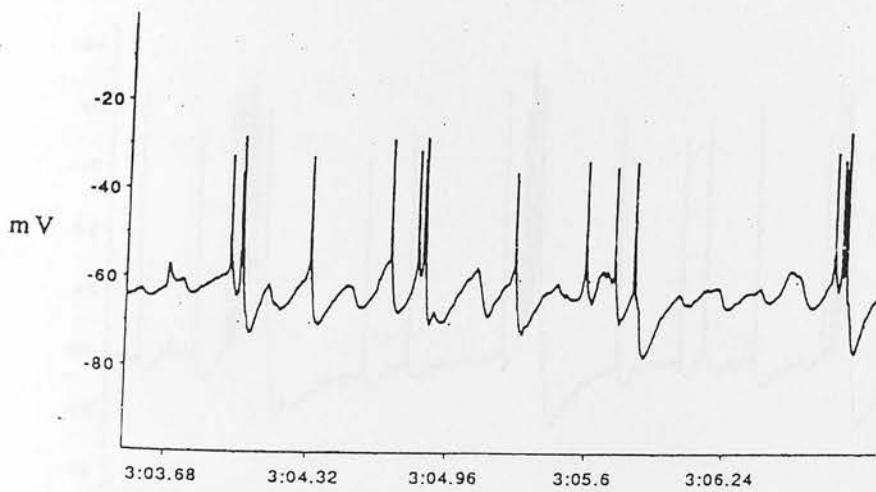


Figure 30. A typical example of a camera lucida reconstructed IB1 neuron (scale bar 100  $\mu\text{m}$ ) and its response to piezoelectric whisker stimulation. The trace shown is a 'Chart' recording and as a result the position of the stimulus is unknown (although the stimulus amplitude and duration remains the same) ( see sections 11.3 and 27.0). The neuron is orientated with the pia towards the top of the page, the callosum to the bottom and the midline to the left.

## IB 2

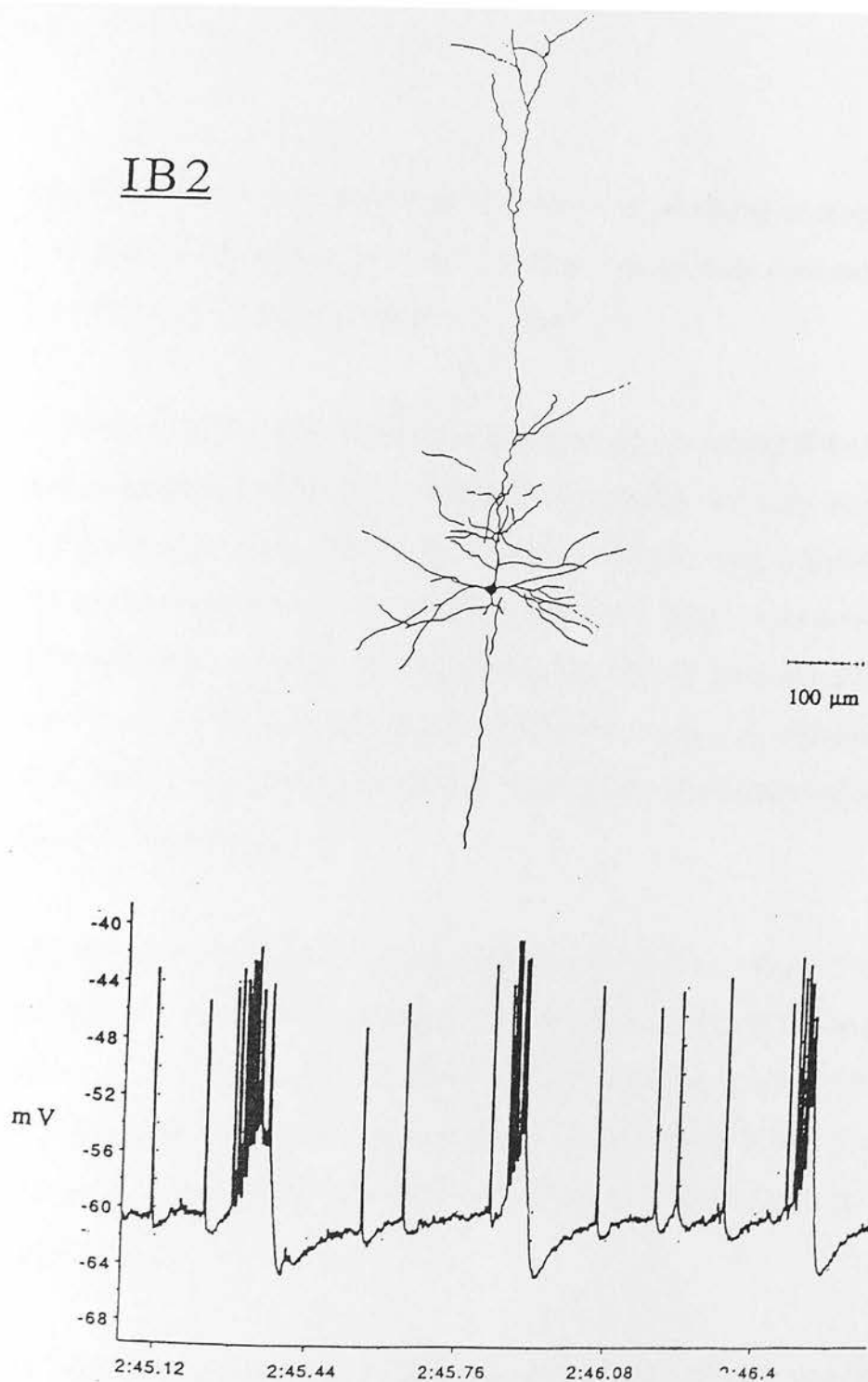


Figure 31. A typical example of a camera lucida reconstructed IB2 neuron (scale bar 100 μm) and its response to piezoelectric whisker stimulation. The trace shown is a 'Chart' recording and as a result the position of the stimulus is unknown (although the stimulus amplitude and duration remains the same) ( see sections 11.3 and 27.0). The neuron is orientated with the pia towards the top of the page, the callosum to the bottom and the midline of the left.

Another difference in the physiology seen here is that the resting membrane potentials were much higher than in vitro. The spike heights in this study were smaller than would be expected and they rarely crossed zero.

There were two important differences between in vivo recordings of the IB neuron and the in vitro literature. The first difference was that as well as having background synaptic activity, the bursts themselves appeared different to those described in vitro. The typical shape of a burst is described in vitro is 3-5 action potentials riding on a slow depolarising envelope. The depolarising envelope and the burst were typically similar to those seen in figures 30, 31, 36 and 37. In this in vivo preparation rather than the first action potential in the burst riding on the depolarising envelope it appeared to precede it.

Secondly the burst firing seen throughout this study was very varied. It was very uncommon to see the typical arrangement of burst firing that is seen in the in vitro studies of the literature where bursts are highlighted as being the sole response to a stimulus. In this study it was very uncommon for a burst firing neuron to solely fire bursts. The most common patterns were a combination of bursts and single action potentials.

In contrast the firing patterns of RS neurons in this study were similar to those described in the literature. Their only response to stimulation was to fire either single or double action potentials. Under no conditions investigated in this study did cells classed as RS fire bursts. An interesting fact to note is that it was difficult to distinguish RS2 and IB1 neurons on the basis of their physiology. This was because IB1 neurons may predominantly fire single or double action potentials in response to a

non principal whisker (see firing patterns across whiskers). Thus an IB1 neuron may be incorrectly classed as an RS2 neuron.

### 2.5.1 Introduction

With all cell classes action potentials were followed by afterhyperpolarisations (AHP). In the case of burst firing cells, the depth of the hyperpolarisation was to some extent dictated by the number of action potentials in a burst. Increasing the number of action potentials in a burst usually resulted in a more hyperpolarised AHP but they were also associated with the single action potentials of RS neurons.

An important observation was that after the stimulation of the neuron by a whisker its initial response was to fire an action potential (single, double or burst). That was followed by a variable period where the cell was inhibited before it resumed the firing pattern characteristic of the cell class.

## 28.0 RESULTS 'SCOPE'/VCR ANALYSIS

### 28.1 Introduction

From the intracellular 'Scope' recordings in this study it appears that the layer Va intrinsically bursting neurons form the largest group ( $n = 47$  IB neurons compared to  $n = 34$  RS neurons). Both the physiological and morphological classifications were compared to the extensive literature available from *in vitro* preparations (See Connors and Gutnick, 1990). Whilst there are obvious differences in the physiology of the neurons the main classification of morphology is unchanged.

Generally, the intrinsically bursting neurons were identified by their ability to generate a cluster of 3 or more action potentials riding on a depolarising envelope.

Morphologically the neurons were identified by their large and extensive apical and basilar dendritic trees as well as the branch in the apical dendrite within layer III (Connors and Gutnick, 1990).

In all cases where filled neurons were visible the morphological and physiological classifications were determined independently of each other. Cases where the physiological and morphological classifications matched were used as the 'benchmark' for that classification. The same approach was used for the RS neurons. Initially the physiological class was determined using 'Scope' records and confirmed using VCR/'Chart' records.

### 28.2 'Scope' Records

In the cases where 'Scope' records were available a number of data values were obtained from the traces in order to calculate mean and standard deviation values for a

number of aspects of the traces these aspects included the response latency, number of action potentials within the initial response to the stimulus and the length of the inhibitory period. Each average and standard deviation value was obtained from 8 consecutive whisker stimulations for a predetermined whisker. As with the classifications, the data analysis were performed independently to the cell's morphology. Upon analysis of the data a number of patterns became evident:

### **28.3 Latency Values**

There were slight but noticeable differences between response latencies recorded in IB neurons in layer Va throughout this study.

### **28.4 Single Whisker Recordings (n = 15)**

All of the neurons recorded have response latencies that are within the values that are typical of layer Va from extracellular recordings (Armstrong-James et al, 1992; Armstrong-James, 1995).

### **28.5 Multi-Whisker Recordings (n = 37)**

Where multi whisker recordings were made it was possible to compare the response latencies to different whisker deflections within an arc. In these cases two patterns were evident.

1) In some recordings it was apparent that there was little difference in response latencies between the three whiskers. There were however two whiskers that had very similar latencies, the third had a longer latency (see figure 35). In these cases it was assumed that the neuron was located within either the side (or septa) of one of the

barrels closest to the barrel corresponding to the whisker producing the similar latency. The neuron was assumed to be furthest away from the whisker barrel producing the longest latency. In these cases the pattern of response latency closely resembled the whisker pattern. For example where the PW was assumed to be either D1 or B1 the closest adjacent whisker was C1.

2) In some cases a single whisker produced a noticeably shorter response latency. In these cases it was assumed that the neuron was located within the centre of that barrel (see figure 34).

In both cases the location of the neuron is speculative as tangential sections were not taken through the cell to confirm the position of the neuron within the barrelfield.

	<b>Intrinsically bursting</b>	<b>Regular spiking</b>
<b>mean</b>	13.05	13.91
<b>standard error</b>	0.76	1.29
<b>median</b>	11.73	13.38
<b>count</b>	34	13

Mann Whitney U test shows that the two values are not significantly different from each other

Figure 32. Examples of the variations in latency and standard deviations of the IB and RS layer V pyramidal projection neurons.

When all the PW data for a cell class is plotted on a histogram the following patterns are observed:

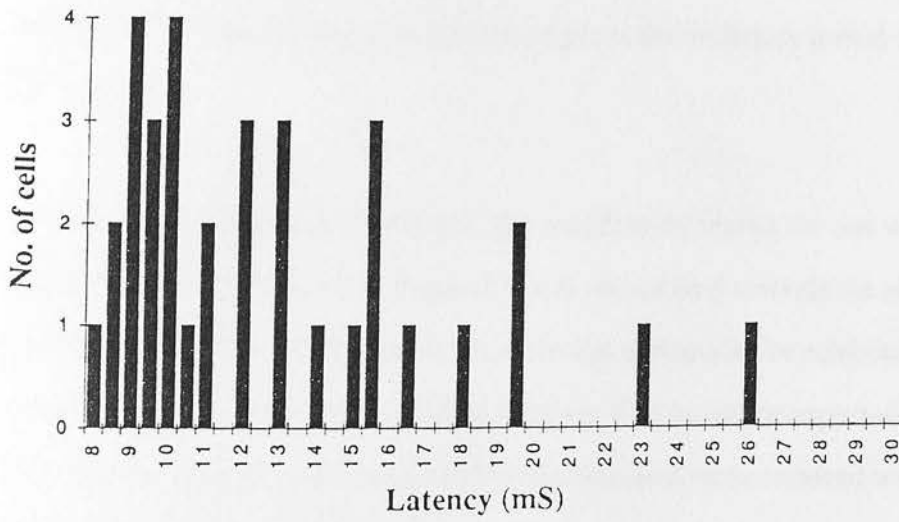
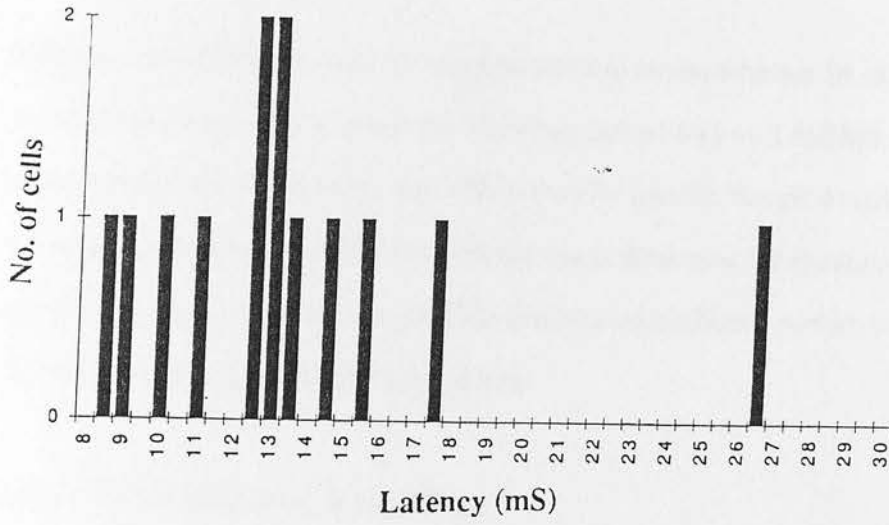


Figure 33. A frequency histogram showing the variations in latencies seen within a) the RS and b) the IB neurons.

## 28.6 INHIBITORY PERIOD

### 28.7 Single Whisker Recordings

Inhibitory period values were obtained in order to assess whether IB or RS neurons showed differences and whether the inhibitory period was well defined (taken as indicating that the cell was located within the PW barrel). 'Scope' overlay records of the original traces were obtained and examined to determine the duration of the inhibitory period assuming it is possible that shorter inhibitory periods indicated that the neuron was located in the barrel centre.

### 28.8 Multi-Whisker Recordings

Where inhibitory period data was available for more than one whisker the data was used to try to confirm the location of the neuron within the barrelfield. From the results in this study it became apparent that the length of the inhibitory period was related to the latency.

Where the inhibitory period of a cell was significantly shorter for one whisker than for the other two whiskers it was assumed that it was located towards the centre of that barrel. The cell that had the fastest response and appeared to be subjected to fewer inhibitory effects from intracortical processing. This would be expected from the literature as incoming thalamocortical information is directly received within the PW barrel before being relayed to adjacent columns and coming under the influence of inhibitory intracortical mechanisms (Armstrong-James and Fox, 1987; Armstrong-James et al., 1992).

	<b>C1</b>	<b>B1</b>	<b>D1</b>
Latency (mS)	13.09	11.29	14.92
SD	2.49	2.79	2.05
Inhibitory period (mS)	170.25	150.75	316.75
SD	43.21	50.27	114.63

	<b>C1</b>	<b>B1</b>	<b>D1</b>
Latency (mS)	17.77	17.93	15.79
SD	1.90	1.56	3.55
Inhibitory period (mS)	141.63	108.63	90.63
SD	20.18	22.83	21.28

Figure 34. An example of latency and inhibitory period data observed within (top) an IB and (bottom) an RS neuron. The neuron was assumed to be located in the centre of a barrel.

In cases where the two whiskers generated very similar latency responses in a cell, it was assumed that the cell was located at the edge of a barrel or in the septa between the two.

	<b>C1</b>	<b>B1</b>	<b>D1</b>
Latency (mS)	9.66	14.28	9.55
SD	0.41	1.56	0.93
Inhibitory period (mS)	123.4	459.8	200.38
SD	27.81	59.35	171.3

Figure 35. An example of multi whisker recordings of latency and PW values for an IB neuron. It was assumed the neuron was located in either the side of a barrel or in the septa between the two indicated barrels.

Within the data presented here activity gradients could be observed. For example if D1 had the shortest latency either C1 or D1 had the shortest inhibitory period and B1 always had both the longest latency and longest inhibitory period. If C1 was the PW then either B1 or D1 may have been the adjacent whisker.

In all cases it appeared that if either D1 or B1 had the shortest latency or inhibitory period it was C1 that was the corresponding partner. It was unusual for D1 and B1 to be complementary partners in this arrangement. From this it was clear that the data was related to the position of the neuron within the arc of barrels and was not random.

## **29.0 FIRING PATTERNS/CELL CLASS ACROSS WHISKERS**

In order to determine whether there was a difference between the firing patterns of neurons (both IB and RS) depending upon which whisker was deflected both VCR/'Chart' and 'Scope' records were examined. These records were examined in a bid to determine whether what was deemed to be the PW produced a different firing pattern within a cell than the other adjacent whiskers. In order to eliminate any bias the VCR/'Chart' records were examined independently of previously determined classifications. The firing patterns were classed for each whisker as either IB or RS and then further within these classes. Once completed the classifications for each cell were compared to the previously determined classifications. On doing so the following became clear.

### **29.1 'Scope' Records versus VCR/'Chart'**

In the majority of cases there was a good correlation in firing patterns between the two systems although some cells classed as RS in 'Scope' records were reclassified as IB neurons upon examination of the VCR/'Chart' recordings. The reverse however was never true.

It became apparent that the longer time periods and greater data available from VCR/'Chart' records made them more reliable for cell classification but the 'Scope' records have provided the quantitative data for each cell.

## 29.2 VCR/'Chart' Recordings of Multiple Whiskers

Once it was established that the VCR/'Chart' records provided a method for more reliable cell classification the differences in response to whiskers across the chosen arc was then investigated. When examining IB neuronal records two things became clear:

1) There were two common and quite distinct patterns of intrinsically bursting firing patterns within a neuron.

The first pattern consisted of a train of single action potentials, variable in number, ending in a burst. The number of action potentials within the burst varied but the burst was always followed by an afterhyperpolarisation. Long trains of single action potentials were always followed by a burst containing fewer action potentials. The firing pattern was extremely rhythmic and was termed pattern 1.

The second pattern observed in these neurons was less complex and consisted in the main of regular repetitive burst of action potentials with an almost total absence of the single action potentials and complex firing of pattern 1. This was termed pattern 2.

Where 'Scope' overlays were possible examination of multi whisker recordings revealed that the overlays of the PW in both RS and IB neurons resulted in a greater degree of overlap between individual traces. Stated simply this implies that the response to PW deflection was most likely to result in rhythmic and co-ordinated firing. The significance of this rhythmicity and co-ordination may be to enhance relay of information to post synaptic targets and ensure that only the neurons within the PW barrel stimulate neurons in the post synaptic target (in this case the striatum) (See discussion and Lisman, 1997). Examples of co-ordinated firing patterns can be seen in figures 38 and 39.

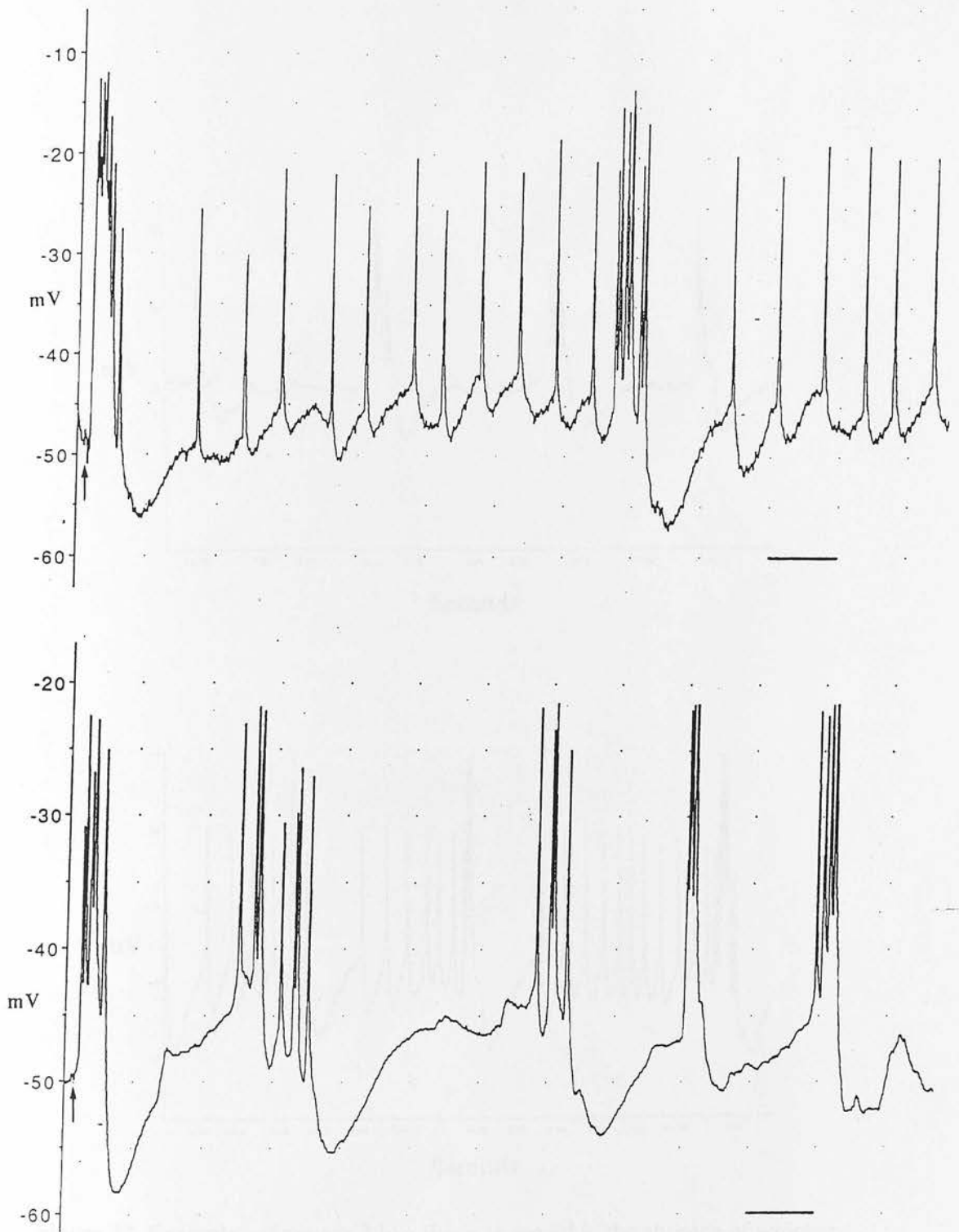


Figure 36. The top figure shows a typical example of pattern 1 firing. The lower figure shows a typical example of pattern 2 firing. Scale bar 100 mS. The position of the piezoelectric stimulation of the whisker is shown (↑).

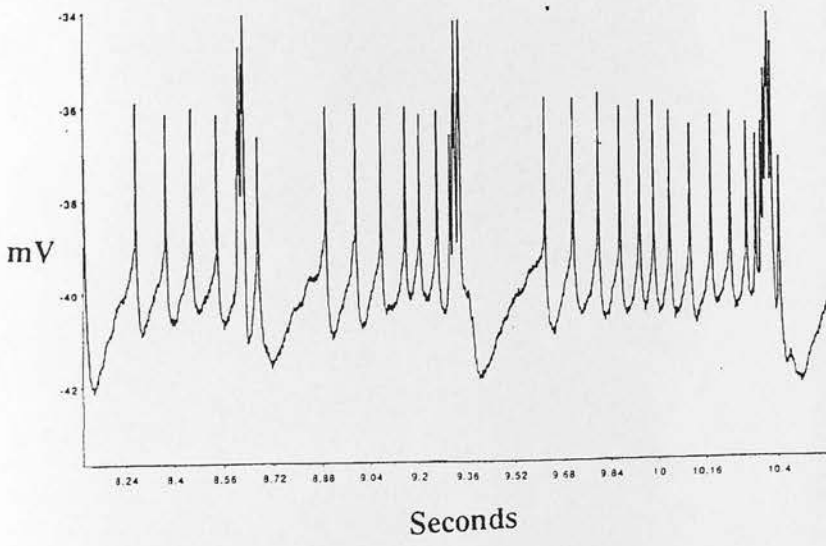
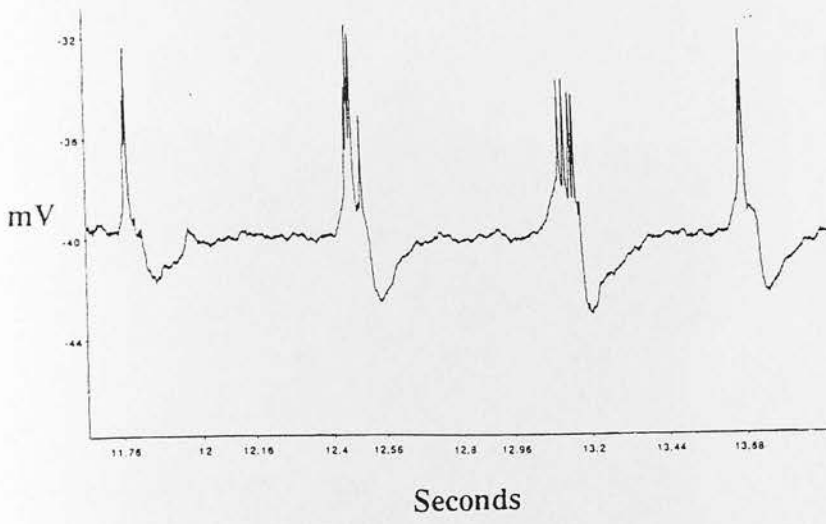


Figure 37. Examples of pattern 2 like firing observed in the absence of whisker stimulation. The lower figure shows the same neuron responding to whisker deflection (demonstrating pattern 1 like firing). The recordings shown have been made using 'Chart'. As a result the exact location of the stimulus is unknown (although stimulus amplitude and duration are the same as in 'Scope' records ( see sections 11.3 and 27.0)). The records therefore show an example of typical neuronal firing.

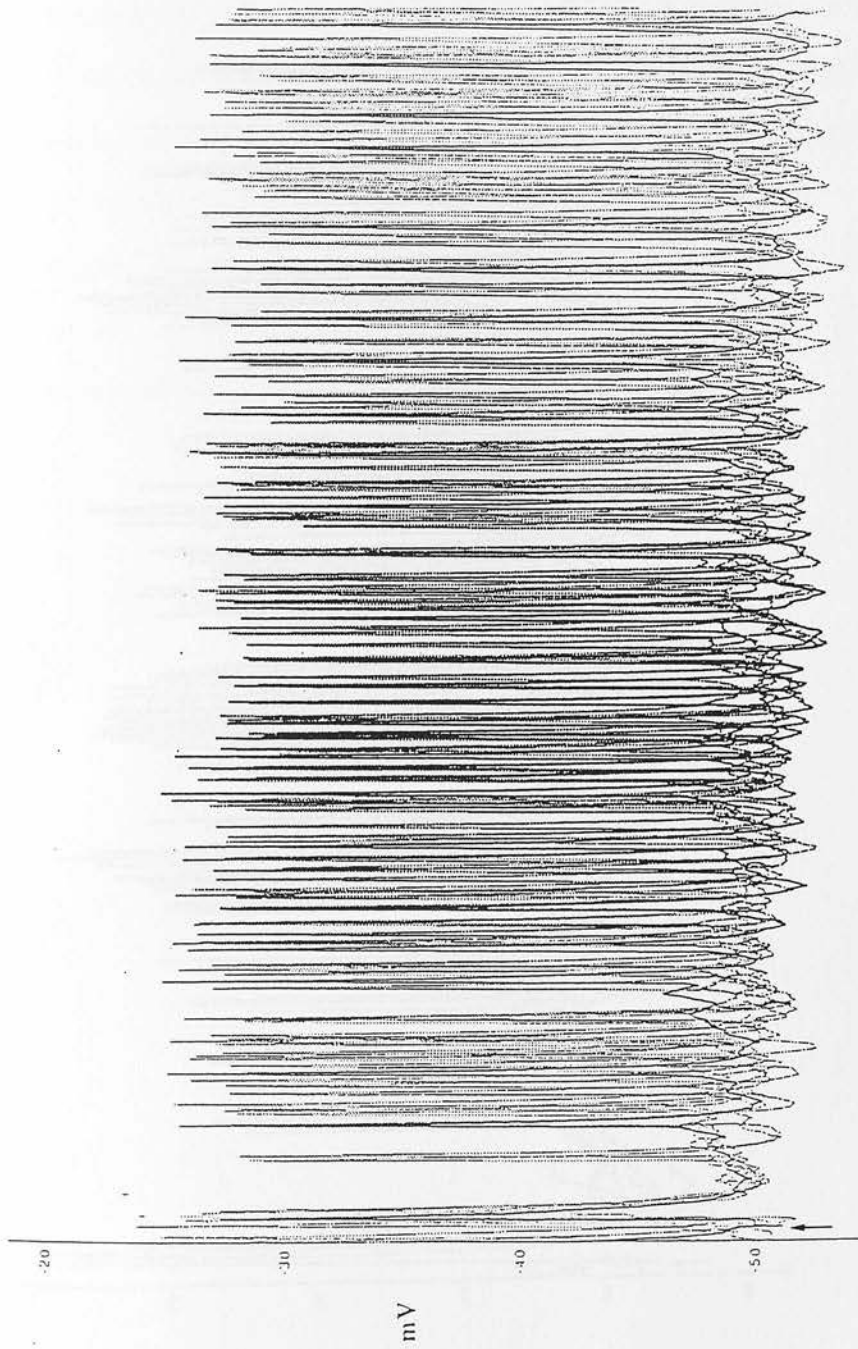


Figure 38. An example of an overlay of 8 consecutive 'Scope' traces of an RS neuron responding to piezoelectric whisker stimulation (shown as  $\uparrow$ ), note the synchronicity. Scale bar 100 mS.

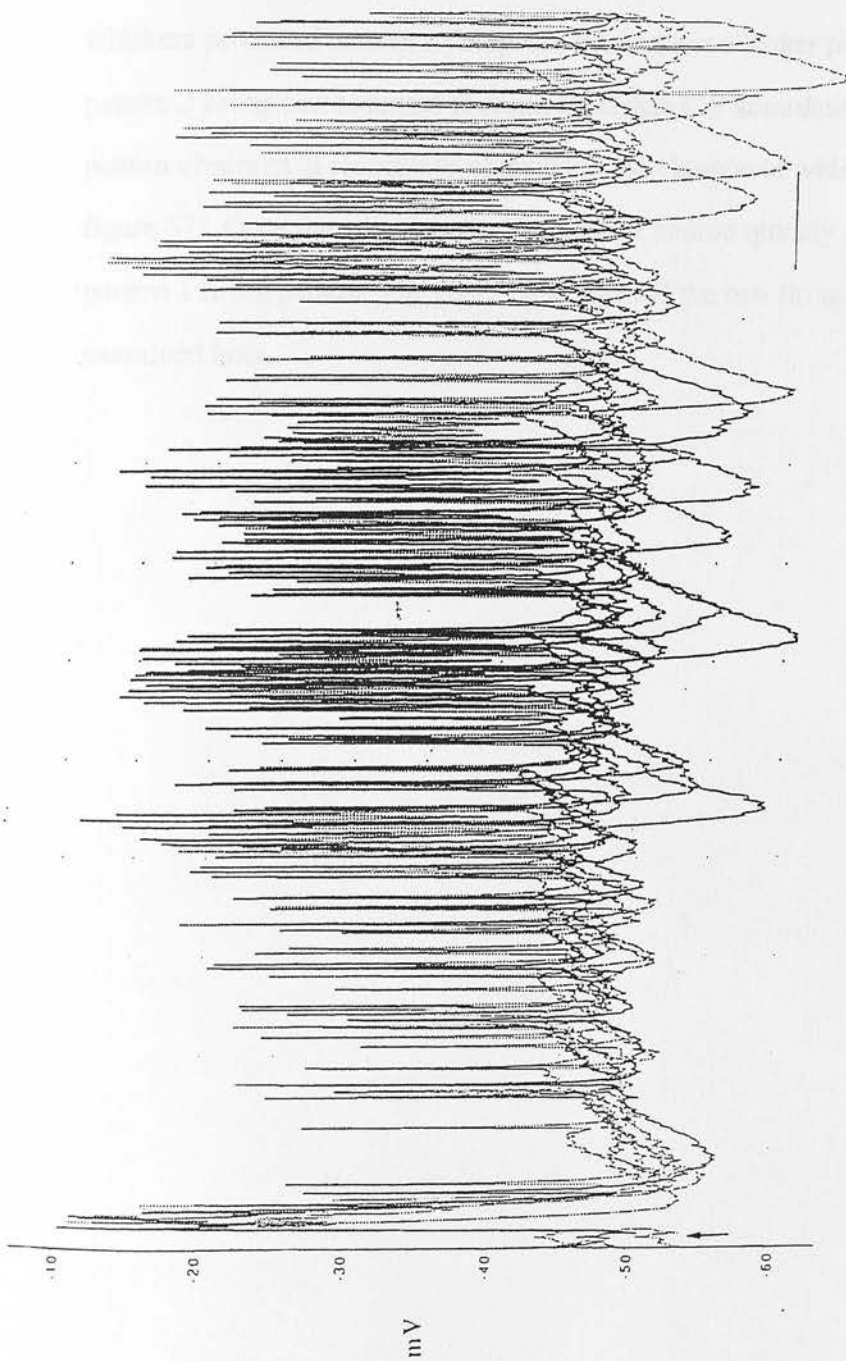


Figure 39. An example of an overlay of 8 consecutive 'Scope' traces of an IB neuron responding to piezoelectric whisker stimulation (shown as  $\uparrow$ ). Scale bar 100 mS.

Examination of the cell classification and the statistical data for latency and inhibitory periods showed that the PW produced pattern 1 firing whereas non-PW stimulations were more likely to result in pattern 2 firing. This was most clear in cases where there was a whisker that produced what was referred to as a barrel centre recording i.e. latency and inhibitory period were noticeably shorter than for the other two whiskers. In cases where the recorded cell was possibly between barrels or in a barrel side two whiskers produced pattern 1 firing and the furthest whisker produced pattern 2 firing. pattern 2 firing was assumed to result from non-PW stimulation as it was the firing pattern observed in recordings obtained in the absence of whisker deflection (see figure 37). Once the stimulus was applied the neuron quickly switched to resemble a pattern 1 firing pattern. The significance behind the two firing patterns will be examined later.

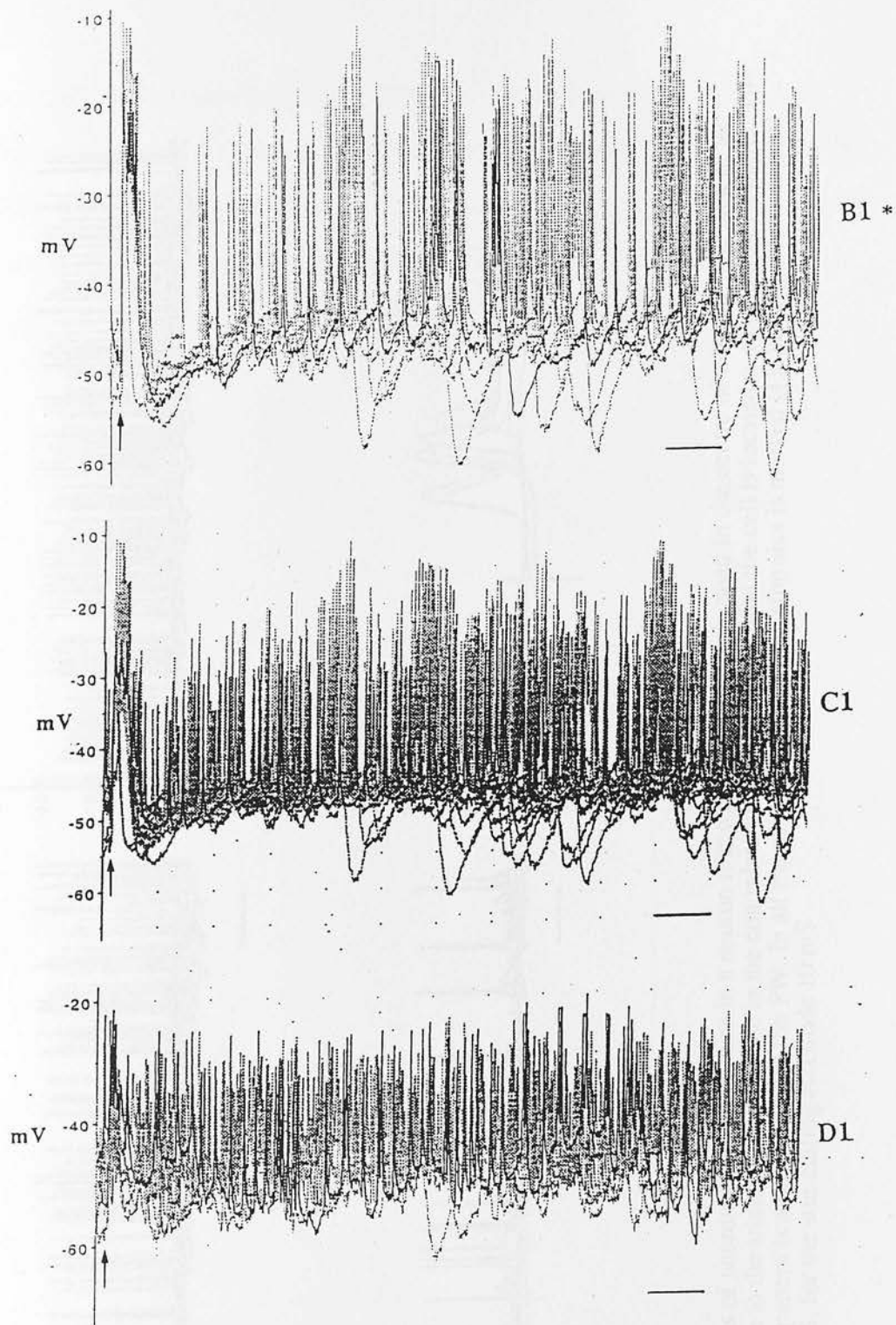


Figure 40. Examples of neuronal responses seen in a neuron that was thought to be located in the centre of a barrel. The co-ordinated firing is associated with the PW. The position of the piezoelectric stimulation of the whisker is shown on each trace ( $\uparrow$ ). Scale bar 100 mS.

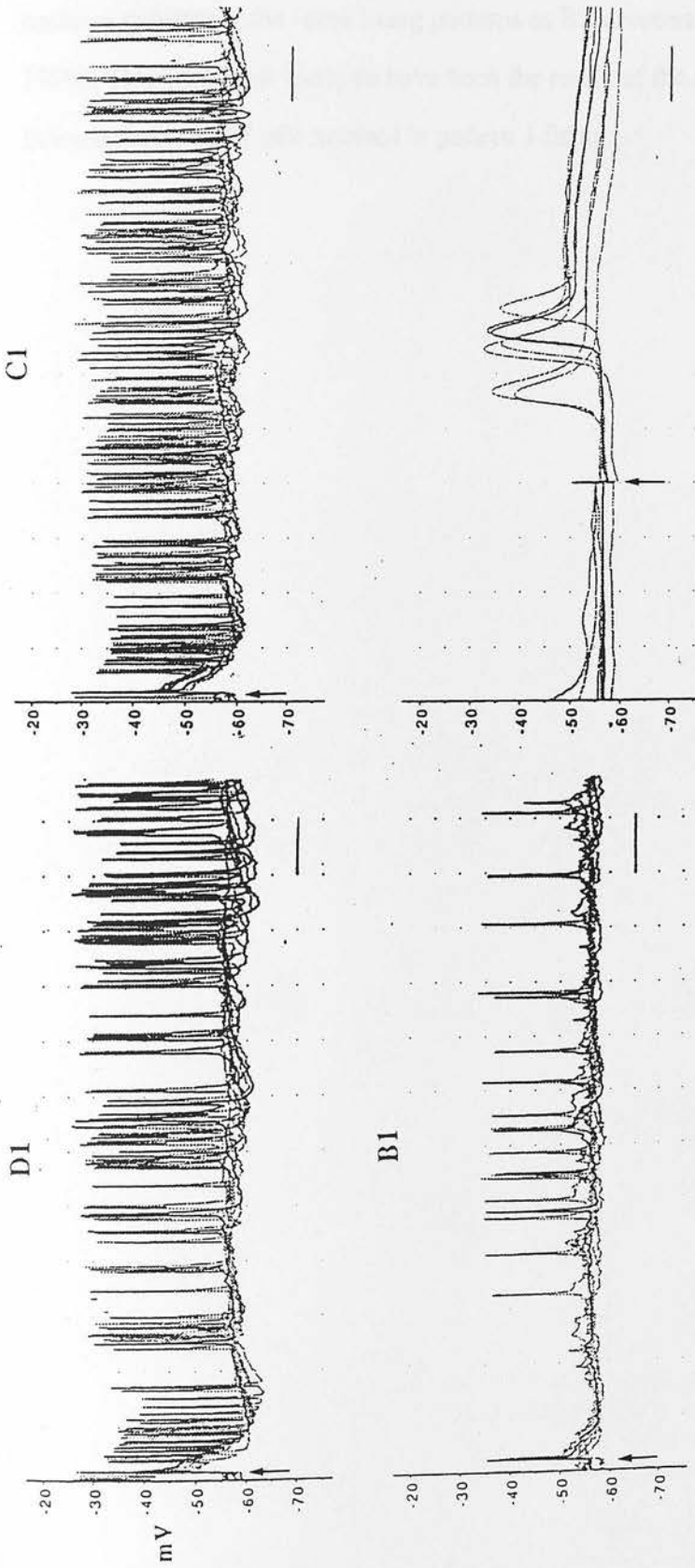


Figure 41. Examples of neuronal responses seen in a neuron that was thought to be located in the centre of a barrel. The lack of an antidromic response to the stimulating electrode in the contralateral cortex suggests that the cell is located in the centre of a barrel. The co-ordinated firing pattern is associated with the PW. In all traces the position of the stimulus is marked ( $\uparrow$ ). Scale bar for neuronal responses is 100 mS, for the stimulating electrode 10 mS

As already described in the in vitro literature, this study sometimes showed IB neurons exhibiting the same firing patterns as RS neurons (Connors and Gutnick, 1990). This was most likely to have been the result of the stimulation of a non-PW. Stimulating the PW still resulted in pattern 1 firing.

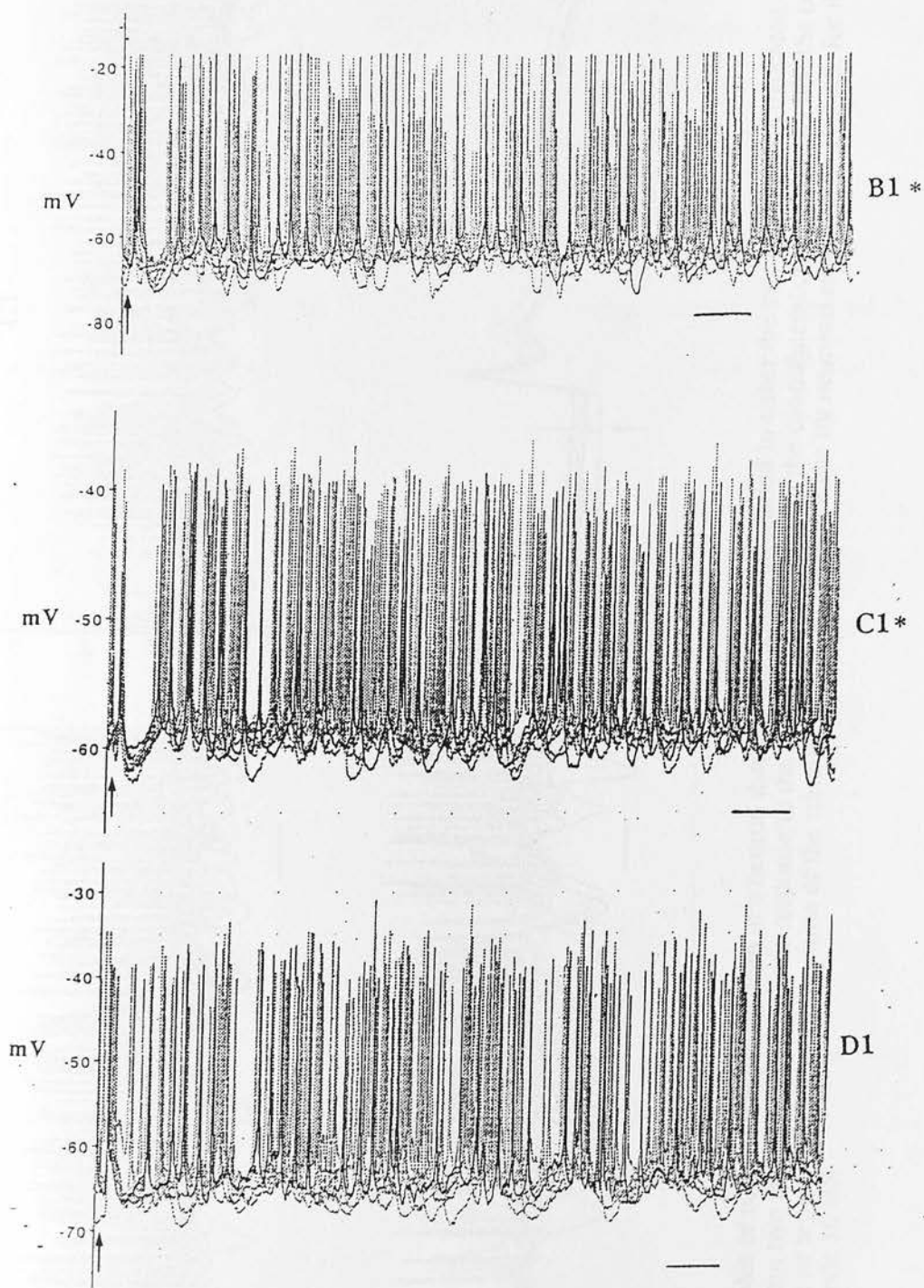


Figure 42. Examples of neuronal responses from a neuron that was thought to be located either in the side of the highlighted barrel (and closest to another barrel) or in the septa between the two barrels indicated. The position of the piezoelectric stimulation of the whisker is shown on each trace ( $\uparrow$ ). Scale bar 100 mS.

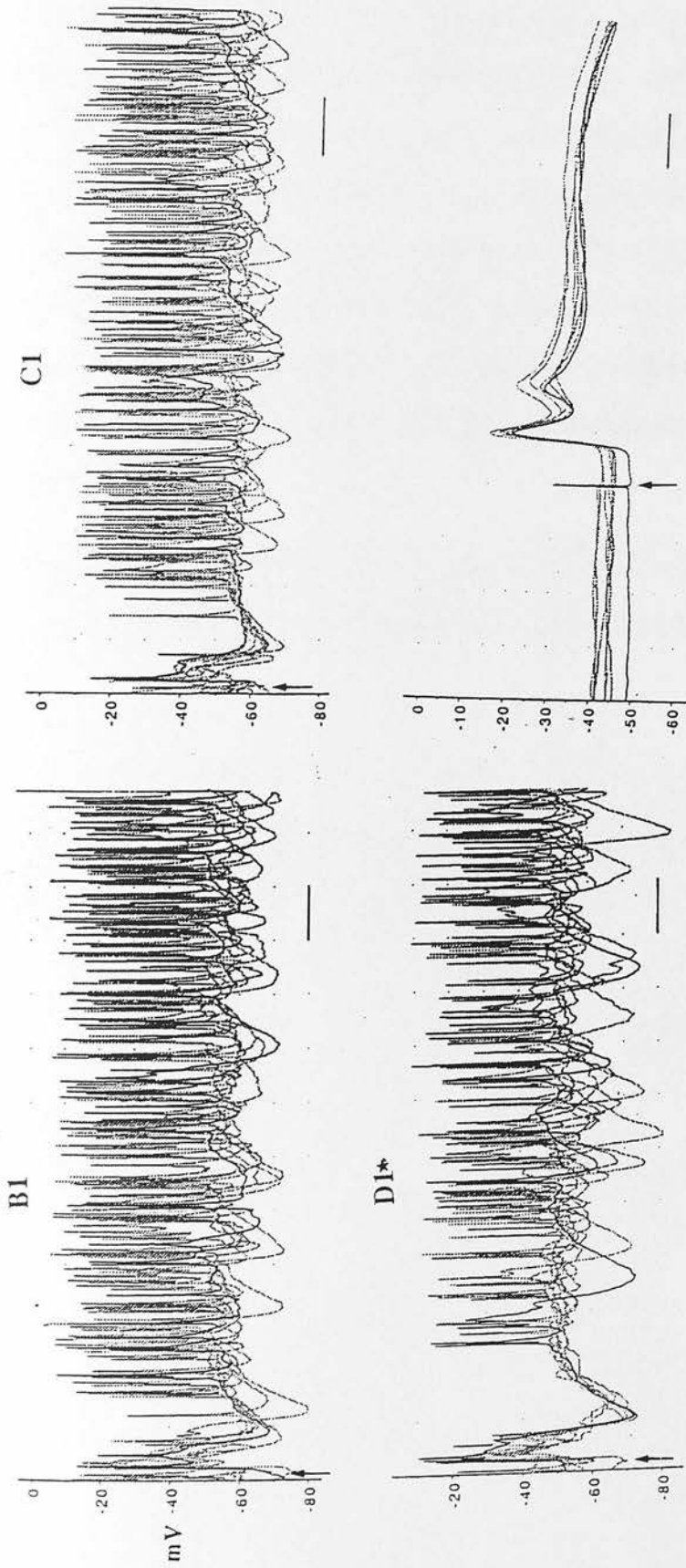


Figure 43. Examples of neuronal responses seen in a neuron that was thought to be located in either the side of the barrel indicated (\*) or in the septa between two barrels. The antidromic response to the stimulating electrode in the contralateral cortex suggests that the cell is located in the side or septa. In all traces the position of the stimulus is marked (\*). Scale bar for neuronal responses is 100 mS, for the stimulating electrode 10 mS

The RS firing patterns observed in this study were similar to those described in the literature (Agmon and Connors, 1992). RS1 neurons tended to show non-variable firing patterns, mainly resulting in single action potentials. RS2 neurons showed variable firing patterns as well as a greater proportion of doublets. Under no conditions did these neurons generate a burst. If a burst was observed the neuron was classed as intrinsically bursting. It is not certain from either the physiological or morphological data presented here whether the two firing transitions described above comprise two different subsets of intrinsically bursting neurons (although one might expect that they do).

The significance of IB neuronal firing, coding of sensory information and the firing patterns of the medium spiny GABAergic neurons of the striatum will be discussed later.

### 30.0 MORPHOLOGY RESULTS

All intracellularly filled neurons in this study were examined initially at the light microscope level to determine whether they were filled by the deliberate injection of current into a physiologically identified neuron or by some other means (see section 23.0). Neurons were initially classed as RS or IB according to their morphology rather than their physiology. The morphology corresponded most closely to the in vitro data. In the preparation of slices ascending pathways have been severed and the slice must be stimulated electrically rather than by mechanical whisker deflections. The morphology on the other hand would only be affected in that the cell would not be seen in its full extent.

The morphological class of a cell was established from a camera lucida reconstruction of the entire neuron. The entire group of filled cells was examined and clear examples of each cell class were established. These cells were used as standards against which other cells were matched. The most difficult cells to class morphologically were RS2 and IB1 cells as these two groups appeared very similar. Other cells that were not entirely filled were also difficult to classify although generally they could be classed as either RS or IB on the basis of the branch point of the apical dendrite. To remove any classification bias each neuron was independently classified by three observers without access to physiological records.

### 31.0 CELL CLASSIFICATION

Within cortex the neuron was investigated for axon collaterals (and whether or not they appeared to run horizontally or vertically), the branching pattern of the apical dendrite and the basilar dendritic pattern. The neurons were then reconstructed using a camera lucida system attached to a light microscope. The neurons were reconstructed from serial sections using a x40 objective. In all cases if a section could not be successfully matched with the camera lucida drawing it was not added to the drawing. Thus in some cases the full extent of the neuron may not be seen.

Once reconstructed the neurons were classed according to the system described by Cauller and Connors (1994).

Initial classification was performed according to the branch point of the apical dendrite which established the cell as either RS or IB (and possibly to a subclass 1 or 2). The cell was then subclassed by examining its basilar dendrites which established it as either 1 or 2). The more classic examples of the four cell classes were first identified followed by those cells that were not as easily classifiable. The results were then compared and any discrepancies discussed and the cells reclassified where necessary. Typical examples of RS1, RS2, IB1 and IB2 neurons from this study of the vibrissal region of rat SI are shown in figures 31-34. In all cases the presence and pattern of axon collaterals are not shown in the camera lucida classification drawings as they confused the drawing.

A total of 26 layer V pyramidal projection neurons were successfully reconstructed from serial coronal sections and examples of each cell type were filled. Of these neurons, 11 were classed as RS (3 RS1 and 8 RS2) and 11 as IB (9 IB1 and 2 IB2) two neurons could not be classified. In this study all classes of pyramidal neuron have

been successfully identified in the vibrissal region of rat primary somatosensory cortex.

The serial sections were then investigated to establish the presence of an axon and its subcortical path. The sections were also investigated to establish whether or not post-synaptic boutons were visible in any subcortical sites i.e. terminal fields. Once established the axonal path and terminal field were drawn using x10 objective. The stereotaxic co-ordinates of the soma, main axon or axonal branch point and the terminal field were then established. The axonal path and cellular morphology were then compared to establish whether or not there was a morphological link between cellular morphology and post-synaptic target site.

In order to compare the morphology of the filled neurons the drawings were photocopied to approximately a quarter of their original size.

## 32.0 SUBCORTICAL PROJECTIONS

Once the position of the cell body had been established the position of the axon path was determined.

In some cases examination revealed more than two stained cells, either through direct filling of two cells or as a result of the processes described previously (see figures 49, 50 and 55-58). It was therefore important to tie an axon to a particular cell body. In most cases where only a single neuron was filled this could be done reliably as the axon was clearly seen (in a single section) to leave the body and enter the corpus callosum. In some cases the axon could also be seen to enter the striatum. In the majority of cases a single axon was observed and this could be traced back to the cell body. The axonal path was then carefully followed in serial sections. Sometimes the axon split and ran in both an anterior and posterior direction. In the majority of cases however the axon ran in an anterior direction. The axon was also investigated for any branching (indicating two potential subcortical targets and possible terminal fields). The axon was also investigated for collaterals as it passed through the striatum giving off *en passant* terminals *en route* to its main subcortical target (e.g. brainstem). (see figures 55-61).

The axon was followed through the serial sections as far as possible until it either faded out or ended in a terminal field. In cases where the axon ended abruptly it may be because there was insufficient incubation time between cell filling and time of sacrifice to prevent axonal transport to the terminal field or it could be that axonal transport ended abruptly due to the death of the filled neuron.

In some cases where the axon appeared to be heading in a posterior direction towards the brainstem and the spinal cord there were insufficient serial sections to trace the full

entirety of the axonal path. In these cases terminals were not visible but it was assumed that the target of these neurons was the brainstem. The axon path of these neurons were similar to those seen from iontophoretic injections into barrel cortex (not shown). These neurons have therefore been classed as brainstem projecting neurons.

In all cases axonal paths became very difficult to trace through white matter areas especially within the fibre bundles of the striatum. This was probably due to the reduced penetration of the ABC through the axon at points where it was heavily myelinated.

### **33.0 TERMINAL FIELDS**

Suspected terminal fields were examined using x40 and x100 oil immersion to assess whether they were connected via thin fibres, there were swellings on the fibres, if appeared to be in 3D running through the thickness of the tissue and whether or not they could be traced back to connect to the axon. If the terminals fulfilled these criteria they were assumed to be real. Terminals that did not were dismissed as surface dirt or background staining.

## **34.0 NEURONS WITH TERMINAL FIELDS**

A total of 4 corticostriatal and 2 corticothalamic neurons resulting in terminal fields were filled in this study. Each one these neurons will be discussed in detail below.

### **34.1 STRIATAL TERMINALS**

#### **34.1.1 Topographic Innervation 1**

The neuron was recorded and filled using the original extracellular surgical procedure and visualised using the initial histology protocol.

The neuronal cell body was located at a stereotaxic co-ordinate between AP -3.14 and AP -2.80. The neuron was classed as an IB1. The axon left the cortex (see figure 48) and had both anterior and posterior located post synaptic targets. The axon initially ran in an anterior direction before branching within a striatal fibre bundle (AP -2.56). The branch ran within the striatal tissue at right angle to the parent axon and parallel to the corpus callosum. As the axon ran through the corpus callosum it appeared to branch and send an axon collateral to the reticular thalamus. It could not be determined however whether the collateral ended in a terminal field or not (not shown). The axon continued its path through the striatum crossing fibre bundles before ending as a hand like arrangement of terminals within the striatal tissue (AP -2.12). The posterior projecting axon ran through the striatal fibre bundle and into the internal capsule. The axon then continued towards the brainstem.

This cell was classed as an IB neuron on the basis of its morphological characteristics. It had extensive apical and basilar dendritic trees as well as an apical dendrite that tapered as it ascends from the soma. The apical dendrite can be clearly seen to branch

in layer III of cortex. All these features are characteristic of an IB1 neuron. In addition to the extensive basilar dendritic branching and extensive axon collateral network within layer V the neuron also sent an axon collateral to SII. The collateral arose in layer V and terminated within layer V of SII (not shown). Unfortunately in this recording and filling no physiology was recorded so this classification is on the basis of morphology alone.

In this case, and in all the following cases the photomicrographs and camera lucida reconstructions are orientated as follows: medial is always to the left of the figure when looking at the figure legend. Lateral is always right, dorsal to the top of the figure and ventral is always at the bottom of the figure. In all cases described in this section the position of the terminal fields in whole cell reconstructions are marked with a ★ and the terminal fields within photomicrographs are highlighted with arrows.



*[Faint, illegible text, likely a figure legend or caption describing the image above.]*



Figure 44. A photomicrograph of the filled layer Va neuron. The layer III neuron also seen did not possess a subcortically projecting axon. The orientation is as follows: pia towards the top of the photograph, the corpus callosum to the bottom of the photograph and the midline to the left of the photograph. Scale bar 100  $\mu\text{m}$ .

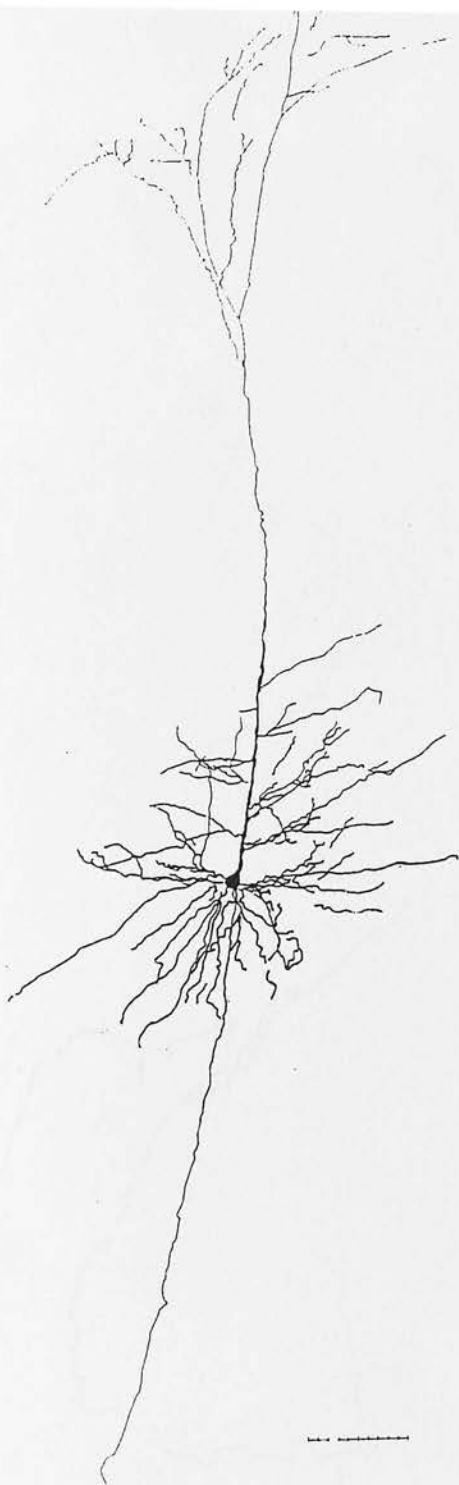


Figure 45. A camera lucida reconstruction of the filled neuron. The orientation is as follows: pia towards the top of the photograph, the corpus callosum to the bottom of the photograph and the midline to the left of the photograph. Scale bar 100  $\mu\text{m}$ .

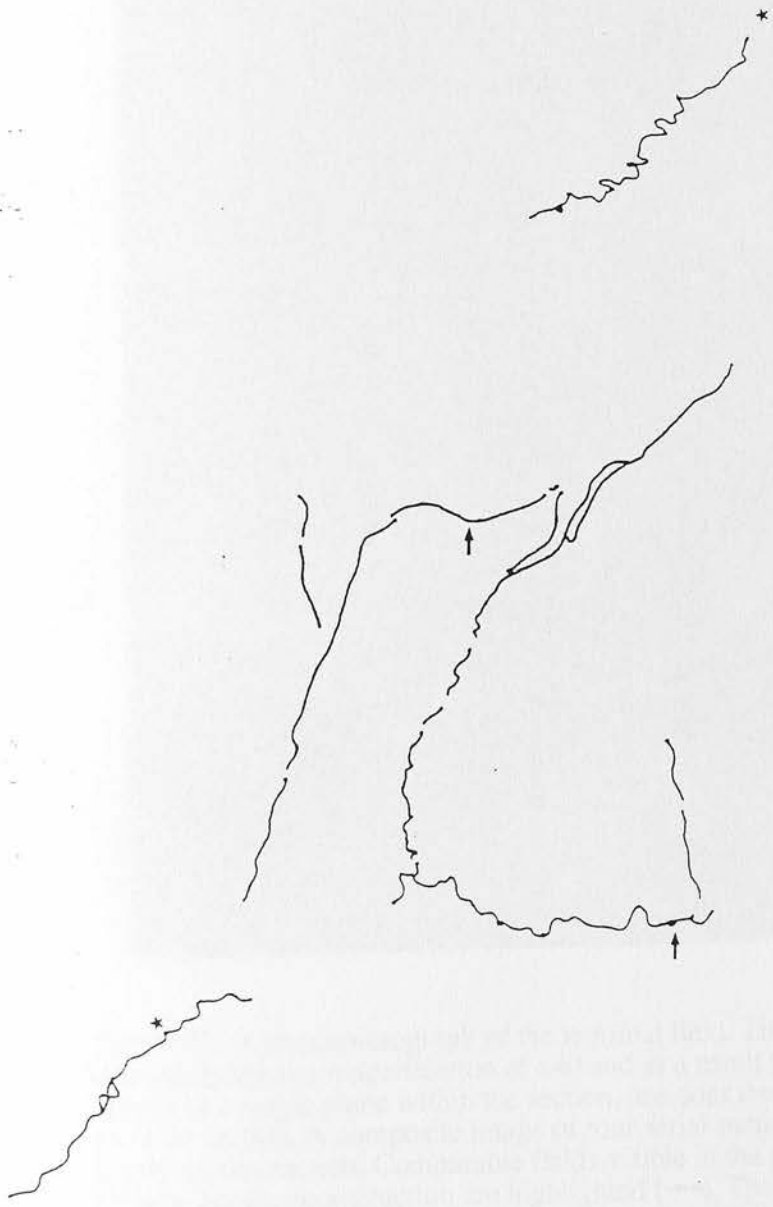


Figure 46. A camera lucida reconstruction of a terminal field. The reconstruction was made in a total of 4 serial sections and through all the planes of view. It was possible to construct this drawing as landmarks could be aligned through serial sections to build a composite image. A comparison of the photomicrograph view and the entire terminal field seen in the camera lucida reconstruction can be compared using the markers ( $\rightarrow$ ). The orientation is as follows: pia towards the top of the drawing and the midline to the left of the drawing. Scale bar 50  $\mu\text{m}$ .



Figure 47. A photomicrograph of the terminal field. The terminal field was photographed at a magnification of x40 and as a result the entire terminal field does not appear in a single plane within the section, nor does the entire terminal field appear in just one section. A composite image of four serial sections can be seen in the camera lucida reconstruction. Comparable fields visible in the photomicrograph and the camera lucida reconstruction are highlighted ( $\rightarrow\star$ ). The orientation is as follows: pia towards the top of the photograph and the midline to the left of the photograph. Scale bar 50  $\mu\text{m}$

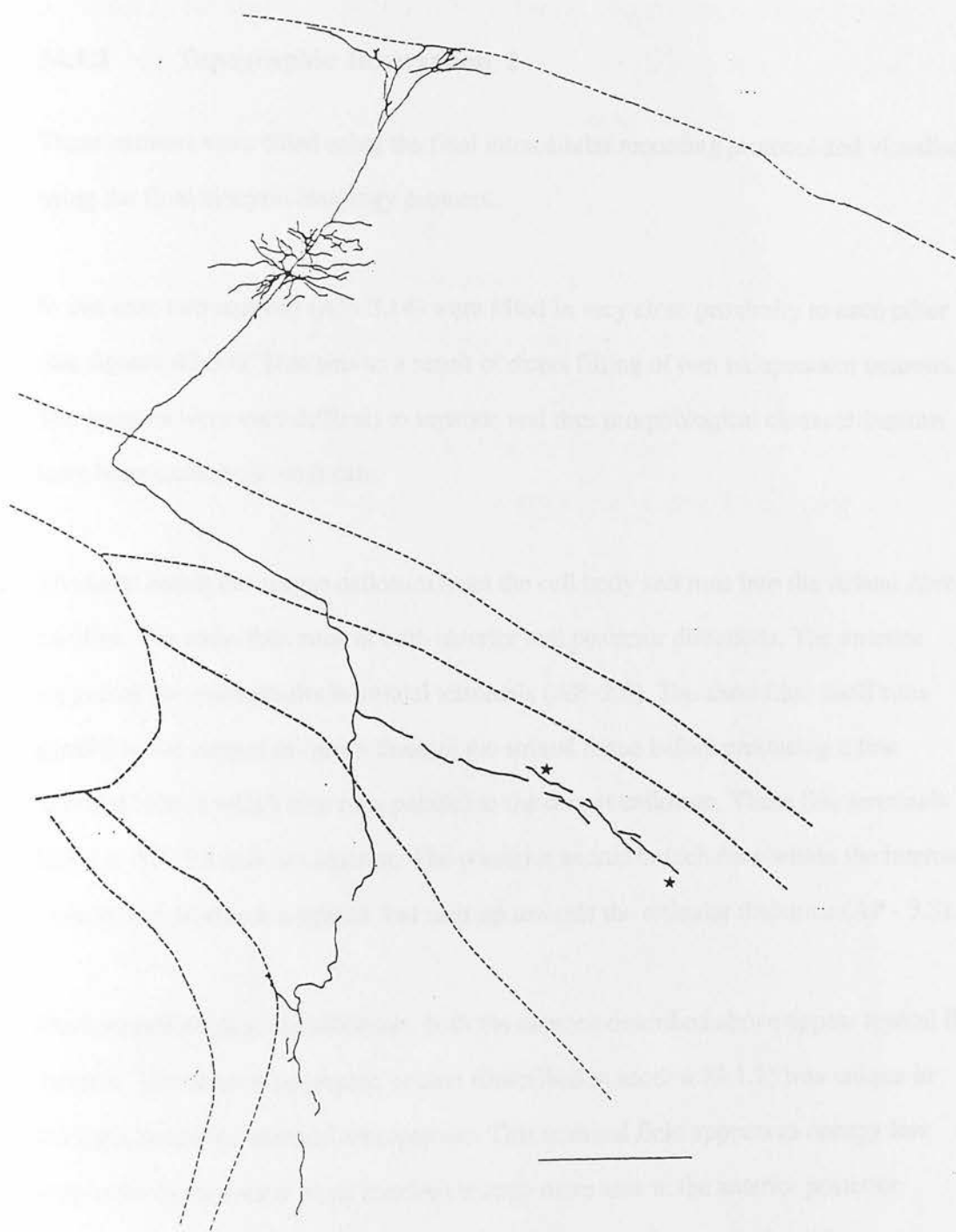


Figure 48. A camera lucida reconstruction of the neuron in its entirety (including cell body, axon path and terminal field). The section is orientated with the pia towards the top of the drawing and the midline to the left. Scale bar 500  $\mu\text{m}$ .

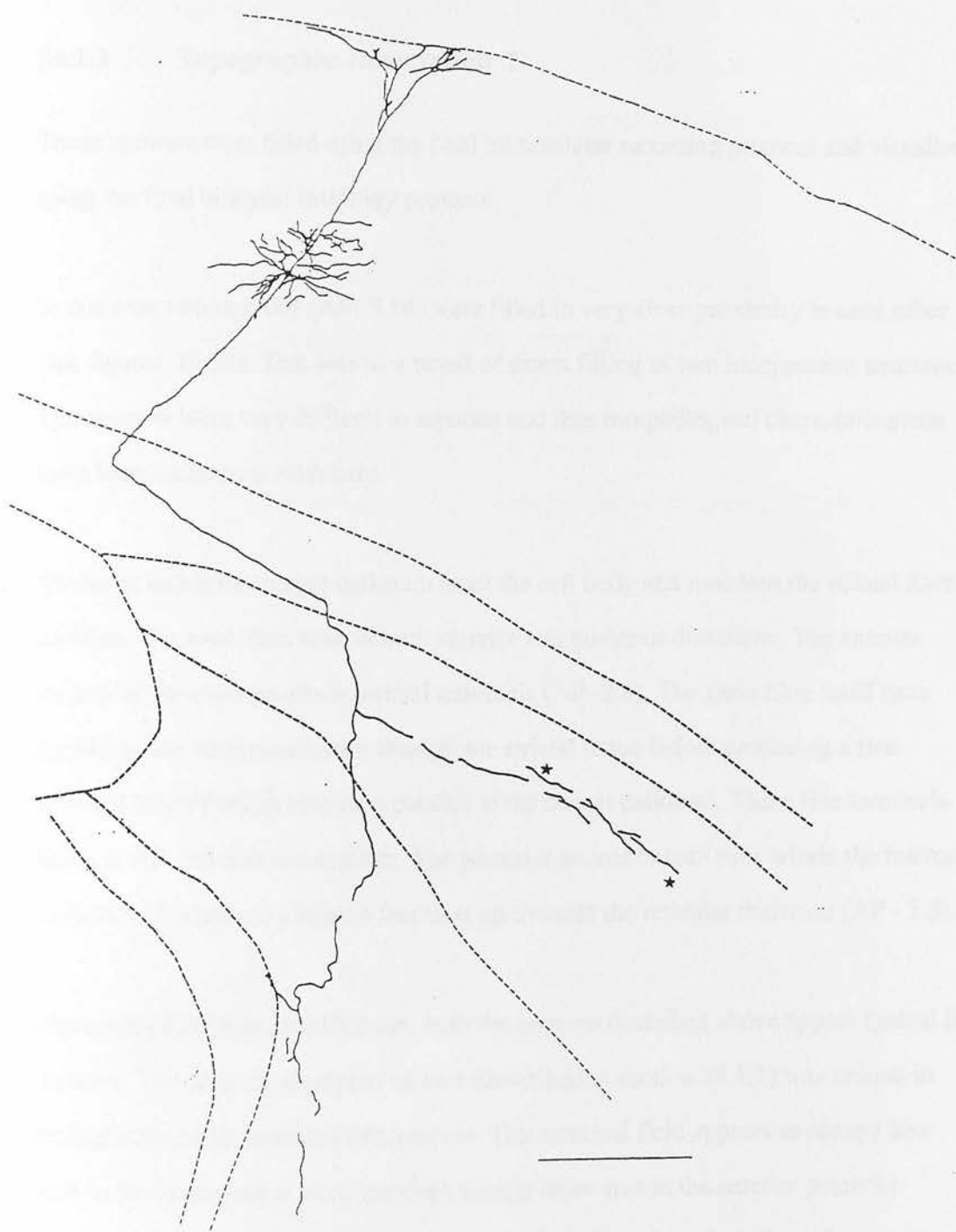


Figure 48. A camera lucida reconstruction of the neuron in its entirety (including cell body, axon path and terminal field). The section is orientated with the pia towards the top of the drawing and the midline to the left. Scale bar 500  $\mu\text{m}$ .

### 34.1.2 Topographic Innervation 2

These neurons were filled using the final intracellular recording protocol and visualised using the final biocytin histology protocol.

In this case two neurons (AP- 3.14) were filled in very close proximity to each other (see figures 49-53). This was as a result of direct filling of two independent neurons. The neurons were very difficult to separate and thus morphological characterisations have been carried out with care.

The axon enters the corpus callosum from the cell body and runs into the striatal fibre bundles. The axon then runs in both anterior and posterior directions. The anterior section of the axon results in striatal terminals (AP -2.8). The axon fibre itself runs parallel to the corpus callosum through the striatal tissue before producing a fine terminal branch which also runs parallel to the corpus callosum. These fine terminals begin at AP -1.8 and run anterior. The posterior axonal branch runs within the internal capsule and produces a branch that runs up towards the reticular thalamus (AP - 3.3).

From morphological classification, both the neurons described above appear typical IB neurons. The other topographic neuron (described in section 34.1.1) was unique in having a hand-like terminal arrangement. This terminal field appears to occupy less area in the mediolateral plane but does occupy more area in the anterior posterior direction. The limited lateral branch innervations arising from branches of axons (see sections 34.3 and 34.4) running through the striatal fibre bundles appear to produce a sparse terminal field. The one thing all the neurons have in common is that as well as innervating the striatum they all appear to innervate a thalamic nucleus (e.g. reticular, VPm or POM). Thus the role of each of these cortical projection neurons must

influence thalamic processing in a variety of ways. It is not known whether there is a separation of the thalamic innervation according to the position of the projection neuron with respect to cortical depth and/or position within the septa/barrel arrangement.

As well as having subcortical projections one of these neurons also appears to innervate layers III and V of secondary somatosensory cortex (SII).

Thus both of the neurons that innervate striatum via an extensive topographic terminal field also innervate thalamus and SII. The significance of these additional innervations is not known.

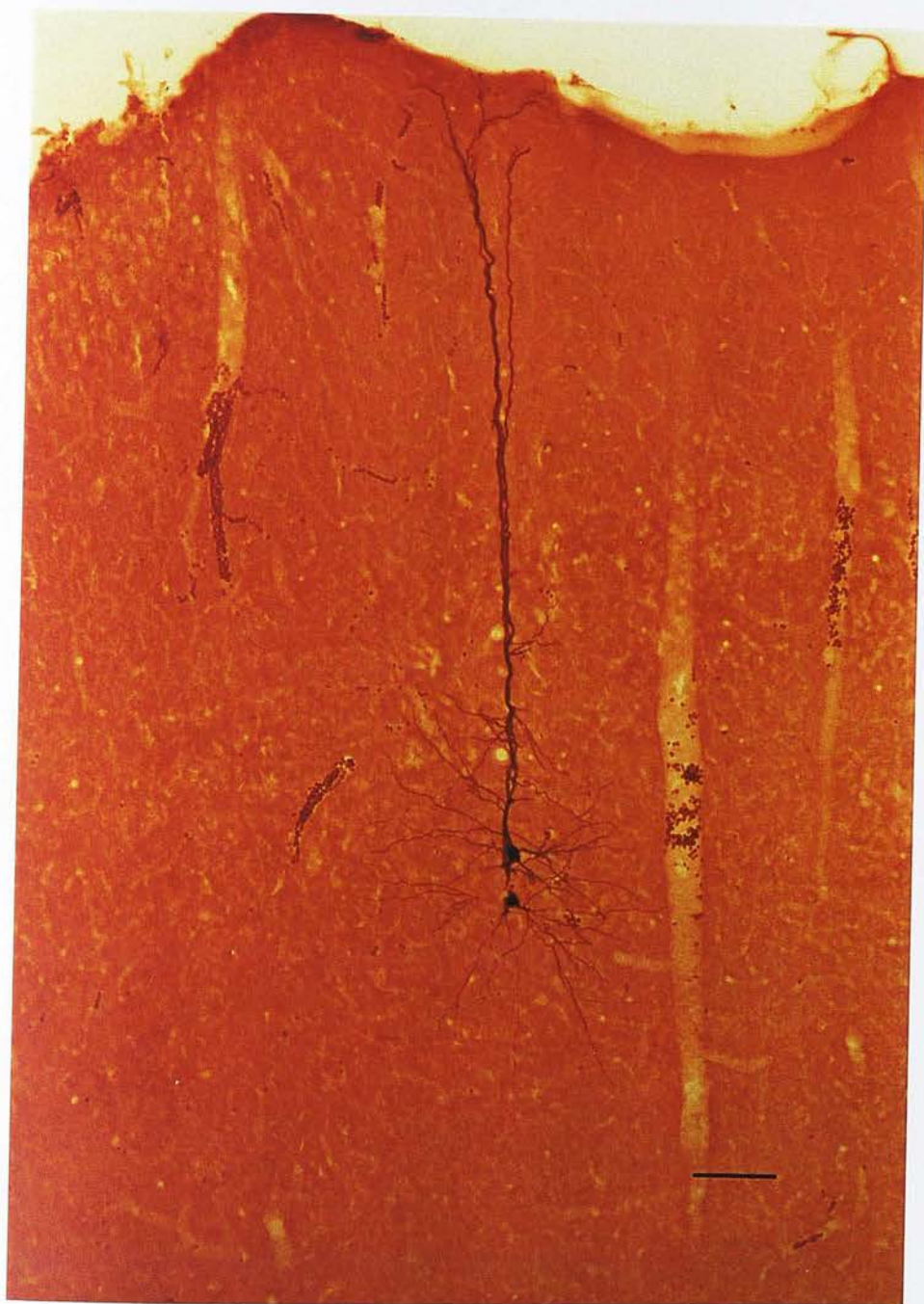


Figure 49. A photomicrograph of the filled neurons. The orientation is as follows: pia towards the top of the photograph, the corpus callosum to the bottom of the photograph and the midline to the left of the photograph. Scale bar 100  $\mu\text{m}$ .

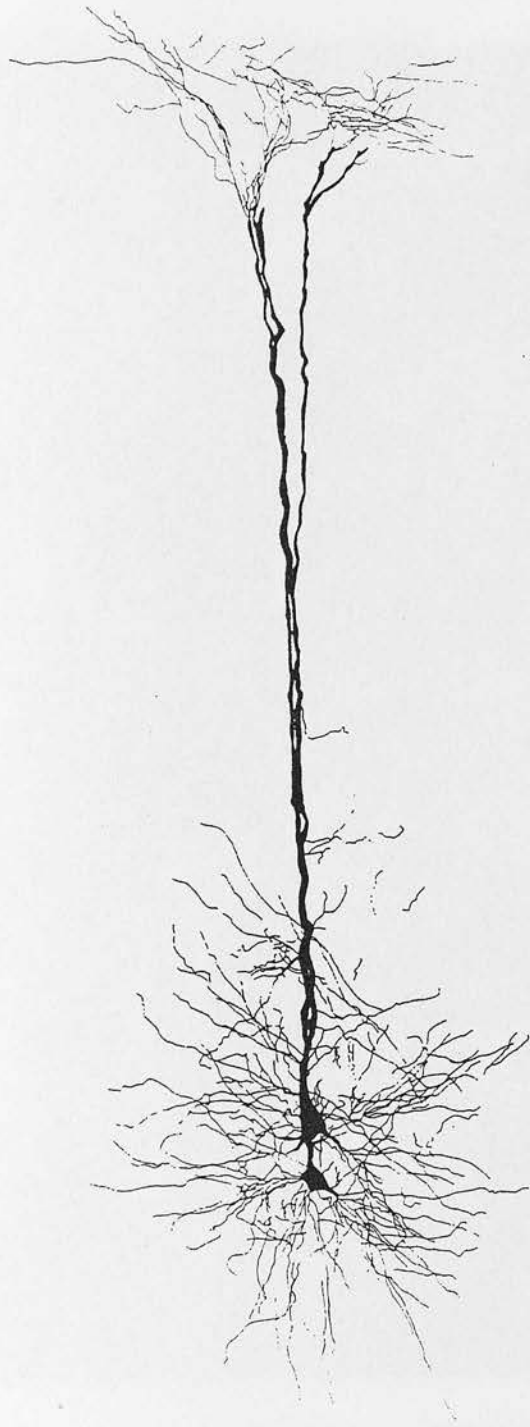


Figure 50. A camera lucida reconstruction of the filled neurons. The orientation is as follows: pia towards the top of the drawing, the corpus callosum to the bottom and the midline to the left. Scale bar 100  $\mu\text{m}$ .



Figure 51. A photomicrograph of the terminal field. The entire extent of the terminal field in this section is not visible in a single plane as the the photomicrograph was taken at a magnification of  $\times 100$  (oil immersion). The section and plane shown highlights the position and extent of the terminal field (shown by  $\rightarrow$ ). A camera lucida reconstruction was not drawn as the terminal field extends in the anterior-posterior direction and thus very little of the terminal field is visible in a section. It is impossible at a magnification of  $\times 100$  (oil immersion) to reliably and accurately align tissue landmarks to build a composite picture of the terminal field. The orientation is as follows: pia towards the top of the photograph and the midline to the left of the photograph. Scale bar  $10 \mu\text{m}$ .

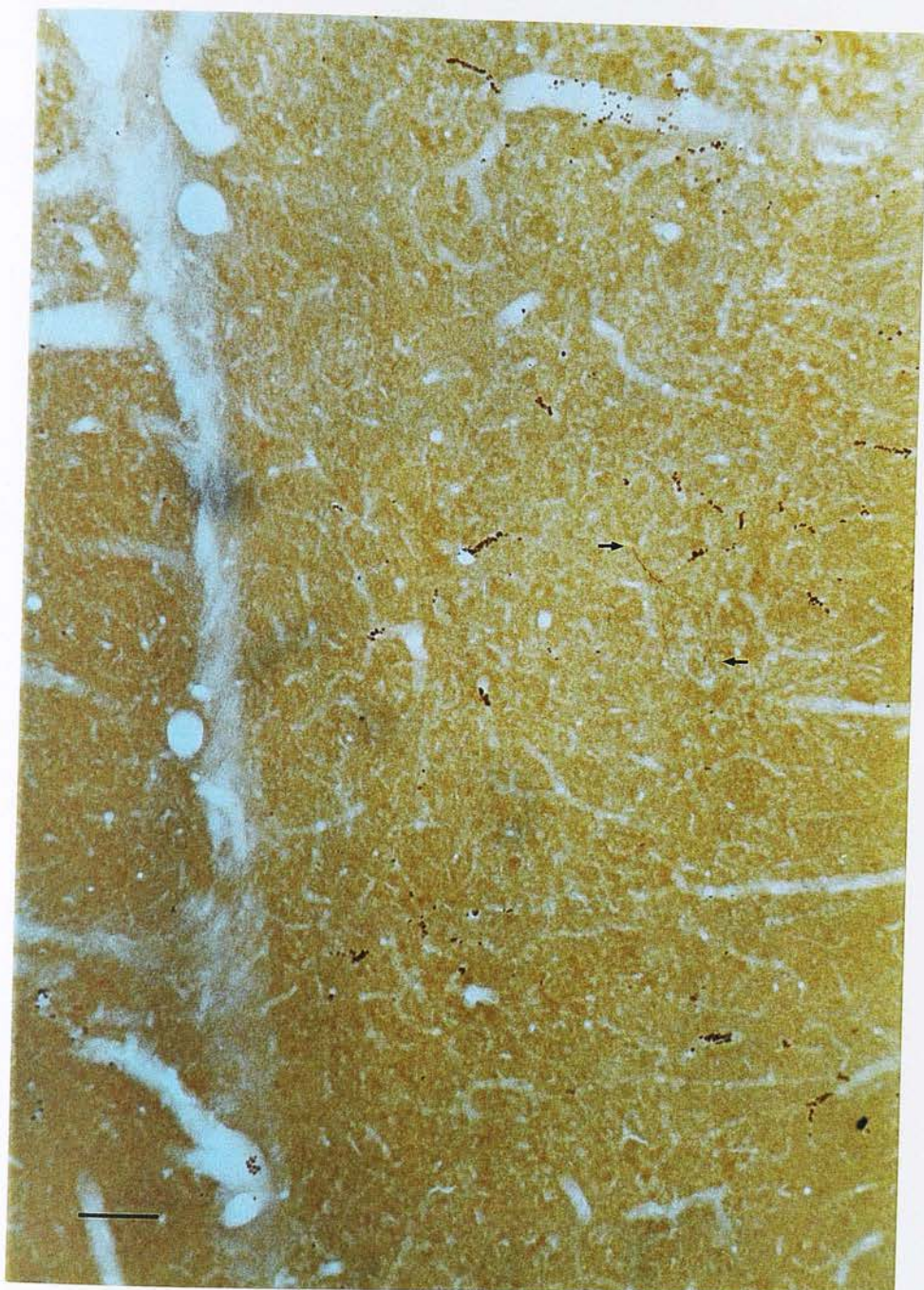


Figure 52. A photomicrograph of the SII innervation. The orientation is as follows: pia towards the top of the photograph and the midline to the left. Scale bar 100  $\mu\text{m}$ .

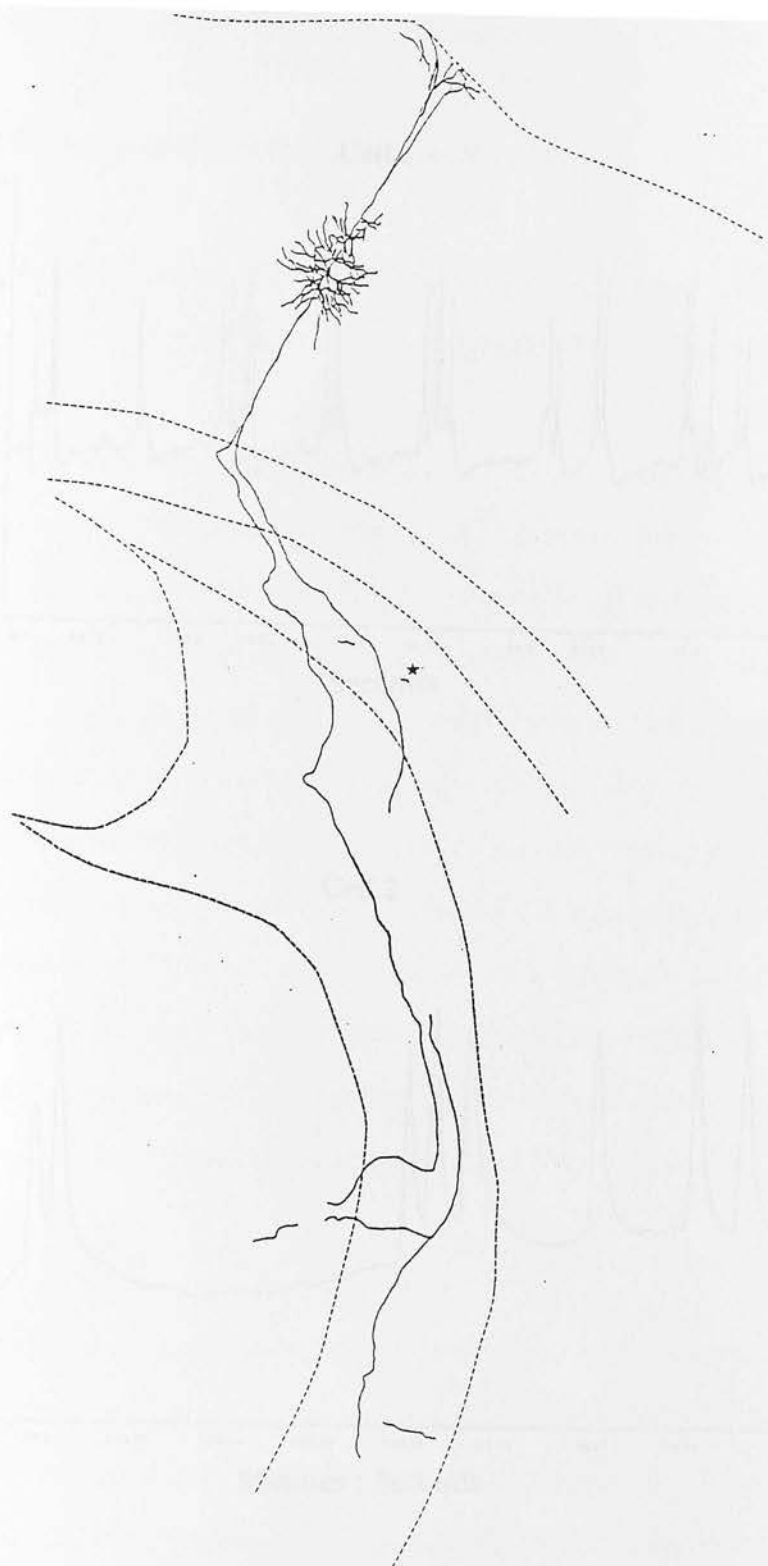


Figure 53. A camera lucida reconstruction of the neuron in its entirety (including cell body, axon path and terminal field). The section is orientated with the pia towards the top of the drawing and the midline to the left. Scale bar 500  $\mu\text{m}$ .

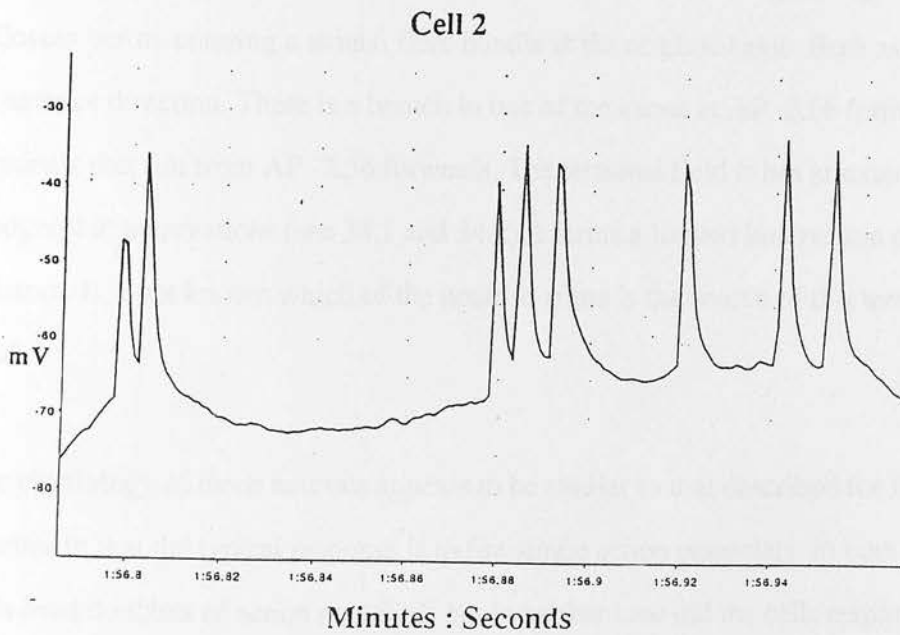
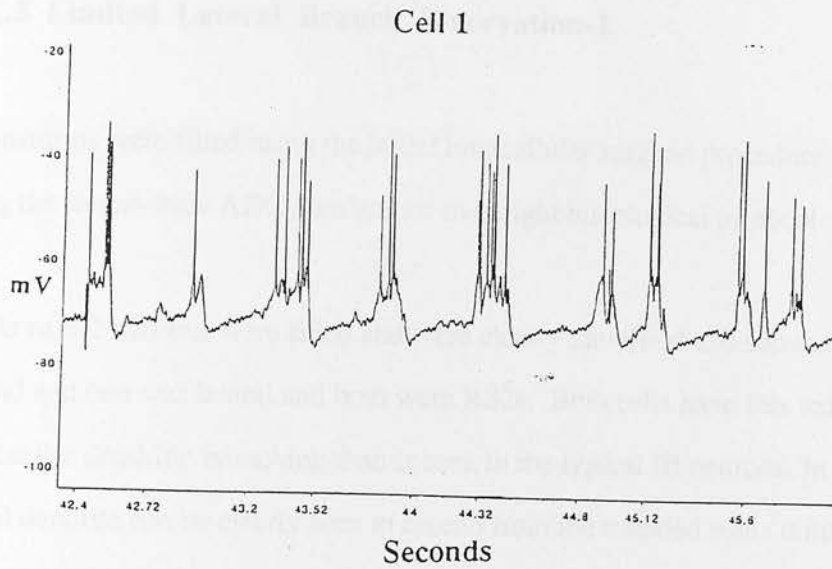


Figure 54. Examples of the filled neuron's response to whisker deflection. The recordings shown were made from vcr and viewed using 'Chart'. As a result the exact location of the stimulus in the record is unknown (the amplitude and duration remain the same as for 'Scope' ( see sections 11.3 and 27.0). The record shown here highlights the typical responses of the two neurons to piezoelectric whisker stimulation.

### 34.1.3 Limited Lateral Branch Innervation-1

The neurons were filled using the initial intracellular surgical procedure and visualised using the freeze-thaw ABC standard kit overnight histological protocol.

In this case 2 neurons were filled and were clearly identified and separated. One was medial and one was lateral and both were RS2s. Both cells have less extensive apical and basilar dendritic branching than is seen in the typical IB neurons. In both cases the apical dendrite can be clearly seen to ascend from the rounded soma unlike the tapering cortical origin that is characteristic of IB neurons. The more medial neuron is located stereotaxically at AP -3.3 and the more lateral at AP -4.6. Both axons clearly leave the cortex and enter the corpus callosum where they turn 90°, running through the corpus callosum before entering a striatal fibre bundle at the original angle. Both axons run in an anterior direction. There is a branch in one of the axons at AP -2.56 forming terminals that run from AP -2.56 forwards. The terminal field is not as extensive as the topographic innervations (see 34.1 and 34.2) it forms a limited innervation of the striatum. It is not known which of the neurons filled is the source of this terminal field.

The physiology of these neurons appears to be similar to that described for RS neurons in that the typical response is to fire single action potentials. In both cases the cells fired doublets of action potentials but in neither case did the cells respond by firing bursts (classed as clusters of 3-5 action potentials associated with a depolarising envelope).

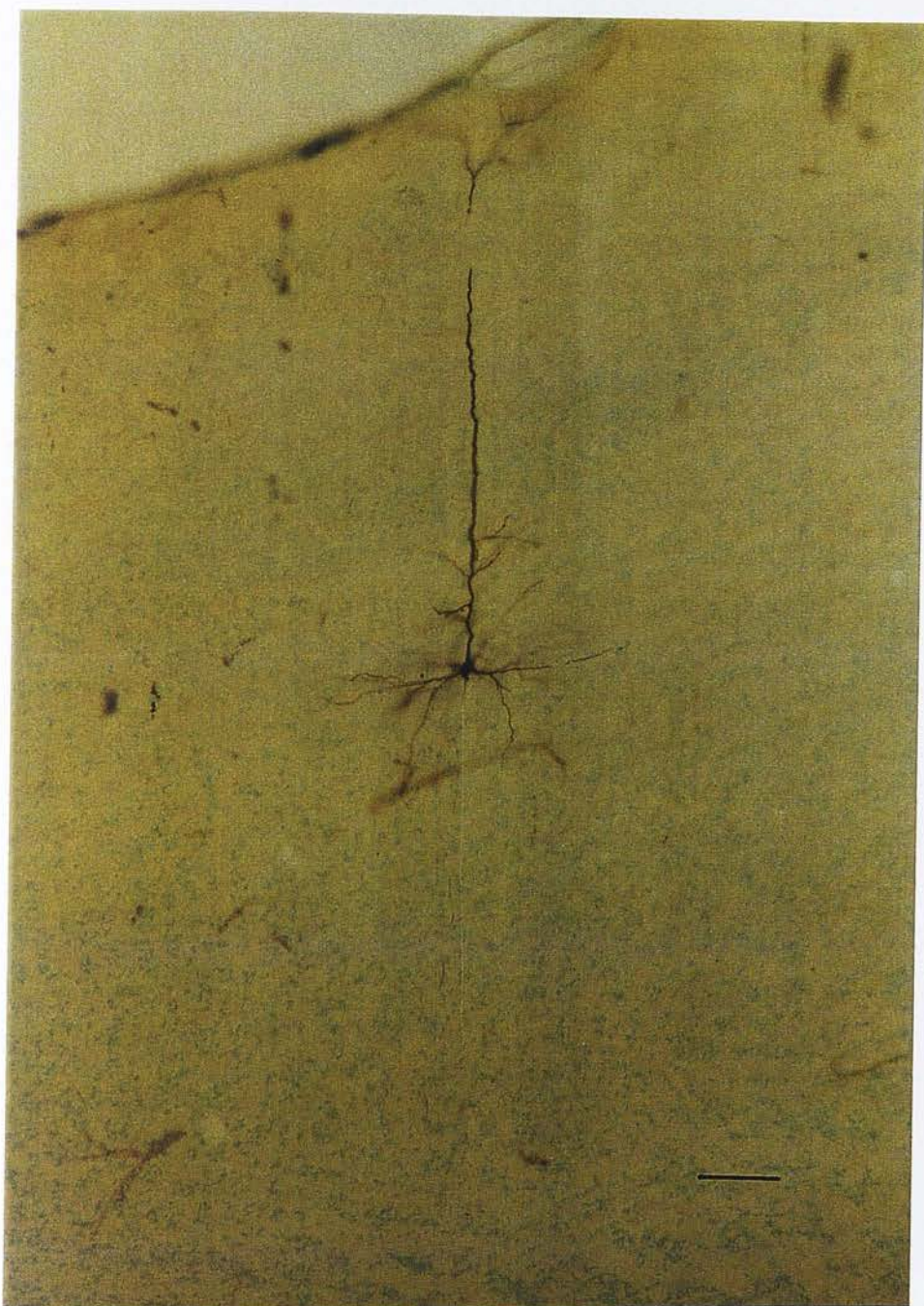


Figure 55. A photomicrograph of one of the filled neurons. The orientation is as follows: pia towards the top of the photograph, the corpus callosum to the bottom of the photograph and the midline to the left of the photograph. Scale bar 100  $\mu\text{m}$ .

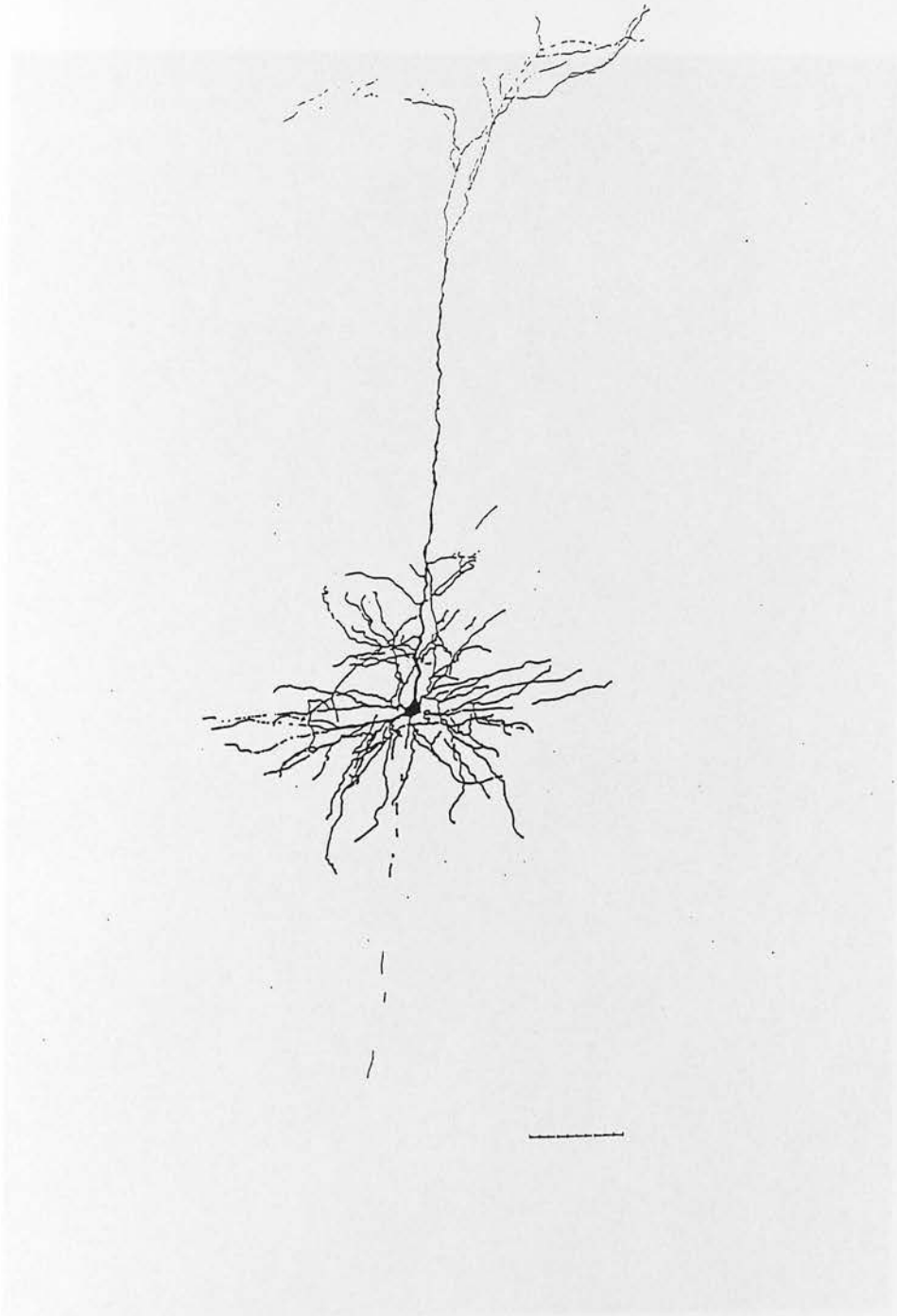


Figure 56. A camera lucida reconstruction of one of the filled neurons. The orientation is as follows: pia towards the top of the drawing, the corpus callosum to the bottom and the midline to the left. Scale bar 100  $\mu\text{m}$ .



Figure 57. A photomicrograph of the other filled neuron. The orientation is as follows: pia towards the top of the photograph, the corpus callosum to the bottom and the midline to the left of the photograph. Scale bar 100  $\mu\text{m}$ .

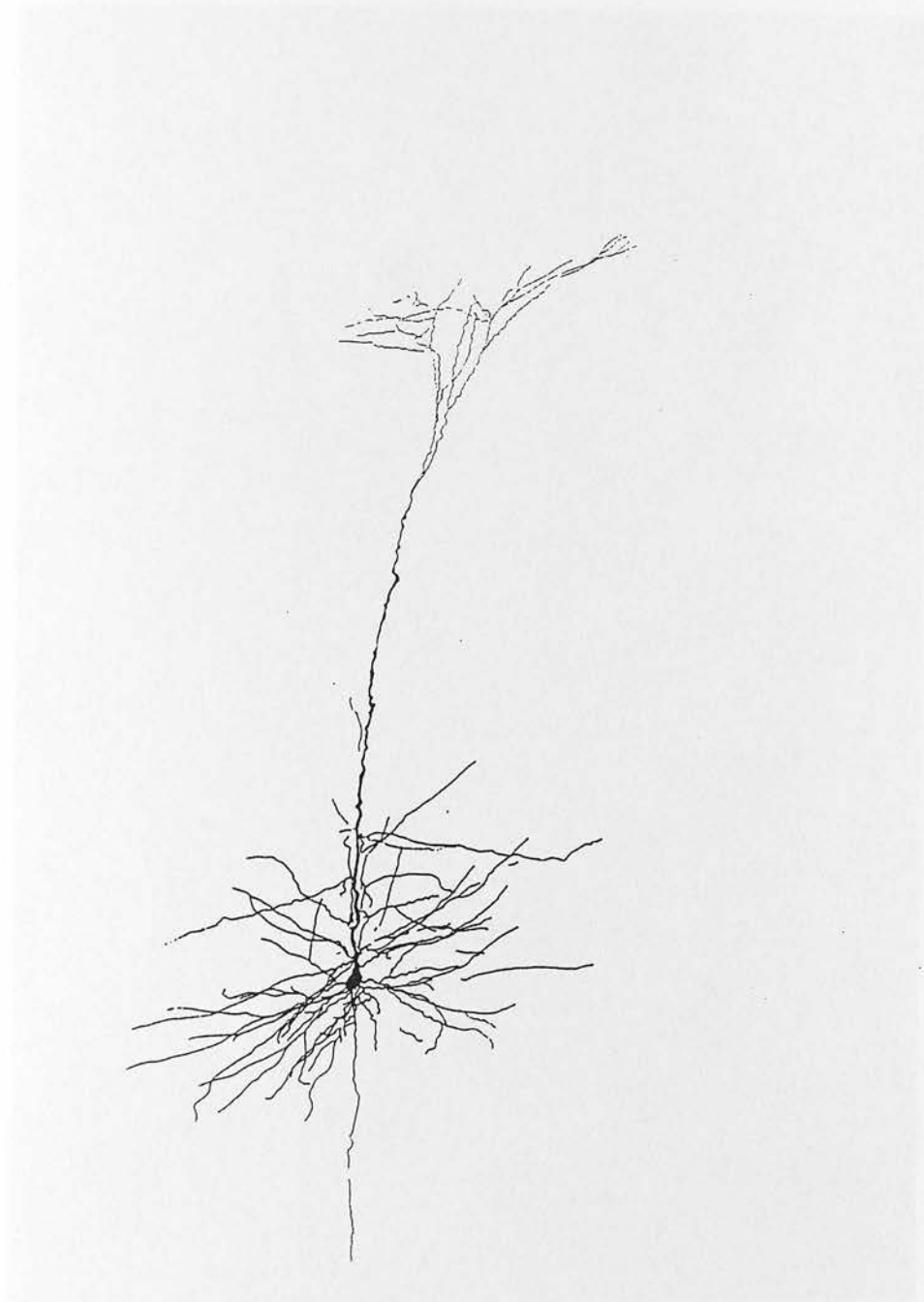


Figure 58. A camera lucida reconstruction of the other filled neuron. The orientation is as follows: pia towards the top of the drawing, the corpus callosum to the bottom and the midline to the left. Scale bar 100  $\mu\text{m}$ .



Figure 59. A photomicrograph of the terminal field. The terminal field was photographed at a magnification of  $\times 100$  (oil immersion) and as a result the entire terminal field does not appear in a single plane within the section. The photograph taken shows a single plane within the section that contains most of the terminal field in a single view. The camera lucida reconstruction contains the entire terminal field within a single section. The fields visible within the photomicrograph and the reconstruction are highlighted ( $\rightarrow$ ). The orientation is as follows: pia towards the top of the photograph and the midline to the left of the photograph. Scale bar  $10\ \mu\text{m}$ .

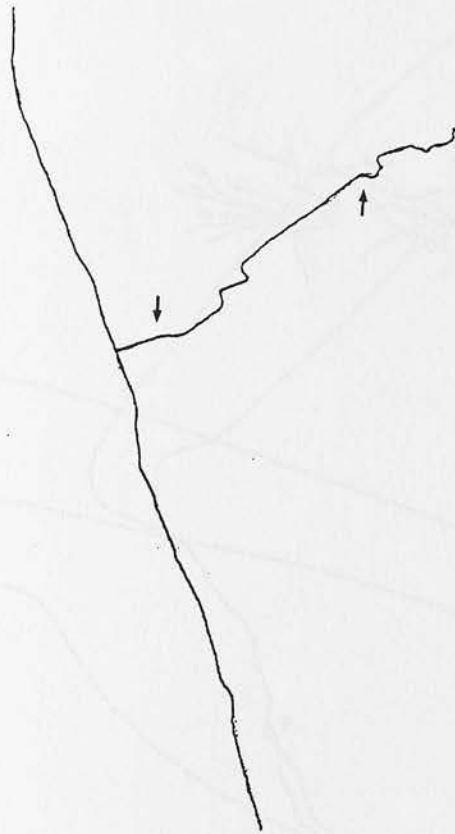


Figure 60. A camera lucida reconstruction of the terminal field. The reconstruction was made in a single section through all the planes of view as it was impossible to reliably align tissue landmarks between serial sections. Limited lateral branch innervations are restricted within serial coronal sections and it is not always possible to detect the terminal field within more than one section. The view shown also contains the greatest part of the terminal field. A comparison of the photomicrograph view and the entire terminal field seen in the camera lucida reconstruction can be compared using the markers ( $\rightarrow$ ). The orientation is as follows: pia towards the top of the drawing and the midline to the left of the drawing. Scale bar 50  $\mu\text{m}$ .

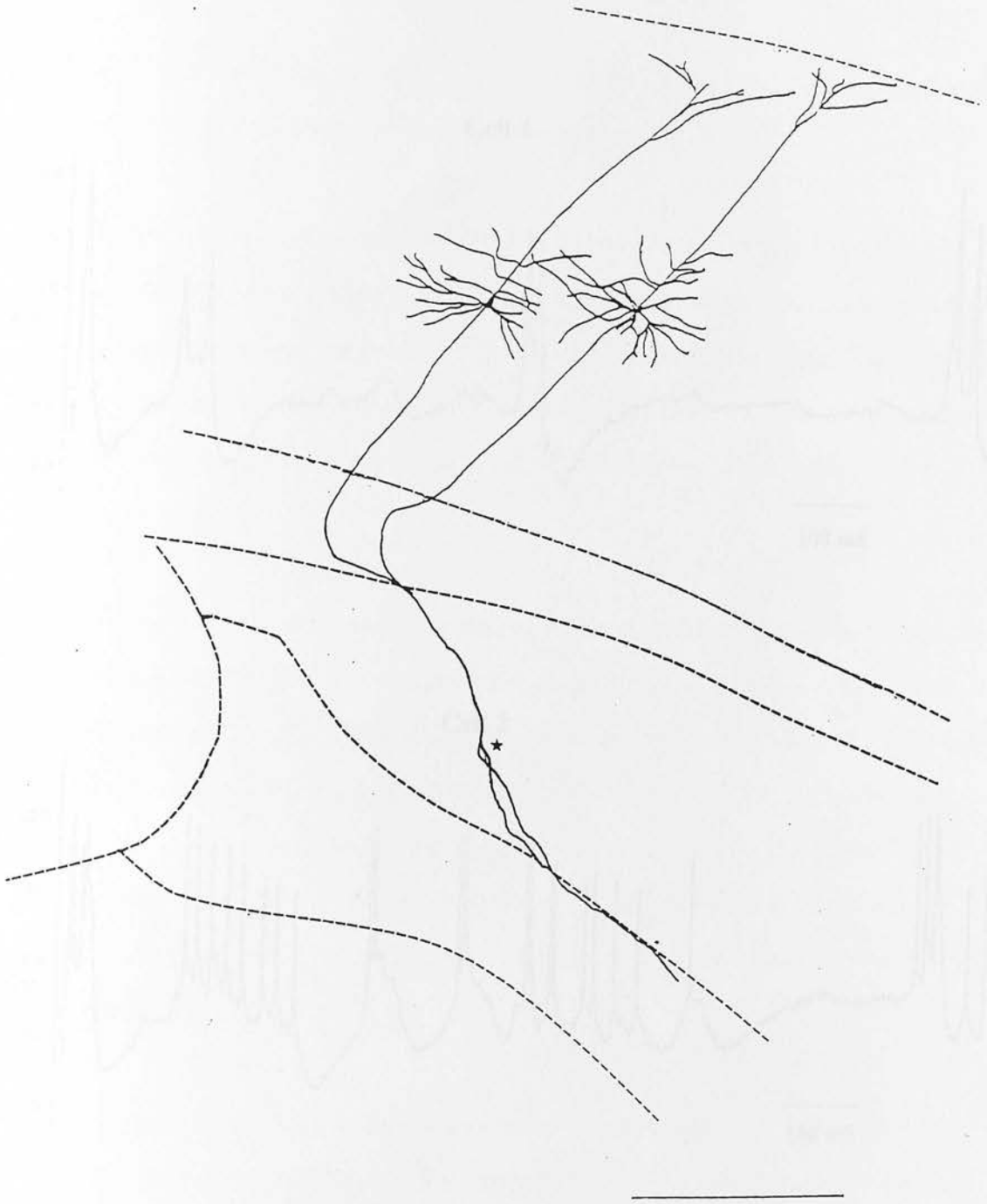


Figure 61. A camera lucida reconstruction of the neurons in their entirety (including cell body, axon path and terminal field). The section is orientated with the pia towards the top of the drawing and the midline to the left. Scale bar 500  $\mu\text{m}$ .

The cell was filled with 1% of the piezoelectric material and recorded using the method described in the text.

Figure 62 shows examples of the filled neurons responses to whisker deflection.

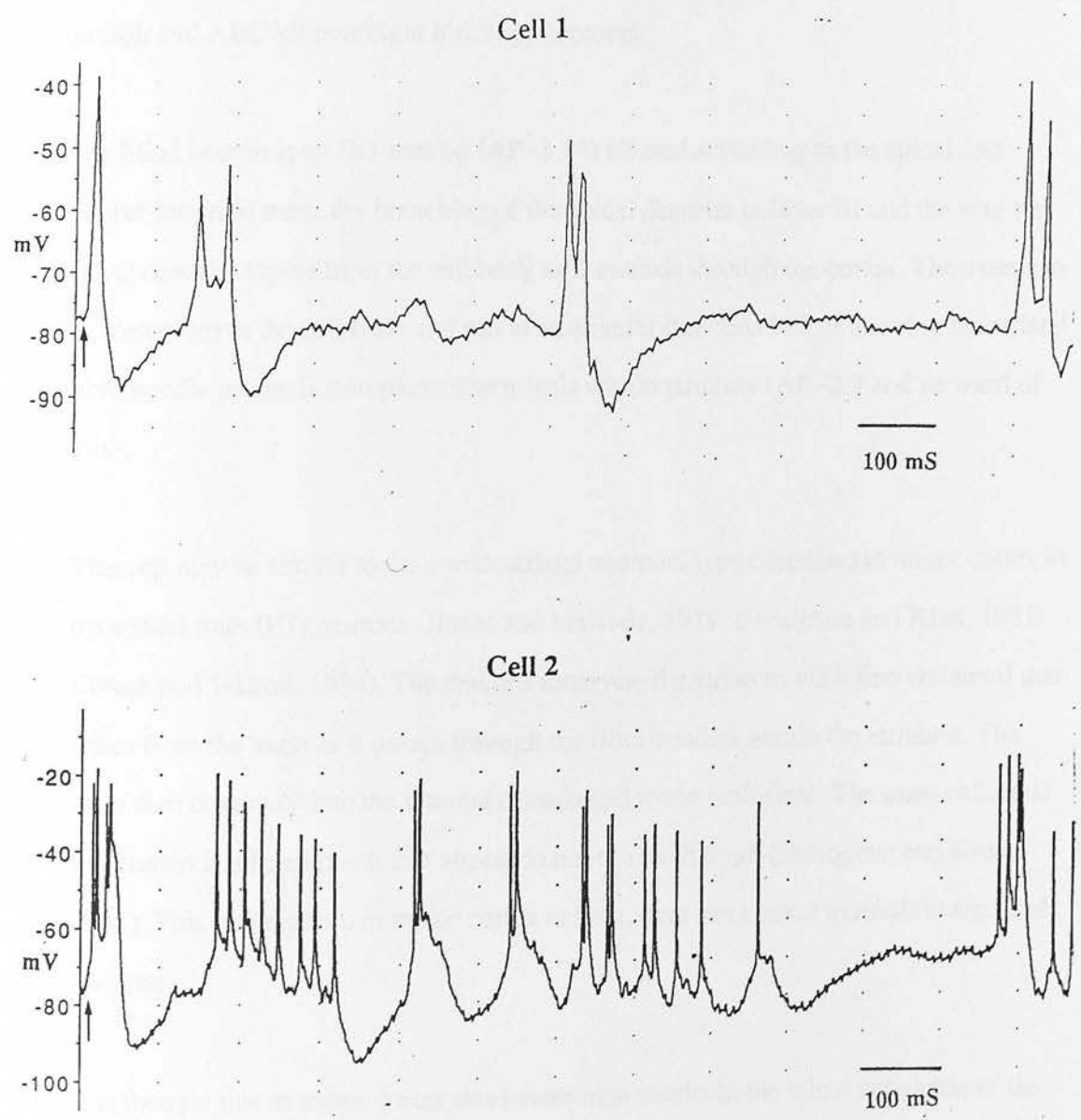


Figure 62. Examples of both the filled neurons responses to whisker deflection. The position of the piezoelectric stimulus is highlighted (↑).

#### 34.1.4 Limited Lateral Branch Innervation 2

The cell was filled using the initial surgical procedure and revealed using the methanol quench and ABC kit overnight histology protocol.

The filled neuron is an IB1 neuron (AP -3.14) classed according to the apical and basilar dendritic trees, the branching of the apical dendrite in layer III and the way the apical dendrite tapers from the cell body as it ascends through the cortex. The axon can be seen to leave the cell body and run in an anterior direction before entering the striatal fibre bundle producing en passant terminals within striatum (AP -2.3 and forward of this).

This cell may be similar to the corticostriatal neuronal type described in motor cortex as pyramidal tract (PT) neurons (Jinnai and Matsuda, 1979; Donoghue and Kitai, 1981; Cowan and Wilson, 1994). The neurons innervate the striatum via a fine collateral that arises from the axon as it passes through the fibre bundles within the striatum. The axon then continues into the internal capsule and to the brainstem. The axon collateral in striatum is a fine branch that appear to travel 100-200  $\mu\text{m}$  (Donoghue and Kitai, 1981). This innervation, in motor cortex at least, does not appear to result in terminal boutons.

It is thought that in motor cortex this innervation results in the initial activation of the striatum from cortical stimulation. The stimulation of cortex results in a short latency EPSP activation of the medium spiny cells in the striatum.

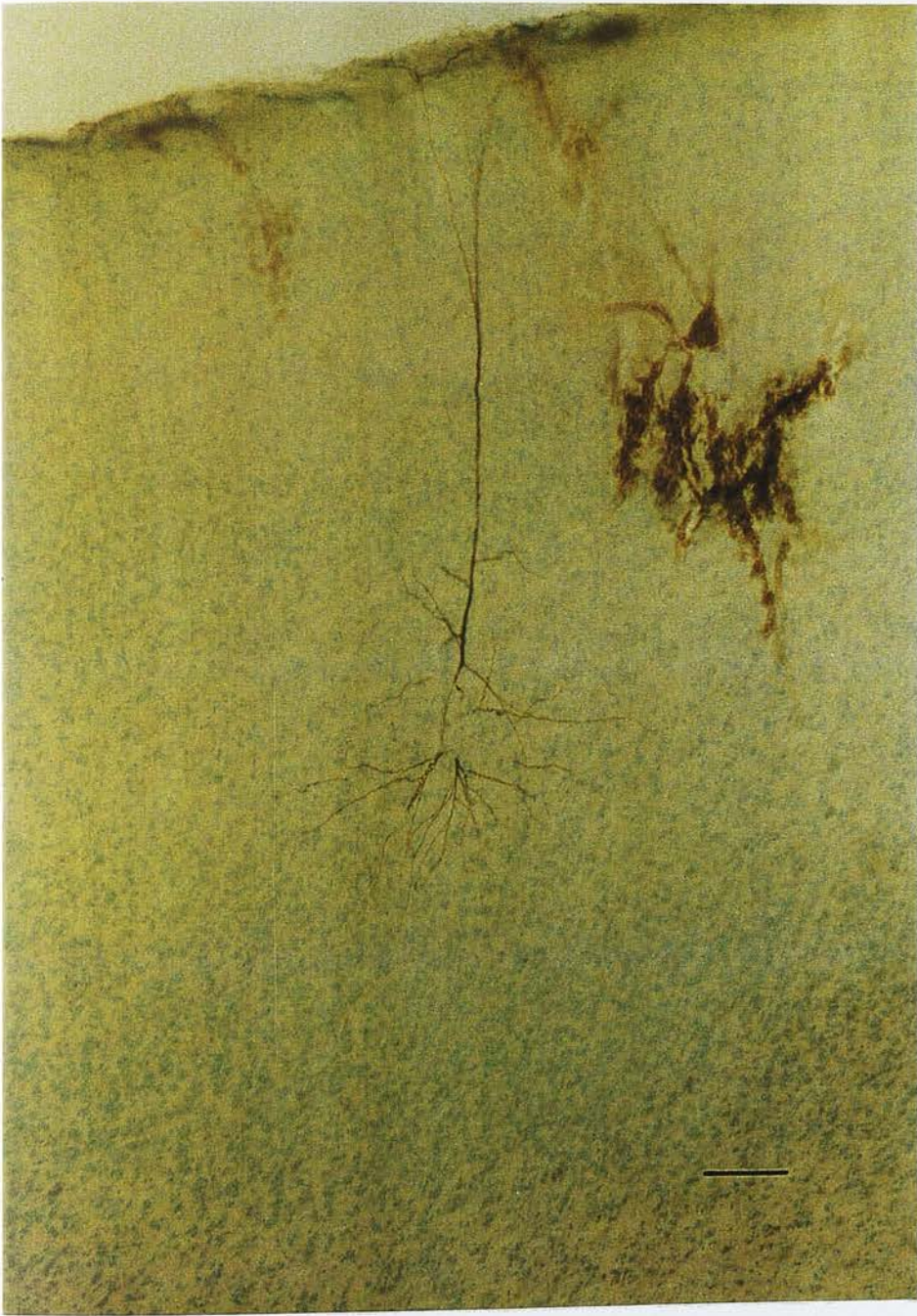


Figure 63. A photomicrograph of the filled neuron. The orientation is as follows: pia towards the top of the photograph, the corpus callosum to the bottom and the midline to the left. Scale bar 100  $\mu\text{m}$ .

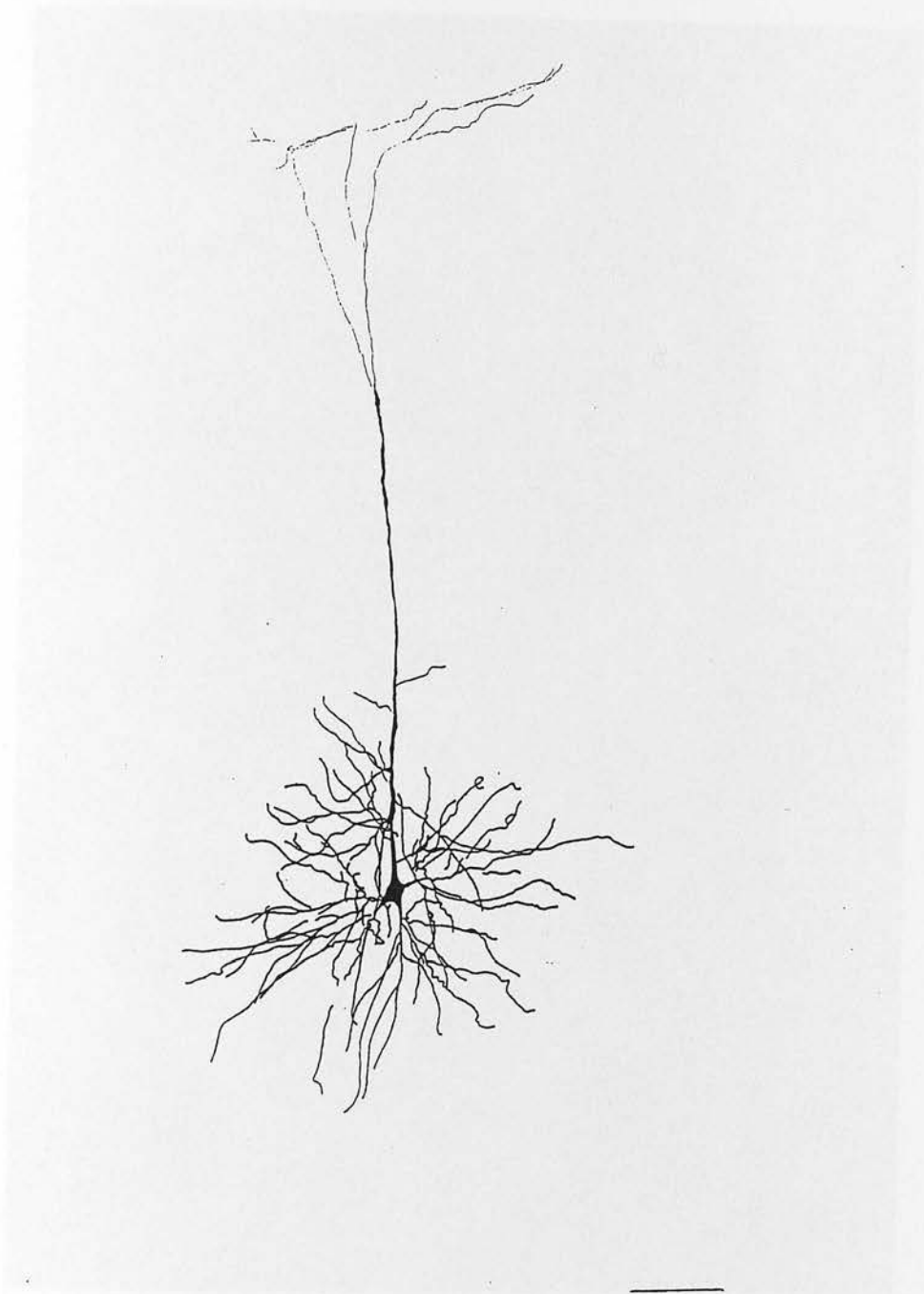


Figure 64. A camera lucida reconstruction of the filled neuron. The orientation is as follows: pia towards the top of the drawing, the corpus callosum to the bottom and the midline to the left. Scale bar 100  $\mu\text{m}$ .



Figure 65. A photomicrograph of the terminal field. The terminal field was photographed at a magnification of  $\times 100$  (oil immersion) and as a result the entire terminal field does not appear within a single plane within the section. The photograph taken shows a single plane within the section that contains most of the terminal field in a single view. The camera lucida reconstruction contains the entire terminal field within the same single section. The comparable fields visible in the photomicrograph and the camera lucida reconstruction are highlighted ( $\leftrightarrow$ ). The orientation is as follows: pia towards the top of the photograph and the midline to the left of the photograph. Scale bar  $10\ \mu\text{m}$ .

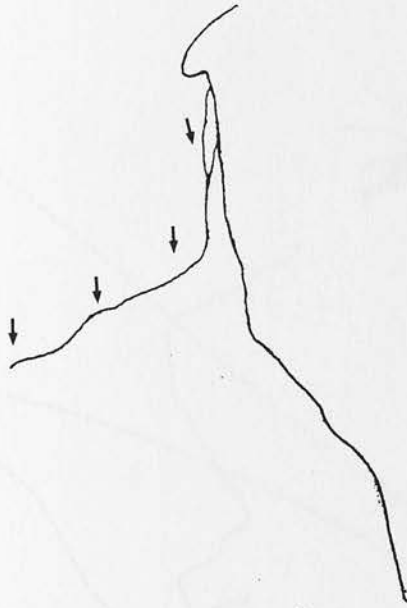


Figure 66. A camera lucida reconstruction of the terminal field. The reconstruction was made in a the same section as the photomicrograph through all the planes of view. A composite picture was not made using adjacent serial sections as the limited lateral branch innervations are restricted within serial coronal sections and it is not always possible to detect the terminal field in more than one section. Where is is detected it is not possibly to reliably align landmarks within the tissue to build a composite image. A comparison of the photomicrograph image and the entire terminal field seen in the camera lucida reconstruction can be compared using the markers ( $\rightarrow$ ). The orientation is as follows: pia towards the top of the drawing and the midline to the left of the drawing. Scale bar 50  $\mu$ m.

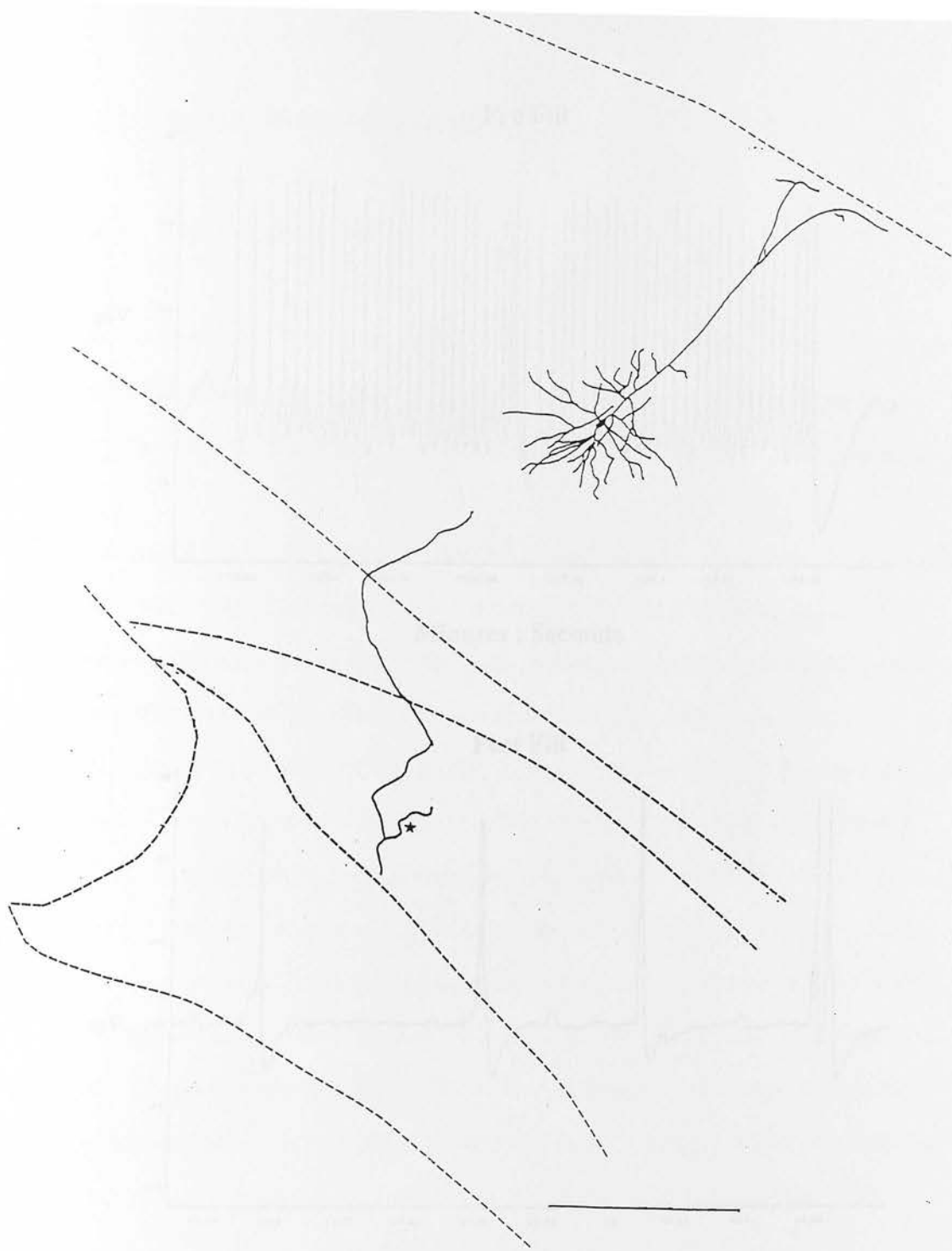


Figure 67. A camera lucida reconstruction of the neuron in its entirety (including cell body, axon path and terminal field). The section is orientated with the pia towards the top of the drawing and the midline to the left. Scale bar 500  $\mu\text{m}$ .

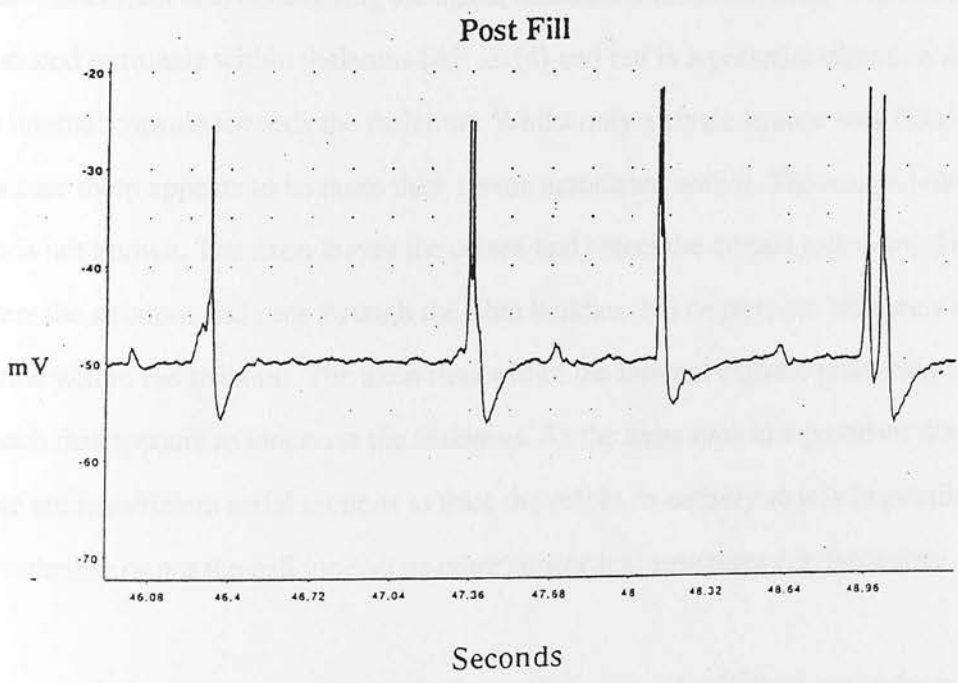
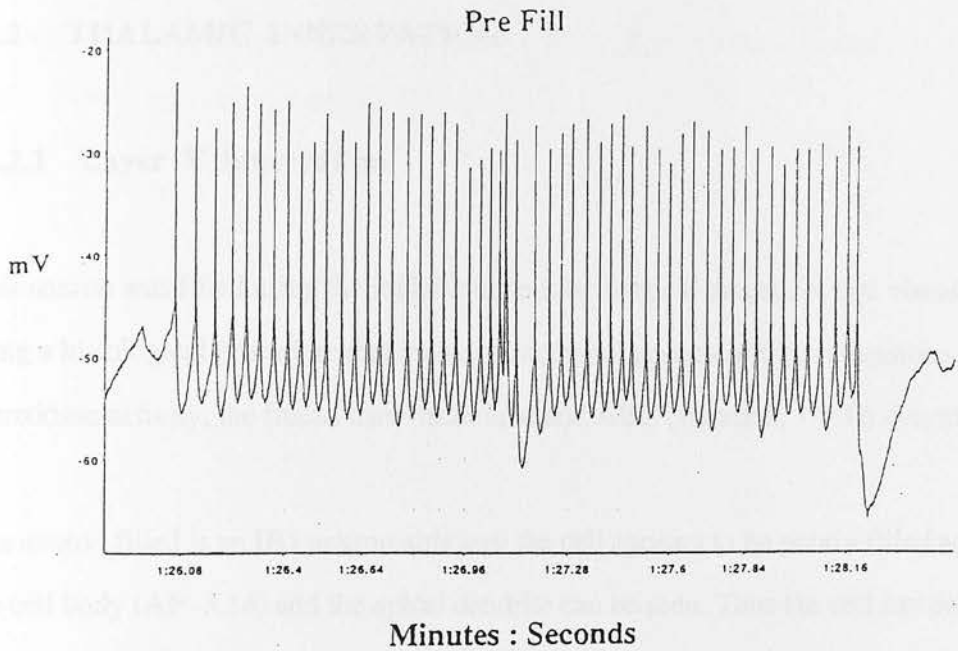


Figure 68. Examples of the filled neuron's response to whisker deflection. Both responses were recorded using vcr and visualised using 'Chart'. As a result the exact location of the stimulus within the trace is unknown ( see sections 11.3 and 27.0) although the amplitude and duration of the stimulus is that same as in 'Scope' recordings. The responses seen here highlight the firing pattern seen in response to piezoelectric whisker stimulation.

## 34.2 THALAMIC INNERVATION

### 34.2.1 Layer V innervation

This neuron was filled using the initial intracellular surgical procedure and visualised using a histological procedure that included methanol quench of the endogenous peroxidase activity, the freeze thaw-technique and ABC (standard, 1:100) overnight.

The neuron filled is an IB1 neuron although the cell appears to be poorly filled as only the cell body (AP -3.14) and the apical dendrite can be seen. Thus the cell has been classed morphologically as IB1 on the basis of the branch point of the apical dendrite alone rather than also considering the apical and basilar dendritic trees. The axon produced terminals within thalamus (AP -3.14) and ran in a posterior direction through the internal capsule towards the thalamus. Whilst only a single neuron was filled in this case there appears to be more than 1 axon associated with it. The reason behind this is not known. The axon leaves the cortex and enters the corpus callosum, then enters the striatum and runs through the fibre bundles. No *en passant* terminals were visible within the striatum. The axon runs within the internal capsule producing a branch that appears to innervate the thalamus. As the axon runs in a posterior direction there are insufficient serial sections to trace the cell in its entirety so it is impossible to say whether or not the cell innervates other subcortical structures e.g. brainstem.

The animal died under anaesthesia which may have caused cell death and reduced fixation of the tissue, possible resulting in the degradation of the biocytin (as the animal could not be successfully perfused). Another possibility is that in order to visualise terminals the cell morphology must sometimes be sacrificed as a compromise if limited tracer is introduced into the actively transporting neuron. For whatever

reason in this case the fill was successful enough to fill the terminals clearly in their entirety but it was not possible to view the entire cell.

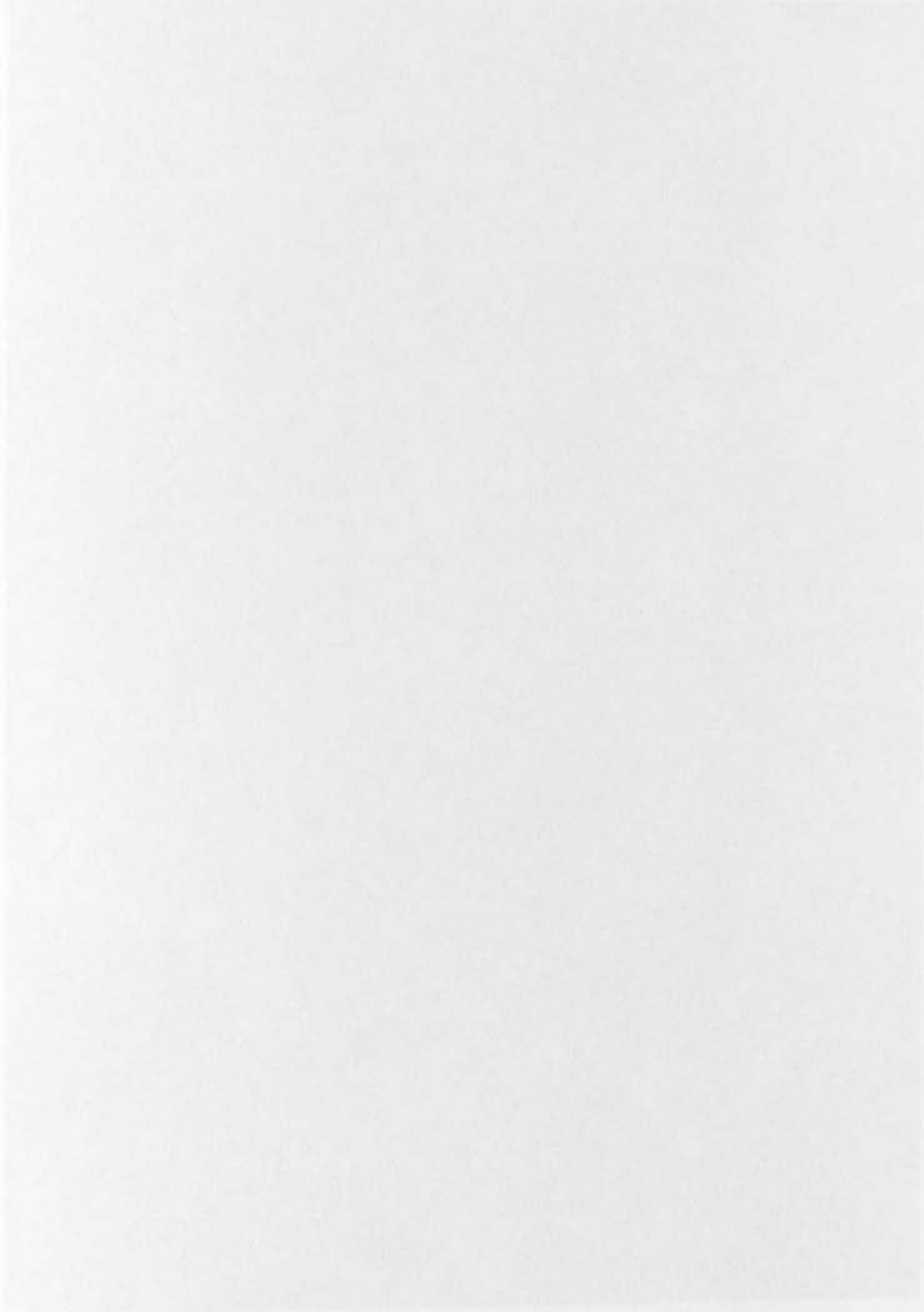


Figure 10. A photomicrograph of a filled neuron. The dendritic tree is at the top of the photograph, the nucleus is at the bottom, and the axon is at the left. Scale bar = 100  $\mu$ m.



Figure 69. A photomicrograph of the filled neuron. The orientation is as follows: pia towards the top of the photograph, the corpus callosum to the bottom and the midline to the left. Scale bar 100  $\mu\text{m}$ .

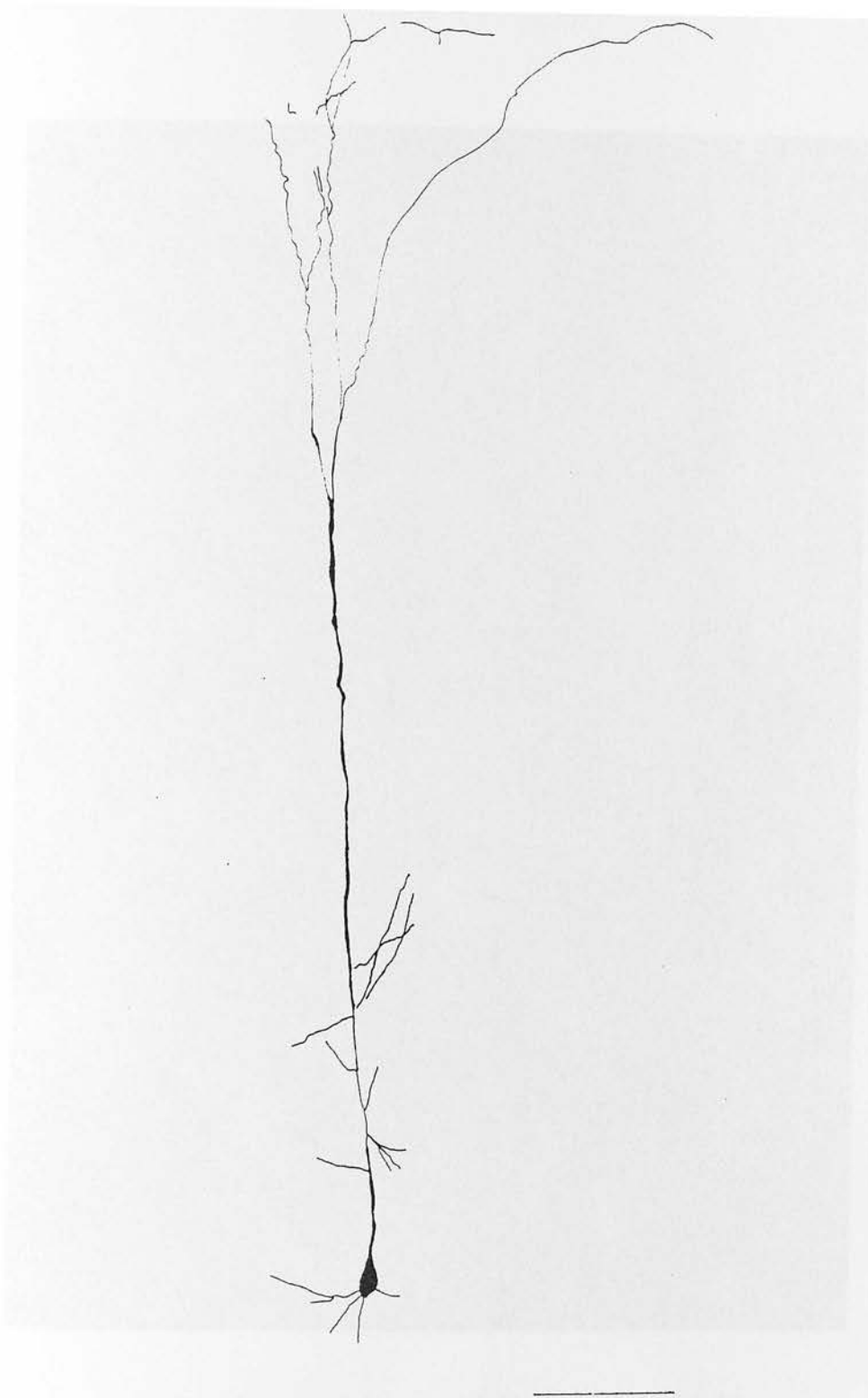


Figure 70. A camera lucida reconstruction of the filled neuron. The orientation is as follows: pia towards the top of the drawing, the corpus callosum to the bottom and the midline to the left. Scale bar 100  $\mu\text{m}$ .



Figure 71. A photomicrograph of a terminal field. The terminal field was photographed at a magnification of  $\times 40$  and as a result the entire terminal field does not appear within a single plane within the section. The photograph taken shows a single plane within the section that contains most of the terminal field in a single view. The camera lucida reconstruction contains the entire terminal field within the same single section. The comparable fields visible in the photomicrograph and the camera lucida reconstruction are highlighted ( $\leftrightarrow$ ). The orientation is as follows: pia towards the top of the photograph and the midline to the left of the photograph. Scale bar  $50 \mu\text{m}$ .

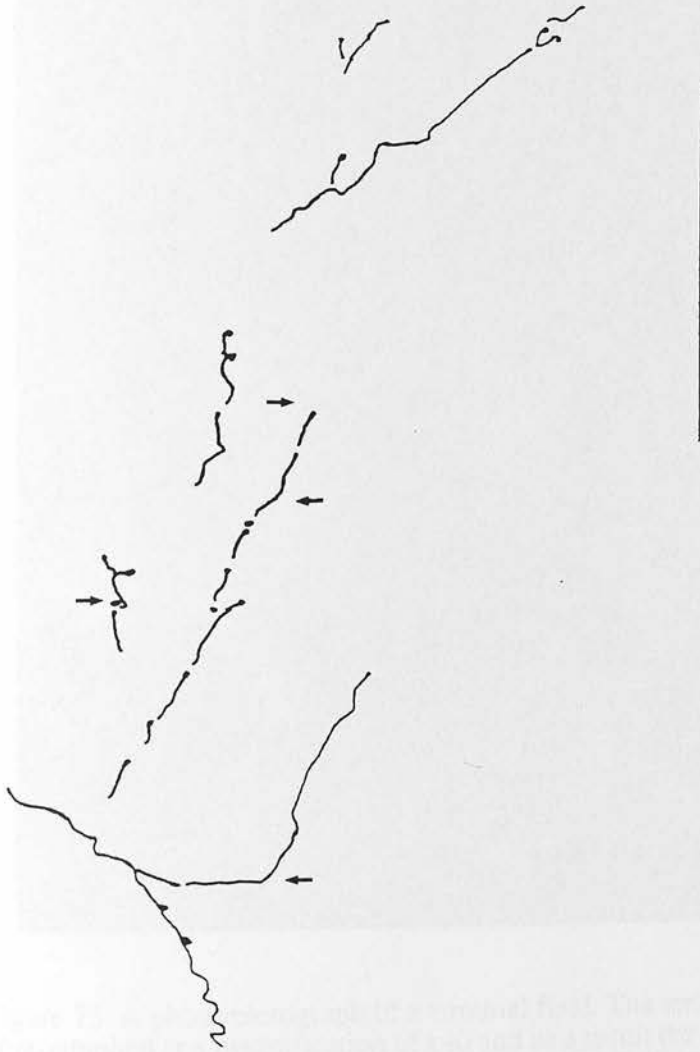


Figure 72. A camera lucida reconstruction of a terminal field. The reconstruction was made in a single section through all planes of view as it was impossible to reliably construct an image from serial coronal sections (due to the difficulty in aligning tissue landmarks between sections). A comparison of the photomicrograph view and the entire terminal field see in the camera lucida reconstruction can be compared using the markers ( $\rightarrow$ ). The orientation is as follows: pia towards the top of the drawing and the midline to the left of the drawing. Scale bar 50  $\mu\text{m}$ .

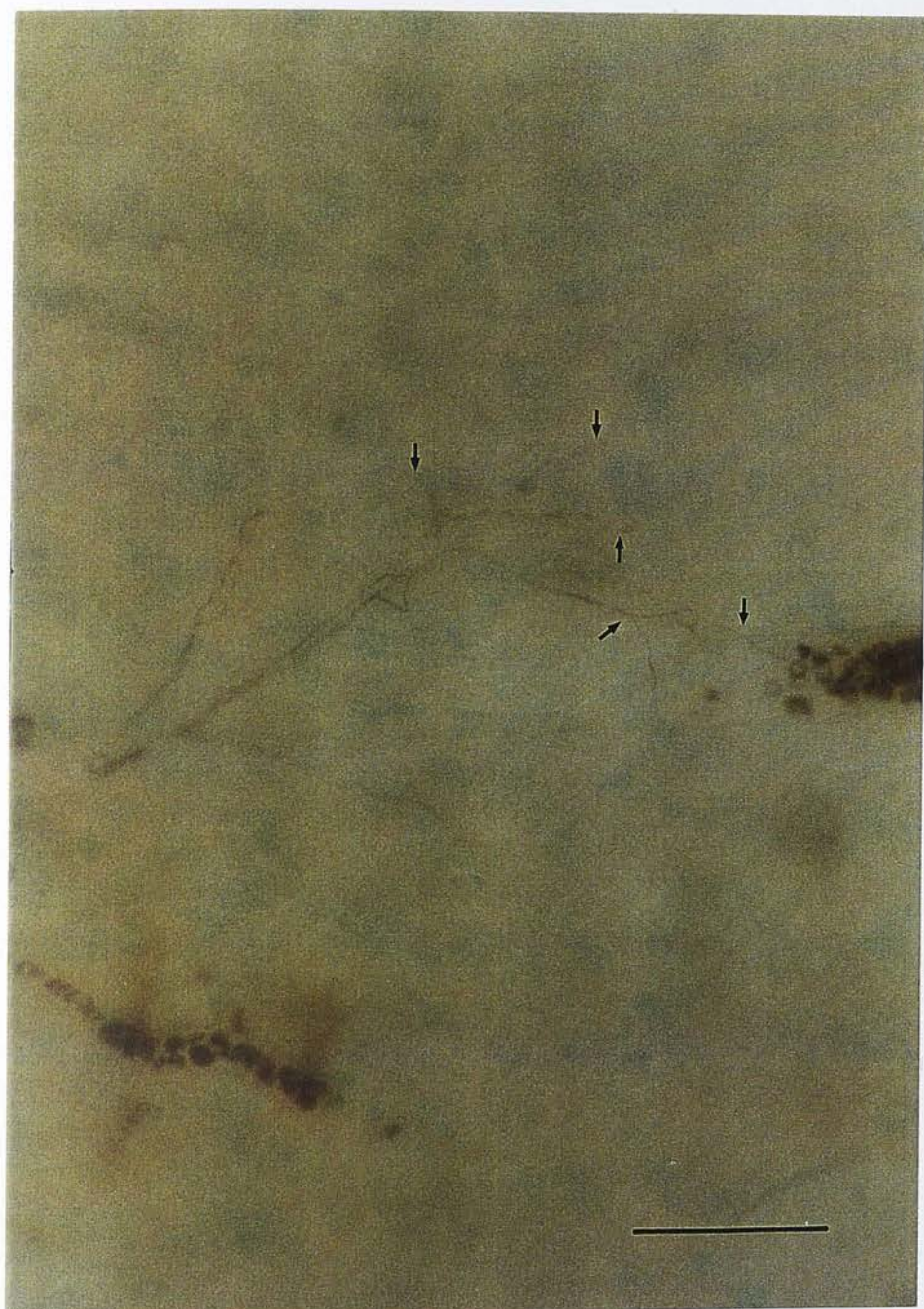


Figure 73. A photomicrograph of a terminal field. The terminal field was photographed at a magnification of x40 and as a result the entire terminal field does not appear within a single plane within the section. The photograph taken shows a single plane within the section that contains most of the terminal field in a single view. The camera lucida reconstruction contains the entire terminal field within the same single section. The comparable fields visible in the photomicrograph and the camera lucida reconstruction are highlighted ( $\leftrightarrow$ ). The orientation is as follows: pia towards the top of the photograph and the midline to the left of the photograph. Scale bar 50  $\mu$ m.

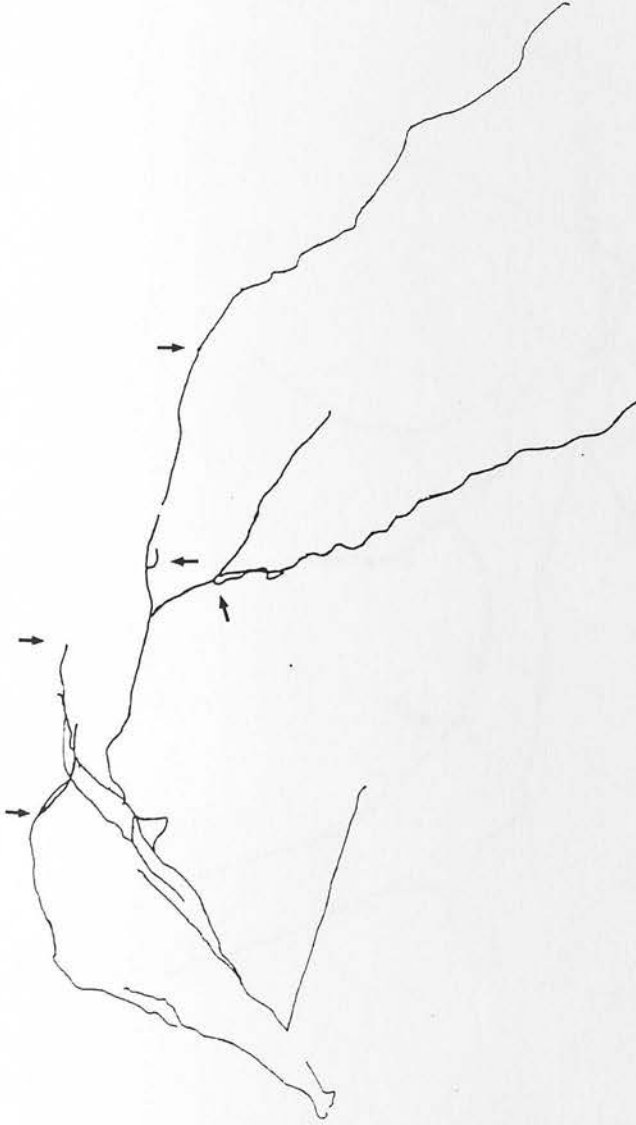


Figure 74. A camera lucida reconstruction of a terminal field. The reconstruction was made in a single section through all planes of view as it was impossible to reliably construct an image from serial coronal sections (due to the difficulty in aligning tissue landmarks between sections). A comparison of the photomicrograph view and the entire terminal field see in the camera lucida reconstruction can be compared using the markers ( $\rightarrow$ ). The orientation is as follows: pia towards the top of the drawing and the midline to the left of the drawing. Scale bar 50  $\mu\text{m}$ .

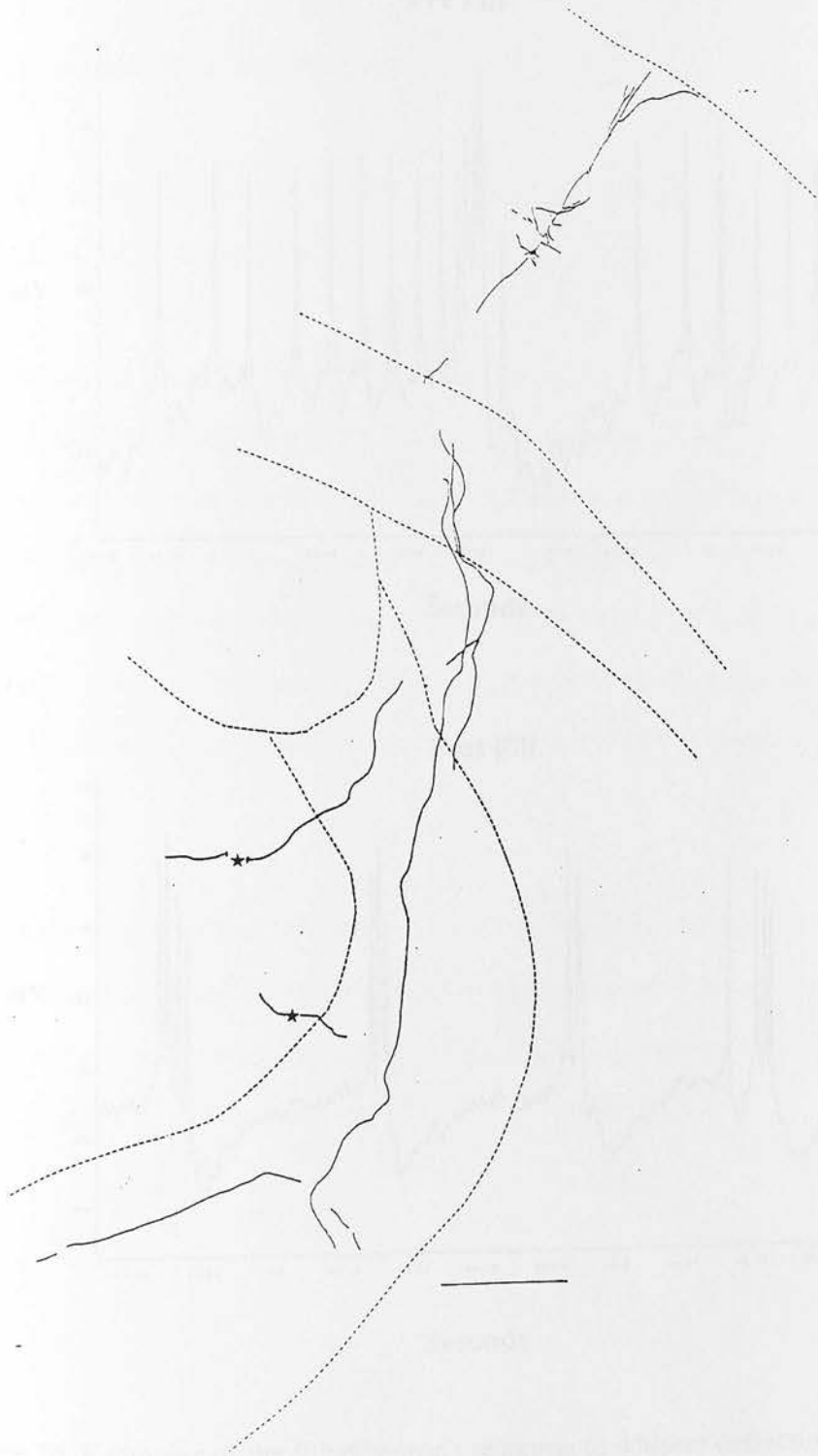


Figure 75. A camera lucida reconstruction of the neuron in its entirety (including cell body, axon path and terminal field). The section is orientated with the pia towards the top of the drawing and the midline to the left. Scale bar 500  $\mu\text{m}$ .

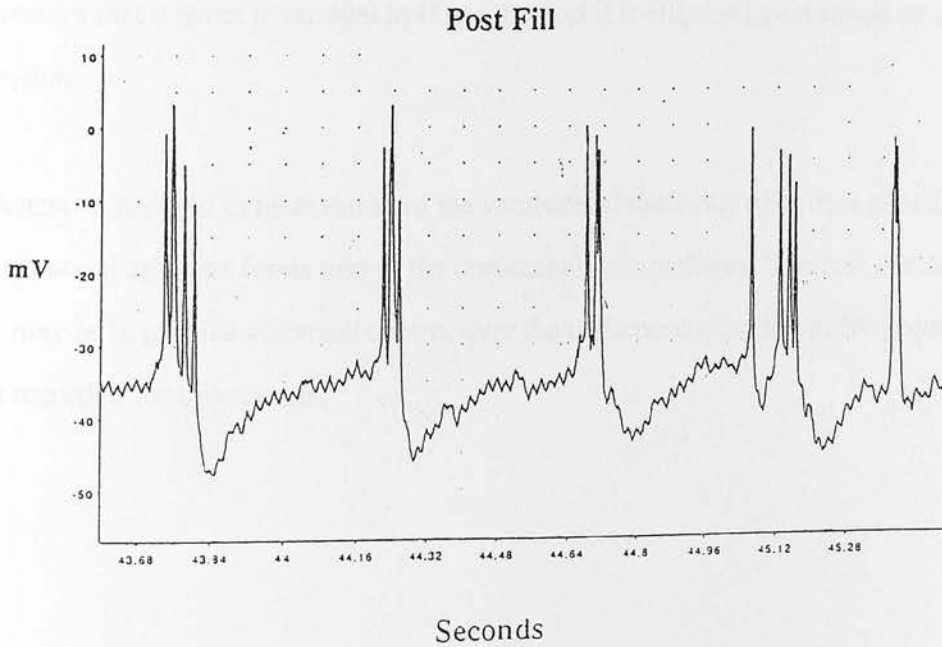
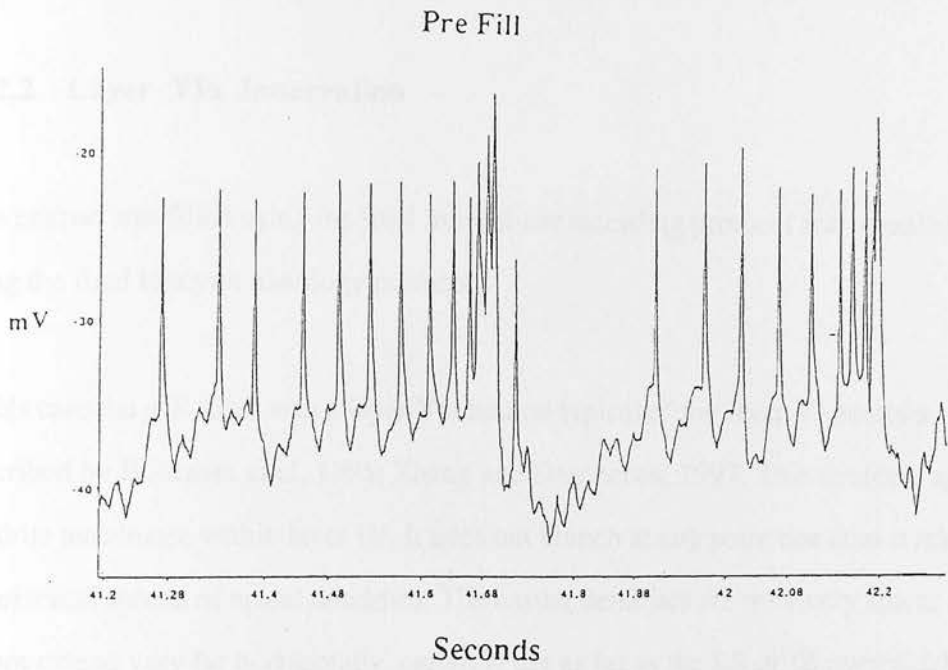


Figure 76. Examples of the filled neuron's response to whisker deflection. Both responses were re-recorded using vcr and visualised using 'Chart'. As a result the exact location of the stimulus within the trace is unknown ( see sections 11.3 and 27.0) although the amplitude and duration of the stimulus is that same as in 'Scope' recordings. The responses seen here highlight the firing pattern seen in response to piezoelectric whisker stimulation.

### 34.2.2 Layer VIa Innervation

This neuron was filled using the final intracellular recording protocol and visualised using the final biocytin histology protocol.

In this case the cell filled was a layer VIa neuron typical of the layer VI neurons described by Bourassa et al, 1995; Zhang and Deschenes, 1997. This neuron's apical dendrite terminates within layer IV. It does not branch at any point nor does it result in a horizontal spread of apical dendrites. The basilar dendrites are relatively sparse and do not extend very far horizontally, certainly not as far as the RS or IB pyramidal projection neurons. The soma is unlike those described for the other projection neurons in that it is not pyramidal in shape, instead it is ellipsoid and is much smaller in diameter.

This neuron resulted in innervation of the ventrobasal thalamus only. It is possible that this neuronal cell type forms part of the corticothalamic pathway. The role of such a link may be to provide a cortical control over the thalamocortical input. No physiology was recorded for this neuron.

Figure 11. A photomicrograph of the filled neuron. The soma is small and ellipsoid. The apical dendrite extends upwards towards the top of the photograph, the axon extends downwards. Scale bar: 100  $\mu$ m.



Figure 77. A photomicrograph of the filled neuron. The orientation is as follows: pia towards the top of the photograph, the corpus callosum to the bottom and the midline to the left. Scale bar 100  $\mu\text{m}$ .

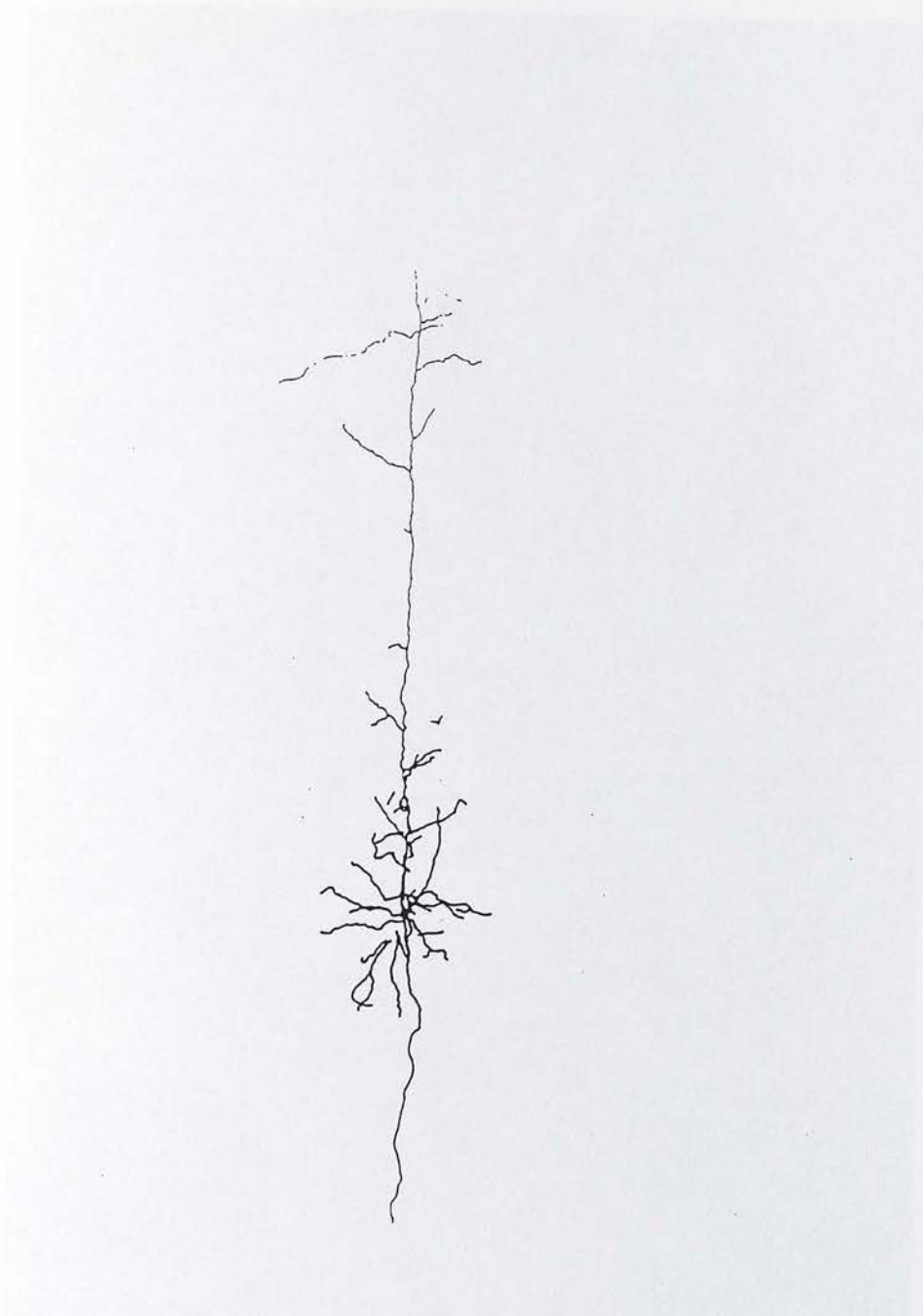


Figure 78. A camera lucida reconstruction of the filled neuron. The orientation is as follows: pia towards the top of the drawing, the corpus callosum to the bottom and the midline to the left of the photograph. Scale bar 100  $\mu$ m.



Figure 79. A photomicrograph of the terminal field. The terminal field was photographed at a magnification of  $\times 100$  (oil immersion) and as a result the entire terminal field in this section does not appear within a single plane. The photograph taken shows a single plane within the section that contains most of the terminal field in a single view. The camera lucida reconstruction contains an entire terminal field within the same single section. The comparable fields visible in the photomicrograph and the camera lucida reconstruction are highlighted. The orientation is as follows: pia towards the top of the photograph and the midline to the left of the photograph. Scale bar  $10\ \mu\text{m}$ .



Figure 79. A camera lucida reconstruction of a terminal field. The reconstruction was made in a single section through all planes of view as it was impossible to reliably construct an image from serial coronal sections (due to the difficulty in aligning tissue landmarks between sections). A comparison of the photomicrograph view and the entire terminal field see in the camera lucida reconstruction can be compared using the markers ( $\rightarrow$ ). The orientation is as follows: pia towards the top of the drawing and the midline to the left of the drawing. Scale bar 50  $\mu\text{m}$ .

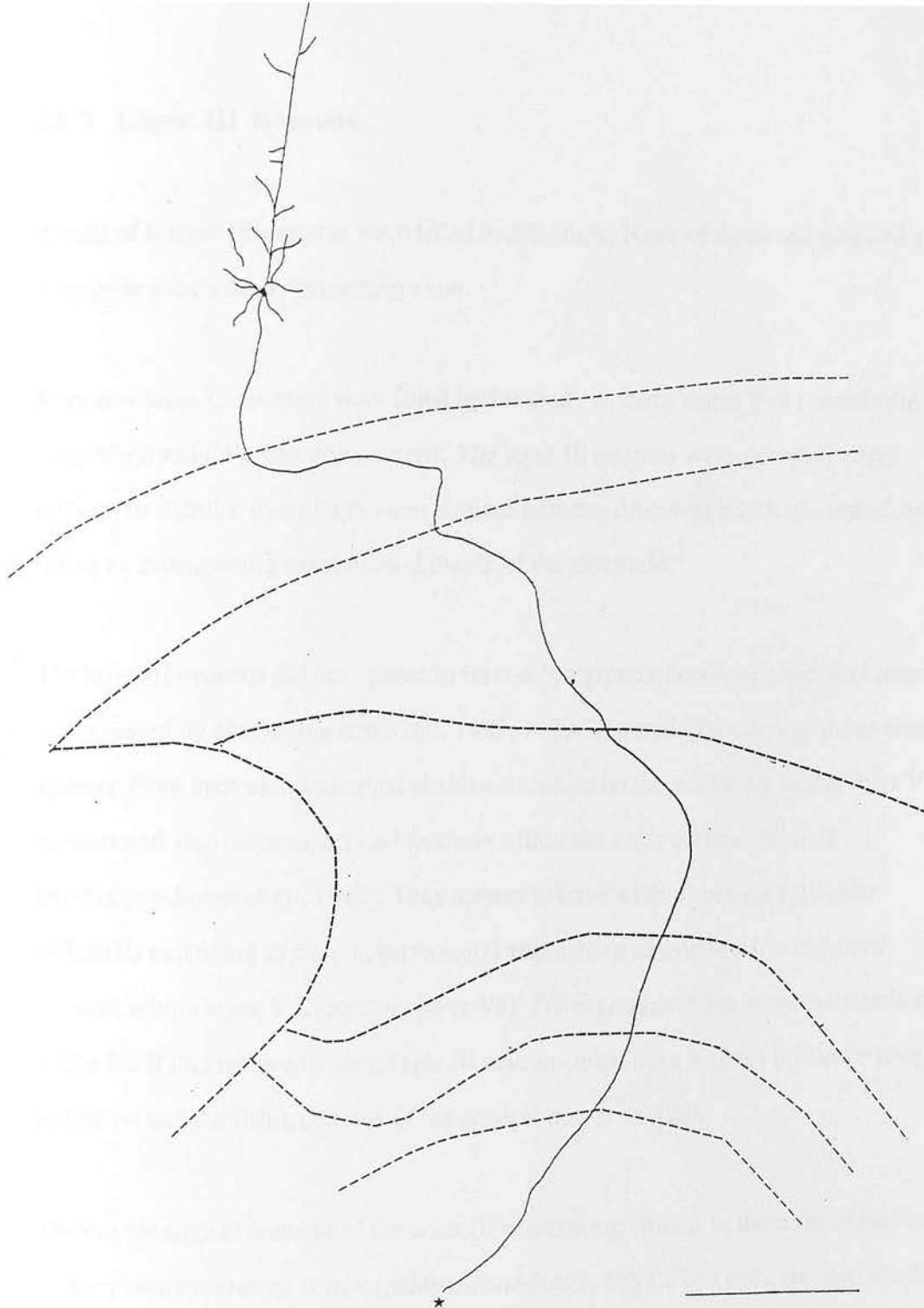


Figure 81. A camera lucida reconstruction of the neuron in its entirety (including cell body, axon path and terminal field). The orientation is as follows: pia towards the top of the drawing and the midline to the left. Scale bar 500  $\mu\text{m}$ .

### 34.3 Layer III Neurons

A total of 6 layer III neurons were filled in this study. None of these neurons had a detectable subcortically projecting axon.

Very few layer III neurons were filled in this study as there was a bias towards the layer V pyramidal projection neurons. The layer III neurons were generally more difficult to stabilise upon impalement perhaps because there was a lack of cortical tissue acting as a dampening agent around the tip of the electrode.

The layer III neurons did not appear to form a sub group of cortical projection neurons as suggested by McGeorge and Faull, 1987; 1989. The main function of these neurons appears, from their morphological characteristics, to be the activation of the layer V neurons and also more superficial neurons within the same cortical column (Armstrong-James et al., 1992). They appear to have a dense network of axon collaterals extending to the pial surface and also a more extensive axon collateral network within layer V (especially layer Va). For examples of the axon collaterals see figure 83. If this is the case then layer III neurons must have a direct influence over the activation and the firing patterns of the cortical output neurons.

The morphological features of the layer III neurons are similar to those described in cat primary somatosensory cortex (Schwark and Jones, 1989). The cells are also similar to those described in the primary motor cortex of rat (Miyashita et al., 1994; Weiss and Keller, 1994), cat (Keller, 1993; Keller and Asanuma, 1993) and primate (Huntley and Jones, 1991) as well as those described for the primary visual cortices in rats (Burkhalter, 1989) and cats (Nicoll et al., 1993; Larkman and Mason, 1990; Mason and Larkman, 1990) and the primary auditory cortex in cats (Ojima et al., 1991; 1992; Wallace et al., 1991b).

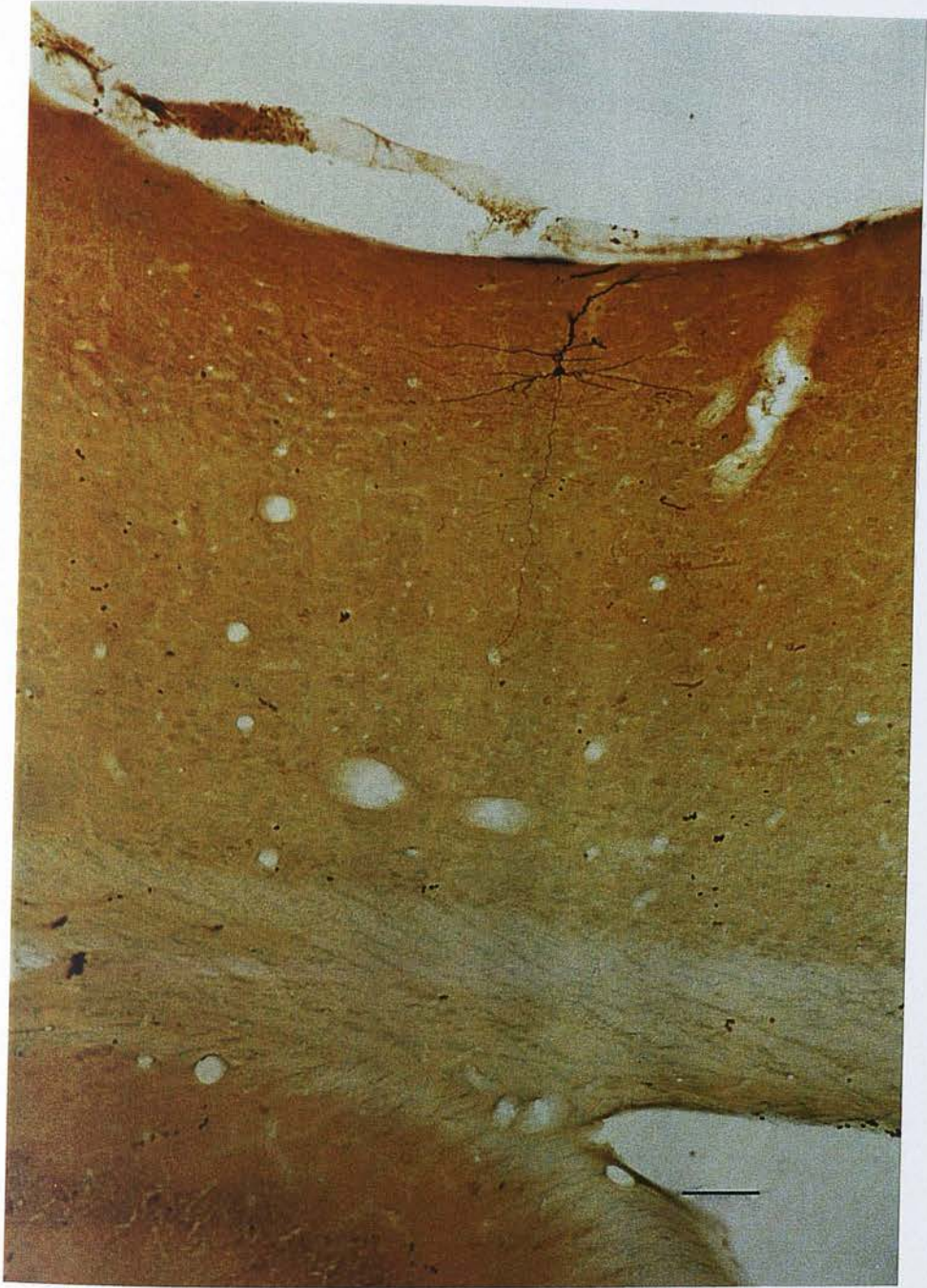


Figure 82. A low power photomicrograph of a layer III neuron showing the laminar position of the neuron. The orientation is as follows: pia towards the top of the photograph, the corpus callosum to the bottom and the midline to the left. Scale bar 100  $\mu\text{m}$ .

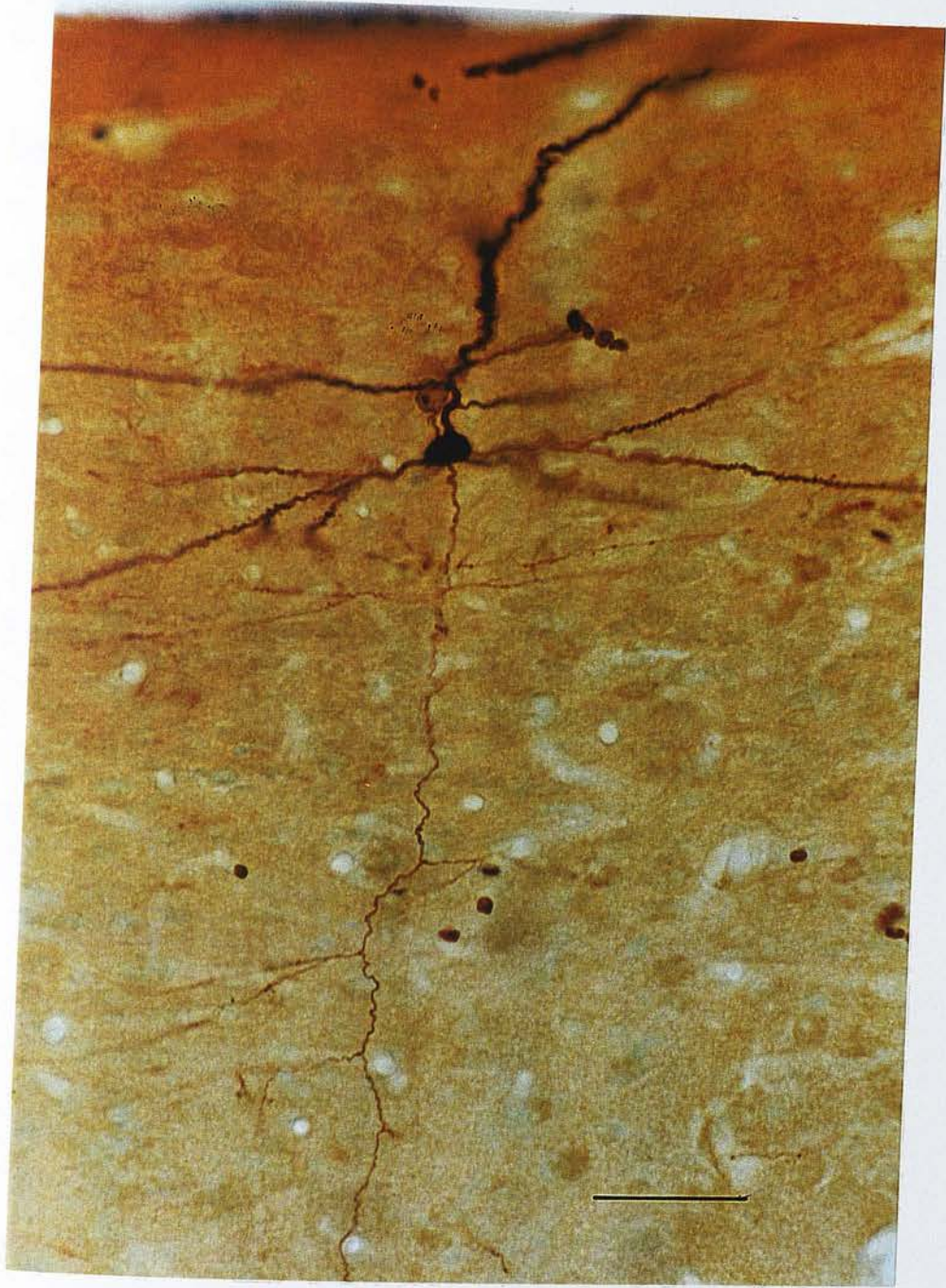


Figure 83. A higher power photomicrograph of the layer III neuron showing the axon collaterals. The orientation is as follows: pia towards the top of the photograph, the corpus callosum to the bottom and the midline to the left. Scale bar 10  $\mu$ m.

## DISCUSSION

### 35.0 Different Classes of Layer V Pyramidal Projection Neurons

In this study the four main classes of layer V pyramidal projection neurons described by Cauller and Connors, 1994 were identified (with IB neurons being the most numerous) as well as two classes of corticostriatal innervation patterns (similar to those previously described in agranular (motor) cortex (Jinnai and Matsuda, 1979; Donoghue and Kitai, 1981; Royce, 1982; 1983; Landry et al., 1984; Wilson, 1987; Cowan and Wilson, 1994) and the whisker region of rat primary somatosensory cortex (Wright et al., 1998)).

The morphology of the neurons in this study were similar to those described *in vitro* within somatosensory cortex (Chagnac-Amitai et al., 1990; Connors and Gutnick, 1990; Cauller and Connors, 1994) visual cortex (Larkman and Mason, 1990; Mason and Larkman, 1990) and motor cortex of rats (Donoghue and Kitai, 1981; Landry et al., 1984; Cowan and Wilson, 1994).

#### 35.1 Classification Criteria

##### Morphology

Morphological classification was performed on a limited number of criteria i.e. branch point of the apical dendrite, the extension of the apical and basilar dendritic trees (and in some cases the orientation of the axon collaterals) described *in vitro* (See Connors and Gutnick, 1990 for a review). As the criteria used are physical it is thought that the classification criteria ( and cell class) will not differ between *in vivo* and *in vitro* recording systems. As the classification criteria are limited there is a greater scope for

the misclassification of RS and IB neurons e.g. in cases where the branch point of the apical dendrite is not clear or where the apical and basilar dendritic trees are not entirely filled or visible. Increasing the number of reliable classification criteria would limit the scope for misclassification. Despite the number of limited criteria those described here have proved successful for the classification of neurons both in vivo and in vitro. In a bid to strengthen the classification where is possible the physiological class of a neuron has also been taken into account when a neuron is classified.

### **Physiology**

The physiological classification criteria used in this study with respect to burst firing have been taken from in vitro studies (for a review see Connors and Gutnick, 1990). The major differences between the two experimental procedures are the nature and duration of the stimulus. In vitro recordings are obtained by the injection of a current pulse into the neuron in question and the response is recorded during the stimulation of the neuron. In this in vivo study the stimulus takes the form of a rapid (4 mS) stimulation of an individual whisker in the periphery. The response to the stimulus is recorded after the stimulation i.e. there is no direct current pulse into the neuron and there is no continuous stimulation of the neuron during the recording of the response.

Although the stimuli in the two systems are quite different examination of the neuronal firing patterns in the in vivo preparation reveals that the response patterns observed within the in vivo and in vitro recordings of RS and IB neurons remain basically the same. For example IB neurons fire in characteristic burst that have been noted in vitro (see Connors and Gutnick, 1990), RS neurons do not burst fire in response to either PW or non-PW deflections. The similarity was confirmed by examining the morphology of the neurons where possible and relating this to the physiology.

From the literature it is assumed that the RS neurons have shorter response latencies than the IB neurons. This does not appear to be the case in this study for the two reasons highlighted below:

1) As the firing patterns of RS and IB neurons are variable compared to *in vitro* there is scope for the misclassification of neurons. Although RS neurons do not fire bursts and cannot be misclassified as IB neurons the reverse is not true. As IB neurons are capable of showing RS like firing (firing single action potentials or doublets in response to whisker stimulation) it is possible in cases where no morphology and limited physiology are available IB neurons could be misclassified as RS neurons. Thus the IB neuronal group contains purely IB neurons but the RS group may contain a mixture of RS and IB neurons.

This becomes a problem when considering the average latency value for RS neurons. In the activation of a single cortical column layer Va (and possibly IB neurons) have the longest response latencies as they do not receive a direct monosynaptic thalamocortical input (Armstrong-James et al., 1992). RS neurons in layer Vb do receive monosynaptic thalamocortical inputs and as a result have shorter response latencies. Thus in the case of principal whisker activation of a column the presence of IB neurons in the RS group would lengthen the average response latency.

2) In cases where the neuronal response to a single whisker is recorded it is possible that as described above an IB neuron may be misclassified as an RS neuron. If the neuron is however a true RS neuron it is still possible that the recording can artificially lengthen the response latency of the entire group. In single whisker recordings a characteristically short latency would only be seen in response to stimulation of the principal whisker for the barrel the neuron was located in (through a direct thalamocortical activation). If a recording is not obtained from the deflection of

the principal whisker a longer latency would be observed. This latency would reflect the direct thalamocortical activation of the principal whisker barrel and then the intracortical activation of the barrel in which the neuron in question is located (Armstrong-James et al., 1992).

For the two reasons highlighted above it is thought that the fact IB neurons have a shorter response latency is an artefact. It is assumed that as in the literature RS (and neurons within layer Vb) have shorter response latencies than IB (and layer Va) neurons.

In this study the distribution of IB or RS neurons appears to be uniform within layer V. Possible confusions within the literature may arise from the fact that in some cases it is very difficult to distinguish the RS2 and IB1 neurons. The majority of the literature predates the RS1 and 2 and IB1 and 2 classification. Prior to this cells were classed as either RS or IB and it is possible that there is a degree of overlap between these two groups. What is not clear from this study is whether the distribution varies between the barrel and septal regions. In order to perform such a study the ideal system to use would be the *in vitro* thalamocortical slice described by Agmon and Connors (1991).

### 35.2 Physiology Data

From the scope data in this study it appears that there are differences in response latency, inhibitory period duration and firing pattern between IB and RS neurons when what appears to be the PW is deflected.

### 35.3 Principal versus adjacent whisker

In barrel centre recordings PW deflection results in a shorter response latency and inhibitory period. This may relay precise information regarding object location to the striatum, thalamus and brainstem. For example where D1 is the PW for a neuron from the set of whiskers (D1, C1 and B1) then information from whisker C1 is likely to have a shorter latency and inhibitory period than B1. However the latency and inhibitory period are clearly shorter for the PW. The response latency depends on the initial trigger for the activation of striatal neurons by IB neurons within cortex. Inhibitory period duration may encode spatial information regarding the position of the object with respect to the vibrissal field and possibly the path of the object across the whisker pad. Thus there may be a gradient system that subtly encodes position.

In side or septal recordings deflections of two whiskers give short almost identical response latencies and inhibitory periods (see figure 35). The slight differences between both the latency and inhibitory period values may reveal neuron position within the barrel. For example where the neuron is located almost in the centre of the septa between two barrels there may be little difference in the latency and inhibitory period. In cases where D1 has a shorter latency or inhibitory period C1 is its adjacent barrel. B1 in these cases has a noticeably longer latency and inhibitory period.

Where the 'Scope' records of successive PW deflections were overlayed a clear consistent inhibitory period was observed. Deflections of a non PW resulted in either no obvious inhibitory period or an inhibitory period that was not 'clean' i.e. was interrupted by stray action potentials (see figures 38 and 39). This may ensure that the co-ordination of PW information results in the co-ordinated firing of striatal neurons. The uncoordinated firing pattern of non-PW deflections may ensure that striatal

neurons are not activated by the volley of information arising from cortex (Lisman, 1997).

The firing patterns of neurons are also interesting. Where a neuron is located within the centre of a barrel (evidenced by the shortest response latency and shortest inhibitory period), pattern 1 firing is observed when the PW is deflected. The other whiskers result in a firing pattern that resembles pattern 2 firing. Pattern 1 firing could increase the contrast between activation of a neuron and the background (pattern 2) firing of the IB neuron (see figures 36 and 37).

IB neurons can also show pattern 2 firing in the absence of whisker deflection and pattern 1 like firing upon whisker deflection. This suggests that pattern 2 firing is the intrinsic firing pattern of IB neurons (which is similar to the activity observed in the medium spiny neurons within the striatum (Stern et al., 1997)). Thus where this pattern 2 firing is observed when a whisker is deflected it seems that this whisker has little influence over the neuron in question.

The complexity of pattern 1 firing is generated intrinsically and may encode a variety of information including velocity, direction of travel, shape or even texture of the object in question from peripheral inputs. From cortex this information can then be reliably relayed to other cortical regions as well as to subcortical targets.

#### **35.4 RS and IB firing patterns with respect to striatal innervation**

The literature suggests that innervation from an RS population would have the following features:

1) It would be likely to be under the control of the thalamus as RS neurons receive direct inputs from the thalamus (Agmon and Connors, 1992).

2) With their axon collaterals and dendrites generally confined to the parent barrel and ascending vertically to the pia they are likely to result in a response that is under the influence of the parent barrel and receive inputs, via their dendrites, from the more superficial layers (Chagnac-Amitai and Connors, 1989a; 1989b; Chagnac-Amitai et al., 1990; Connors and Gutnick, 1990).

3) As RS neurons tend to have less apical dendritic branching it is thought that they are less capable of receiving inputs from other areas than IB neurons.

4) With a limited input to the striatum they are likely to form a simple and restricted topographic input (Cowan and Wilson, 1994; Gerfen and Wilson, 1996). This innervation may prime the striatal neurons for the subsequent, longer latency, and more complex input from IB neurons.

IB neurons on the other hand are likely to possess the following characteristics:

1) IB neurons are more likely to be under the control of cortical influences than thalamic ones as intrinsically bursting cells do not receive a direct thalamic input (Agmon and Connors, 1992). Intrinsically bursting neurons are thought to be associated in some instances with layer Va (Connors et al., 1982; McCormick et al., 1985; Chagnac-Amitai and Connors, 1989a; 1989b; Armstrong-James et al., 1992; Agmon and Connors, 1992) and be activated via layer III and other layer V axon collaterals both within and between barrels as well as in cat SI (Schwark and Jones, 1989), in MI of primates (Huntley and Jones, 1991), in cat AI (Wallace et al., 1991a; 1991b).

2) The IB neurons have extensive basilar dendritic branching extending upto 600  $\mu\text{m}$  from the soma within the output layers of cortex (layer V and VI) (Connors and Gutnick, 1990; Chagnac-Amitai et al., 1990). They are therefore likely to receive cortically integrated information predominantly from output neurons.

3) They receive inputs from more than one barrel and as a result they are more suited to integration of information between rather than within barrels.

The IB neurons possess one important characteristic lacking in RS neurons: they are capable of acting in a network. It is known that IB neurons in layer V are both necessary and sufficient to generate cortically based rhythm. These neurons are able to initiate and activate other IB neurons into rhythmic and co-ordinated firing pattern that can amplify and co-ordinate cortical firing patterns within populations of intrinsically bursting neurons (Connors, 1984; Chagnac-Amitai and Connors, 1989a; Guatteo et al., 1994; Francashetti et al., 1995). These neurons may serve to increase the contrast between strong and weak signals in incoming information (Simons, 1995). The complex firing patterns generated within IB neurons may influence neuronal activity within the striatum and ultimately result in the execution of a wide variety of movements appropriate to the cortical signal.

## Anatomy

### 35.5 Pyramidal tract neurons and striatal innervation in rat motor cortex

In previous studies it has been established that rats only possess slow pyramidal tract neurons and do not possess the fast pyramidal tract neurons described in cat and monkey (Landry et al., 1984).

In the corticostriatal pathway in rat motor cortex it appears that there are two classes of pyramidal tract innervations (Landry et al., 1984; Cowan and Wilson, 1994). The most common innervation arises from cortical neurons with axonal trees that are confined to layers V and VI, rarely extend to the pia and have wide apical and basilar dendritic trees. This is suggestive of IB neuronal morphology. These neurons tend to be located within the superficial third of layer V which also correlates with the positioning of IB neurons (Connors et al., 1982; McCormick et al., 1985; Chagnac-Amitai and Connors, 1989a; 1989b; Chagnac-Amitai et al., 1990; Armstrong-James et al., 1992; Agmon and Connors, 1992). Anatomical tracing performed by Mercier et al., 1990 suggests that the majority of layer Vb neurons innervate brainstem targets whereas the majority of layer Va neurons appear to innervate the striatum. Previous studies in motor cortex (Jinnai and Matsuda, 1979; Donoghue and Kitai, 1981; Wilson et al., 1982; Landry et al., 1984; Wilson, 1986; Cowan and Wilson, 1994) have established that the pyramidal tract neurons innervate the striatum via a lateral branch of the axon as it runs through the fibre bundles within the striatum (see sections 34.1.3 and 34.1.4). The innervation arises at a right angle and appears to be approx.  $0.5\ \mu\text{m}$  in diameter (compared to  $2.0\text{--}2.5\ \mu\text{m}$  of the axon itself) and runs for approximately  $100\text{--}200\ \mu\text{m}$  and may or may not result in visible terminal swellings within the striatum (Donoghue and Kitai, 1981). This cell type also innervates the brainstem. Thus this

cell type sends identical information to both the striatum and the brainstem. Previous studies have also shown that when the cortex is stimulated the medium spiny projection neurons in the striatum respond to cortical stimulation with an initial single EPSP with a latency of approximately 3 mS (Jinnai and Matsuda, 1979; Wilson, 1986) followed by a period of inhibition lasting 100-300 mS (Wilson et al., 1983).

Another type of pyramidal tract neuron that innervates the striatum has axon collaterals that are more commonly associated with RS neurons i.e. they have axon collaterals that extend vertically towards the pia rather than horizontally (for review see Connors and Gutnick, 1990). They also have more limited basilar and apical dendritic trees.

The axon collaterals are more vertically orientated and tend to terminate in layer III or extend towards the pia. These neurons form the least common pyramidal tract neuronal innervation of the striatum (Landry et al., 1984). These cells innervate striatum from an axon which enters a capsular bundle, and then produces a relatively larger collateral that is approximately 1.8  $\mu\text{m}$  in diameter and extends laterally for approximately 1 mm (Miller, 1975; Jinnai and Matsuda, 1979; Donoghue and Kitai, 1981; Landry et al., 1984; Wilson, 1986).

Studies in motor cortex (Cowan and Wilson, 1994) suggest that the most common pyramidal tract neurons that innervate the striatum are large deep cortical cells that have extensive intracortical axon collaterals and limited intrastriatal innervation. The less common class of pyramidal tract neurons are medium sized pyramidal cells with limited intracortical axon collateralisation and more extensive intrastriatal arbourisation.

In this study of the primary somatosensory cortex it appears that the limited striatal innervation (described here as a limited lateral branch innervation) originates from RS neurons. IB neurons in this study provide the more extensive and topographic

innervation of the striatum (described here as a topographic innervation of the striatum).

### 35.6 Vibrissal region of primary somatosensory cortex

Intracellular recordings of corticostriatal neurons and anatomical tracing of the corticostriatal pathway in this region of cortex (Wright et al., 1998) have revealed that there are at least two distinct ipsilateral corticostriatal pathways:

1) An extensive, topographically innervation which does not appear to be *en passant*. This innervation appears to be a major post synaptic target of these neurons. These neurons have similar innervation patterns to those described in motor cortex (although the topography is more clearly seen in somatosensory cortex) (Wilson, 1986; Cowan and Wilson, 1994). These neurons are probably pyramidal tract neurons and do not resemble the extensive striatal innervation seen in the exclusively corticostriatal neurons seen in motor cortex.

The terminals from the topographic innervation arise from a lateral axonal branch as the axon runs through the fibre bundles within the striatum. The branch occurs at right angles to the parent axon and runs parallel to the corpus callosum. The positioning of the terminal field within the striatum depends on the source of the parent cell and is arranged topographically within rows. Row A represented closest to the corpus callosum and row E the most medial. The terminal field of an individual neuron forms a hand like arrangement. The neuron filled in this class would appear to be located within row C (see figures 46 and 47).

2) A limited innervation that arises from the axons of pyramidal tract neurons as they run through the striatal fibre bundles. This innervation is finer and is similar to those

of pyramidal tract neurons described in rat motor cortex (Jinnai and Matsuda, 1979; Donoghue and Kitai, 1981; Landry et al., 1984; Wilson, 1986; Cowan and Wilson, 1994).

Examples of 1) and 2) above have been filled and will be discussed later (see sections 34.1.1 and 34.1.4).

Another class of corticostriatal neurons exist that have not been filled in this study- the crossed corticostriatal neurons (Wright et al., 1998). Anatomical tracing studies have revealed crossed corticostriatal neurons (but these are rare within somatosensory cortex (Gerfen and Wilson, 1996)). The bilateral neurons innervate the ipsilateral striatum as well as contralateral cortex and striatum. The terminal fields arising from these neurons resembles those of the fine extensive ipsilateral corticostriatal cells rather than those seen from the pyramidal tract neurons (Wilson, 1987; Cowan and Wilson, 1994). The contralateral does appear to be located more rostral than the innervation seen in the ipsilateral striatum (Ebrahimi et al., 1992; Wright et al., 1998). They are located within superficial layer V (within somatosensory cortex layers II/III does not appear to project subcortically so therefore it is assumed that these neurons will be located within layer Va). It is likely that these neurons are located within the septa as the septae are known to receive and project information to the contralateral hemisphere (Ackers and Killackey, 1978; Olavarria et al., 1984; Welker et al., 1988).

### **35.7 Limited lateral branch innervation of the striatum.**

In this study the neurons providing this striatal innervation pattern was classed morphologically and physiologically as an RS neurons. Whether in this area of cortex RS neurons are the only source of this striatal innervation is impossible to say.

### **35.8 Topographic Innervation of the Striatum**

In this study, the neurons that resulted in the topographic innervation of the striatum were classed morphologically as IB neurons. Unfortunately there was no physiology available so physiological confirmation was not possible. This striatal innervation is similar to that seen in anatomical studies (see earlier section 34.1.1 and figures 44-48). It is possible that these neurons correspond to the other class of pyramidal tract neurons described in motor cortex.

### **35.9 Relation to ascending sensory systems**

Examination of the anatomy of the topographic corticostriatal innervation seen in both intracellular and anatomical studies (Wright et al., 1998) with relation to the ascending somatosensory system reveals interesting parallels:

1) In the ascending vibrissal system and within cortex itself there appears to be a dominant, in row preference for the relay of sensory information (Durham and Woolsey, 1978; 1985; Simons, 1978; Simons and Woolsey, 1979; 1984; Armstrong-James and Fox, 1987; McCasland and Woolsey, 1988; Bernardo et al., 1990a; 1989b). Symmetric surround receptive fields also show a preference for relay within rows of barrels rather than across arcs (Simons, 1978; Simons and Woolsey, 1979; 1984; Chapin, 1986; Chmielowska et al., 1986a; Armstrong-James and Fox, 1987; Bernardo et al., 1990a; 1990b; Fabri and Burton, 1991; Armstrong-James et al., 1992; McCasland et al., 1992; Simons et al., 1992; Diamond et al., 1993; Welker et al., 1993). In striatum too these the terminals seem to be arranged in rows (see figures 46-48). Thus is it possible that the interconnectivity seen between areas in primate motor and somatosensory cortex may exist in rat. Interconnectivity within the rostrocaudal

plane in striatum also indicates that as in cortex there is a preferential relay of information within rows rather than across arcs.

2) In anatomical studies (Wright et al., 1998) in the vibrissal region of primary somatosensory cortex the topographically arranged corticostriatal innervation appears in rows running parallel to the corpus callosum in a mediolateral orientation (row A is closest to the corpus callosum, row E most medial). A single cell filled in this study appears to back up this arrangement (see figures 44 and 45). From the anatomical studies (Wright et al., 1998) and from the single topographic striatal terminal field filled in this study it is impossible to say whether the corticostriatal link is similar to that seen in the corticothalamic innervation. In that innervation by the corticothalamic input is from a single barrel to an arc of barreloids rather than from a single barreloid to a single barrel seen in the ascending system (Van der Loos, 1976). It may be that the cortical innervation of the striatum is from a single cortical barrel to an area of striatum that represents a row of barrels.

### **35.10 Relation to other cortical regions**

In the primate somatosensory corticostriatal pathway the discrete topography of the cortex is not maintained within the striatum. Areas in striatum that represent a particular body part cover a greater in area than the corresponding cortical area. When the cortex innervates the striatum there is a greater degree of overlap seen in the striatum than in the cortex (Yeterian and van Hoesen, 1978; Jinnai and Matsuda, 1979; Royce, 1982; Wilson, 1986; Selemon and Goldman-Rakic, 1985; 1987; Flaherty and Graybiel, 1991; 1993; 1994; Giminez-Amaya and Graybiel, 1990; Ragsdale and Graybiel, 1990; Cavada and Goldman-Rakic, 1991; Parthasarathy et al., 1992; Eblen and Graybiel, 1995; Gerfen and Wilson, 1996). This overlap is arranged so that areas that are heavily interconnected in the cortex tend to show a greater degree of overlap in

the striatum (with preferential orientation in the rostrocaudal plane). Areas that are concerned with a particular body part, muscle combination or movement, tend to show greater overlap. The function of this overlap may be to bring together certain inputs (from common modalities) and separate others that are not related (Jiminez-Castellanos and Graybiel, 1989).

As a given area of cortex projects to an area of striatum that is proportionally larger in order to accommodate all the cortical inputs to the striatum there must be a degree of overlap. Thus it is unlikely that there is a 1:1 arrangement seen in ascending systems (Yeterian and van Hoesen, 1978; Selemon and Goldman-Rakic, 1985; 1988).

The purpose of the striatum appears to be the integration of the information it receives, in this case somatosensory information from the vibrissae, before relaying it to other stations in the basal ganglia for processing. It is possible that the system seen in the primate somatosensory system occurs in the rodent system when comparing the innervation patterns seen in rat and those seen in the primate.

### **35.11 Intrinsically Bursting Neurons and Striatal Innervation**

The previous literature on intrinsically bursting neurons may provide clues to the importance in striatal activation of the intrinsically bursting inputs from cortex:

1) Intrinsic bursting occurs after that caused by the pyramidal tract neurons.

Throughout the ascending system the secondary information that is relayed to a nucleus is more detailed with respect to directional specificities, texture, and shape. Short latency inputs are more generally associated with stimulus velocity and frequency. Intrinsically bursting neurons with their complex firing patterns would be able to encode a wide variety of stimulus factors including slight differences in texture and

would be ideal for use in building up a picture of the environment. Fast latency responses which may encode the peripheral stimulus in a very precise and less integrated manner and may better reflect movements in a single whisker than the IB neurons.

2) Intrinsically bursting neurons burst at a rate of approximately 15 Hz. Whisking behaviour occurs within the range of 5-15 Hz and at 8 Hz when an object is detected (Connors, 1984; Agmon and Connors, 1989; Chagnac-Amitai et al., 1990; Silva et al., 1991b; Wang and McCormick, 1993; Franceschetti et al., 1995; Carvell and Simons, 1996). Whisking frequency and intrinsic bursting may be closely linked as intrinsic bursting within neurons is not evident until approx. P15 (P0 = day of birth) (Armstrong-James, 1975). Whisking behaviour develops within the second to third postnatal weeks (Welker, 1964; Guic-Robel et al., 1989). Receptive fields within cortex (arising from sensory experience) are generated within the first few postnatal weeks (Simons, 1985; Simons and Land, 1987; McCasland and Woolsey, 1988; McCasland et al., 1992; Diamond et al., 1993). Thus it can be assumed that whisking and intrinsically bursting neurons are important for the relay of complex sensor information. The formation of the receptive fields is also due in part to GABAergic influence. GABA levels reach the adult state within the first two postnatal weeks and at this stage the RF's are much smaller and more finely tuned (Luhman and Prince, 1991; Micheva and Beaulieu, 1996).

3) Examination of the striatal medium spiny cells reveals that they fire in a slow rhythmic pattern of approx. 3-10 Hz (Wilson and Groves, 1981; Wilson et al., 1983). The firing patterns of the striatal cells after cortical activation mimics that of the cortex (Cowan and Wilson, 1994).

4) The innervation of the striatum from the cortex reveals that cortical cells do not form extensive and dense terminal contact within the striatum, rather a single cortical cell may only connect with very few striatal cells and each cell may only form a single synapse with any one striatal cell (Gerfen and Wilson, 1996). This makes the detection of corticostriatal terminals very difficult in single cell studies. Similarly, a small area of the striatum is innervated by a larger area of the cortex. Striatal neurons with their limited input from single cortical neurons would therefore require inputs from a large network of co-ordinated cortical cells. The IB neurons with their ability to synchronise and co-ordinate their firing (and amplify any input they receive) would be ideally suited to the activation of medium spiny striatal neurons (Connors, 1984; Agmon and Connors, 1989; Chagnac-Amitai and Connors, 1989a; Chagnac-Amitai et al., 1990; Mason and Larkman, 1990; Tseng and Prince, 1993; Guatteo et al., 1994; Franceschetti et al., 1995; Flint and Connors, 1996). Examination of the anatomical studies using retrograde tracing of the corticostriatal pathway reveals that the projection neurons arise mainly in layer V (occasionally layer VI) and small injections of tracer label into striatum results in the labelling of large numbers of neurons in cortex (an area of striatum approximately 1 mm<sup>3</sup> is innervated by 1480 layer V pyramidal neurons (A. Wright and G. Arbuthnott, personal communication)).

From the literature it would appear that the initial activation in cortex is via RS neurons as this cell type is found throughout the cortical layers (Mountcastle et al., 1969; Oshima, 1969; Simons, 1978; Connors et al., 1982; Stafstrom et al., 1984; McCormick et al., 1985; Agmon and Connors, 1989; Chagnac-Amitai and Connors, 1989a; 1989b; Connors and Gutnick, 1990; White et al., 1994). This activation is driven by a direct thalamic input and would produce short latency responses within cortex and striatum. With the activation pattern in a cortical column in this region of cortex (Armstrong-James et al., 1992) it would seem that RS neurons initiate firing in the IB neuronal population. Thus it is likely that RS activation provides a seed from

which the activation of the IB network grows. It is possible that the initial discrete activation of the striatum is via the RS pyramidal tract neurons. This may then be followed, as in cortex, by a volley of information arising from the IB cells.

The RS neurons are ideal candidates for such activation as they are activated at shorter latencies within cortex (Armstrong-James et al., 1992) and would provide an ideal priming system. IB neurons tend to have longer latencies than RS neurons and their longer conduction velocities implies that their input to the striatum occurs at a much longer latency than that of the RS neurons. The main corticostriatal innervation from motor cortex is thought to arise from a population of neurons that evoke EPSP's with a longer latency (approx. 10 mS) (Jinnai and Matsuda, 1979; Wilson, 1986).

The important role of IB neurons in striatal activation is highlighted by literature on cortical activation of the striatal neurons. The literature consistently shows that each cortical neuron only makes a few synapses with each striatal neuron (Wilson, 1993) and that several thousand excitatory inputs are required from nearly as many afferent inputs to maintain striatal neurons in their 'up' membrane state and in order to maintain this 'up' state excitatory cortical activity is necessary.

From computer models of the corticostriatal system (Wickens and Arbuthnott, 1993) the order of activation of striatal neurons in response to a stimulus is determined by the efficacy of the corticostriatal neurons. The most strongly excited neurons become activated first and then a gradient system operates where the strength of excitation dictates which neurons fire next. From this model and the data obtained in this study it may be that the shorter latencies and shorter inhibitory period allows this information to flow through the striatum first. This may result in a gradient of information flowing through the striatum dictated by activation and interconnectivity of barrels.

## 36.0 Conclusion

Thus from this study it appears possible that the IB neurons innervate much larger and more topographically specific regions of the striatum than the RS pyramidal tract neurons. This innervation pattern is also observed within the corticostriatal connections within motor cortex (Jinnai and Matsuda, 1979; Donoghue and Kitai, 1981).

From the results of this study the following two points are clear:

1) IB neurons in this in vivo study have shorter latencies than the RS neurons. It is not known if this is a true representation of the response latencies observed in vivo or whether this is an artefact of the recording protocol.

2) IB recordings are more numerous than those of RS neurons. This may also be an artefact of the recording protocol revealing a bias towards IB recordings. On the other hand there may be an anatomical or physiological reason.

All recordings in this study were performed in the region of the B1, C1 and D1 arc of barrels. From the literature (see introduction) the large caudal whiskers are associated with roughness discrimination. If IB neurons are ideally suited for interpretation and coding of such complex information (as is suggested here) it may be possible that the caudal barrel region may contain a higher proportion of IB neurons than the rostral region.

Another possibility is that as the recording area remained constant the IB neurons may be concentrated within groups within the barrelfield (either within barrels or septae). The bias in the recording area may therefore reveal a higher proportion of IB neurons.

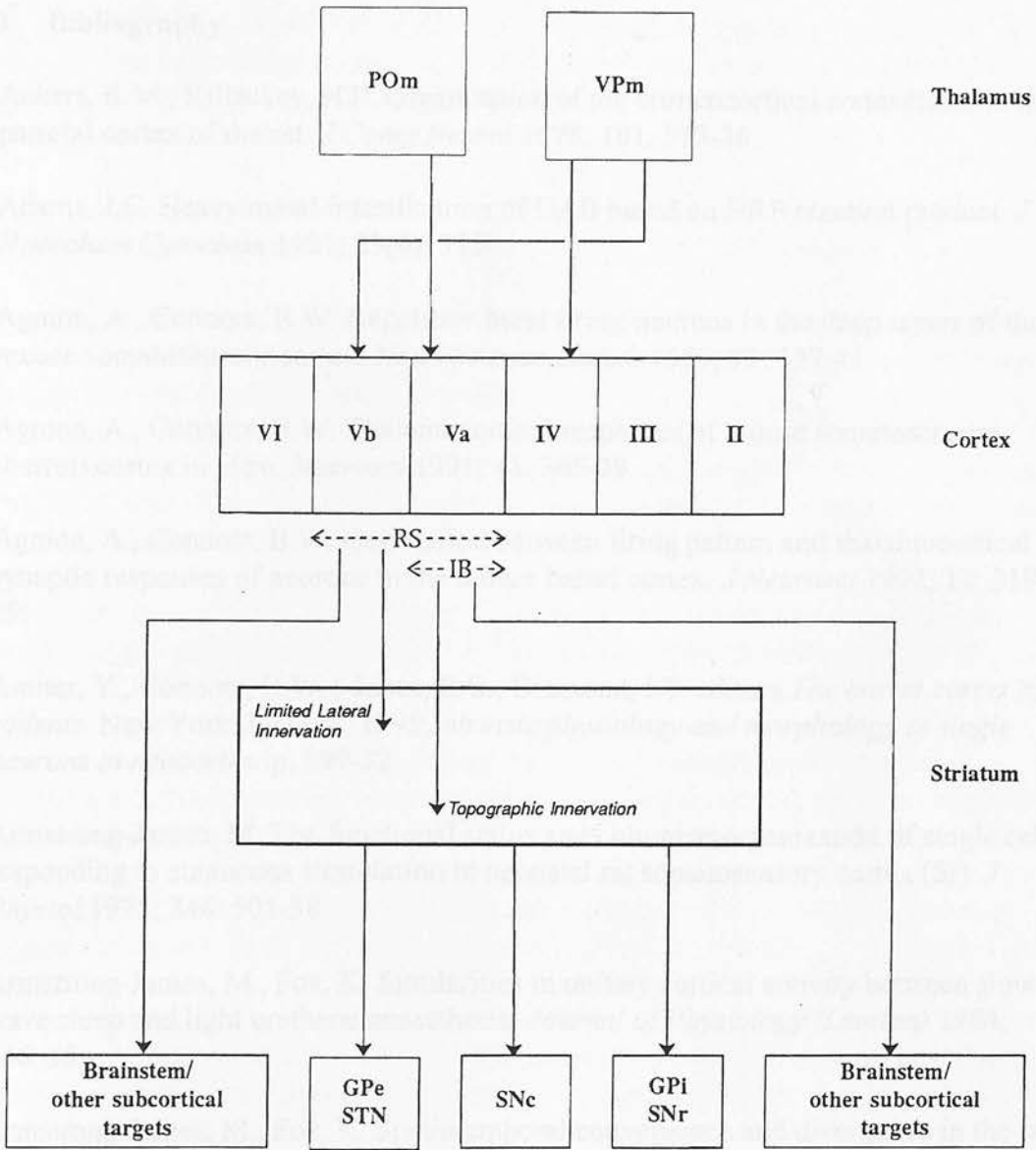
Aside from the anatomical possibilities the choice of anaesthetic may also have biased the recordings in favour of IB neurons. It is known that urethane anaesthesia is advantageous for the recording of IB neurons. Chloralose was also included in the anaesthesia mix to ensure that peripheral inputs are reliably relayed through the ascending system to cortex. It is possible that the use of chloralose allows a greater proportion of IB driven information from the periphery to the cortex where it is enhanced by the presence of urethane.

Allowing for experimental bias is a possible cause for increased numbers of IB neurons it is also possible that IB neurons are more numerous within primary somatosensory cortex than in motor, visual or auditory cortices.

Examination of firing patterns within the striatum mirror the responses of IB neurons. Both neurons respond to stimulation by firing an initial single or double EPSP followed by a slow membrane hyperpolarisation before the neurons resume firing (Wilson et al., 1983). From the firing patterns it appears that IB neurons are most likely to dictate firing within the medium spiny neurons within the striatum. The controlling mechanism with this large network of IB neuronal firing and the lack of inhibitory mechanisms controlling the IB neurons may be related to synchronisation of firing. In most neuronal systems activation by a large volley of incoming information is limited by the receiving system. This receiving system in most cases is only activated by highly synchronised and co-ordinated information (For a review see Lisman, 1997)).

If this system operates within the vibrissal region of primary somatosensory cortex striatal activation only occurs when whisker deflection results in highly co-ordinated firing within the principal barrel. When an adjacent barrel is activated the firing is not

tightly linked to the stimulus. In PW deflection the co-ordination of the response is seen when scope records are overlaid as tightly coupled initial responses to whisker deflection and an inhibitory period that appears consistent between responses. When firing resumes after the inhibitory period it is highly synchronised with periods of intense activity interrupted by periods of brief inhibition (see figures 38 and 39). Where synchrony is observed there is an activation of the striatum, in non-synchronous activity from adjacent whiskers there may be a lack of striatal activation or possibly a priming of the neurons that may receive from the next whisker to be deflected.



Key  
 POm            Posteriomedial thalamic nucleus  
 VPm            Ventroposteriomedial thalamic nucleus  
 GPe/GPi        Globus Pallidus (external and internal segments)  
 STN            Subthalamic nucleus  
 SNc/SNr        Substantia Nigra pars compacta/reticulata

Figure 84. A summary diagram showing the possible cortical activation of striatum based on the data presented. The diagram does not show the complex circuitry of the basal ganglia

## 37.0 Bibliography

1. Ackers, R.M., Killackey, H.P. Organisation of the corticocortical connections in the parietal cortex of the rat. *J Comp Neurol* 1978; **181**: 513-38.
2. Adams, J.C. Heavy metal intensification of DAB based on HRP reaction product. *J Histochem Cytochem* 1981; **29**(6): 775
3. Agmon, A., Connors, B.W. Repetitive burst firing-neurons in the deep layers of the mouse somatosensory cortex. *Neuroscience Letters* 1989; **99**: 137-41.
4. Agmon, A., Connors, B.W. Thalamocortical responses of mouse somatosensory (barrel) cortex in vitro. *Neurosci* 1991; **41**: 365-79.
5. Agmon, A., Connors, B.W. Correlation between firing pattern and thalamocortical synaptic responses of neurons in the mouse barrel cortex. *J Neurosci* 1992; **12**: 319-29.
6. Amitai, Y., Connors, B.W. ; Jones, E.G., Diamond, I.T. editors. *The barrel cortex of rodents*. New York: Plenum, 1995; *Intrinsic physiology and morphology of single neurons in neocortex*. p. 299-32.
7. Armstrong-James, M. The functional status and columnar organization of single cells responding to cutaneous stimulation in neonatal rat somatosensory cortex (SI). *J Physiol* 1975; **246**: 501-38.
8. Armstrong-James, M., Fox, K. Similarities in unitary cortical activity between slow wave sleep and light urethane anaesthesia. *Journal of Physiology (London)* 1984; **346**: 55p
9. Armstrong-James, M., Fox, K. Spatiotemporal convergence and divergence in the rat S1 "barrel" cortex. *J Comp Neurol* 1987; **263**: 265-81.
10. Armstrong-James, M., George, M.J. Influence of anaesthesia on spontaneous activity and receptive field size of single units in rat SmI neocortex. *Exp Neurol* 1988; **99**: 369-88.
11. Armstrong-James, M., Callahan, C.A. Thalamo-Cortical Processing of Vibrissal Information in the Rat. II. Spatiotemporal Convergence in the Thalamic Ventroposterior Medial Nucleus (VPM) and Its Relevance to Generation of Receptive Fields of SI Cortical "Barrel" Neurones. *J Comp Neurol* 1991; **303**: 211-24.

12. Armstrong-James, M., Callahan, C.A., Friedman, M.A. Thalamo-Cortical Processing of Vibrissal Information in the Rat. I. Intracortical Origins of Surround But Not Centre-Receptive Fields of Layer IV Neurones in the Rat S1 Barrel Field Cortex. *J Comp Neurol* 1991; **303**: 193-210.
13. Armstrong-James, M., Fox, K., Das-Gupta, A. Flow of excitation within rat barrel cortex on striking a single vibrissa. *J Neurophysiol* 1992; **68**: 1345-58.
14. Armstrong-James, M. ; Jones, E.G., Diamond, I.T. editors. *The barrel cortex of rodents*. New York: Plenum, 1995; *The nature and plasticity of sensory processing within adult rat barrel cortex*. p. 333-76.
15. Arvidsson, J., Rice, F.L. Central projection of primary sensory neurons innervating different parts of the vibrissae follicles and intervibrissal skin on the mystacial pad of the rat. *J Comp Neurol* 1991; **309**: 1-16.
16. Barbaresi, P., Spreafico, R., Frassoni, C., Rustioni, A. GABA-ergic neurons are present in the dorsal column nuclei but not in the ventroposterior complex of rats. *Brain Res* 1986; **382**: 305-26.
17. Bates, C.A., Erzurumlu, R.S., Killackey, H.P. Central correlates of peripheral alterations in the trigeminal system of the rat. III. Neurons of the principal sensory nucleus. *Dev Brain Res* 1982; **5**: 108-13.
18. Belford, G.R., Killackey, H.P. Vibrissae representation in Subcortical Trigeminal Centers of the Neonatal Rat. *J Comp Neurol* 1979; **183**: 305-22.
19. Bennett-Clarke, C.A., Chiaia, N.L., Jacquin, M.F., Rhoades, R.W. Parvalbumin and calbindin immunocytochemistry reveal functionally distinct cell groups and vibrissa-related patterns in the trigeminal brainstem complex of the adult rat. *J Comp Neurol* 1992; **320**: 323-38.
20. Benshalom, G., White, E.L. Quantification of thalamocortical synapses with spiny stellate neurons in layer IV of mouse somatosensory cortex. *J Comp Neurol* 1986; **253**: 303-14.
21. Berendse, H.W., Galis-de Graaf, Y., Groenewegen, H.J. Topographical organization and relationship with ventral striatal compartments of prefrontal corticostriatal projections in the rat. *J Comp Neurol* 1992; **316**: 314-47.
22. Bernardo, K.L., Woolsey, T.A. Axonal trajectories between mouse somatosensory thalamus and cortex. *J Comp Neurol* 1987; **258**: 542-64.

23. Bernardo, K.L., McCasland, J., Woolsey, T.A., Strominger, R.N. Local and intra- and inter laminar connections in mouse barrel cortex. *J Comp Neurol* 1990a; **291**: 231-55.
24. Bernardo, K.L., McCasland, J.S., Woolsey, T.A. Local axon trajectories in mouse barrel cortex. *Exp Brain Res* 1990b; **82**: 247-53.
25. Bindman, L.J., Meyer, T., Prince, C.A. Comparison of the electrical properties of neocortical neurones in slices in vitro and in the anaesthetised rat. *Exp Brain Res* 1988; **69**: 489-96.
26. Bourassa, J., Pinault, D., Deschênes, M. Corticothalamic projections from the cortical barrel field to the somatosensory thalamus in rats: A single-fibre study using biocytin as an anterograde tracer. *Eur J Neurosci* 1995; **7**: 19-30.
27. Braun, L.D., Miller, L.P., Pardridge, W.M., Oldendorf, W.H. Kinetics of regional blood-brain barrier glucose transport and cerebral blood flow determined with the carotid injection technique in conscious rats. *Journal of Neurohistochemistry* 1985; **44**: 911-5.
28. Brumberg, J.C., Pinto, D.J., Simons, D.J. Spatial gradients and inhibitory summation in the rat whisker barrel system. *J Neurophysiol* 1996; **76**: 130-40.
29. Burkhalter, A. Intrinsic Connections of Rat Primary Visual Cortex: Laminar Organization of Axonal Projections. *The Journal of Comparative Neurology* 1989; **279**: 171-86.
30. Calvin, W.H., Sypert, G.W. Fast and slow pyramidal tract neurons: An intracellular analysis of their contrasting repetitive firing properties. *J Neurophysiol* 1976; **39**: 420-34.
31. Caretta, D., Sbriccoli, A., Santarelli, M., Pinto, F., Grantò, A., Minciaahi, D. Crossed thalamo-cortical and cortico-thalamic projections in adult mice. *Neuroscience Letters* 1996; **204**: 69-72.
32. Carvell, G.E., Simons, D.J. Thalamic and corticocortical connections of the second somatic sensory area of the mouse. *J Comp Neurol* 1987; **265**: 409-27.
33. Carvell, G.E., Simons, D.J. Membrane Potential changes in Rat Sm1 Cortical Neurons evoked by Controlled Stimulation of Mystacial Vibrissae. *Brain Res* 1988; **448**: 186-91.
34. Carvell, G.E., Simons, D.J. Biometric analyses of vibrissal tactile discrimination in the rat. *J Neurosci* 1990; **10(8)**: 2638-48.

35. Carvell, G.E., Simons, D.J., Lichtenstein, S.H., Bryant, P. Electromyographic activity of the mystacial pad musculature during whisking behaviour in the rat. *Somatosen Motor Res* 1991; **8**: 159-64.
36. Carvell, G.E., Simons, D.J. Abnormal tactile experience early in life disrupts active touch. *J Neurosci* 1996; **16**: 2750-7.
37. Cauller, L.J., Connors, B.W. Synaptic physiology of horizontal afferents to layer I of primary somatosensory cortex in rats. *J Neurosci* 1994; **14**: 751-62.
38. Cavada, C., Goldman-Rakic, P.S. Topographic segregation of corticostriatal projections from posterior parietal subdivisions in the macaque monkey. *Neurosci* 1991; **42**: 683-96.
39. Caviness, V.S. Patterns of cell and fiber distribution in the neocortex of the 'reeler' mutant mouse. *J Comp Neurol* 1976; **170**: 435-48.
40. Celio, M.R. Calbindin D-28K and parvalbumin in the rat nervous system. *Neurosci* 1990; **35**: 375-475.
41. Chagnac-Amitai, Y., Connors, B.W. Synchronised excitation and inhibition driven by intrinsically bursting neurons in neocortex. *J Neurophysiol* 1989a; **62**: 1149-62.
42. Chagnac-Amitai, Y., Connors, B.W. Horizontal spread of synchronised activity in neocortex and its control by GABA-mediated inhibition. *J Neurophysiol* 1989b; **61**: 747-58.
43. Chagnac-Amitai, Y., Luhman, H.J., Prince, D.A. Burst generating and regular spiking layer 5 pyramidal neurons of rat neocortex have different morphological features. *J Comp Neurol* 1990; **296**: 598-613.
44. Chapin, J.K., Lin, C.-S. Mapping the body representation in the SI cortex of the anaesthetised and awake rat. *J Comp Neurol* 1984; **229**: 199-213.
45. Chapin, J.K. Laminar Differences in Sizes, Shapes and Response Profiles of Cutaneous Receptive Fields in the Rat SI Cortex. *Exp Brain Res* 1986; **62**: 549-59.
46. Chapin, J.K., Sadeq, M., Guise, L.U. Corticocortical connections within the primary somatosensory cortex of the rat. *J Comp Neurol* 1987; **263**: 326-46.

47. Chiaia, N.L., Rhoades, R.W., Bennett-Clarke, C.A., Fish, S.E., Killackey, H.P. Thalamic processing of vibrissal information in the rat: I. Afferent input to the medial ventral posterior nuclei. *J Comp Neurol* 1991a; **314**: 201-16.
48. Chiaia, N.L., Rhoades, R.W., Fish, S.E., Killackey, H.P. Thalamic processing of vibrissal information in the rat: II. Morphological and functional properties of medial ventral posterior nucleus and posterior nucleus neurons. *J Comp Neurol* 1991b; **314**: 217-36.
49. Chmielowska, J., Kossut, M., Chmielowski, M. Single vibrissal cortical column in the mouse labelled with 2-deoxyglucose. *Exp Brain Res* 1986a; **63**: 607-19.
50. Chmielowska, J., Stewart, M.G., Bourne, R.C., Hamori, J. Gamma-aminobutyric acid immunoreactivity in mouse barrel field: A light microscopical study. *Brain Res* 1986b; **368**: 371-4.
51. Chmielowska, J., Stewart, M.G., Bourne, R.C.  $\gamma$ -aminobutyric acid (GABA) immunoreactivity in the mouse and rat first somatosensory (SI) cortex: Description and comparison. *Brain Res* 1988; **439**: 155-68.
52. Chmielowska, J., Carvell, G.E., Simons, D.J. Spatial organization of thalamocortical and corticothalamic projection systems in the rat Sm1 barrel cortex. *J Comp Neurol* 1989; **285**: 325-38.
53. Cippolloni, P.B., Peters, A. The bilaminar and banded distribution of the callosal terminals in the posterior neocortex of the rat. *Brain Res* 1979; **176**: 33-47.
54. Connors, B.W., Gutnick, M.J., Prince, D.A. Electrophysiological properties of neocortical neurons in vitro. *J Neurophysiol* 1982; **48**: 1302-20.
55. Connors, B.W. Initiation of synchronised neuronal bursting in neocortex. *Nature* 1984; **310**: 685-7.
56. Connors, B.W., Gutnick, M.J. Intrinsic firing patterns of diverse neocortical neurons. *Trends neurosci* 1990; **13**: 99-104.
57. Cowan, R.L., Wilson, C.J. Spontaneous firing patterns and axonal projections of single corticostriatal neurons in the rat medial agranular cortex. *J Neurophysiol* 1994; **71**: 17-32.
58. Crandall, J.E., Korde, M., Caviness, V.S.J. Somata of layer V projection neurons in the mouse barrelfield cortex are in preferential register with the sides and the septa of barrels. *Neuroscience Letters* 1986; **67**: 19-24.

59. De Biasi, S., Frassoni, C., Spreafico, R. The intrinsic organization of the ventroposteriolateral nucleus and related reticular thalamic nucleus of the rat: A double-labelling ultrastructural investigation with gamma-aminobutyric acid immunolod staining and lectin-conjugated horseradish peroxidase. *Somatosen Res* 1988; **5**: 187-203.
60. deCharms, R., Merzenich, M.M. Primary cortical representation of sounds by the coordination of action-potential timing. *Nature* 1996; **381**: 610-3.
61. DeFelipe, J., Farinas, I. The pyramidal neuron of the cerebral cortex: Morphological and chemical characteristics of the synaptic inputs. *Progress in Neurobiology* 1992; **39**: 563-607.
62. Di, S., Baumgartner, C., Barth, D.S. Laminar analysis of extracellular field potentials in rat vibrissa/barrel cortex. *J Neurophysiol* 1990; **63**: 832-40.
63. Diamond, M.E., Armstrong-James, M., Budway, M.J., Ebner, F.F. Somatic sensory responses in the rostral sector of the posterior group (POm) and in the ventral posterior medial nucleus (VPM) of the rat thalamus: Dependance on barrel cortex. *J Comp Neurol* 1992a; **319**: 66-84.
64. Diamond, M.E., Armstrong-James, M., Ebner, F.F. Somatic sensory responses in the rostral sector of the posterior group (POm) and in the ventral posterior medial nucleus (VPM) of the rat thalamus. *J Comp Neurol* 1992b; **318**: 462-76.
65. Diamond, M.E., Armstrong-James, M., Ebner, F.F. Experience dependant plasticity in adult rat barrel cortex. *Proceedings of the National Academy of Science (USA)* 1993; **90**: 2082-5.
66. Doherty, D.W., Killackey, H.P., Jacquin, M.F. Receptive field synthesis in rat nucleus principalis spinal trigeminal contributions. *Soc Neurosci Abstr* 1992; **18**
67. Donaldson, L., Hand, P.J., Morrison, A.R. Cortico-thalamic relationships in the rat. *Exp Neurol* 1975; **47**: 448-58.
68. Donoghue, J.P., Kitai, S.T. A collateral pathway to the neostriatum from corticofugal neurons of the rat sensory-motor cortex: An intracellular HRP study. *J Comp Neurol* 1981; **201**: 1-13.
69. Dorfl, J. The musculature of the mystacial vibrissae of the white mouse. *J Anat* 1982; **135**: 147-54.

70. Dorfl, J. The innervation of the mystacial region of the white mouse. A topographical study. *J Anat* 1985; **142**: 173-84.
71. Durham, D., Woolsey, T.A. Acute Whisker Removal Reduces Neuronal Activity in Barrels of Mouse SmI Cortex. *J Comp Neurol* 1978; **178**: 629-44.
72. Durham, D., Woolsey, T.A. Functional organization in cortical barrels of normal and vibrissae-damaged mice: A 2-deoxyglucose study. *J Comp Neurol* 1985; **235**: 97-110.
73. Dykes, R.W. Afferent fibres from mystacial vibrissae of cats and seals. *J Neurophysiol* 1975; **38**: 650-62.
74. Dykes, R.W. Parallel processing of somatosensory information: A theory. *Brain Research Reviews* 1983; **6**: 47-115.
75. Eblen, F., Graybiel, A., M. Highly restricted origin of prefrontal cortical inputs to striosomes in the macaque monkey. *J Neurosci* 1995; **15**: 5999-6013.
76. Ebrahimi, A., Pochet, R., Roger, M. Topographical organization of the projections from physiologically identified areas of the motor cortex to the striatum in the rat. *Neuroscience Research* 1992; **14**: 39-60.
77. Elhanany, E., White, E.L. Intrinsic circuitry: Synapses involving the local axon collaterals of corticotectal projection neurons in the mouse primary somatosensory cortex. *J Comp Neurol* 1990; **291**: 43-54.
78. Fabri, M., Burton, H. Ipsilateral cortical connections of primary somatic sensory cortex in rats. *J Comp Neurol* 1991; **311**: 405-24.
79. Feldman, M.L., Peters, A. A study of the barrels and pyramidal dendritic clusters in the cerebral cortex. *Brain Res* 1974; **77**: 55-76.
80. Flaherty, A.W., Graybiel, A.M. Corticostriatal Transformations in the Primate Somatosensory System. Projections from Physiologically Mapped Body-Part Representations. *J Neurophysiol* 1991; **66**: 1249-63.
81. Flaherty, A.W., Graybiel, A.M. Two input systems for body representations in the primate striatal matrix: Experimental evidence in the squirrel monkey. *J Neurosci* 1993; **13**: 1120-37.
82. Flaherty, A.W., Graybiel, A.M. Input-output organization of the sensorimotor striatum in the squirrel monkey. *J Neurosci* 1994; **14**: 599-610.

83. Flint, A.C., Connors, B.W. Two types of network oscillations in neocortex mediated by distinct glutamate receptor subtypes and neuronal populations. *J Neurophysiol* 1996; **75**: 951-7.
84. Foehring, R.C., Lorenzon, N.M., Herron, P., Wilson, C.J. Correlation of physiologically and morphologically identified neuronal types in human association cortex in vitro. *J Neurophysiol* 1991; **66**: 1825-37.
85. Fonesca, M., DeFelipe, J., Fairen, A. Local connections in transplanted and normal cerebral cortex of rats. *Exp Brain Res* 1988; **69**: 387-98.
86. Fox, K., Armstrong-James, M. The role of the anterior intralaminar nuclei and N-methyl D-aspartate receptors in the generation of spontaneous bursts in rat neocortical neurones. *Exp Brain Res* 1986; **63**: 505-18.
87. Franceschetti, S., Guatteo, E., Panzica, F., Sancini, G., Wanke, E., Avanzini, G. Ionic mechanisms underlying burst firing in pyramidal neurons: Intracellular study in rat sensorimotor cortex. *Brain Res* 1995; **696**: 127-39.
88. Gerfen, C.R., Wilson, C.J. ; Swanson, L.W., Bjorkland, A., Hokfelt, T. editors. *Integrated systems of the CNS, part III. Cerebellum, basal ganglia and olfactory system*. Amsterdam: Elsevier Press, 1996; *The basal ganglia*.
89. Gibson, J.M. A quantitative comparison of stimulus-response relationships of vibrissa-activated neurons in subnuclei oralis and interpolaris of the rat's trigeminal sensory complex: Receptive field properties and threshold determinations. *Somatosen Motor Res* 1987; **5**: 137-55.
90. Gilbert, C.D., Wiesel, T.N. Morphology and intracortical projections of functionally characterized neurons in the cat visual cortex. *Nature* 1979; **280**: 120-5.
91. Gimenez-Amaya, J.M., Graybiel, A.M. Compartmental origins of the striatopallidal projection in the primate. *Neurosci* 1990; **34**: 111-26.
92. Gonzalez, M.F., Sharp, F.R. Vibrissae tactile discrimination (<sup>14</sup>C) 2-deoxyglucose uptake in rat brainstem, thalamus and cortex. *J Comp Neurol* 1985; **231**: 457-72.
93. Good, K.E., Killackey, H.P. Areal distribution of corticothalamic projection neurons to the posterior thalamic complex in rat somatosensory cortex. *Society of Neuroscience Abstracts* 1992; **18**: 1390

94. Gottschaldt, K.M., Iggo, A., Young, D.W. Functional characteristics of mechanoreceptors in sinus hair follicles of the cat. *J Physiol (Lond)* 1973; **235**: 287-315.
95. Greenough, W.T., Chang, F.-L.F. Dendritic pattern formation involves both oriented regression and oriented growth in the barrels of mouse somatosensory cortex. *Dev Brain Res* 1988; **43**: 148-52.
96. Guatteo, E., Bacci, A., Franceschetti, S., Avanzini, G., Wanke, E. Neurones dissociated from neocortex fire with 'burst' and 'regular' trains of spikes. *Neurosci.Letts.* 1994; **175**: 117-20.
97. Guic-Robel, E., Valdiviesco, C., Guajardo, G. Rats can learn roughness discrimination using only thir vibrissal system. *Behavioural Brain Research* 1989; **31**: 285-9.
98. Guiffrida, R., Rustioni, A. Glutamate and aspartate immunoreactivity in corticocortical neurons of the sensorimotor cortex of rats. *Exp Brain Res* 1989; **74**: 41-6.
99. Gustafson, J.W., Felbain-Keramidas, S.L. Behavioural and neural approaches to the function of the mystacial vibrissae. *Psychological bulletin* 1977; **84**: 477-88.
100. Halata, Z., Munger, B.L. Sensory nerve endings in the rhesus monkey sinus hair. *J Comp Neurol* 1980; **192**: 645-63.
101. Harding, G.W., Stogsdill, R.M., Towe, A.L. Relative effects of pentobarbital and chloralose on the responsiveness of neurons in sensorimotor cerebral cortex of the domestic cat. *Neurosci* 1979; **4**: 369-78.
102. Harris, R.M., Woolsey, T.A. Computer-assisted analyses of barrel neuron axons and their putative synaptic contacts. *J Comp Neurol* 1983; **220**: 63-79.
103. Harris, R.M. Morphology of physioloically identified thalamocortical relay neurons in the rat ventrobasal thalamus. *J Comp Neurol* 1986; **251**: 491-505.
104. Harris, R.M. Axon collaterals in the thalamic reticular nucleus from thalamocortical neurons of rat ventrobasal thalamus. *J Comp Neurol* 1987; **258**: 397-406.
105. Herkenham, M. Laminar organization of thalamic projections to the rat neocortex. *Science* 1980; **207**: 532-5.

- 106.Hersch, S.M., White, E.L. Thalamocortical synapses with corticothalamic projection neurons in mouse SmI cortex: Electron microscopic demonstration of a monosynaptic feedback loop. *Neuroscience Letters* 1981a; **24**: 217-55.
- 107.Hersch, S.M., White, E.L. Thalamocortical synapses involving identified neurones in mouse primary somatosensory cortex: A terminal degeneration and Golgi/EM study. *J Comp Neurol* 1981b; **195**: 253-63.
- 108.Hersch, S.M., White, E.L. A quantitative study of the thalamocortical and other synapses in layer IV of pyramidal cells projecting from mouse SmI cortex to the caudate-putamen nucleus. *J Comp Neurol* 1982; **211**: 217-25.
- 109.Hoogland, P.V., Welker, E., Van der Loos, H. Organizations of the projections from barrel cortex to thalamus in mice studied with Phaseolus vulgaris-leucoagglutinin and HRP. *Exp Brain Res* 1987; **68**: 73-87.
- 110.Huettner, J.E., Baughman, R.W. The pharmacology of synapses formed by corticocollicular neurons in primary cultures of rat visual cortex. *J Neurosci* 1988; **8**: 160-75.
- 111.Huntley, G.W., Jones, E.G. Relationship of intrinsic connections to forelimb movement representations in monkey motor cortex: A correlative anatomical and physiological study. *Jouranl of Neurophysiology* 1991; **66**: 390-413.
- 112.Hutson, K.A., Masterson, R.B. The sensory contribution of a single vibrissas cortical barrel. *J Neurophysiol* 1986; **56(4)**: 1196-223.
- 113.Ito, M. Some quantitative aspects of vibrissa-driven neuronal responses in rat neocortex. *J Neurophysiol* 1981; **46**: 705-15.
- 114.Ito, M. Processing of vibrissal sensory information within the rat neocortex. *J Neurophysiol* 1985; **54(3)**: 479-90.
- 115.Ito, M. Responsive properties and topography of vibrissa-sensitive VPM neurons in the rat. *J Neurophysiol* 1988; **60**: 1181-97.
- 116.Jacobson, S., Trojanowski, J.Q. The cells of origin of the corpus callosum in rat, cat and rhesus monkey. *Brain Res* 1974; **23**: 103-12.
- 117.Jacobson, S., Trojanowski, J.Q. Corticothalamic neurons and thalamocortical terminal fields: An investigation in rat using horseradish peroxidase and autoradiography. *Brain Res* 1975; **85**: 385-401.

118. Jacquin, M.F., Rhoades, R.W. Central projections of the normal and "regenerate" infraorbital nerve in adult rats subjected to neonatal infraorbital lesions: A transganglionic horseradish peroxidase study. *Brain Res* 1983; **269**: 137-44.
119. Jacquin, M.F., Moone, R.D., Rhoades, R.W. Morphology, response properties, and collateral projections of trigeminothalamic neurons in brainstem subnucleus interpolaris of rat. *Exp Brain Res* 1986; **61**: 457-68.
120. Jacquin, M.F., Rhoades, R.W. Development and plasticity in hamster trigeminal primary afferent projections. *Dev Brain Res* 1987; **31**: 161-75.
121. Jacquin, M.F., Golden, J., Panneton, W.M. Structure and function of barrel 'precursor' cells in trigeminal nucleus principalis. *Dev Brain Res* 1988a; **43**: 309-14.
122. Jacquin, M.F., Stennett, R.A., Renehan, W.E., Rhoades, R.W. Structure-function relationships in rat brainstem subnucleus interpolaris. II. Low and high threshold trigeminal primary afferents. *J Comp Neurol* 1988b; **267**: 107-30.
123. Jacquin, M.F., Barcia, M., Rhoades, R.W. Structure-Function relationships in rat brainstem subnucleus interpolaris. IV. Projection neurons. *J Comp Neurol* 1989a; **282**: 45-62.
124. Jacquin, M.F., Golden, J.P., Rhoades, R.W. Structure -function relationships in the rat brainstem subnucleus interpolaris. III. Local circuit neurons. *J Comp Neurol* 1989b; **282**: 22-44.
125. Jensen, K.F., Killackey, H.P. Terminal arbors of axons projecting to the somatosensory cortex of the adult rat. 1. The normal morphology of specific thalamocortical afferents. *J Neurosci* 1987; **7**: 3529-43.
126. Jimenez-Castellanos, J., Graybiel, A.M. Compartmental origins of striatal efferent projections in the cat. *Neurosci* 1989; **32**: 297-321.
127. Jinnai, K., Matsuda, Y. Neurons of the motor cortex projecting commonly to the caudate nucleus and the lower brainstem in the cat. *Neuroscience Letters* 1979; **13**: 121-6.
128. Johansson, K., Arvidsson, J. Central plasticity in rat trigeminal primary sensory neurons innervating vibrissae after neonatal peripheral nerve injury. *Neurosci Lett* 1994; **167**: 187-90.

129. Johansson, R.S., Vallbo, A.B. detection of tactile stimuli. Thresholds of afferent units related to psychophysical thresholds in the human hand. *J Physiol (Lond)* 1979; **297**: 405-22.
130. Karmy, G., Carr, P.A., Yamamoto, T., Chan, S.H., Nagy, J.I. Cytochrome oxidase immunohistochemistry in rat brain and dorsal root ganglia: Visualization of enzyme in neuronal perikarya and in parvalbumin positive neurons. *Neurosci* 1991; **40**: 825-39.
131. Kasper, E., Larkman, A.U., Blakemore, C., Judge, S. Physiology and morphology of identified projection neurons in the rat visual cortex studied in vitro. *Society of Neuroscience Abstracts* 1991; **17**: 114
132. Kawaguchi, Y. Groupings of nonpyramidal cells with specific physiological and morphological characteristics in the rat frontal cortex. *J Neurophysiol* 1993; **69**: 416-31.
133. Kawaguchi, Y., Kubota, Y. Correlation of physiological subgroupings of nonpyramidal cells with parvalbumin-immunoreactive and calbindin (D28K)-immunoreactive neurons in layer V of rat frontal cortex. *J Neurophysiol* 1993; **70**: 387-96.
134. Keller, Asanuma, H. Synaptic relationships involving local axon collaterals of pyramidal neurons in the cat motor cortex. *J Comp Neurol* 1993; **336**: 229-42.
135. Keller, A., White, E.L., Cipolloni, P.B. The identification of thalamocortical axon terminals in barrels of mouse SmI cortex using immunohistochemistry of anterogradely transported lectin (*Phaseolus vulgaris* leucoagglutinin). *Brain Res* 1985; **343**: 159-65.
136. Keller, A., White, E.L. Distribution of glutamic acid decarboxylase-immunoreactive structures in the barrel region of mouse somatosensory cortex. *Neuroscience Letters* 1986; **66**: 245-50.
137. Keller, A., White, E.L. Synaptic organization of GABAergic neurons in the mouse SmI cortex. *J Comp Neurol* 1987; **262**: 1-12.
138. Keller, A. Patterns of intrinsic connections between motor representation zones in the cat motor cortex. *NeuroR* 1993; **4**: 515-8.
139. Killackey, H.P. Anatomical evidence for cortical subdivisions based on vertically discrete thalamic projections from the ventral posterior nucleus to cortical barrels in the rat. *Brain Res* 1973; **51**: 326-31.

140. Killackey, H.P., Leshin, S. The organization of specific thalamocortical projections to the posteromedial barrel subfield of the rat somtic sensory cortex. *Brain Res* 1975; **86**: 469-72.
141. Killackey, H.P., Belford, G., Ryugo, R.G., Ryugo, D.K. Anomalous organization of thalamocortical projections consequent to vibrissal removal in newborn rat and mouse. *Brain Res* 1976; **104**: 309-15.
142. Kim, H.G., Connors, B.W. Apical dendrites of the neocortex: A correlation between sodium- and calcium dependant spiking and pyramidal cell morphology. *J Neurosci* 1993; **13**: 5301-11.
143. King, M.A., Louis, P.M., Hunter, B.E., Walker, D.W. Biocytin: a versatile anterograde neuroanatomical tract-tracing alternative. *Brain Res* 1989; **497**: 361-7.
144. Koralek, K.-A., Jensen, K.F., Killackey, H.P. Evidence for two complementary patterns of thalamic input to the rat somatosensory cortex. *Brain Res* 1988; **463**: 346-51.
145. Kossut, M., Hand, P. The development of the vibrissal cortical column: a 2-deoxyglucose study in the rat. *Neuroscience Letters* 1984; **46**: 1-6.
146. Land, P.W., Simons, D.J. Metbolic and structural correlates of the vibrissae representation in the thalamus of the adult rat. *Neuroscience Letters* 1985; **60**: 319-24.
147. Landry, P., Deschenes, M. Intracortical arborizations and receptive fields of identified ventrobasal thalamocortical afferents to the primary somatic sensory cortex in the cat. *J Comp Neurol* 1981; **199**: 345-71.
148. Landry, P., Wilson, C.J., Kitai, S.T. Morphological and electrophysiological characteristics of pyramidal tract neurones in the rat. *Exp Brain Res* 1984; **57**: 177-90.
149. Larkman, A., Mason, A. Correlations between morphology and electrophysiology of pyramidal neurones in slices of rat visual cortex. I Establishment of cells. *J Neurosci* 1990; **10**(5): 1407-14.
150. Larkman, A.U. Dendritic morphology of pyramidal neurons in the visual cortex of the rat: I. Branching patterns. *J Comp Neurol* 1991; **306**: 306-19.

151. Levesque, M., Charara, A., Gagnon, S., Parent, A., Deschenes, M. Corticostriatal projections from layer V cells in the rat are collaterals of long-range corticofugal axons. *Brain Res* 1996; **709**: 311-5.
152. Lichtenstein, S.H., Carvell, G.E., Simons, D.J. Responses of rat trigeminal ganglion neurons to movements of vibrissae in different directions. *Somatosens Motor Res* 1990; **7**: 47-65.
153. Lin, C., Lu, S.M., Yamawaki, R.M. Laminar and synaptic organization of terminals from the ventrobasal and posterior thalamic nuclei in rat barrel cortex. *Neuroscience Abstracts* 1987; **13**: 248
154. Lin, C.S., Lu, S.M., Schmechel, D. Glutamic Acid Decarboxylase Immunoreactivity in Layer IV of Barrel cortex of Rat and Mouse. *Neurosci* 1985; **5**: 1934-9.
155. Lisman, J.E. Bursts as a unit of neural information: Making unreliable synapses reliable. *Trends neurosci* 1997; **20**: 38-43.
156. Lorenzon, N.M., Foehring, R.C. Relationship between repetitive firing and hyperpolarizations in human neocortical neurons. *J Neurophysiol* 1992; **67**: 350-63.
157. Lu, S.-M., Lin, R.C.-S. Thalamic afferents of the rat barrel cortex: A light- and electron-microscopic study using *Phaseolus vulgaris* leucoagglutinin as an anterograde tracer. *Somatosens Mot Res* 1993; **10**: 1-16.
158. Luhmann, H.J., Prince, D.A. Postnatal maturation of the GABAergic system in rat neocortex. *J Neurophysiol* 1991; **65**: 247-63.
159. Ma, P.-K.M., Woolsey, T.A. Cytoarchitectonic correlates of the vibrissae in the medullary trigeminal complex of the mouse. *Brain Res* 1984; **306**: 374-9.
160. Ma, P.-K.M. The barrelettes - architectonic vibrissal representations in the brainstem trigeminal complex of the mouse. I. Normal structural organisation. *J Comp Neurol* 1991; **309**: 161-99.
161. Mason, A., Larkman, A. Correlations between morphology and electrophysiology of pyramidal neurones in slices of rat visual cortex. II: Electrophysiology. *J Neurosci* 1990; **10**(5): 1415-28.
162. McAllister, J.P., Wells, J. The structural organization of the ventral posterolateral nucleus in the rat. *J Comp Neurol* 1981; **197**: 271-301.

163. McCasland, J.S., Woolsey, T.A. High resolution 2-deoxyglucose mapping of functional cortical columns in mouse barrel cortex. *J Comp Neurol* 1988; **278**: 555-69.
164. McCasland, J.S., Carvell, G.E., Simons, D.J., Woolsey, T.A. Functional Asymmetries in the Rodent Barrel Cortex. *Somatosen Motor Res* 1991; **8**: 111-6.
165. McCasland, J.S., Hibbard, L.S. GABAergic neurons in barrel cortex showing strong, whisker-dependant metabolic activation during normal behaviour. *J Neurosci* 1991; **17**: 5509-27.
166. McCasland, J.S., Bernardo, K.L., Probst, K.L., Woolsey, T.A. Cortical local circuit axons do not mature after early deafferentation. *Proceedings of the National Academy of Science (USA)* 1992; **89**: 1832-6.
167. McCormick, D.A., Connors, B.W., Lighthall, J.W., Prince, D.A. Comparative electrophysiology of pyramidal and sparsely spiny stellate neurones of the neocortex. *J Neurophysiol* 1985; **54(4)**: 782-806.
168. McGeorge, A.J., Faull, R.L.M. The organization and collateralization of corticostriate neurones in the motor and sensory cortex of the rat brain. *Brain Res* 1987; **423**: 318-24.
169. McGeorge, A.J., Faull, R.L.M. The organization of the projection from the cerebral cortex to the striatum in the rat. *Neurosci* 1989; **29**: 503-37.
170. Mercier, B.E., Glickstein, M., Legg, C.R. Basal ganglia and the cerebellum receive different somatosensory information in rats. *Proceedings of the National Academy of Science (USA)* 1990; **87**: 4388-92.
171. Metz, C.B., Schneider, S.P., Fyffe, R.E.W. Selective supression of endogenous peroxidase activity: Application for enhancing appearance of HRP-labeled neurones in vitro. *J Neurosci Methods* 1989; **26**: 181-8.
172. Micheva, K.D., Beaulieu, C. Quantitative aspects of synaptogenesis in the rat barrelfield cortex with special reference to GABA circuitry. *J Comp Neurol* 1996; **373**: 340-54.
173. Miller, M.W., Chiaia, N.L., Rhoades, R.W. Intracellular recording and injecyion study of corticospinal neurons in the rat somatosensory cortex: Effect of prenatal exposure to ethanol. *J Comp Neurol* 1990; **297**: 91-105.

174. Miller, R. Distribution and properties of commissural and other neurons in cat sensorimotor cortex. *J Comp Neurol* 1975; **164**: 361-73.
175. Miyashita, E., Keller, A., Asanuma, H. Input-output organization of the rat vibrissal motor cortex. *Exp Brain Res* 1994; **99**: 223-32.
176. Montoro, R.J., Lopez-Bareno, J., Jassik-Gershenfeld, D. Differential bursting modes in neurons of the mammalian visual cortex in vitro. *Brain Res* 1988; **460**: 168-72.
177. Mosconi, T.M., Rice, F.L., Song, M.J. Sensory innervation in the inner conical body of the vibrissal follicle-sinus complex of the rat. *J Comp Neurol* 1993; **328**: 323-51.
178. Mountcastle, Talbot, W.H., Sakata, H., Hyvarinen, J. Cortical neuronal mechanisms in flutter-vibration studied in unanaesthetized monkeys. Neuronal periodicity and frequency discrimination. *J Neurophysiol* 1969; **32**: 452-84.
179. Neagele, J.R., Katz, L.C. Cell surface molecules containing N-acetylgalactosamine are associated with basket cells and neurogliaform cells in cat visual cortex. *J Neurosci* 1990; **10**: 540-57.
180. Nicoll, A., Kim, H.G., Connors, B.W. Spatial organization of inhibitory synaptic responses onto pyramidal neurons of rat neocortex. *Society of Neuroscience Abstracts* 1993; **19**: 1704
181. Nothias, F., Peschanski, M., Besson, J.-M. Somatotopic reciprocal connections between the somatosensory cortex and thalamic Po nucleus in the rat. *Brain Res* 1988; **447**: 169-74.
182. Ojima, H., Honda, C.N., Jones, E.G. Patterns of axon collateralization of identified supragranular pyramidal neurons in the cat auditory cortex. *Cerebral Cortex* 1991; **1**: 80-94.
183. Ojima, H., Honda, C.N., Jones, E.G. Characteristics of intracellularly injected infragranular pyramidal neurons in cat primary auditory cortex. *Cerebral Cortex* 1992; **2**: 197-216.
184. Olavarria, J., Van Sluyters, R.C., Killackey, H.P. Evidence for the complementary organization of callosal and thalamic connections within rat somatosensory cortex. *Brain Res* 1984; **291**: 364-8.
185. Oshima, T. ; Jasper, H.H., Ward, A.A., Pope, A. editors. *Basic mechanisms of the epilepsies*. Boston: Little Brown, 1969; *Studies of pyramidal tract neurons*. p. 253-61.

186. Pare, D., Smith, Y. Thalamic collaterals of corticostriatal axons: Their termination field and synaptic targets in cats. *J Comp Neurol* 1996; **372**: 551-67.
187. Parthasarathy, H.B., Schall, J.D., Graybiel, A.M. Distributed but convergent ordering of corticostriatal projections: Analysis of the frontal eye field and the supplementary eye field in the macaque monkey. *J Neurosci* 1992; **12**: 4468-88.
188. Patel, U. Non-random distribution of blood vessels in the posterior region of the rat somatosensory cortex. *Brain Res* 1983; **289**: 65-70.
189. Patel-Viadya, J. Ultrastructural organization of the posterior and anterior barrels in the somatosensory cortex of the rat. *Journal of Neuroscience Research* 1985; **14**: 357-71.
190. Peschanski, M. Trigeminal afferents to the diencephalon in the rat. *Neurosci* 1984; **12**: 465-87.
191. Peters, A., Walsh, M.T. A study of the organization of apical dendrites in the somatic sensory cortex of the rat. *J Comp Neurol* 1972; **144**: 253-68.
192. Pockberger, H. Electrophysiological and morphological properties of rat motor cortex in vivo. *Brain Res* 1991; **539**: 181-90.
193. Pollard, C.E., Angel, A. Spontaneous single cell discharge in rat somatosensory cortical slices and relationship to discharge in the urethane-anaesthaized rat. *Brain Res* 1990; **518**: 120-6.
194. Porter, L., White, E.L. Afferent and efferent pathways of the vibrissal region of primary motor cortex in the mouse. *J Comp Neurol* 1983; **214**: 279-89.
195. Porter, L.L., Izraeli, R. Connections of vibrissal regions in rat sensory-motor cortex. *Soc Neurosci Abstr* 1992; **18**
196. Ragsdale, C.W.J., Graybiel, A.M. A simple ordering of neocortical areas established by the compartmental organization of their striatal projections. *Proc.Natl.Acad.Sci.USA* 1990; **87**: 6196-9.
197. Renehan, W.E., Jacquin, M.F., Mooney, R.D., Rhoades, R.W. Structure-function relationships in rat medullary and cervical dorsal horns. II. Medullary dorsal horn cells. *J Neurophysiol* 1986; **55**: 1187-201.

198. Rhoades, R.W., Belford, G.R., Killackey, H.P. Receptive-field Properties of Rat Ventral Posterior Medial Neurons Before and After Selective Kainic Acid Lesions of the Trigeminal Brainstem Complex. *J Neurophysiol* 1987; **57**: 1577-600.
199. Rice, F.L., Mance, A., Munger, B.L. A comparative light microscopic analysis of the sensory innervation of the mystacial pad I: innervation of the vibrissal follicle-sinus complexes. *J Comp Neurol* 1986; **252**: 154-74.
200. Rice, F.L., Kinnman, E., Aldskogius, H., Johansson, O., Arvidsson, J. The innervation of the mystacial pad of the rat as revealed by PGP 9.5 immunofluorescence. *J Comp Neurol* 1993; **337**: 366-85.
201. Robinson, D.A. Eye movements evoked by collicular stimulation in the alert monkey. *Vision Res* 1972; **12**: 1795-808.
202. Royce, G.J. Laminar origin of cortical neurons which project upon the caudate nucleus: A horseradish peroxidase investigation in the cat. *J Comp Neurol* 1982; **205**: 8-29.
203. Royce, G.J. Cortical neurons with collateral projections to both the caudate nucleus and the centromedian-parafascicular thalamic complex: a fluorescent retrograde double labelling study in the cat. *Exp Brain Res* 1983; **50**: 157-65.
204. Ryugo, R., Ryugo, D.K., Killackey, H.P. Differential effect of enucleation on two populations of layer V pyramidal cells. *Brain Res* 1975; **88**: 554-9.
205. Salt, T.E. Excitatory amino acid receptors and synaptic transmission in the rat ventrobasal thalamus. *Journal of Physiology (London)* 1987; **391**: 499-510.
206. Salt, T.E., Eaton, S.A. Function of non-NMDA receptors and NMDA receptors in synaptic responses to natural somatosensory stimulation in the ventrobasal thalamus. *Exp Brain Res* 1989; **77**: 646-52.
207. Saporta, S., Kruger, L. The organization of thalamocortical relay neurons in the rat ventrobasal complex studied by the retrograde transport of horseradish peroxidase. *J Comp Neurol* 1977; **174**: 187-208.
208. Schiller, P.H., Stryker, M.P. Single unit recording and stimulations in superior colliculus of the alert rhesus monkey. *J Neurophysiol* 1972; **35**: 915-24.
209. Schwark, H.D., Jones, E., G. The distribution of intrinsic cortical axons in area 3b of cat primary somatosensory cortex. *Exp Brain Res* 1989; **78**: 501-13.

210. Schwindt, P., O'Brien, J.A., Crill, W. Quantitative analysis of firing properties of pyramidal neurons from layer V of rat sensorimotor cortex. *J Neurophysiol* 1997; **77**: 2482-98.
211. Selemon, L.D., Goldman-Rakic, P.S. Longitudinal topography and interdigitation of corticostriatal projections in the rhesus monkey. *J Neurosci* 1985; **5**: 776-94.
212. Selemon, L.D., Goldman-Rakic, P.S. Common cortical and subcortical targets of the dorsolateral prefrontal and posterior parietal cortices in the rhesus monkey: Evidence for a distributed neural network subserving spatially guided behaviour. *J Neurosci* 1988; **8**: 4049-68.
213. Sharp, F.R., Evans, K. Regional (14C) 2-deoxyglucose uptake during vibrissae movements evoked by rat motor cortex stimulation. *J Comp Neurol* 1982; **208**: 255-87.
214. Shipley, M.T. Response characteristics of single units in the rat's trigeminal nuclei to vibrissa displacements. *J Neurophysiol* 1974; **37**: 73-90.
215. Silva, L.R., Connors, B.W. Spatial distribution of intrinsic cortical neurons that excite or inhibit layer 2/3 pyramidal cells: A physiological study of the neocortex in vitro. *Society of Neuroscience Abstracts* 1986; **12**: 1435
216. Silva, L.R., Amitai, Y., Connors, B.W. Intrinsic oscillations of neocortex generated by layer 5 pyramidal neurons. *Science* 1991a; **251**: 432-5.
217. Silva, L.R., Gutnick, M.J., Connors, B.W. Laminar distribution of neuronal membrane properties in neocortex of normal and reeler mouse. *J Neurophysiol* 1991b; **66**: 2034-40.
218. Simons, D.J. Response properties of vibrissa units in the rat S1 somatosensory neocortex. *J Neurophysiol* 1978; **41**: 798-820.
219. Simons, D.J., Woolsey, T.A. Functional organisation in mouse barrel cortex. *Brain Res* 1979; **165**: 327-32.
220. Simons, D.J., Woolsey, T.A. Morphology of Golgi-Cox-impregnated barrel neurons in rat SmI cortex. *J Comp Neurol* 1984; **230**: 119-32.
221. Simons, D.J. Temporal and spatial integration in the rat S1 vibrissa cortex. *J Neurophysiol* 1985; **54**: 615-35.

222. Simons, D.J., Land, P.W. Early experience of tactile stimulation influences organization of somatic sensory cortex. *Nature* 1987; **326**: 694-7.
223. Simons, D.J., Carvell, G.E. Thalamocortical Response Transformation in the Rat Vibrissa/Barrel System. *J Neurophysiol* 1989; **61**: 311-30.
224. Simons, D.J., Carvell, G.E., Hershey, A.E., Bryant, D.P. Responses of barrel cortex neurons in awake rats and effects of urethane anesthesia. *Exp Brain Res* 1992; **91**: 259-72.
225. Simons, D.J. ; Jones, E.G., Diamond, I.T. editors. *The barrel cortex of rodents*. New York: Plenum, 1995; *Neuronal integration in the somatosensory whisker/barrel cortex*. p. 263-98.
226. Smith, R.L. The ascending fiber projections from the principal sensory trigeminal nucleus in the rat. *J Comp Neurol* 1973; **148**: 423-46.
227. Smith, Y. ; Bolam, J.P. editors. *Experimental neuroanatomy*. Oxford: IRI press, 1992; *Antrograde tracing with PHA-L and biocytin at the electron microscopic level*. p. 61-79.
228. Stafstrom, C.E., Schwindt, P.C., Crill, W.E. Repetitive firing in layer V neurons from cat neocortex in vitro. *J Neurophysiol* 1984; **52**: 264-77.
229. Staiger, J.F., Zilles, K., Freund, T.F. Distribution of GABAergic elements post-synaptic to ventroposteromedial thalamic projections in layer IV of rat barrel cortex. *Eu J Neurosci* 1996; **8**: 2273-85.
230. Stern, E.A., Kincaid, A.E., Wilson, C.J. Spontaneous subthreshold membrane potential fluctuations and action potential variability of rat corticostriatal neurons in vivo. *J Neurophysiol* 1997; **77**: 1697-715.
231. Stryker, M.P., Schiller, P.H. Eye and head movements evoked by electrical stimulation of the monkey superior colliculus. *Exp Brain Res* 1975; **23**: 103-12.
232. Stryker, M.P., Jenkins, W.M., Merenich, M. Anaesthetic state does not affect the map of the hand representation within area 3b somatosensory cortex in owl monkey. *J Comp Neurol* 1988; **258**: 297-303.
233. Tseng, G.F., Prince, D.A. Heterogeneity of rat corticospinal neurons. *J Comp Neurol* 1993; **335**: 92-108.

234. Valverde, F. Intrinsic neocortical organisation: Some comparative aspects. *Neurosci* 1986; **18**(1): 1-23.
235. van Brederode, J.F., Mulligan, K.A., Hendrickson, A.E. Calcium-binding proteins as markers for subpopulations of GABAergic neurons in monkey striate cortex. *J Comp Neurol* 1990; **298**: 1-22.
236. van Brederode, J.F., Helliesen, M.K., Hendrickson, A.E. Distribution of the calcium-binding proteins parvalbumin and calbindin-D28K in the sensorimotor cortex of the rat. *Neurosci* 1991; **44**: 157-71.
237. van Brederode, J.F.M., Snyder, G.L. A Comparison of the Electrophysiological Properties of Morphologically Identified Cells in Layers 5B and 6 of the Rat Neocortex. *Neurosci* 1992; **50**: 315-37.
238. Van der Loos, H. Barreloids in the Mouse Somatosensory Thalamus. *Neurosci Lett* 1976; **2**: 1-6.
239. Waite, P.M., Jacquin, M.F. Dual innervation of the rat vibrissa: Responses of trigeminal ganglion cells projecting through deep or superficial nerves. *J Comp Neurol* 1992; **322**: 233-45.
240. Waite, P.M.E. The responses of cells in the rat thalamus to mechanical movements of the whiskers. *Journal of Physiology (London)* 1973; **228**: 541-61.
241. Wallace, M.N., Kitzes, L.M., Jones, E.G. Chemoarchitectonic organization of the cat primary auditory cortex. *Exp Brain Res* 1991a; **86**: 518-26.
242. Wallace, M.N., Kitzes, L.M., Jones, E.G. Intrinsic inter- and intralaminar connections and their relationship to the topographic map in the cat primary auditory cortex. *Exp Brain Res* 1991b; **86**: 527-44.
243. Wang, Z., McCormick, D.A. Control of firing mode of corticotectal and corticopontine layer V burst-generating neurons by norepinephrine, acetylcholine, and 1S,3R-ACPD. *J Neurosci* 1993; **13**: 2199-216.
244. Weiss, D.S., Keller, A. Specific patterns of intrinsic connections between representational zones in the rat motor cortex. *Cerebral Cortex* 1994; **4**: 295-314.
245. Welker, C., Woolsey, T.A. Structure of layer IV in the somatosensory neocortex of the rat: Description and comparison with the mouse. *J Comp Neurol* 1974; **158**: 437-54.

246. Welker, E., Hoogland, P.V., Van der Loos, H. Organization of feedback and feedforward projections of the barrel cortex: a PHA-L study in the mouse. *Exp Brain Res* 1988; **73**: 411-35.
247. Welker, E., Soriano, E., Van der Loos, H. Plasticity in the barrel cortex of adult mouse: Effects of peripheral deprivation on GAD-immunoreactivity. *Exp Brain Res* 1989; **74**: 441-52.
248. Welker, E., Armstrong-James, M., Van der Loos, H., Kraftsik, R. The mode of activation of a barrel column: Response properties of single units in the somatosensory cortex of the mouse upon whisker deflection. *European Journal Neuroscience* 1993; **5**: 691-712.
249. Welker, W.I. Analysis of sniffing in the albino rat. *Behaviour* 1964; **22**: 223-44.
250. White, E.L., DeAmicis, R.A. Afferent and efferent projections of the region in mouse SmI cortex which contains the posteriomedial barrel subfield. *J Comp Neurol* 1977; **175**: 455-82.
251. White, E.L. Identified neurones in mouse SmI cortex which are postsynaptic to thalamocortical axon terminals: A combined Golgi-electron microscopic and degeneration study. *J Comp Neurol* 1978; **181**: 627-39.
252. White, E.L., Rock, M.P. Distribution of thalamic input to different dendrites of a spiny stellate cell. *Neuroscience Letters* 1979; **15**: 115-9.
253. White, E.L., Hersch, S.M. Thalamocortical synapses of pyramidal cells which project from SmI to MsI cortex in the mouse. *J Comp Neurol* 1981; **198**: 167-81.
254. White, E.L., Rock, M.P. A comparison of thalamocortical and other synaptic inputs to dendrites of two non-spiny neurons in a single barrel of mouse SmI cortex. *J Comp Neurol* 1981; **195**: 265-77.
255. White, E.L., Benshalom, G., Hersch, S.M. Thalamocortical and other synapses of non-spiny multipolar cells in mouse SmI cortex. *J Comp Neurol* 1984; **229**: 311-20.
256. White, E.L. ; Jones, E.G., Peters, A. editors. *Cerebral cortex*. New York: Plenum Press, 1986; *Termination of thalamic afferents in the cerebral cortex*. p. 271-89.
257. White, E.L., Keller, A. *Intrinsic circuitry involving the local axon collaterals of corticothalamic projection cells in mouse SmI cortex*. *J Comp Neurol* 1987; **262**: 13-26.

258. White, E.L., Peters, A. Cortical modules in the posteromedial barrel subfield (Sml) of the mouse. *J Comp Neurol* 1993; **334**: 86-96.
259. White, E.L., Amitai, Y., Gutnick, M.J. Axosomatic synapses onto intrinsically bursting neurons in rat Sml (barrel) cortex. *J Comp Neurol* 1994; **342**: 1-14.
260. Wickens, J.R., Arbuthnott, G.W. ; Arbuthnott, G.W., Emson, P.C. editors. *Chemical signalling in the basal ganglia*. Elsevier Science Publishers B.V. Amsterdam, 1993; *The corticostriatal system on computer simulation: an intermediate mechanism for sequencing of actions*. p. 325-40.
261. Williams, M.N., Faull, R.L. The distribution and morphology of identified thalamocortical projection neurons and glial cells with reference to the question of interneurons in the ventrolateral nucleus of the rat thalamus. *Neurosci* 1987; **21**: 767-80.
262. Williams, M.N., Zham, D.S., Jacquin, M.F. Differential foci and synaptic organization of the principal and spinal projections to the thalamus in rat. *Eu J Neurosci* 1993; **6**: 429-53.
263. Wilson, C.J., Groves, P.M. Spontaneous firing patterns of identified spin neurons in the rat neostriatum. *Brain Res* 1981; **220**: 67-80.
264. Wilson, C.J., Chang, H.T., Kitai, S.T. Origins of postsynaptic potentials evoked in identified rat neostriatal neurons by stimulation in substantia nigra. *Exp Brain Res* 1982; **45**: 157-67.
265. Wilson, C.J., Groves, P.M., Kitai, S.T., Linder, J.C. Three-dimensional structure of dendritic spines in the rat neostriatum. *The Journal of Neuroscience* 1983; **3**: 383-93.
266. Wilson, C.J. Postsynaptic potentials evoked in spiny neostriatal projection neurons by stimulation of ipsilateral and contralateral neocortex. *Br Res* 1986; **367**: 201-13.
267. Wilson, C.J. Morphology and synaptic connections of crossed corticostriatal neurons in the rat. *J Comp Neurol* 1987; **263**: 567-80.
268. Wilson, C.J. ; Arbuthnott, G.W., Emson, P.C. editors. *Chemical signalling in the basal ganglia*. Elsevier: Amsterdam, 1993; *The generation of the natural firing patterns in neostriatal neurons*. p. 277-97.
269. Wise, S.P., Jones, E.G. The organisation and positional development of the commissural projection of the rat somatic sensory cortex. *J Comp Neurol* 1976; **168**: 313-44.

270. Wise, S.P., Jones, E.G. Developmental studies of the thalamocortical and commissural connections in the rat somatic sensory cortex. *J Comp Neurol* 1978; **178**: 187-208.
271. Wong-Riley, M.M.T. Changes in the visual system of monocularly sutured cats demonstratable with cytochrome oxidase histochemistry. *Brain Res* 1979; **171**: 11-28.
272. Woolsey, T.A., Van der Loos, H. The structural organization of layer IV in the somatosensory region (S1) of mouse cerebral cortex: the description of a cortical field composed of discrete cytoarchitectonic units. *Brain Res* 1970; **17**: 205-42.
273. Woolsey, T.A., Welker, C., Schwartz, R.H. Comparative anatomical studies of the SmI face cortex with special reference to the occurrence of "barrels" in layer IV. *J Comp Neurol* 1975; **164**: 79-94.
274. Woolston, D.C., LaLonde, J.R., Gibson, J.M. Comparison of response properties of cerebellar- and thalamic projecting intercalated neurons. *J Neurophysiol* 1982; **48**: 160-73.
275. Wright, A.K., Norrie, L., Ingham, C.A., Hutton, E.A.M., Arbuthnott, G.W. Double anterograde tracing of outputs from adjacent 'barrel columns' of rat somatosensory cortex. Neostriatal projection patterns and terminal ultrastructure. *Neurosci* 1998, **in press**.
276. Yeterian, E.H., Van Hoesen, G.W. Cortico-striate projections in the rhesus monkey: the organization of certain cortico-caudate connections. *Brain Res* 1978; **139**: 43-63.
277. Yohoro, Y. Structure of the sinus hair follicle in the big-clawed shrew, *Sorex unguiculatus*. *Journal of Morphology* 1977; **257**: 333-54.
278. Zhang, Z.W., Deschenes, M. Intracortical axon projections of lamina VI cells of the primary somatosensory cortex in the rat: A single-cell labelling study. *J Neurosci* 1997; **17**: 6365-79.
279. Zucker, E., Welker, W.I. Coding of somatic sensory input by vibrissae neurones in the rats trigeminal ganglion. *Brain Res* 1969; **12**: 138-56.

### 38.0 APPENDIX

List of neurons recorded, filled and traced in this study (including figure references).

Case	Depth	Filled	Visible	Whiskers	Class	Scope	VCR	Fig. No.
37	756	√	III	1	x	x	x	44
37	1062	√	IB	1	x	x	x	44-56
44	858	√	IB	1	IB	IB	IB	
48	882	x	x	1	IB	RS	IB	
48	1248	√	x	1	RS	RS	RS	
49	1062	√	IB	1	IB	RS	IB	
49	282	√	x	1	x	x	x	
53	585	√	IB	1	IB	IB	IB	
54	894	√	x	1	IB	RS	IB	
57	900	√	RS	1	RS	RS	RS	
58	342	√	IB	1	IB	IB	IB	
59	573	√	RS	1	RS	RS	RS	}55-62
59	711	√	RS	1	RS	RS	RS	
60	1077	√	x	1	RS	RS	RS	
60	939	x	x	1	x	x	x	
60	951	x	x	1	x	x	x	
63	387	x	x	1	IB	x	IB	
63	666	x	x	1	IB	x	IB	
64	1050	√	x	1	IB	IB	IB	
64	729	√	x	1	IB	x	IB	
64	975	x	x	1	IB	x	IB	
64	864	x	x	1	IB	x	IB	
66	648	x	x	1	IB	x	IB	
66	1143	√	RS	1	RS	x	RS	
67	645	x	x	1	IB	x	IB	
67	1125	√	III	1	x	x	x	

#### KEY

- √ Neuron filled
- x Cell was not filled OR no physiology was available for this neuron (either because no record was taken or the available record was unsuitable for cell classification).
- ? A number of neurons were filled in this case and it is impossible to say which results in the visible neuron
- contra Contralateral stimulating electrode

Case	Depth	Filled	Visible	Whiskers	Class	Scope	VCR	Fig. No.
67	456	x	x	1	IB	x	IB	
68	582	x	x	1	RS	x	RS	
68	804	x	x	1	IB	x	IB	
69	1026	√	x	1	IB	x	IB	
69	1008	x	x	1	IB	x	IB	
70	318	√	IB	1	IB	x	IB	69-76
72	645	√	x	1	IB	x	IB	
72	1023	x	x	1	IB	x	IB	
72	1005	x	x	1	IB	x	IB	
73	540	x	x	1	IB	x	IB	
74	759	x	x	1	IB	x	IB	
74	924	x	x	1	IB	x	IB	
74	1041	√	IB	1	IB	x	IB	
74	1119	x	x	1	RS	x	RS	
75	156	x	x	1	IB	x	IB	
75	480	x	x	1	RS	x	RS	
75	492	x	x	1	IB	x	IB	
76	756	x	x	1	IB	x	IB	
78	915	x	x	1	IB	x	IB	
78	1014	√	IB	1	IB	x	IB	31
79	1173	x	x	1	RS	x	RS	
79	636	x	x	1	IB	x	IB	
79	642	x	x	1	IB	x	IB	
79	942	√	IB	1	IB	x	IB	
80	780	√	RS	1	RS	x	RS	

KEY

- √ Neuron filled  
x Cell was not filled OR no physiology was available for this neuron (either because no record was taken or the available record was unsuitable for cell classification).  
? A number of neurons were filled in this case and it is impossible to say which results in the visible neuron  
contra Contralateral stimulating electrode

Case	Depth	Filled	Visible	Whiskers	Class	Scope	VCR	Fig. No.
80	720	x	x	1	IB	x	IB	
81	786	x	x	1	IB	x	IB	
81	867	x	x	1	IB	x	IB	
81	636	x	x	1	RS	x	RS	
81	798	x	x	1	RS	x	RS	
81	210	x	x	1	RS	x	RS	
82	1134	x	x	1	x	x	x	
82	1140	x	x	1	IB	x	IB	
82	1143	x	x	1	IB	x	IB	
82	882	x	x	1	RS	x	RS	
82	885	x	x	1	RS	x	RS	
82	471	√	x	1	RS	x	RS	
82	873	x	x	1	RS	x	RS	
82	921	x	x	1	RS	x	RS	
82	534	x	x	1	RS	x	RS	
83	747	x	x	1	RS	x	RS	
83	819	√	IB	1	IB	x	IB	30
83	792	x	x	1	IB	x	IB	
83	894	x	x	1	IB	x	IB	
83	897	x	x	1	IB	x	IB	
83	990	x	x	1	IB	x	IB	
83	990	x	x	1	IB	x	IB	
83	996	x	x	1	IB	x	IB	
83	732	x	x	1	IB	x	IB	
84	1134	√	x	1	IB	x	IB	

KEY

- √ Neuron filled  
x Cell was not filled OR no physiology was available for this neuron (either because no record was taken or the available record was unsuitable for cell classification).  
? A number of neurons were filled in this case and it is impossible to say which results in the visible neuron  
contra Contralateral stimulating electrode

Case	Depth	Filled	Visible	Whiskers	Class	Scope	VCR	Fig. No.
84	765	x	x	1	IB	x	IB	
84	1710	√	x	1	RS	x	RS	
84	279	x	x	1	IB	x	IB	
84	693	x	x	1	IB	x	IB	
84	699	x	x	1	IB	x	IB	
84	714	x	x	1	IB	x	IB	37
84	843	x	x	1	IB	x	IB	
84	837	x	x	1	IB	x	IB	
84	843	x	x	1	IB	x	IB	
85	837	x	x	2	IB	x	IB	
85	915	x	x	3	IB	x	IB	
85	285	√	x	3	IB	x	IB	
85	1116	√	RS	3	RS	x	RS	64-68
85	993	x	x	3	IB	x	IB	
85	540	√	x	3	IB	x	IB	
87	630	x	x	3	IB	RS	IB	
87	726	x	x	3	IB	RS	IB	
88	897	√	x	3	IB	RS	IB	41
88	213	x	x	2	IB	RS	IB	
88	639	√	x	3	IB	IB	IB	
90	927	√	?	1	IB	IB	IB	
90	1197	√	?	3	IB	IB	IB	
90	1131	x	x	1	IB	IB	IB	
91	1143	x	x	2	IB	RS	IB	
92	927	x	x	1	IB	RS	IB	

KEY

- √ Neuron filled  
x Cell was not filled OR no physiology was available for this neuron (either because no record was taken or the available record was unsuitable for cell classification).  
? A number of neurons were filled in this case and it is impossible to say which results in the visible neuron  
contra Contralateral stimulating electrode

Case	Depth	Filled	Visible	Whiskers	Class	Scope	VCR	Fig. No.
92	750	x	x	2	IB	IB	IB	
92	759	x	x	3	IB	IB	IB	36+39
93	813	√	x	3	IB	RS	IB	42
93	1032	x	x	2	RS	RS	RS	
93	861	√	x	3	IB	IB	IB	
93	897	√	x	3	IB	RS	IB	
94	753	x	x	3	IB	IB	IB	
94	912	√	IB	3	IB	IB	IB	
94	858	x	x	3	IB	IB	IB	
94	960	x	x	3	RS	RS	RS	
94	1053	√	x	3	IB	IB	IB	
94	726	x	x	3	IB	RS	IB	
95	165	x	x	3	IB	IB	IB	
95	816	√	?	3	IB	IB	IB	} 28
95	474	√	?	3	IB	RS	IB	
95	801	√	?	3	IB	IB	IB	
103	810	x	x	2+contra	IB	RS	IB	
104	852	√	x	3	RS	RS	RS	38
109	993	√	x	3	RS	RS	RS	
113	321	x	x	2	RS	RS	x	
113	513	√	III	contra	RS	RS	x	
113	1506	√	x	3+contra	RS	RS	RS	
117	603	x	x	1	RS	RS	x	
117	870	√	x	3	RS	RS	RS	
117	615	x	x	3+stim	RS	RS	RS	41

KEY

- √ Neuron filled  
x Cell was not filled OR no physiology was available for this neuron (either because no record was taken or the available record was unsuitable for cell classification).  
? A number of neurons were filled in this case and it is impossible to say which results in the visible neuron  
contra Contralateral stimulating electrode

Case	Depth	Filled	Visible	Whiskers	Class	Scope	VCR	Fig. No.
117	1359	x	x	3	RS	RS	RS	
117	809	√	x	3+contra	IB	IB	IB	
117	801	√	x	3+contra	IB	IB	IB	36
119	1107	x	x	2	IB	IB	x	
119	567	√	x	2	IB	IB	IB	
119	447	√	x	3+contra	IB	RS	IB	
119	567	√	x	3+contra	IB	IB	IB	43
147	723	√	III	3	III	x	x	
149	843	√	IB	3	IB	x	IB	}49-54
149	1053	√	IB	2	IB	x	IB	
150	957	√	?	?	x	x	x	}77-81
150	891	√	?	?	x	x	x	
151	951	√	x	1	x	x	x	
152	951	√	x	1	IB	x	x	
152	672	√	x	3	IB	x	x	
160	756	√	x	1	RS	x	x	
160	1071	√	√	1	IB	x	x	
162	918	√	x	1	IB	x	x	
167	219	x	x	1	IB	x	x	
167	831	√	x	1	IB	x	x	
168	162	√	x	1	IB	x	x	
168	261	√	III	3	IB	x	x	82-83
121	1041	√	RS	3	RS	x	x	
131	840	√	III	3	III	x	x	
120	672	√	x	3+contra	x	x	x	
120	768	√	x	3+contra	x	x	x	
151	909	√	x	1	x	x	x	
161	390	√	x	1	IB	x	x	

KEY

- √ Neuron filled  
x Cell was not filled OR no physiology was available for this neuron (either because no record was taken or the available record was unsuitable for cell classification).  
? A number of neurons were filled in this case and it is impossible to say which results in the visible neuron  
contra Contralateral stimulating electrode